AN ABSTRACT OF THE DISSERTATION OF

Matthew P. Adams for the degree of Doctor of Philosophy in Civil Engineering presented on May 28, 2015.

Title: Factors Influencing Conversion and Volume Stability in Calcium Aluminate Cement Systems

Abstract approved: _____

Jason H. Ideker

There is renewed interest in North America for the use of calcium aluminate cement (CAC) in infrastructure repair. The interest is driven by the specialty properties that make CAC the ideal candidate for particular applications. These include rapid strength gain, even at temperatures approaching 0°C, the ability to customize fresh property characteristics, high abrasion resistance, and resistance to chemical corrosion. Despite the advantages that CAC can bring to infrastructure repair projects, it is still not well understood within the North American construction community. There are three main topics that are limiting the use of CAC in the construction industry today: (1) a general lack-of-understanding within the construction industry of the conversion process that occurs in CAC systems; (2) there is no standardized accelerated test method for determining the minimum converted strength of CAC concrete; and (3) there are insufficient data on the long-term performance of concrete made with CAC, particularly as a repair material in transportation infrastructure. The work presented in this dissertation addresses these topics in an effort to provide information for and tools for construction professionals interested in using CAC in infrastructure repair situations.

Conversion of the hydration products of concrete where CAC is the only binder is a well-known phenomenon which is accompanied by the formation of porosity and strength loss. Presented in this dissertation is an accelerated test method for determining the converted strength of CAC concrete that is convenient for use in the field. Robustness of this test method is examined. The effects of water to cement materials ratio (w/cm), curing temperature during initial 24 hours after casting, length of time prior to being placed in 50°C water bath, and aggregate source are examined. Results indicated that the test method is viable for use in the field, however writing of a standard based on

this method will require careful consideration to take into account impact of temperature impact and aggregate source on time to conversion. Variability of the test method between four laboratories was also examined and showed that variability within CAC systems is higher when compared to ordinary portland cement (OPC) systems. Also presented is a study of the impact of replacing CAC with finely ground limestone (FGLS) at rates of 1%, 2%, 5%, and 10%. These results showed that replacement rates up to 5% can significantly improve the converted strength of CAC concrete without impacting rapid strength gain prior to conversion.

A further examination of the impact of aggregate type on hydration, conversion, and strength development in CAC systems is also presented. Concrete systems made with nine different coarse aggregate sources and six different fine aggregate sources were cast. Carbonate limestone aggregate systems experienced delayed times to conversion and experienced less strength reduction due to conversion compared to siliceous limestone and siliceous river gravel aggregates. Further examination was done to study the pore solution chemistry, porosity, and microstructure of one carbonate limestone and one siliceous river gravel system. These results indicated that the siliceous river gravel system had lower ionic activity within its pore solution at all ages, and had significantly lower pH compared to the carbonate limestone system. Additionally, the siliceous river gravel system formed poor interfacial transition zones and had higher overall porosity compared to the carbonate limestone system. Theories explaining the differences between these two systems are presented.

Finally, an examination of volume stability of CAC systems compared to calcium sulfoaluminate cement (CSA) and OPC systems is presented. Systems based on CAC experienced the highest levels of chemical, autogenous, and drying shrinkage. It was found that the rapid setting nature of CAC and CSA systems caused the pore structures to develop quickly resulting in an increase in the rate of early age shrinkage compared to the OPC system. Additionally, the impact of length of curing on drying shrinkage was examined for CSA and CAC systems. Results showed that length of curing did not impact overall drying shrinkage in either system.

Factors Influencing Conversion and Volume Stability in Calcium Aluminate Cement Systems

by
Matthew P. Adams

A DISSERTATION

submitted to

Oregon State University

in partial fulfillment of
the requirements for the
degree of

Doctor of Philosophy

Presented May 28, 2015
Commencement June 2015

Doctor of Philosophy dissertation of Matthew P. Adams presented on May 28, 2015

APPROVED

Major Professor, representing Civil Engineering

Head of the School of Civil and Construction Engineering

Dean of the Graduate School

I understand that my dissertation will become part of the permanent collection of Oregon State University libraries. My signature below authorizes release of my dissertation to any reader upon request.

Matthew P. Adams, Author

ACKNOWLEDGEMENTS

The last five years that I have spent at Oregon State University have been wonderful and amazing in ways I could never describe. I owe all of this to my strong support group of friends and colleagues. Doctoral dissertations come with a single author listed, which is quite misleading. The work presented is the result of the combined efforts and support of many people. It is the support of these people that make the strings of failed experiments, days of low inspiration, and long nights in the office trying to finish up the report that was due two weeks ago possible, and enjoyable. I would like to take the next pages to acknowledge these people. The list is long, and despite my best efforts, I apologize if I unintentionally leave anyone out.

First I would like to thank my family: Mom, Dad, Mo, Mike, and Melissa. Your unwavering support as I moved all the way across the country to be an academic has been remarkable. You have been unbelievably encouraging and I couldn't appreciate it more, thank you. To Madeline, may you be afforded the same support and opportunities to pursue what makes your heart beat fast throughout your whole life.

Thank you to Dr. David Gress, at University of New Hampshire. Over 10 years ago you introduced me to the wonders of concrete, and I've been amazed by the material ever since. Your infectious love of research and learning got to me, and it is the reason I am still studying the material all these years later. To Dr. Cynthia Maris and Jane Raymond of Manchester High School Central, who showed me that chemistry and science could be fun, and not a chore. You are two of the best teachers I've ever had, and each student that comes into your classrooms is lucky to have you as a teacher. I can only hope I will be as good of a teacher for my future students, and inspire them in the ways that the three of you have inspired me.

I would also like to thank my very strong support group of friends, who help me relax, laugh, and make sure I think about things other than concrete. Todd Page, you are the best friend I have ever had. You make me smile and laugh more than anyone ever has. You bring out my silly, and I can't tell you how much I need and appreciate that. Brien Saputo, you keep me thinking, and you help me appreciate the humor in the ridiculousness that is the world. 10 years on, both of us moving to the middle of nowhere, and we're still chatting almost every day. Christopher Petrilli, you've been a

mentor, a friend, and you've always made me feel good about my know-it-all tendencies. Kathryn Magura, you were one of my first friends in Corvallis, and are one of my best. Thank you for all the advice, countless dinners together, and true support. Clare Cady, I am so excited that we are both moving on to the next stages of our careers together, and also I am excited for brunch. Tyler Deboodt thank you for all the puns and afternoon candy stops at Circle K, all the conversations about concrete, answering my questions about hiking and climbing, and great conversations on travel. To everyone else that I won't write sentences for but you know how awesome you are: Andrea Brush, Karla Kruse, Brian Malone, Gordon Stratton, Justin Saputo, Kate Jones, Julie and Brian Whitmore, Charles Sacre, and Guillaume Bouche, you have all supported me in so many ways, I'm grateful for each of you.

Thanks as well to all of my colleagues: Monica Morales, David Rodriguez, and Skylar Warner, Ben Sohn, Kelsey Schumacher, Jose Banuelos. All of the extremely helpful UGAs that have helped on this project over the years: Nick Briesach, Silas Shields, Adal Guerra Cabrera. Aaron Strand who is a whiz with the pore press and polishers and Travis Moore who is one of the hardest workers I've ever met. Chang Li, thank you for all the endless hours of help figuring out how to do certain tests and helping me with chemistry. Tengfei Fu, thank you for being my roommate all over the world, and being my go to guy to bounce ideas off of. You're a brilliant engineer and I'm looking forward to a career of working together.

Thank you to my committee members Dr. Belinda Batten and Dr. David Trejo for agreeing to serve. Thank you to Bukan Isgor, you've been a great mentor and friend over the past few years, I'm glad you joined the OSU faculty. I'm looking forward to continuing to work with you in the future. Thank you also to Andy Ungerer for letting us use the ICP-OES all the time; and to Theresa Sawyer and Peter Eschbach for all the great training and availability for use of the SEM in the OSU Microscopy Facility. Your support and friendliness has not gone unnoticed.

Thank you to everyone in the front office at CCE, and throughout the University who have helped on the administrative end of this process. Cindy Olsen, you're always a bright spot when I stop in, friendly and helpful. Dana Ainsworth, the pile of paperwork on your desk seems never-ending but you always made sure we got what we needed, as if you were there just for our group despite the large amount of people you help on a daily basis. Kathy Westberg, thank you for all the hard work

making sure all the endless paperwork gets through so I could get paid, graduate, heave health insurance etc. You really make this department tick. Thank you to Angela Franklin and Fran Severiano who made the fellowship possible and helped every term to make sure things went smoothly. Finally thank you to Paul Montagne and Jordan Jones for all the IT support through the years.

Thank you to everyone involved with the Kerneos Scientific Network, each of you has taught me so much about this crazy, wonderful, weird specialty cement. Dr. Michael Thomas, thank you for serving on my committee, being a great mentor, teacher and friend over the past few years. Dr. Kevin Folliard, you taught me never to take anything too seriously, thank you for your friendship, and thank you for teaching Jason to be such a great mentor. Ted Moffatt, Dr. Anthony Bentivegna, Dr. Julien Bizzozero, Dr. Thano Drimalas and Rachael Lute: We've had some amazing experiences as a part of this research group, learning from each other and exploring the world together. It has been so much fun, and I don't think I would have enjoyed this experience nearly as much without you. I'm looking forward to all of the research and conferences we'll be going to together in the future.

Dr. Karen Scrivener, thank you so much for allowing me to come learn from you at EPFL in Lausanne. The two months there taught me skills that I will use for the rest of my career and gave me a personal experience I will never forget. Thank you to everyone at EPFL (and associates) that helped me learn new things: Elise Berodier, Berta Mota Gasso, Pawel Durdzinski, John Rossen, Arnaud Muller, Cyrille Dunant, Ruben, Snellings, Hadi Kazemi-Kayab, and Cristophe Gosselin.

To everyone at Kerneos Aluminate Technologies: Fancois Saucier, Pascal Taquet, Herve Fryda, and Charles Alt. Your support of this Ph.D. means the world to me and I will forever be in your debt. Your trust in our group to produce good quality research was not misplaced, and I hope this dissertation makes you proud.

And finally, thank you to my advisor Dr. Jason H. Ideker. I can't put into words how much your support has meant to me. You are my mentor, and my friend. I know that we will continue to work together for the rest of our careers, but I can't help but be a bit sad leaving OSU and not being able to come see you when I'm feeling a bit overwhelmed. You took a chance on some guy you met out of the blue, and I can't thank you enough for doing so. You've given me opportunities I've never

dreamed of, and made me believe I can do things I never would have thought possible. I can only hope to be half as good of a researcher and writer that you are, and I will strive to make you proud every day.

CONTRIBUTION OF AUTHORS

Dr. Jason H. Ideker advised on data collection, analysis, and interpretation of results, as well as edits for the entire document. Dr. Michael Thomas, Dr. Charles Alt, Dr. Kevin Folliard, Edward Moffatt, Rachael Lute, and Thano Drimalas assisted in data collection for the inter laboratory study presented in Chapter 2, and the multiple aggregate study presented in Chapter 4. Aaron Strand, Silas Shields, Nick Briesach, and Travis Moore assisted in data collection for Chapters 2, 3, 4, and 5. Dr. O. Burkan Isgor, Dr. Tengfei Fu, Monica Morales, and Adal Guerra Cabrera assisted in data collection, analysis, interpretation, and writing of Appendix A.

TABLE OF CONTENTS

TABLE OF CONTENTS (Continued)

Page

TABLE OF CONTENTS (Continued)

TABLE OF CONTENTS (Continued)

TABLE OF CONTENTS (Continued)

TABLE OF CONTENTS (Continued)

TABLE OF CONTENTS (Continued)

LIST OF FIGURES

LIST OF FIGURES (Continued)

LIST OF FIGURES (Continued)

LIST OF TABLES

LIST OF APPENDICES

LIST OF APPENDICES (Continued)

LIST OF APPENDIX FIGURES

LIST OF APPENDIX FIGURES (Continued)

LIST OF APPENDIX TABLES

DEDICATION

To my grandmother, Mary Adams, thank you for always encouraging me to be exactly whoever I wanted. You are missed.

1 Introduction and Background

1.1 Scope and Layout of This Dissertation

This dissertation follows the manuscript option for the Doctor of Philosophy Thesis in the Oregon State University Graduate School Thesis Guide 2014-2015. This dissertation contains an examination of calcium aluminate cement (CAC) concrete properties. CAC is an alternative cement material that gains strength rapidly even in cold temperatures (nearing 0°C), making it an ideal material for use in rapid concrete repairs. The work presented in this dissertation was undertaken to develop a better understanding of the properties of CAC concrete, particularly the role of aggregate source in strength development, hydration, and system chemistry. Additionally, work was completed tofurther develop a test method that that can be used to measure the converted strength of CAC concrete. The research is presented through a literature review, experimental methods, a series of four individual manuscripts, and a unifying conclusion. The dissertation is outlined as follows:

Chapter 1: *Background and Introduction* – This chapter provides an introduction to the work presented in this dissertation as well as the motivation for completing that work. Also presented in a review of literature examining current understanding of CAC history and production, CAC uses, CAC hydration, CAC concrete properties, and test methods for determining conversion in CAC concrete systems. Special consideration is paid to the impact of carbonate bearing materials (limestone filler and aggregates) on CAC hydration and conversion.

Chapter 2: *Experimental Methods* – This chapter provides an overview of the experimental methods used for the work presented in this dissertation. Images of the equipment used to complete the testing presented in this dissertation are also included.

Chapter 3: *Manuscript 1* – The first manuscript presented in this dissertation is entitled "Procedure for Determining the Converted Strength of Calcium Aluminate Cement Concrete." This chapter examines the robustness and variability of a test method used to rapidly determine the converted strength of calcium aluminate cement concrete. Mixture design and curing parameters were examined to determine their impact on time to conversion and converted strength in CAC concrete. These variables included aggregate source, w/cm, temperature of curing environment during initial 24 hours, and length of time spent in the initial curing environment. Inter-laboratory variability was investigated through a four laboratory round robin study. Also presented is an examination of the impact of finely

ground limestone on strength when used as a replacement for CAC in concrete mixtures. Dosage rates of 1%, 2%, 5%, and 10% were investigated.

Chapter 4: *Manuscript 2* – The second manuscript presented in this dissertation is entitled "Pore Solution Chemistry of Calcium Aluminate Cement Concrete Undergoing Accelerated Conversion." This paper examines the pore solution chemistry in calcium aluminate cement paste, and concrete containing a siliceous and a limestone aggregate. Pore solution chemistry was examined over a period of 28 days. Conversion was accelerated in the CAC systems and occurred between days 1 and 3. A study examining possible leaching of ions into the curing water in which the samples were stored was also done. This paper has been submitted, and is under review as of the time of publication of this dissertation, for acceptance in the Proceedings of the 14th International Congress on Cement Chemistry to be held in Beijing, China in October of 2015.

Chapter 5: *Manuscript 3* – The third manuscript presented in this dissertation is entitled "Influence of Aggregate Type on Conversion and Strength in Calcium Aluminate Cement Concrete." This paper examined the impact of aggregate source on strength, conversion, and hydration in CAC concrete systems. Nine different concrete systems were examined using nine coarse aggregate and six fine aggregate sources. Impact of aggregate properties (grading, absorption capacity, G_s, fineness modulus, and D50 number) on strength development was examined for four of the systems. Microstructural examinations and porosity quantification was done through the use of SEM image analysis and mercury intrusion porosimetry for two systems. Elemental analysis of pore solution and energy dispersive X-ray mapping of hardened concrete were also examined for two systems. Theories explaining the reason for differences in converted strength of CAC concrete caused by aggregate source are presented.

Chapter 6: *Manuscript 4* – The fourth manuscript presented in this dissertation is entitled "Volume Stability of Calcium Aluminate Cement and Calcium Sulfoaluminate Cement Systems" and was published in an alternate form in the Proceedings of the 2014 International Conference on Calcium Aluminate Cements [1]. This paper examined the chemical shrinkage, autogenous shrinkage, and drying shrinkage of calcium aluminate cement, calcium sulfoaluminate cement (CSA) and ordinary portland cement (OPC) systems at room temperatures. The study compares the speed of hydration and its impact on volume stability between each system, noting how rapid hydration in alternative

cement systems may affect long-term properties. Also examined was the impact of length of curing on drying shrinkage in CAC and CSA systems.

Chapter 7: *General Conclusions* – This chapter summarizes the goals and findings of this research and provides conclusions tying the research from all manuscripts together. Future work based on this research is also suggested.

Chapter 8: *References* – This chapter includes a comprehensive list of references used in the dissertation, including those cited as a part of the appendices.

Appendix A: *Additional Manuscript A* – The additional manuscript included in Appendix A is entitled "Cracking Susceptibility of Concrete Made with Recycled Concrete Aggregates." This paper was produced from a research project initiated by the author during his time as a Ph.D. student. This work examines the cracking resistance of concrete made with recycled concrete aggregates from two different sources. This study examined cracking resistance through use of the restrained shrinkage ring test. These results were compared with free shrinkage data and mechanical properties of the systems to examine understand if RCA poses a greater risk of cracking compared to natural aggregate systems. This manuscript does not examine CAC concrete; however it does examine the greater themes of the impact of aggregate type on concrete properties and volume stability of concrete and is included in this dissertation for that reason.

Appendix B: *Additional Data and Images* – This section includes additional data and images not used in the manuscripts presented here, but collected as a part of the work presented in this dissertation. References will be made to this section throughout the dissertation, but will be removed prior submitting any individual manuscript for publication.

1.2 Notation

Cement chemistry notation is used throughout this dissertation where applicable. Standard chemical notation will be used where cement chemistry notation is not applicable. The following is a list of the cement chemistry notation and other abbreviations used throughout the dissertation

1.2.1 Cement Chemistry Notation for Oxide Compounds

A: Al_2O_3 C: CaO S: SiO_2 F: Fe_2O_3 $: SO_3 H: H_2O

1.2.2 Materials and Mixtures

CAC	Calcium Aluminate Cement
CSC	Calcium Silicate Cements
OPC	Ordinary Portland Cement (a type of CSC)
FLGS	Finely Ground Limestone
G_s	Specific Gravity
w/cm	Water to cementitious materials ratio

1.2.3 Techniques

XRD	X-Ray Diffraction
TGA	Thermogravimetry Analysis
SEM	Scanning Electron Microscopy
EDX	Energy Dispersive X-Ray
MIP	Mercury Intrusion Porosimetry

1.3 Introduction

America's bridges are deteriorating at an alarming rate and need over $76 Billion in repairs to repair, rehabilitate, or retrofit structurally deficient bridges such that they meet current design standards [2]. Cement-based rapid repair materials are an integral tool that will be needed for repairing and extending the life of our deteriorating infrastructure without disturbing the economic activities (e.g. transportation of goods and people) that utilize that infrastructure. Calcium aluminate cement (CAC) is a specialty cement that can be used in a wide range of specialty applications such as rapid repair but also including refractory applications, building chemistry applications and sewer pipe linings. Concrete materials that are made with CAC gain strength rapidly, even in low (e.g. nearing 0°C) temperature

environments. This has led to an increase in interest in using the material in concrete for rapid repair applications, particularly in the transportation industry. Despite the higher cost of the cement, CAC concrete can provide a solution for particular repair situations where ordinary portland cement nor other construction materials cannot address. However, beyond cost concerns, the use of the material for technical concrete applications in the United States has been limited for three main reasons:

1. There is a general lack-of-knowledge, by construction professionals, concerning conversion, a process in which meta-stable calcium aluminate cement hydrates convert to stable hydrates which results in increased porosity and strength loss; and
2. There is no standardized accelerated test method for minimum converted concrete strength; and
3. There is insufficient data on the long-term performance of concrete made with CAC, particularly as a repair material in transportation infrastructure.

This dissertation presents work that addressed these items. This work examined the influence of various factors on conversion including aggregate mineralogy, finely ground limestone additions, initial curing temperature, and w/cm on conversion in CAC concrete (addresses challenge 1&3). Additionally, this work presents robustness and variability testing for a proposed accelerated test method to determine the converted strength of CAC concrete that is simple to use in the field (addresses challenge 2). This will allow designers to determine the minimum converted strength of CAC concrete within an accelerated time period and specify CACs for use in construction. Finally, an examination of volume stability in calcium aluminate cement concrete systems as compared to OPC and calcium sulfoaluminate cement (CSA) concrete systems is presented (addresses challenge 1 and 2).

1.4 Background

1.4.1 History of Calcium Aluminate Cements

The development of high alumina cement began with a theory proposed by Louis Vicat that a cement with a ratio of $(SiO_2 + Al_2O_3)/(CaO + MgO) > 1$ would be indestructible. There were difficulties in developing this cement, however, as high SiO_2 amounts in the clinker caused very low reactivity in the cement, and high Al_2O_3 contents caused flash setting. In the early 1900s Jules Bied (among others) decided to examine this concept further [3]. Bied was able to develop a cement through fusion, rather than clinkering that had a high alumina content but did not undergo flash setting. The

commercialization of this process took some time and was eventually perfected by Bied, while working at J and A Pavin de Lafarge, by 1913 [3-5]. This is largely the cement we know today as calcium aluminate cement [3, 6]. The fusion process that Bied developed is still mostly unchanged [3] and is still used for low alumina (40-50% Al_2O_3 content) CACs. CACs with higher alumina contents (70-80% Al_2O_3), use clinkering (similar to the process for ordinary portland cement) as the preferred method of manufacture [3].

CAC was originally developed as a sulfate resistant and chemical corrosion resistant cement [3, 5], however it was initially used primarily due to its rapid strength gain properties [5]. During WWI a significant amount of the material was used by the French government for gun emplacements [5, 7], and in the late 1910s and 1920s began to be used in tunnel lining systems [5]. One tunnel, built in France in 1871, was reinforced with CAC in 1922. This tunnel was still in good condition in 2013, having undergone only minimal maintenance in the intervening years [8].

By 1940, the building codes in the United Kingdom were modified to allow the use of CAC in structural concrete and in the 1950s the material was being used in precast concrete construction because of its rapid strength gain properties [5]. In the 1970s three structural collapses of prestressed concrete beams made with CAC changed the overall perception of CACs and resulted in limitations on the use of the material in structural applications [4, 5, 9]. The first two collapses, at the University of Leicester and the Camden School for Girls were mainly attributed to poor structural steel detailing. While the collapse was due to poor structural steel detailing, the strength loss in concrete due to conversion (discussed further in Section 1.4.4) contributed to a reduced safety factor, increasing the likelihood of collapse [5, 9]. A third building collapse at the John Cass School was attributed to loss of strength due to conversion and subsequent sulfate attack due to the CAC concrete beams having been in contact with gypsum plaster [5, 9]. An image of the collapsed roof beams in the swimming pool at the John Cass School can be seen in Figure 1-1 [10].

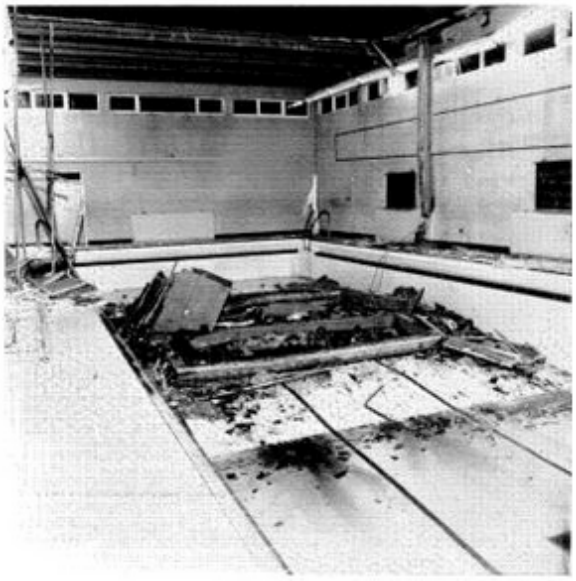

Figure 1-1: John Cass School Roof Beam Collapse [10]

The collapse at John Cass School, combined with the earlier issues suffered by CAC concrete led to significant limitations on the use of the material in structural applications [9]. This was mainly due to a poor understanding of the conversion process [5], a problem that still exists today in the general construction community. This problem has been compounded by a lack of a convenient, standardized method for determining the converted strength of CAC concrete [9, 11].

Recently, however, interest in CAC use in the construction community has increased due to its rapid hardening properties, especially at low temperatures and our need for repair solutions that provide long-term performance. The material has been particularly useful for rapid concrete repair in cold environments [9, 12-15]. Therefore, through better understanding of conversion by the construction and design community, coupled with the development of standardized quality control procedures, the use of CAC in the technical concrete market may see an increase in the coming years.

1.4.2 Specialty Uses for CAC

CACs have more traditionally been used in specialty areas beyond technical concrete applications due to cost and a range of unique properties that the material has. CAC materials cost around four to five times that of ordinary portland cements due to the expense of raw materials (bauxite mainly), and the relatively small amount of material manufactured every year [7]. CAC was originally designed as a sulfate resistant cement based off of original ideas by Louis Vicat [3]. The material has been found to

perform quite well in sulfate environments[16, 17], including when anhydrite was used as an aggregate in concrete made with CAC in a railway tunnel in France [4].

One of the main uses for CAC is in the refractory industry as kiln liners due to its adequate refractoriness. Refractoriness is the ability for a concrete to maintain adequate mechanical strengths after repeated cycles of cooling and heating, and without deteriorating when exposed to moist air or water [4, 18]. Upon initial firing of refractory concretes, the system will lose strength due to conversion and loss of water from the system. After initial firing, the minimum strength remains quite stable in CAC refractory concretes, unlike in calcium silicate cement (CSC) systems. In CSC systems, upon heating above 450°C, CaO will form within the system as the CH is dehydrated. Upon contact with moisture, the re-hydration of CaO will cause significant increases in volume. Therefore, the long-term strength of fired CSC systems will not be stable for use in refractory concretes. CaO does not form upon firing in CAC systems, making it an ideal candidate for refractory applications [18]. A significant amount of work has been published on the use of CACs in refractory applications [4, 18-29]. The improved performance of CAC materials as a refractory cement over calcium CSC has been related to the low amount of hydrated lime products in the system, which easily break down at higher temperatures. Therefore, higher aluminum to calcium ratios result in better refractoriness for cements, subsequently higher grade CACs (high Al_2O_3, low CaO) are preferred for refractory applications [4, 19].

CAC's are also more resistant to chemical corrosion and acid attack compared to CSC materials. In CSC materials the calcium hydroxide (CH) dissolves rapidly in the presence of acids, which opens up porosity in the system allowing further ingress of corrosive chemicals. Hydrated CAC paste does not contain CH; additionally, the alumina hydrate, AH_3, that is present in hydrated CAC's is stable to pHs as low as 3, providing more resistance against acid attack compared to CSCs. Additionally, dissolution of other calcium aluminate hydrates due to acid attack results in the formation of additional AH_3, further slowing the progression of the chemical corrosion [4, 7, 30]. The material's resistance to chemical corrosion and acid attack make it ideal for use in industrial floors [7]. Additionally, it has been used and studied extensively as a material for rehabilitation of concrete pipelines affected by biogenic corrosion, and as a pipe-lining in new pipes to increase long-term performance of concrete pipes [31-39].

CAC concrete, particularly when made with aggregates created from crushed hardened CAC cement paste, also has high abrasion resistance. This property has resulted in the materials use in industrial floors where heavy equipment is regularly in use, as a wearing surface on roadways, and in spillways on dams [4, 7].

Besides these applications, CACs have also become an integral part of the building chemistry industry. Building chemistry refers to a wide range of non-structural products used in construction including floor levelers, grouts, and expansive mortars [4, 40, 41]. These systems generally are made from blends of multiple cement types and admixtures to produce very specific setting time, workability, color, and drying properties [4].

1.4.3 Calcium Aluminate Cement Composition

CACs are available in a variety of compositions that are graded based on the alumina content in each cement. Al_2O_3 contents can range from 40% to over 80%. Table 1-1, adapted from reference [4], shows different grades of calcium aluminate cements and a typical oxide breakdown for each grade; also shown are a typical cement oxide breakdown for a type I/II portland cement (typical CSC) and a calcium sulfoaluminate (CSA) cement, for comparison.

Table 1-1: Cement Oxide Compositions [4]

Type	Color	Composition Range [%]							
		Aluminum Oxide	Calcium Oxide	Silicon Dioxide	Iron Oxides	Titanium Oxide	Magnesium Oxide	Sodium Oxide	Potassium Oxide
		Al_2O_3	CaO	SiO_2	Fe_2O_3 + FeO	TiO_2	MgO	Na_2O	K_2O
Standard low alumina CAC	Gray or buff to black	36-42	36-42	3 - 8	<2	<2	~1	~0.1	~0.15
Low alumina, low iron CAC	Light buff or gray to white	48-60	36-42	3 - 8	<2	<2	~0.1	~0.1	~0.05
Medium alumina CAC	White	65-75	25-35	<0.5	<0.5	<0.05	~0.1	<0.3	~0.05
High alumina CAC	White	≥80	<20	<0.2	<0.2	<0.05	<0.1	<0.2	<0.05
Type I/II Portland Cement	Gray	5	63	20	3.5	0.2	0.9	0.3	0.3
Calcium Sulfoaluminate Cement	White	14	52	12	1	0.9	2	0.01	0.9

Table 1-1 shows that CACs have relatively high levels of aluminum oxide compared to other cements, with low levels of silicon dioxide and calcium oxide. For the purposes of this dissertation, further references to CAC will indicate standard low grade CAC, which is the focus of this dissertation. Discussions referring to other grades of CAC will be noted as such.

1.4.3.1 *Unhydrated Cement Phases*

CACs have several different crystalline phases present in the unhydrated cement. The main phase present is monocalcium aluminate ($CaAl_2O_4$ or CA) and generally comprises 40% or more of the overall composition of the cement, depending on grade of CAC [4]. This phase often has inclusions of iron in the solid solution, and sometime silicon [4, 42]. CA has a density of 2945 kg/m^3. The composition of this phase was described as $Ca_xAl_yFe_zSi_tO_{x+3/2(y+z)+2t}$ where x can range from 4.4-4.8, y=4.7-5.0, z<=2.13 and t<=0.1 [42]. This phase has high reactivity compared to other phases present in CAC. Hydration of CA is described in Section 1.4.4.

Calcium dialuminate (CA_2, $CaAl_4O_7$, or grossite) is also present in CAC systems as $CaAl_2O_7$. Iron inclusions have also been observed in this phase. The amount and importance of this phase in CAC systems increases with aluminum oxide contents [42]. This phase has low reactivity at room temperatures, but becomes more reactive at higher temperatures [43]. Dodecacalcium heptaluminate (Mayenite, $Ca_{12}Al_{14}O_{33}$, or $C_{12}A_7$) can also form in CAC systems, and recently has come to attention as being a system which has a high level of reactivity [44]. Increasing amountsof $C_{12}A_7$ have been shown to decrease the length of the induction period and increase reactivity in CAC systems, and therefore this phase plays an important role in overall set time for CAC concrete [45, 46].

Other minor calcium aluminate phases include dicalcium aluminate (C_2A), and hibonite (CA_6) which are both present mainly in high alumina CACs [42]. Further discussion of these phases can be found in the following references [4, 42, 47]. They will not be addressed as a part of this dissertation however, as the focus of this dissertation focuses on the use of standard or low alumina CAC systems.

Dicalcium silicate (C_2S, Ca_2SiO_4, or belite) can also form in CAC systems but only in its beta phase, β-C_2S, particularly in CACs with higher silica contents [42]. C_2AS ($Ca_2Al[AlSiO_7]$ or gehlenite) can also form in standard and low grade CACs. Gehlenite is more likely to form during rapid cooling of CAC clinker [42], which is typical of standard grade CACs manufacturing [4]. Gehlenite can also have iron inclusions in its system [42].

Calcium aluminum ferrites also exist in CAC systems, and their presence increases as the iron content increases (lower grade CACs) [4, 42]. While the composition of this phase varies with impurities, the basic formula for these systems can be C_2F, C_6A_2F, and C_4AF_2. Impurities such as MgO, TiO_2, SiO, and MnO often substitute into this phase [4].

1.4.4 Hydration of Calcium Aluminate Cements

Hydration of CAC systems has been studied extensively since the material was originally produced, as is evidenced by the number of book chapters written on this topic [4, 42, 47, 48] and the four international conferences dedicated solely to calcium aluminate cements [49-52]. The hydration of calcium aluminate cements are very different compared to calcium silicate cements. The reaction that occurs in these systems is strongly influenced by the temperature history of the sample. The following section examines the hydration of monocalcium aluminate (CA) specifically. The hydration process examined herein applies only to pure CAC systems; additions of other cementitious materials will result in different hydrates formed than those discussed below.

1.4.4.1 *Hydration and Conversion of Monocalcium Aluminate*

CA will hydrate to form four main phases: CAH_{10}, C_2AH_8, C_3AH_6, and AH_3. These hydrates fall into two main categories, metastable (CAH_{10}, C_2AH_8) and stable hydrates (C_3AH_6, and AH_3) [4, 42, 45]. Which hydrate is initially formed depends upon the temperature history of the system. When cured isothermally at temperatures below 15°C, CAH_{10} is primarily formed during initial hydration. When cured isothermally at temperatures between 15°C and 27°C, both CAH_{10} and C_2AH_8 are formed during initial hydration [4, 42], however as the temperature approaches 27°C, formation of neither hydrate is favored, which causes an increase in setting time compared to other temperatures with CACs at 27°C [53-57]. Setting time will be discussed further in Section 1.4.8. When cured isothermally at temperatures above 27°C, C_2AH_8 is the primary hydrate formed during initial hydration. The equations that describe these reactions can be seen in Equation 1-1 and Equation 1-2 [4, 42].

Equation 1-1
$$CA + 10H \rightarrow CAH_{10}$$

Equation 1-2
$$2CA + 11H \rightarrow C_2AH_8 + AH_3$$

Equation 1-2 shows that AH_3, a stable gel hydrate, will also form during the hydration reaction of CA which forms C_2AH_8. As stated above, CAH_{10} and C_2AH_8 are both metastable hydrates and will undergo transitions to form the stable hydrates AH_3 and C_3AH_6. The speed at which this reaction

occurs is dependent on the temperature and moisture state of the system [4, 42, 45] as well as w/cm [4]. However, it is important to note that this reaction is thermodynamically inevitable and will occur at all temperatures [42, 45]. This process is known as conversion. Equations 1-3 and 1-4 describe the chemical reaction that occurs when CAH_{10} and C_2AH_8 undergo conversion [4, 42, 45].

Equation 1-3 $$2CAH_{10} \rightarrow C_2AH_8 + AH_3 + 9H$$

Equation 1-4 $$3C_2AH_8 \rightarrow 2C_3AH_6 + AH_3 + 9H$$

These reactions show that the conversion of the metastable hydrates to C_3AH_6 is accompanied by further formation of AH_3 gel and the release of water. The formation of C_3AH_6 is always preceded by the formation of the metastable hydrates, even at high temperatures [45, 58, 59]. However the process of conversion at high temperatures can occur quickly. Gosselin [45] showed that when CAC paste was cured at 70°C, C_2AH_8 formation peaked at 30 minutes, but converted to C_3AH_6 and AH_3 within the first three hours. Rashid et al. [60] observed C_2AH_8 as an intermediate phase before the presence of C_3AH_6 was observed at 90°C. It has also been suggested that direct conversion of CAH_{10} to C_3AH_6 can occur through a solid state reaction [60], however Scrivener [61] notes that this is not possible and that the similarities between crystalline structures of C_2AH_8 and C_3AH_6 indicates that C_2AH_8 is always an intermediate phase in the conversion of CAH_{10} to C_3AH_6. Nucleation of C_3AH_6 has been shown to be quite difficult, and therefore it is kinetically advantageous for the metastable hydrates to form first, and then convert to the stable C_3AH_6 [62]. Further work has shown, however, that once C_3AH_6 has nucleated, direct formation of C_3AH_6 from CA can occur according to Equation 1-5 [4, 61-63], and that C_3AH_6 may grow through incorporation of dissolved CAH_{10} ions [61]. This was shown to occur even when CAC was cured at an elevated temperature of 70°C. At this temperature, C_2AH_8 precipitated instantaneously and was followed by a rapid conversion to C_3AH_6 within three hours [64].

Equation 1-5 $$3CA + 11H \rightarrow C_3AH_6 + 2AH_3$$

The density of the main hydrate structures in CAC paste have been reported in literature and are summarized in Table 1-2 along with their molar masses [4, 11, 62].

Table 1-2: Molar mass and densities of calcium aluminate hydrates [4, 11, 62]

	CA	CAH_{10}	C_2AH_8	C_3AH_6	AH_3
Molar Mass (g)	158	338	358	378	78
Density (g/cm^3)	2.98	1.72	1.95	2.52	2.4

During hydration of CA, the formation of CAH_{10} and C_2AH_8 metastable hydrates binds a relatively large amount of water into their chemical structures. The rapid precipitation of these hydrates, along with the low density of the hydrates results in rapid space filling within the hydrating system [65]. The impact of this on strength is discussed below in Section 1.4.10. The conversion of metastable hydrates to stable hydrates is accompanied by the release of water [4, 45, 62], which can be seen in Equation 1-3 and Equation 1-4. Additionally, as seen in Table 1-2 conversion also results in a densification of the hydrates in CAC systems. This densification results in the opening of porosity in the system (impact on strength also discussed in Section 1.4.10). The opening of porosity and release of water into the system allows for further hydration of CA after conversion, which will result in long-term continuous strength gain after conversion occurs [4, 11, 61, 62].

1.4.4.2 *Mechanism of Hydration in CAC*

The mechanism of hydration of CA is widely accepted to be that of 'through solution' [4, 65, 66], which is the dissolution of anhydrous phases followed by precipitation in solution. Once CA contacts water, a surface layer composed of $Ca[Al(OH)_4]_2$ will form [47]. This surface layer will subsequently dissolve, and then reform as fresh anhydrous material is exposed [45]. Before nucleation of hydrates occurs, an induction period can be observed in which the Ca^{2+} and $Al(OH)_2^-$ exist in relatively high concentrations in the solution [61]. Once the solution reaches a critical level of supersaturation, hydrates will precipitate out of solution [4, 45, 47] and form the calcium aluminate hydrates described above. During the initial reaction, both aluminum and calcium go into solution throughout the matrix, such that when precipitation of hydrates does occur, they form everywhere, as opposed to just on the surface of the CA grains [61]. As a result of this, precipitation will occur rapidly after initial nucleation, which will result in rapid space filling and subsequent rapid strength gain [45, 47, 61]. Similar to OPC, the degree of hydration of CA can be increased by increasing the fineness of the anhydrous grains [67].

Scrivener and Taylor (1990) noted the formation of an inner product layer that forms in the space that was previously occupied by anhydrous CA. The outer product that forms during the hydration of CA is the material that exists in the space between previously unhydrated cement grains [68]. The formation of the inner layer of hydration product on CAC was supported by Gessner et al. [69] and it was speculated that this may be the cause of the induction period seen for CACs. However Scrivener [61] refuted this and noted that during the period of dissolution, no hydrate layer is formed around the anhydrous grains, allowing for continuous dissolution of CA, until mass precipitation occurs once the pore solution reaches supersaturation and the hydrates can nucleate. Lamour et al. [65] supported this idea with the use soft X-ray transmission microscopy, through which they were able to observe the mass precipitation of crystalline phases at the end of the induction period. They also noted that there were amorphous hydrates that form throughout the solution during the induction period, but that they did not prevent further dissolution of the anhydrous grains [65]. Therefore, the inner product mentioned above, and the outer product will form simultaneously. This system of "through solution" hydration has been used to explain the reason why CAC hydrates fill space quickly, leading to the rapid strength gain that is not seen in CSCs [45, 65]. In CSCs, rapid growth of hydration products is prevented by the formation of calcium silicate hydrate around the anhydrous cement grains that leads to a decrease in reaction rate shortly after the end of the induction period [70-72].

Conversion of metastable hydrates to stable hydrates also occurs through solution and is initiated by the first nucleation of C_3AH_6 [62]. The solubility of C_3AH_6 is lower than that of the metastable hydrates CAH_{10} and C_2AH_8, and its precipitation from solution is driven by the dissolution of the metastable hydrates [45]. Both metastable hydrates become more soluble as temperature increases [11, 45, 62, 73], which favors the formation of C_3AH_6 and AH_3, both of which have decreasing solubility as temperature increases.

The timescale for conversion varies and is dependent on the temperature history to which the concrete is subjected. While there are several ways to determine the time to full conversion, it is typically measured by periodically testing the compressive strength of the materials until a minimum strength is reached. The time from casting the concrete at which that minimum strength is observed, is considered to be the "time to conversion." Fryda et al.(2001) showed that CAC concrete placed into a heated water bath set to 100°C directly after being cast reached converted strength within 15 minutes. However, when the CAC concrete was placed into a water bath set to 30°C, the concrete reached converted strength at 20 days [62]. These results elucidate the influence that temperature can have on

the time to conversion. Therefore, it is important to monitor the temperature history of CAC specimens. Additionally, any specification written for use with CAC concrete must include specific temperature monitoring procedures as well as ways to adjust the standard's provisions depending on temperature.

1.4.4.3 *Hydration of Minor CAC Phases*

$C_{12}A_7$ hydrates analogously to CA, forming similar hydrates [4, 47]. However, hydration of $C_{12}A_7$ generally results in the formation of C_2AH_8 even at low temperatures, due to the high C/A in the phase [4, 48]. $C_{12}A_7$ along with CA are the only phases present in standard grade CACs that react significantly at early ages [4]. While $C_{12}A_7$ is a relatively minor component in most CAC systems, the amount has been show to have an effect on setting time, with higher amounts reducing the overall induction period of the cements [45, 46].

CA_2 has been found to react slowly, particularly at ambient curing temperatures, however at elevated temperatures the reaction of CA_2 increases significantly. The hydration of CA_2 will form the same hydrates that CA forms (Section 1.4.4) [43]. More recent examinations of the CA_2 phase have shown that it dissolves rapidly when mixed with water on its own [74, 75], however in the presence of CA, the dissolution of CA_2 is significantly delayed [22, 74].

Hydration of C_2AS, gehlenite, will result in the formation of C_2ASH_8, also known as stratlingite [4]. Stratlingite will also form from the hydration of C_2S when there is alumina also in solution (as occurs in CAC systems) [4, 11]. The ferrite phases have a relatively low rate of reaction but will hydrate to form $C_2(A,F)H_x$. Reactivity of the ferrite solid solution phase increases with time and temperature [4].

1.4.4.4 *Heat of Hydration and Rate of Reaction*

Hydration of CAC is an exothermic chemical reaction. The rapid precipitation of hydrates will result in a significant exotherm, which can result in self-heating of CAC elements. While the hydration of CSC systems also produces an exotherm, the rapid hydration in CAC leads to much higher, and quicker heat evolution. The total heat evolved in both CAC and CSC systems is similar, however.

Gosselin et al. examined the heat flow through isothermal calorimetry in standard grade CAC system at varying w/cm at 20°C. The heat flow curves from this study can be seen in Figure 1-2 [76].

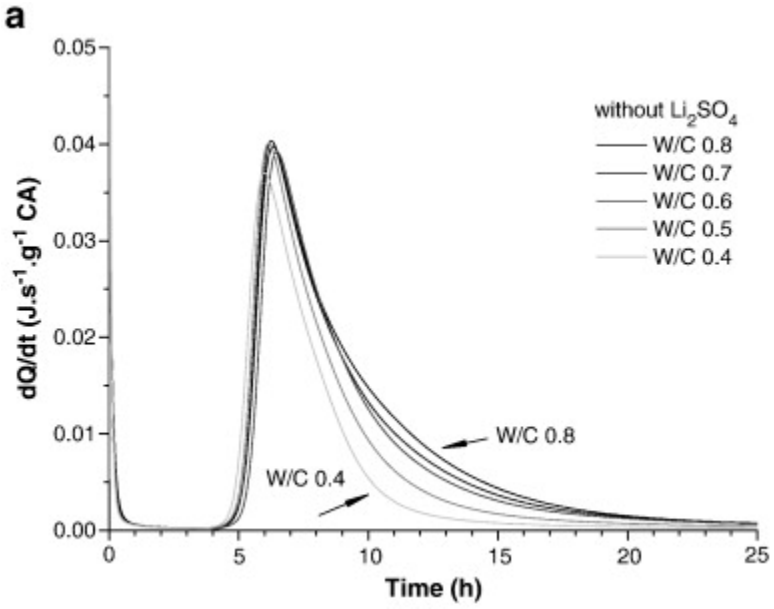

Figure 1-2: Heat flow curve of CAC Hydrated at 20°C [76]

Figure 1-2 shows that initial heat flow under isothermal calorimetry is characterized by an early peak that is associated with the dissolution of cement. This is known as the heat of wetting, and is typically not included in total heat flow calculations [77]. This period is followed by an induction period, where little exothermic activity can be observed. The length of the induction period is controlled by the presence of nucleation sites, and the influence of accelerators and retarders. Lower w/cm will reduce the length of the induction period slightly because the critical concentrations in solution that cause hydrate precipitation are reached earlier due to the overall lower water content [45, 76]. The single sharp peak observed during hydration at 20°C indicates the rapid precipitation of hydrates from solution [77]. The rapid decrease in heat flow after the sharp peak indicates a sharp decline hydration shortly after initial hydration begins. The sharp reduction in hydration activity can be attributed to three possibilities: lack of reactant (anhydrous cement), lack of water, and lack of space. It has been shown, however, that there are still significant amounts of anhydrous CAC at 24 hours, so the slowdown of hydration was not caused by a lack of reactant [76]. As discussed above, the metastable hydrates formed at 20°C bind significant amounts of water, so it is likely that in some areas, a lack of water prevents further dissolution and hydration of anhydrous cement, slowing down the reaction significantly. Additionally, the metastable hydrates rapidly fill space reducing the available space available for new hydrates to precipitate [76].

Gosselin also examined the heat flow through isothermal calorimetry in a standard grade CAC system at 0.4 w/cm at 38°C with and without a lithium sulfate accelerator. The heat flow curves from this study can be seen in Figure 1-3 [45].

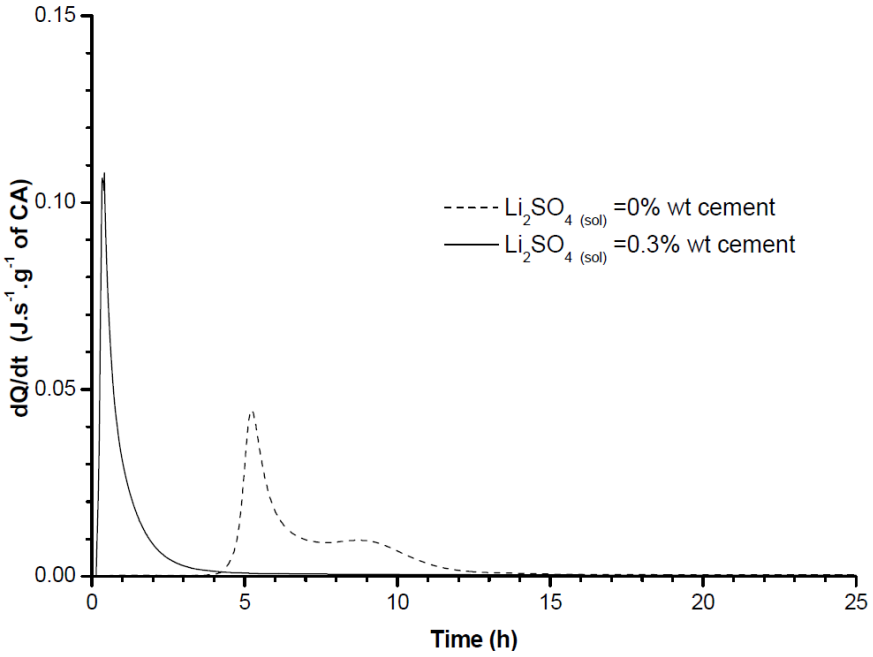

Figure 1-3: Heat flow curve of CAC Hydrated at 38^0C [45]

The heat flow of CAC at 38°C is significantly different compared to the results from 20°C. Without an accelerator, the reaction is characterized by a sharp initial peak, followed by a second peak of lower intensity. This second peak was correlated with the dissolution of the C_2AH_8 during conversion [76]. When an accelerator was included at this temperature, the reaction was characterized by one single peak, and the majority of the heat evolved happened within the first 5 hours of hydration. It was not clear why no second peak was observed in the accelerated system, but the heat released due to dissolution of C_2AH_8 may have occurred concurrently with the initial formation of new C_2AH_8 resulting in concurrent peaks from these exotherms.

1.4.4.5 *Heat Generation in Concrete Elements*

The rapid release of heat into the system, when not controlled to maintain isothermal conditions, can result in significant levels of self-heating in CAC specimens and elements. The rate at which heat dissipates from a CAC system is critical to the temperature that is reached within the system during

hydration. Larger elements or elements cast in insulated forms will reach higher temperatures during hydration than smaller or less insulated systems. As described above, the temperature of a system during hydration dictates the rate of conversion of metastable hydrates to stable hydrates. Therefore, due to the possibility of self-heating, it is important to monitor the temperature of CAC systems during hydration, to have an understanding of the level of conversion that may have occurred.

Fryda et al. examined self-heating in pure CAC systems to determine the impact of element size and form insulation on self-heating [11]. The authors monitored the temperatures of three systems, a concrete block measuring 1.2 m x 1.8 m x 7 m, a concrete slab measuring 20 cm x 5 m x 5 m, and another concrete slab 8 cm x 5 m x 5 m. The temperature profiles from the first 15 hours of curing is presented below in Figure 1-4 [11].

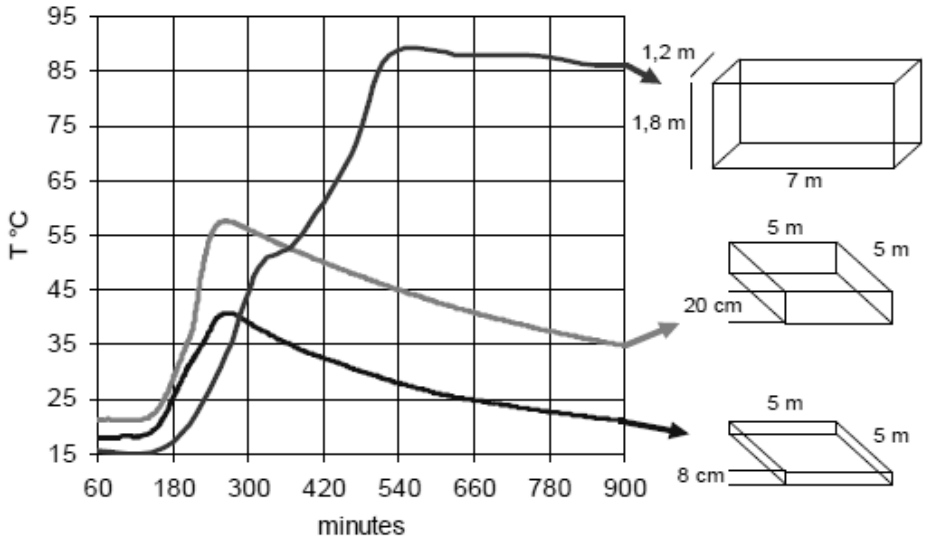

Figure 1-4: Internal temperature in different sized CAC concrete elements[11]

From this work, it can be observed that larger elements will produce higher internal temperatures due to self-heating during hydration. While the 8 cm and 20 cm thick slabs both dissipated heat rather quickly, the larger element maintained temperature, indicating that the slab may have undergone conversion during early-age. Earlier work by Fryda et al. (2001) showed that maximum temperatures during hardening above 70°C will result in rapid conversion to stable hydrates. However if the temperature reached is below 70°C, continued conversion and strength regression after hardening can still occur [62].

Fryda et al. also examined the influence of mold types on internal self-heating during curing, the results from this work are presented below in Figure 1-5 [11].

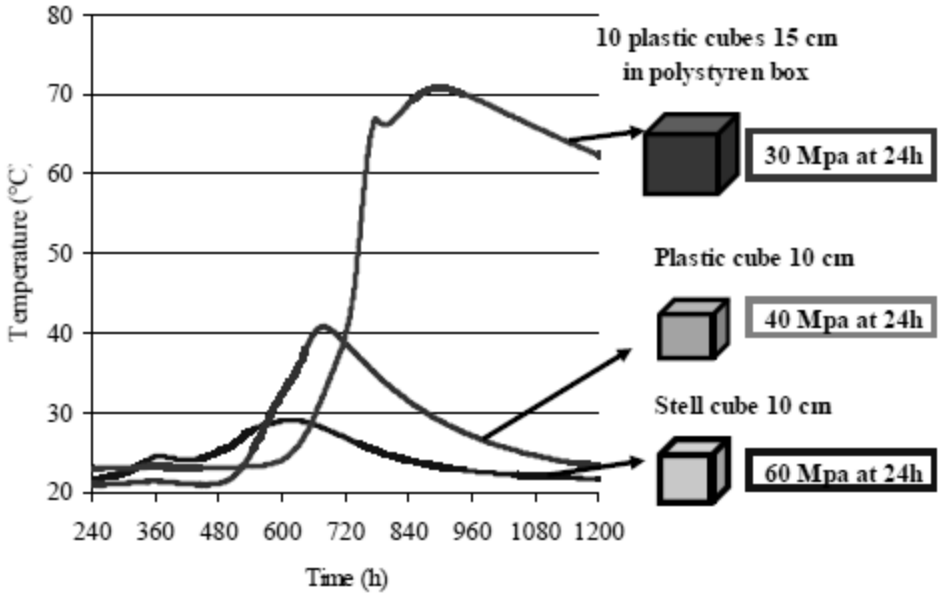

Figure 1-5: Impact of mold type on self-heating on CAC concrete [11]

This study showed that steel molds will dissipate heat better than plastic molds, however, neither mold reached high enough temperatures to cause direct conversion during hardening. However, when multiple cubes were placed together in a polystyrene box, they were able to generate enough self-heat together to increase the temperature above the critical 70°C mark to cause rapid conversion [11]. These results are particularly important for understanding quality control specimens in the field. Typically, quality control specimens will be taken from the fresh concrete mixture as a surrogate measure of strength of the hardened concrete mixture. The current standard used in the United States for curing of these samples states that the samples must be maintained in an environment between 16° and 27°, but the temperature of the concrete itself does not need to be monitored [78]. These results indicate that for CAC concrete the type of mold, and how close together the specimens are placed can impact the generation of self-heating within the concrete, and thus impact the conversion process. That means that the current standard that is used is not applicable for use with CAC concrete and that it is very important to monitor the internal temperature profile of quality controls specimens during construction when using CAC concrete.

1.4.5 Hydration of CAC In the Presence of $CaCO_3$

Research to understand the impact of carbonates ($CaCO_3$ or finely ground limestone [FGLS]) on CAC hydration and conversion has been carried out by several authors [79-81]. Negro and co-workers observed, through the use of calorimetry, that in the presence of calcium carbonate the hydration reaction peaked earlier than pure CAC systems [79]. Fentiman also conducted research where finely ground limestone was incorporated with CAC; it was observed that when the limestone powder was incorporated, calcium monocarboaluminate was formed in the mortar samples and conversion was delayed. However, a drop in compressive strength eventually was reached due to further conversion of calcium monocarboaluminate to C_3AH_6. The converted strength (around 90 days) was found to be similar to the mortar samples without ground limestone (around 5 days). Fentiman claimed that the calcium monocarboaluminate formed as a secondary metastable hydrate and converted to the stable hydrate at a slower rate, which was responsible for the delayed converted strength [82].

Previous research has pointed out that the conversion process was affected by the addition of FGLS or in the presence of limestone (calcareous) aggregate. Monocarboaluminate was detected in many cases and attributed to a reduced or time-delayed conversion process. Some researchers have indicated that the formation of calcium monocarboaluminate would lead to a reduction in the total amount of strength loss due to conversion in CAC pastes and mortars when $CaCO_3$ was present [6, 83-92]. However, the long-term stability of calcium monocarboaluminate is widely debated in the literature. A slight decrease in the formation of C_3AH_6 was observed when there was an increase in the presence of calcium monocarboaluminate [82]. Luz and Pandolfelli showed that in presence of calcium monocarboaluminate, the formation of C_2AH_8 and CAH_{10} were all inhibited due to the formation of calcium monocarboaluminate at temperatures under 37°C, which resulted in higher compressive strength [92].

While research has shown a benefit to the formation of calcium monocarboaluminate in CAC systems, various studies have shown conflicting results in the stability of the calcium monocarboaluminate resulting in decomposition. Based on research by Fentiman, the formation of calcium monocarboaluminate was affected by curing time and temperature [80]. These results are presented in Figure 1-6.

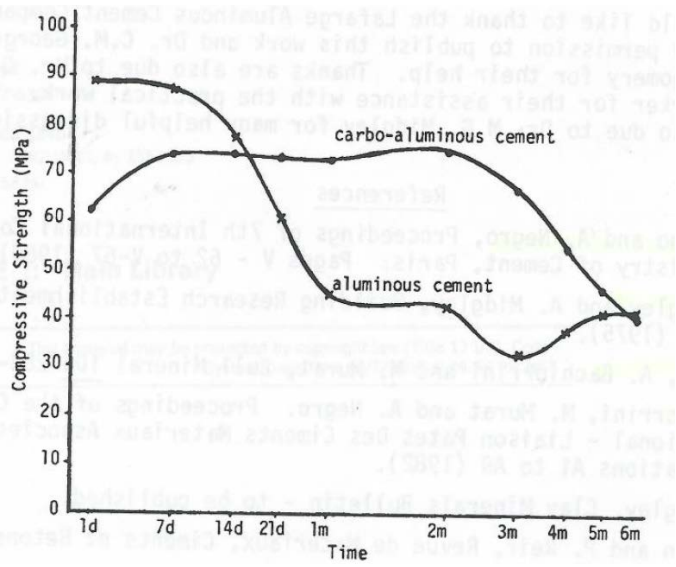

Figure 1-6: Compressive strengths of 100% CAC ("aluminous cement) and 70%CAC/30% FGLS (carbo-aluminous cement) pastes cured for 24 hours at 20°C followed by long-term curing at 38°C [80]

Fentiman observed that long-term strength in CAC pastes made with a 30% replacement of FGLS (labeled "carbo-aluminous cement") maintained "unconverted" high early strengths longer than 100% CAC pastes (labeled "aluminous cement"), but still eventually experienced a strength reduction after 3 months of curing in a 38°C water bath. This was attributed to the decomposition of calcium monocarboaluminate into C_3AH_6, resulting in similar strength as the converted 100% CAC system. Other authors have reported decomposition of calcium monocarboaluminate at higher temperatures, however. In 1984, Midgley showed that calcium monocarboaluminate started to decompose at 60°C through mass analysis by using DTA [93]. In 1996, through XRD analysis, it was reported that C_3AH_6 tended to transform to calcium monocarboaluminate when $CaCO_3$ and H_2O were present and the temperature was below 60°C. Thermal decomposition of calcium monocarboaluminate occurred at 90±5°C [81]. These studies have shown conflicting results in the decomposition of calcium monocarboaluminate at elevated temperatures reporting that decomposition occurred between 37-90°C [81, 82, 86, 92-94]. It has been shown, however, that calcium monocarboaluminate is thermodynamically more stable than C_3AH_6 up to 80°C such that no conversion to C_3AH_6 can take place [95, 96]. In CSC systems, calcium monocarboaluminate destabilized in the presence of ettringite and monosulfate + calcite above 50°C [73]. On the other hand, with small amounts of SiO_2 present in the cement, the transformation of calcium monocarboaluminate was shown to be inhibited due to the formation of a siliceous hydrogarnet with a theoretical composition of $Ca_3Al_2[SiO_4]_{0.4}(OH)_{10.4}$

[81]. Additionally, some research on the stability of calcium monocarboaluminate when exposed to air by Carlson and Berman (1960) showed that manufactured calcium monocarboaluminate was not stable when suspended in an aqueous solution and exposed to carbon dioxide at a partial pressure equal to that of air. The monocarboaluminate decomposed to $CaCO_3$ and hydrated alumina [97].

These studies indicate that the formation and stability of calcium monocarboaluminate in a system with CAC hydrates is not well understood. Subsequently, its impact on conversion cannot be predicted without additional research. The reduction in the degree of conversion by introducing FGLS is not completely understood. It has been shown, however, that FGLS additions may be a viable method of to increase basic strength properties in CAC concrete. Further studies must be completed however, to understand the stability of hydrates formed in the presence of FGLS. Additionally, studying FGLS+CAC systems, may provide insight into ways to improve concrete properties in CAC systems.

1.4.6 Volume Stability and Water Changes in CAC Systems

The critical w/cm required to fully hydrate a standard grade CAC (50% CA, and 30% Ferrite content) is 0.70 at low temperatures (for the formation of CAH_{10}) and 0.35 at higher temperatures (formation of C_3AH_6 and AH_3) [4]. The difference is due to the amount of combined water that that is bound into the calcium aluminate hydrates (see Equations 1-1 through 1-5). As discussed above, the conversion of metastable hydrates results in a significant release of water, and densification of hydrates. Therefore, any excess water over the 0.35 w/c required for full hydration of CAC adds to the porosity of the paste, adversely affecting the long-term strength (described below in Section 1.4.10), particularly after conversion [4].

Similar to CSC systems, CAC cement will undergo chemical shrinkage, the overall decrease in volume that occurs due to hydration. Chemical shrinkage is the difference in absolute volume of solids and liquids that occurs during hydration [98]. Measurements of chemical shrinkage are also commonly used to understand progression of hydration in cement based systems [99]. Chemical shrinkage for the formation of CAH_{10} from CA is 16%, whereas the chemical shrinkage is 25% for the formation of C_3AH_6 and AH_3. These values will alter in true pastes where other phases exist resulting in an average volume decrease of 10-12% in standard grade CAC systems [4].

The chemical shrinkage in CAC systems has been observed to be about 2-4 times higher than CSC systems across all isotherms [1, 100]. Ideker observed lower chemical shrinkage values for the

formation of metastable hydrates compared to stable hydrates [100] which coincides with the larger volume size of the metastable hydrates compared to stable hydrates. Fu observed that time to conversion could be estimated by observing chemical shrinkage in CAC pastes. It was shown that the rate of chemical shrinkage will increase significantly for a short time period when conversion occurs, and the time of the change in rate correlated to the time to conversion [99]. Adams and Ideker noted that the majority of chemical shrinkage happened quite rapidly at 20°C (> 80% before 1 day). The rapid chemical shrinkage rate was attributed to the rapid formation of metastable hydrates that occurs at 20° as described above [1].

Ideker et al. observed that when cured isothermally below 30°C, CAC paste systems experienced shrinkage over time in free deformation testing. However, when the system was cured above 30°C, expansion was observed [100, 101]. This work has shown that the formation of different hydrates can lead to significantly different volume changes in CAC, depending on which reaction listed above is occurring [100, 101].

Autogenous deformation is the macroscopic dimensional change that occurs in a closed, isothermal cementitious system [102]. Autogenous deformation is generally believed to occur when water is removed from a pore to aid in the hydration of cement. As the water is removed from that pore, the pore collapses due to internal pressures caused by the movement of water in the system. When enough pores collapse, macroscopic volume changes can be observed [98]. While autogenous deformation is generally minor compared to other kinds of volume change in cementitious systems, it has been found to be significant enough to induce micro- and macro-cracking in concrete at early ages before concrete is strong enough to resist the stresses induced [103, 104].

Ideker et al. [101] studied autogenous deformation in CAC systems using a free deformation frame that could keep a prism of curing CAC mortar isothermal, despite the large exotherms produced during hydration, and sealed from the environment to prevent moisture loss during curing. With this frame, they were able to measure the autogenous deformation of the mortar during the early stages of hydration at varying isothermal temperatures. Testing in this frame showed some interesting results, particularly concerning the effect of temperature on the autogenous deformation. When the CAC was cured at isothermal temperatures at or below 30°C, shrinkage was observed in the mortars in the free deformation frames. However, when the samples were isothermally cured above 30°C, expansion was observed [100, 101]. These results reflected what was observed in the chemical shrinkage tests.

Ideker et al. (2008) hypothesized that the expansion seen at higher temperatures may be due to the release of water during conversion. As stated earlier, this release of water may exert pressure on the system causing expansion to occur. However, the authors were unable to confirm this [101]. Further research into understanding the cause of the differing deformations depending on temperature is required. Currently there are very few studies available that examine the early-age volume stability of CAC. Work by Ideker et al. [101] and Bentivegna [77] has shown that there is a significant impact from the temperature at curing. Samples of concrete cast in warm environments may experience expansion, whereas samples cast in cool environments may experience shrinkage. Understanding how this deformation occurs, and what level of deformation to expect is essential for achieving a good bond in repair situations. Further research is necessary to verify and expand upon these results.

Drying shrinkage is the contraction of hardened concrete caused by the loss of capillary water to the surrounding environment [105]. Drying shrinkage will occur until the internal relative humidity of the cement paste reaches equilibrium with the atmospheric relative humidity. As water evaporates to the surrounding environment, vapor pressure decreases and tensile stresses form in the concrete. This eventually results in a capillary tension large enough that can lead to shrinkage and residual tensile stresses throughout the entire paste matrix, which may lead to cracking. Many factors affect drying shrinkage of concrete. These factors include the type and fineness of cement, composition and fineness of supplementary cementing materials, type of aggregate, aggregate size, water to cement ratio (w/c), relative humidity, admixtures, duration of curing and the size of the concrete specimen [106]. Early work studying drying shrinkage in CAC concrete has shown that total drying shrinkage of CAC concrete is similar to OPC concrete [4]. However, drying shrinkage happens much more rapidly in CAC concrete, compared to OPC [4, 100]. The rapid shrinkage may affect the tendency for CAC concrete to crack. Since the shrinkage occurs rapidly in the early age of the material, sufficient strength gain to resist cracking during shrinkage may not always be obtained [4]. Conversely, the rapid strength gain observed in CAC systems may work to counteract this effect. This is an area that has not been studied in depth. Conversion appears to have little effect on the drying shrinkage seen in CAC concrete, however this is an area that still requires further research to truly understand how different curing regimes, and times to conversion, may affect the shrinkage and cracking risk of CAC concrete [4].

Adams and Ideker (2014) examined the free drying shrinkage of CAC concrete compared to ordinary portland cement concrete and calcium sulfoaluminate cement concrete. The authors observed that

after 90 days of drying in a 50% relative humidity chamber at 23°C, the CAC system experienced significantly higher levels of drying shrinkage compared to the OPC system (0.06% higher) [1]. Adams and Ideker also examined the impact of length of wet cure on the overall drying shrinkage. They cured samples for 10 hours and 24 hours and found that there was no significant difference in the amount of drying shrinkage observed [1]. This information is important for the use of CAC in rapid repair environments where curing time is minimized to allow for minimal facility or road closures.

Little work, overall, has been completed on the shrinkage propensity of CAC based materials. This area still requires significant amounts of research to understand the mechanisms through which deformation occurs, how temperature affects it, what role conversion plays in the process, and what role curing plays in the process. This last item is particularly important for rapid repair situations where available curing time may be shortened by the need to reopen infrastructure in a timely manner. Additionally, understanding how to better control deformation to achieve desired results, and the effect deformation has on cracking and durability has yet to be examined.

1.4.7 Setting Time in Calcium Aluminate Cement Systems

Setting time behavior in CAC systems differs significantly compared to CSC systems. In CSC systems, setting time decreases inversely with temperature. However, early research showed that CAC systems behave significantly different. CAC cement pastes experienced a retardation of set between 18°C and 30°, but above 30°C set time decreased again [18]. Bushnell-Watson and Sharp confirmed that setting time increased with temperature, reaching a maximum between 26°C and 30°C , followed by a continuous decrease in set time as temperature increased above or decreased below those thresholds [55]. The changes in set time for two difference grades of CAC can be observed in Figure 1-7 from Bushnell-Watson and Sharp's work [55].

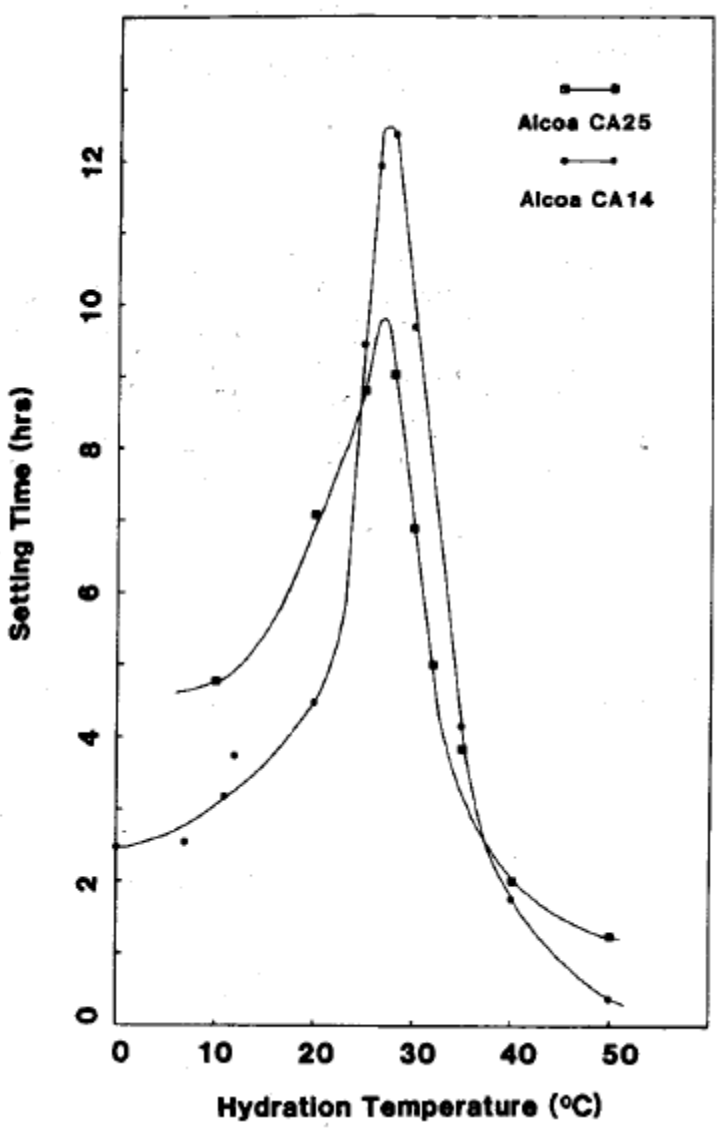

Figure 1-7: Effect of temperature on setting time of CAC paste [55]

As can be seen in Figure 1-7, the set time reaches a maximum around 28°C, decreasing as temperatures decrease below 28°C or increase above 28°C. The rapid setting behavior of CAC at low temperatures is one of the properties that make the material desirable for use in rapid repair in situations where concrete must be cast at low temperatures.

Early theories suggested that the delay in setting time may have been caused by the formation of a crystalline barrier around anhydrous cement grains preventing further dissolution and slowing set time

[53]. X-ray diffraction (XRD) and differential thermos-gravimetric analysis (DTA) studies showed, however, that very little amorphous or crystalline material can be observed in CAC systems until a time that corresponds with setting time, which is accompanied by rapid formation of hydrates. This suggests that the increased set time observed at 28°C was caused by a difficulty for initial nucleation and growth of either CAH_{10} or C_2AH_8, and not by the formation of a barrier preventing further hydration [53].

Another early theory stated that the anomalous setting time behavior was caused by the presence of C_2S in the CAC [87]. However Bushnell-Watson and Sharp [53] observed the same setting time behavior in synthetic CA pastes that did not contain C_2S, and suggested that the behavior is associated with the hydration of CA [53, 56]. The study on pure CA found that setting time increased from 2 hours at 12°C to 12 hours at 27°C, after which it decreased rapidly [56]. Bushnell-Watson and Sharp suggested the setting time increase between 20°C and 30°C may be due to difficulty in nucleating C_2AH_8 between these particular temperatures [55]. Additionally, experimental results indicated that CAH_{10} becomes more and more difficult to nucleate as temperatures increase, and that it does not nucleate above 29°C [66]. Additionally, the formation of C_2AH_8 is slow in the temperature range below 30°C, but above 30°C formation of C_2AH_8 becomes more favorable and forms with increasing rapidity [53]. Therefore, neither hydrate was favored to form as the curing temperature approached 28°C. However, as the temperature moved away from 28°C, either lower or higher, CAH_{10} and C_2AH_8, respectively, become more likely to nucleate and setting time decreases.

Initial research on CACs with higher alumina contents did not have the same problem, and instead saw continued decrease in set time as temperature was increased [87]. However this was found to be due to the presence of admixtures in the particular source of cement examined in the study. Bushnell-Watson and Sharp found that while CACs with higher alumina contents experienced shorter set times overall, the same setting time trend was observed in CAC's with high alumina contents (80% Al_2O_3) as was observed in standard grade CACs [55].

Further studies found that certain accelerating chemical admixtures such as lithium chloride can help to overcome this setting time behavior [21, 56]. Gosselin found that the addition of an accelerator helps to promote nucleation such that the nucleation barrier seen between 20°C and 30°C is overcome [45, 76]. Additionally, the setting time behavior remained consistent with changes in w/cm [53].

These studies indicate, however, that it is important to quote a temperature at which the setting time was determined since it is highly variable with temperature for CAC systems [55]. Additionally, given the difference in hydrates that form depending on temperature, it is important to monitor the temperature in all CAC systems so that one is better able to understand what hydrates may have formed during initial hydration, as well as how likely the cement is to have converted during its lifespan.

1.4.8 Pore Solution Evolution during Hydration of Calcium Aluminate Cements

Minimal research has been done on the pore solution chemistry in CAC systems. Rodger and Double reported on the concentration of aluminum, calcium, and OH^- in dilute solutions of a standard grade CAC in water at 22°C over the initial 6 hours after mixing. The authors found that aluminum and calcium concentrations increase rapidly, upon contact with solution, after reaching a point of saturation, the ionic concentration dropped significantly, which the authors linked to the precipitation of hydrates from solution. The OH^- concentration also dropped as precipitates formed from the solution [107]. Rodger and Double's work supports the general theories about CAC hydration discussed above, that hydration occurs through solution with early increases in elemental concentrations followed by sharp decreases in concentration as a massive precipitation of hydrates occurs after a particular concentration in solution is reached. Barrett et al. (1994) performed experiments that supported this theory. Barrett et al. placed a standard grade CAC in a dilute lime solution and monitored ionic concentrations in the solution over 10 hours [108]. Results from this work indicated that during hydration, as hydrates precipitate from solution, the concentrations of calcium and aluminum in solution decreased significantly. Neither of these studies examined actual concrete pore solution, however. While the information provided is useful for better understanding the hydration process, they still do not provide information regarding actual ionic concentrations in concrete. These values are important to understanding how alterations in mixture design may affect overall concrete properties.

Gaztanaga et al. examined the pore solution chemistry in a CAC paste cured at 20°C using a standard grade CAC out to 30 days [109]. The authors reported that calcium concentrations continued to decrease after initial hydration from 20 ppm at 1 day after casting to 1 ppm at 30 days. Aluminum concentrations also decreased significantly over the curing period. The pH ranged from 12.53 to 12.69 in that same time period. This analysis was performed on systems that had been cured at 20°C over

their lifespan, and therefore examined only unconverted CAC concrete systems [109]. This work did not examine how the pore solution chemistry in hardened systems changed during the conversion process, and therefore it is still not well understood how elemental composition of the pore solution is affected by conversion in hardened systems. Additionally, these authors examined cement paste systems specifically, and the impact of aggregate mineralogy was not observed. As discussed below in Section 1.4.10.2, changes in mineralogy in CAC concrete systems can have significant impacts on strength, particularly after conversion.

1.4.9 Strength Gain and the Impact of Conversion on Strength in CAC Systems

Strength evolution in CAC systems is very different compared to CSC systems due to the conversion of metastable hydrates to stable hydrates. CSC systems typically experience continuous strength gain over their life-span unless the material is compromised by some form of deterioration. In CAC systems, however, strength loss over time can be observed due to the process of conversion, through which porosity opens within the system. Long-term strength is based on the stable hydrates C_3AH_6 and AH_3, whereas early-age strength is mainly dependent on the metastable hydrates CAH_{10} and C_2AH_8. The rapid strength gain observed in CACs is a consequence of the rapid precipitation observed during hydration of CAC. Lamour et al. observed through transmission soft X-ray microscopy that as the induction period ends, there is a rapid formation of metastable hydrates resulting in a significant binding of water and filling of space [4, 65]. The rapid space filling due to the formation of the metastable hydrates provides high early strength in these systems [4]. As discussed in Section 1.4.5, the metastable hydrate CAH_{10} is favored to form and provide rapid strength gain even at low temperatures [53-56], which is why the material is useful for rapid construction in cold environments.

The strength developed from the metastable hydrates is transitory, however, as conversion occurs strength loss is observed in CAC systems. A significant amount of work has been performed to understand the effect of conversion on strength loss. Much of this work has focused on pastes and mortars with only a small percentage focused on concrete mixtures [62, 74, 81-83, 89-91, 93, 110-118]. As discussed earlier, converted CA hydrates are denser than unconverted hydrates. As the hydrates densify, they release water into the system and porosity is formed. The formation of porosity in the system results in a significant loss of strength over the lifespan of the system. As with CSCs, the strength of calcium aluminate cements increases as w/cm decreases [9]. This is due to higher w/cm

resulting in relatively higher levels of porosity in the system. Indelicato [90] and Matusinovic et al. [115] both showed through experimental results that higher porosities resulted in lower overall strengths. Figure 1-8 shows the effect of conversion on strength in CAC concrete as described by Scrivener and Capmas [4].

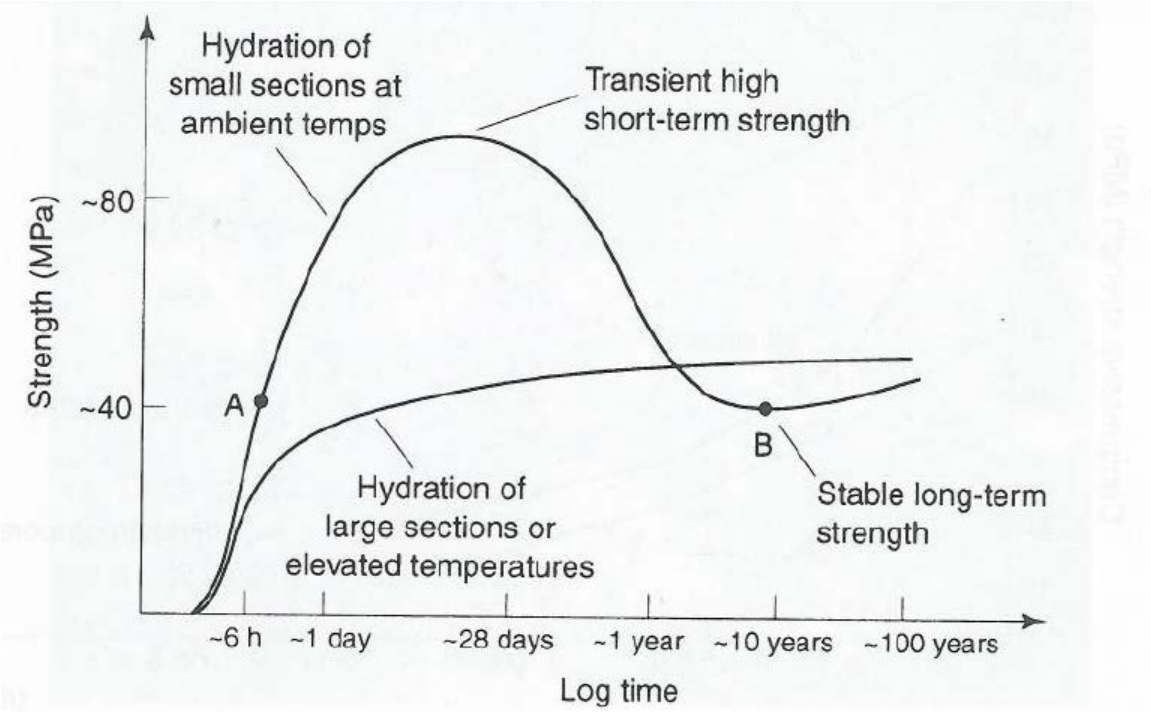

Figure 1-8: Effect of conversion on strength in CAC systems[4]

Figure 1-8 shows the strength evolution for CAC concrete cured at standard ambient temperatures, and for CAC concrete cured at elevated temperatures. The system was cured at ambient temperature reaches a high early strength, which peaks before 28 days. Then over time, as conversion occurs, significant strength reductions were observed due to the opening of porosity during conversion. Point B, as shown in Figure 1-8 indicates "minimum converted strength." Additional strength gain is realized at later ages after the minimum converted strength. This is due to further hydration of anhydrous cement grains which is stimulated by the release of water that occurs during conversion [4]. However it is important to point out that since both conversion and continued hydration of anhydrous grains will happen simultaneously, the point of minimum converted strength may not correspond directly to the point of 100% hydration [4]. As discussed earlier, once conversion of hydrates has occurred, new hydrate formation will result in direct nucleation of C_3AH_6 and AH_3 [4, 60-63], and therefore a second occurrence of strength loss will not occur once the minimum converted strength has happened. As

shown in Figure 1-8, CAC concrete that was cured at elevated temperatures experienced continuous strength gain. This can occur in systems where high temperature causes rapid conversion to stable hydrates [4, 62].

1.4.9.1 *Porosity's Impact on Strength*

Strength is inversely proportional to porosity in solids [105] and this relationship has been studied extensively in cement based materials (particularly for CSC systems). Higher porosities will result in lower overall strengths in cementitious systems. Consequently, strength of the cement paste is dependent on the w/cm and the degree of cement hydration which both influence the porosity [98]. The effect of changing the w/cm has on strength has been demonstrated by a variety of experiments on CSC systems summarized by Eglinton [119] and have shown that high w/cm (and thus higher porosities) produce lower strengths. The effect of porosity on strength is typically associated with the macropores and air voids (50 nm and greater) [105]. Pores of this size cause significant stress concentrations to form within the concrete at the site of the pore. Stress concentrations are caused where there is a change in a material's cross sectional area (such as a void). At these points the stresses do not redistribute equally, and higher stresses occur closer to where the defect is located [120]. This causes the locations of the larger voids to be places where cracks will preferentially form under stress, due to the concentration of loads in those locations [105]. Subsequently, cracking will occur first around these voids. Indelicato confirmed that this relationship held true for CAC mortars as seen in Figure 1-9 [90].

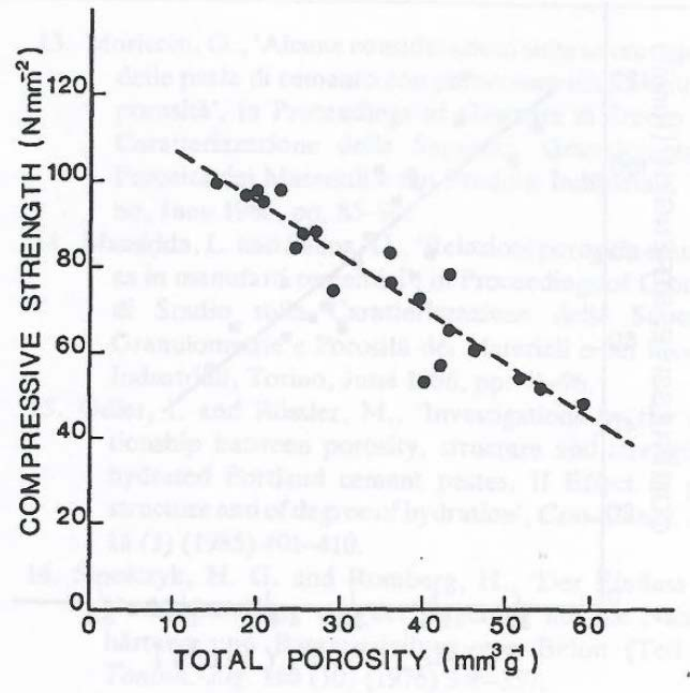

Figure 1-9: Correlation between porosity and compressive strength in CAC mortars as a function of w/cm [90]

Indelicato's results show that as porosity increases, compressive strength deacreased as porosity increased. These results are consistent with the trends normally seen for other hydraulic cement systems.

For CSC systems, a clear relationship between the strength of cement paste and porosity has been described, modeled and widely accepted [105, 121]. Research has been completed to find an analogous model in CAC systems by Indelicato [90] and Matusinović et al. [115] however neither has gained wide acceptance. Additionally, both studies focused on CAC in the unconverted state, and as such, the relationships may not be valid for converted CAC samples. Therefore, there is currently no model available to predict the strength in CAC systems based off of total porosity after conversion.

1.4.9.2 *Impact of Aggregate Mineralogy on Strength in CAC Systems*

Previous work has observed that aggregate mineralogy can have a significant impact on concrete strength and conversion in CAC systems. In an early study by Cussino and Negro in 1980, samples were stored at 20°C for five years and tested in compression periodically. The results from this study are presented in Figure 1-10.

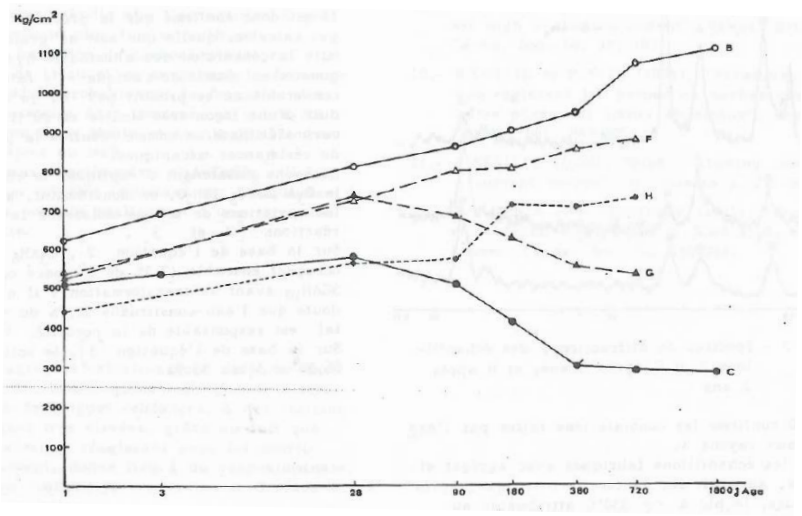

Line B	0.5 w/cm Concrete with Carbonate Limestone Aggregate
Line C	0.5 w/cm Concrete with Siliceous Aggregate
Line F	0.6 w/cm Concrete with Carbonate Limestone Aggregate
Line G	0.54 w/cm Concrete with Siliceous Aggregate
Line H	0.51 w/cm Concrete with Siliceous Limestone Aggregate and a 25% Replacement of CAC with FGLS

Figure 1-10: Concrete compressive strength results from Cussino and Negro (Translated from original French) [91]

The specimens containing siliceous aggregate saw strength reductions due to conversion beginning after 28 days. However, after five years of being stored in the same conditions, mixtures containing either limestone aggregates or limestone powder used as a replacement for CAC were still steadily gaining strength [91]. Scrivener and Capmas also noted that CAC concrete made with limestone typically showed strengths about 20% higher than those made with siliceous aggregates, ascribing the difference to bond strengths between the cement paste and aggregates. The authors did not fully describe the systems which they were discussing, and no in-depth study of the difference between each system was done [4]. Despite the fact that researchers observed an impact of mineralogy in these systems 30 years ago, no systematic, in-depth studies of the impact of aggregate mineralogy on CAC concrete have been done to date.

Cussino and Negro's preliminary analysis observed the formation of calcium monocarboaluminate in the samples containing finely ground limestone [91]. However, this analysis work was conducted through the use of DTA and a study of compressive strength. Additionally, the analysis work focused on systems with finely ground limestone (15 μm to 150 μm particle size diameter), and not larger limestone aggregates (150 μm to 4.75 mm particle size diameter for fine aggregates, 4.75 mm and greater particle size diameter for coarse aggregates). Using a high surface area material such as finely ground limestone to explain how a larger limestone aggregate, with significantly less surface area on which topochemical reactions may occur may not provide an accurate answer to the results discussed above. Cussino and Negro assumed that analogous reactions were occurring in the systems containing

limestone aggregates, however they did not confirm the existence of calcium monocarboaluminates in these systems [91]. Lamour and co-workers observed similar findings in concrete and mortars made with siliceous and limestone aggregates [89], however no examination of the hydrates or microstructure was done to determine the cause. The authors from both studies attributed the difference in conversion and strength to the presence of monocarboaluminate in the system [89, 91]. Lamour and co-workers suggested mechanistic work be performed to further understand the differences between CAC concrete made with limestone and CAC concrete made with siliceous aggregates, however, to date no study has been done [89].

1.4.10 Determination of Minimum Converted Strength in CAC Concrete

A standard method used for sampling and curing hydraulic cement concrete specimens for testing compressive strength, ASTM C31, states that cylinders should be cast on site, and allowed to be cured on site for a period up to 48 hours. The cylinders should then be moved to a moist cabinet where they are cured at 23 ± 2°C until tested [122]. This curing regime will not allow for obtaining the minimum strength of CAC concrete within a convenient time period because the metastable hydrates will not convert quickly to the stable hydrates within an acceptable time period, at this temperature.

There are two main methods that are used to promote conversion of CAC hydrates to obtain a minimum compressive strength of a given CAC concrete within a reasonable time. The method described in EN 14647 is used primarily in Europe. This method states that to achieve the minimum converted strength of CAC concrete rapidly, the test specimens should be placed in a 38°C water bath directly after being cast. According to this standard, the minimum converted strength will occur at five days after casting followed by the subsequent submersion in the heated water bath [123]. This method was also suggested for use in the U.K. by the Concrete Society [9]. Standard SS-4491 used by the Texas Department of Transportation, in Texas, U.S.A. states that the specimens should be placed immediately in a heavily insulated box after casting. The insulated box takes advantage of the high heat of hydration produced during CAC hydration which is captured to encourage "self-heating" of the specimens [124]. The samples that are stored in the insulated box will, collectively, generate enough heat to promote the rapid conversion of the metastable hydrates. A heavily insulted box similar to that suggested by the Texas DOT can be seen below in Figure 1-11.

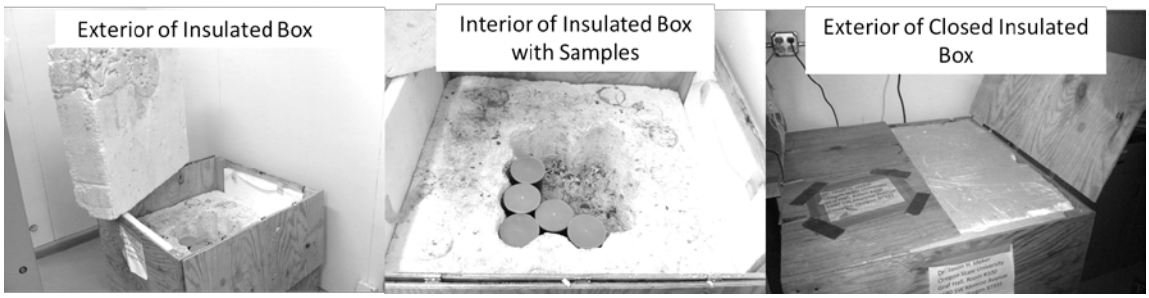

Figure 1-11: Heavily insulated box for curing CAC concrete samples

These test methods, while useful for determining the converted strength of CAC concrete, are not convenient for use in the field because they require bulky equipment, or equipment that requires a power source, to be transported to the site so samples can be directly placed into the heated water bath or the insulated box directly after being cast. Fryda et al. [11] proposed a test method that overcomes these challenges by permitting the specimens to be cast and cured on site under ambient conditions, and then transported to the laboratory at a later time where they can be cured. This method allows for the specimens to be kept on site at ambient temperatures for up to 24 hours after casting; and then transported to the laboratory and placed in a heated water bath [11]. This test method has not been examined in depth, however, to determine the influence of various factors on the reliability of the test method.

In order for this test method to gain wide acceptance within the United States, it must become a standard test method likely approved by a well-recognized standards organization such as ASTM, International. However, there are several barriers that must be overcome prior to acceptance as a test method. The influence of mixture design parameters and curing parameters must be studied to understand their impact on the test method. Understanding the impact of each of these variables will help determine the scope of the test method, as well as the proper procedure and allowable variance, and apparatus requirements [125]. This work is known as ruggedness or robustness testing, and is important to determining the overall accuracy of the test method [126]. Once these are well understood through research, the appropriate language for the test method can be developed to ensure that consistent procedures are followed at all laboratories to produce acceptable variance.

A precision and bias statement should also be developed for all test methods before they can be approved by a standards organization [126]. Precision is "the closeness of agreement among test results obtained under prescribed conditions," and bias is "a systematic error that contributes to the

difference between the mean of a large number of test results and an accepted reference value" [126]. Data for the precision and bias statement can be developed through an interlaboratory study, more commonly known as a "round robin" study in which several laboratories run the test method and the results are compared [126]. It is important to have performed the ruggedness testing prior to conducting round robin testing so that a well written testing procedure is already developed for all laboratories to follow [127]. ASTM Standard E 691, "Standard Practice for Conducting an Interlaboratory Study to Determine the Precision of a Test Method" suggests that at least six laboratories be included in any interlaboratory study to ensure an adequate sampling of different laboratories [127]. Ruggedness testing and a preliminary round robin of the Fryda et al. [11] test method are presented in Manuscript one in Chapter 3 of this dissertation.

1.4.11 Concrete Mixture Design Standards

Recommendations for design of CAC concrete systems have been created and included in the European Standard for CAC to ensure viable strengths after conversion. These rules were developed by the authors of the European Standard [123] as well as CAC manufacturers [9]. These guidelines suggest that a minimum cement content of 400 kg/m^3 be used in all mixtures. Additionally, the guidelines suggest a maximum total w/cm of 0.40 [9, 123].

As discussed in Section 1.4.6 and Section 1.4.10.2 the use of carbonate bearing aggregates and fillers (e.g. limestone) can delay the time to conversion in some systems. This process is not well understood, however, and as such CAC manufacturers have often suggested not using carbonates in CAC concrete mixtures, because their effect is not well understood [12]. The European Standard does not prohibit the use limestone aggregates or other carbonate fillers, however it does note that the standard technique for accelerating conversion by direct immersion in a 38°C water bath (described above) to determine the converted strength of CAC concrete may not be applicable for use with systems including carbonates [123].

It is important to note that no such guidelines exist at the national standards levels in North America (e.g. ASTM, AASHTO, CSA), beyond the recommendations of the manufacturers of CAC, and as such there are no significant restrictions on the use of CAC in North American markets. However, these guidelines were developed through extensive research and case study experience, so it would still be pertinent for anyone using CACs to carefully consider the experience and guidance of the European Standard and other guidelines.

1.5 Summary and Motivation

The aim of this literature review was to familiarize the reader with the various aspects of CAC including: history, use, production, cement chemistry, hydration, conversion, strength development, impact of aggregate choice, and test methods. The work reviewed in the above sections illustrates the significant amount of literature that has been produced examining the properties and hydration of CAC systems. CAC materials have been in use for over 100 years and continue to work successfully in specialty applications. CAC's ability to gain strength rapidly even at temperatures approaching 0°C, resistance to acidic corrosion, and abrasion resistance properties also make it an ideal tool for use in the quickly growing rapid repair of infrastructure market, particularly in North America. Despite this, gaps exist in literature that have limited the use of CAC in rapid repair environments. These include:

1. A lack of a viable, standardized, test method that is convenient for use in the field that will quickly determine the converted strength of CAC concrete for quality assurance purposes;
2. Insufficient understanding of the impact of limestone aggregates and FGLS in CAC concrete mixtures on hydration, strength development and conversion; and
3. Insufficient understanding of the shrinkage propensity of CAC concrete, and in particular the role that curing time, curing temperature, and conversion plays in the cracking susceptibility of the system.

Responding to these gaps in literature and developing an appropriate test method for CAC concrete quality assurance provided the motivation for the studies presented in this dissertation. The following section, Chapter 2, will outline the various experimental techniques and methods used throughout the dissertation. Chapters 3-6 presents the work completed to address the gaps in literature discussed above. This work is presented in the format a four individual manuscripts ready to be submitted (Chapters 3 and 5), already submitted (Chapter 4), or already accepted (Chapter 6) for publication. Chapter 7 concludes the work and unifies all the topics discussed in Chapters 1-6. This work represents a significant addition to the knowledge base concerning CAC concrete and will aid future researchers and engineers in better understanding and utilizing the material.

1.6 Works Cited

[1] M.P. Adams, J.H. Ideker, Volume stability of calcium aluminate cement and calcium sulfoaluminate cement systems, in: C. Fentiman, R. Mangabhai, K. Scrivener (Eds.) International Conference on Calcium Aluminate Cements, IHS, Avignon, FR, 2014.

[2] American Society of Civil Engineers, Report card for America's infrastructure, in, American Society of Civil Engineers, 2013.

[3] K.L. Scrivener, 100 years of calcium aluminate cements, in: C.H. Fentiman, R.J. Mangabhai, K.L. Scrivener (Eds.) Calcium aluminate cements : Proceedings of the centenary conference, IHS BRE Press, Avignon, France, 2008, pp. 3-6.

[4] K.L. Scrivener, A. Capmas, Calcium Aluminate Cements, in: P.C. Hewitt (Ed.) Lea's Chemistry of Cement and Concrete, Elsevier - Butterworth-Heinemann, Oxford, UK, 1998, pp. 713-782.

[5] H.G. Midgley, High alumina cement in construction - A future based on experience, in: R.J. Mangabhai (Ed.) International Symposium on Calcium Aluminate Cements, E & F. N. Spon, London, 1990, pp. 1-13.

[6] C.M. George, Manufacture and performance of aluminous cement: a new perspective, in: R.J. Mangabhai (Ed.) International Symposium on Calcium Aluminate Cements, E&FN Spon, London, UK, 1990, pp. 181-207.

[7] K.L. Scrivener, J.-L. Cabiron, R. Letourneux, High-performance concretes from calcium aluminate cements, Cement and Concrete Research, 29 (1999) 1215-1223.

[8] F. Sorrentino, D. Damidot, Mineralogy of a 90 year old structure "Le Tunnel Des Valois", in: C.H. Fentiman, R.J. Mangabhai, K.L. Scrivener (Eds.) Calcium Aluminates: Proceedings of the International Conference, IHS BRE Press, Avignon, France, 2014, pp. 535-544.

[9] Concrete Society Technical Report, Calcium Aluminate Cements in Construction: A Reassessment, in, Concrete Society, 1997, pp. 63.

[10] Beam failure— conversion of high alumina cement, Building Research and Practice, 2 (1974) 235-240.

[11] H. Fryda, E. Charpentier, J.M. Bertino, Accelerated test for conversion of calcium aluminate cement concrete, in: C.H. Fentiman, R.J. Mangabhai, K.L. Scrivener (Eds.) Calcium Aluminate Cements: The Centenary Conference, IHS BRE Press, Avignon, FR, 2008.

[12] H. Fryda, C. Alt, Conversations with a CAC cement manufacturer, in: M.P. Adams (Ed.), 2013.

[13] C.M. Williams, F. Garrott, Recycling/Reclaiming a savings spree: Chicago reuses to the max on famous shopping mile, in: Illinois Interchange, Illinois Department of Transportation, Springfield, IL, 2012.

[14] M.C.G. Juenger, F. Winnefeld, J.L. Provis, J.H. Ideker, Advances in alternative cementitious binders, Cement and Concrete Research, 41 (2011) 1232-1243.

[15] H. Justnes, Rapid repair of airfield runway in cold weather using CAC mortar, in: C. Fentiman, R. Mangabhai, K. Scrivener (Eds.) Calcium Aluminate Cements: The Centenary Conference, IHS BRE Press, Avignon, FR, 2008.

[16] A. Dunster, I. Holton, A laboratory study of ther esistance of CAC concretes to chemical attack by sulphate and alkali carbonate solutions. , in: R.J. Mangabhai, F.P. Glasser (Eds.) International Conference on Calcium Aluminate Cements, IOM Communications, Edinburgh, UK, 2001, pp. 333-348.

[17] N.J. Crammond, Long-term performance of high alumina cement concrete in sulphate-bearing environments, in: R.J. Mangabhai (Ed.) International Symposium on Calcium Aluminate Cements, Spon Press, London, UK, 1990, pp. 208-221.

[18] T.D. Robson, High Alumina Cements and Concretes, John Wiley & Sons, Inc., New York, NY, 1962.

[19] J. Sawkow, High alumina cements based on calcium aluminate clinker with different phase compositions and sintering degrees, in: R.J. Mangabhai (Ed.) International Symposium on Calcium Aluminate Cements, E & F. N. Spon, London, UK, 1990, pp. 27-38.

[20] W. Gessner, S. Mohmel, J. Kieser, M. Hawecker, Investigations of the composition of phases formed in low cement castables during hydration and after thermal treatment, in: R.J. Mangabhai (Ed.) International Symposium on Calcium Aluminate Cements, E & F. N. Spon, London, UK, 1990, pp. 52-64.

[21] J. H. Sharp, S.M. Bushnell-Watson, D. R. Payne, P.A. Ward, The effect of admixtures on the hydration of refractory calcium aluminate cements, in: R.J. Mangabhai (Ed.) International Symposium on Calcium Aluminate Cements, E. & F. N. Spon, London, UK, 1990, pp. 127-141.

[22] S.R. Klaus, J. Neubauer, F. Goetz-Neunhoeffer, B. A, D. Schmidtmeier, Application of heat flow calculation to synthetic calcium aluminate cement mixes, in: C. Fentiman, R. Mangabhai, K. Scrivener (Eds.) International Conference on Calcium Aluminate Cements, IHS BRE, Avignon, FR, 2014, pp. 65-74.

[23] J.M. Auvray, H. Fryda, C. Zetterstrom, C. Wohrmeye, C. Parr, Hydration and properties of calcium magnesium aluminate cement, in: C. Fentiman, R. Mangabhai, K. Scrivener (Eds.) International Conference on Calcium Aluminate Cements, IHS BRE Press, Avignon, FR, 2014, pp. 130-139.

[24] D. Madej, J. Szczerba, W. Kagan, Investigations on the hydratable compounds in the CaO-Al_2O_3-ZrO_2 system, in: C. Fentiman, R. Mangabhai, K. Scrivener (Eds.) International Conference on Calcium Aluminate Cements, IHS BRE Press, Avignon, FR, 2014, pp. 140-149.

[25] C. Stancu, N. Angelescu, M. Muntean, The influence of mineralogical composition of high alumina cement on its physical-mechanical properties, in: C. Fentiman, R. Mangabhai, K. Scrivener (Eds.) International Conference on Calcium Aluminate Cements, IHS BRE Press, Avignon, FR, 2014, pp. 364-370.

[26] A. Buhr, D. Schmidtmeier, G. Wams, S. Kuiper, S. Klaus, Testing of calcium aluminate cement bonded castables and influence of curing conditions on the strength development, in: C. Fentiman, R. Mangabhai, K. Scrivener (Eds.) International Conference on Calcium Aluminate Cements, IHS BRE Press, Avignon, FR, 2014, pp. 437-449.

[27] J. Kasper, O. Krause, Mixing optimization of an alumina based LC-castable by applying ariable power inputs, in: C. Fentiman, R. Mangabhai, K. Scrivener (Eds.) International Conference on Calcium Aluminate Cements, IHS BRE Press, Avignon, FR, 2014, pp. 450-456.

[28] C. Parr, D. Verat, C. Wohrmeyer, J.P. Letourneux, High purity calcium aluminate binders for demanding high temperature applications, in: C. Fentiman, R. Mangabhai, K. Scrivener (Eds.) Centenary Conference on Calcium Alumiante Cements, IHS BRE Press, Avignon, FR, 2008.

[29] P. Boch, S. Masse, N. Lequeux, CAC in refractory applications: from LCCs to ZCCs, in: R.J. Mangabhai, F.P. Glasser (Eds.) International Conference on Calcium Aluminate Cements, IOM Communications, Edinburgh, UK, 2001.

[30] J.P. Bayoux, J.P. Letourneux, S. Marcdargent, M. Vershaeve, Acidic corrosion of high alumina cement, in: R.J. Mangabhai (Ed.) International Symposium on Calcium Aluminate Cements, E. & F. N. Spon, London, UK, 2014, pp. 230-240.

[31] A.M. Goyns, M.G. Alexander, Performance of various concretes in the Virginia experimental sewer over 20 years, in: C. Fentiman, R. Mangabhai, K. Scrivener (Eds.) International Conference on Calcium Aluminate Cements, IHS BRE Press, Avignon, FR, 2014, pp. 573-584.

[32] M. Valix, A.W.H. Cheung, J. Sunarho, H. Bustamente, The impact of calcium aluminate cement and aggregates on conversion and on field performance in sewers, in: C. Fentiman, R. Mangabhai, K. Scrivener (Eds.) International Conference on Calcium Aluminate Cements, IHS BRE Press, Avignon, FR, 2014, pp. 585-599.

[33] T. Sugiyama, K. Tabara, M. Morioka, E. Sakai, The influence of water/poweder ratio on the resistance fo sulfuric acid on hardened calcium aluminate cement containing blast furnace slag, in: C. Fentiman, R. Mangabhai, K. Scrivener (Eds.) International Conference on Calcium Aluminate Cements, IHS BRE Press, Avignon, FR, 2014, pp. 600-607.

[34] N. Motsieloa, M.G. Alexander, H. Beushausen, Acid resistance of calcium alumiante cement concrete blended with supplementary cementitious materials for application in sewer pipes, in: C. Fentiman, R. Mangabhai, K. Scrivener (Eds.) International Conference on Calcium Aluminate Cements, IHS BRE Press, Avignon, FR, 2014, pp. 608-320.

[35] M.P. Lavigne, J.N. Foussard, A. Cockx, E. Paul, A. Bertron, G. Escadeillas, A new method for evaluation of cement-based material resistance against biogenic attacks in sewer-like environments: comparison between CAC and BFSC linings, in: C. Fentiman, R. Mangabhai, K. Scrivener (Eds.) International Conference on Calcium Aluminate Cements, IHS BRE Press, Avignon, FR, 2014, pp. 621-633.

[36] J. Herisson, E.D.v. Hullebusch, M. Gueguen-Minerbe, T. Chaussadent, Biogenic corrosion mechanism: study of parameters explaining calcium alumiante cement durability, in: C. Fentiman, R. Mangabhai, K. Scrivener (Eds.) International Conference on Calcium Aluminate Cements, IHS BRE Press, Avignon, FR, 2014, pp. 621-659.

[37] J. Herisson, M. Gueguen-Minerbe, T. Chaussadent, E.D.v. Hullesbusch, Development of a reproducible, representative and accelerated biogenic corrosion test to deliver durable structures in sewer networks, in: C. Fentiman, R. Mangabhai, K. Scrivener (Eds.) International Conference on Calcium Aluminate Cements, IHS BRE Press, Avignon, FR, 2014, pp. 645-658.

[38] A. Goyns, Calcium aluminate cement linings for cost-effective sewers, in: R.J. Mangabhai, F.P. Glasser (Eds.) International Conference on Calcium Aluminate Cements, IOM Communications, Edinburgh, UK, 2001, pp. 617-631.

[39] M.G. Alexander, C.W. Fourie, Acid resistance of calcium alumiante cement in concrete sewer pipe mixtures, in: R.J. Mangabhai, F.P. Glasser (Eds.) International Conference on Calcium Aluminate Cements, IOM Communications, Edinburgh, UK, 2001, pp. 633-645.

[40] R. Harebron, A general description of flow-applied floor screeds - An important application for complex formulations based on CAC, in: R.J. Mangabhai, F.P. Glasser (Eds.) International Conference on Calcium Aluminate Cements, IOM Communications, Edinburgh, Scotland, 2001, pp. 597-604.

[41] M. Roberts, The effect of utilising calcium aluminate cements in the development of self-smoothing cementitious floor, in: R.J. Mangabhai, F.P. Glasser (Eds.) International Conference on Calcium Aluminate Cements, IOM Communications, Edinburgh, Scotland, 2001, pp. 605-614.

[42] H. Pöllman, Calcium alumiante cements- Raw materials, differences, hydration and properties, in: M.A.T.M. Broekmans, H. Pöllmann (Eds.) Applied mineralogy of cement & concrete, The Mineralogical Society of Virginia, Chantilly, Virginia, USA, 2012, pp. 1-82.

[43] I.N. Chakraborty, S. Narayanan, D. Venkateswaran, S.K. Biswas, A.K. Chatterjee, Effect of morphology on the hydration characteristics of high alumina cements, in: R.J. Mangabhai (Ed.) International Symposium on Calcium Alumiante Cements, E. & F. N. Spon, London, 1990, pp. 17-26.

[44] B. Touzo, P.A. Andreani, Mineral composition of hydration of a $C_{12}A_7$ rich binder, in: C. Fentiman, R. Mangabhai, K. Scrivener (Eds.) Internation Conference on Calcium Aluminate Cements, IHS BRE, Avignon, FR, 2014, pp. 33-41.

[45] C. Gosselin, Microstructural development of calcium aluminate cement based systems with and without supplementary cementitious materials, in: Faculte sciences et techniques de l'ingenieur, Ecole Polytechniqe Federale de Lausanne, Lausanne, CH, 2009.

[46] P. Barret, D. Bertrandie, Minimum instability curve in metastable solution of CA, in: 7th International Conference on Cement Chemistry, Paris, 1980.

[47] H.F.W. Taylor, Calcium aluminate, expansive and other cements, in: Cement Chemistry, Thomas Telford, London, 1997, pp. 295-322.

[48] I. Odler, Calcium aluminate cement, in: Special Inorganic Cements, E & FN Spon, London, 2000, pp. 173-204.

[49] Various, Calcium Aluminate Cements: Proceedings of the International Symposium in London, England, E & F N Spon, London, 1990.

[50] Various, Proceedings of the International Conference on Calcium Alumiante Cements in Edinburgh, Scotland, IOM Communications, 2001.

[51] Various, Calcium aluminate cements: Proceedings of the centenary conference in Avignon, France, IHS BRE Press, London, England, 2008.

[52] Various, Calcium Aluminates: Proceedings of the International Conference in Avignon France, IHS BRE Press, U. K. , 2014.

[53] S.M. Bushnell-Watson, J.H. Sharp, On the cause of the anomalous setting bahavior with respect to temperature of calcium aluminate cement, Cement and Concrete Research, 20 (1990).

[54] S.M. Bushnell-Watson, J.H. Sharp, The application of thermal analysis to the hydration of conversion reactions of calcium aluminate cements, Materiales De Construccion, 42 (1992) 13-32.

[55] S.M. Bushnell-Watson, J. Sharp, The effect of temperature upon the setting behavior of refractory calcium aluminate cements, Cement and Concrete Research, 16 (1986) 875-884.

[56] S.M. Bushnell-Watson, J.H. Sharp, Further studies of the effect of temperature upon the setting behavior of refractory calcium aluminate cements, cement and Concrete Research, 20 (1990) 623-635.

[57] V. Antonovič, J. Keriene, R. Boris, M. Aleknevičius, The effect of temperature on the formation of the hydrated calcium aluminate cement structure, Procedia Engineering, 57 (2013) 99-106.

[58] S. Rashid, X. Turrillas, Hydration kinetics of $CaAl_2O_4$ using synchrotron energy-dispersive diffraction, Thermochemica Acta, 302 (1997) 25-34.

[59] A. Rettel, W. Gessner, D. Muller, G. Scheler, On the hydration of $CaAl_2O_4$ at various temperatures, Transactions and journal of the British Ceramic Society, 84 (1985) 25-28.

[60] S. Rashid, P. Barnes, X. Turrillas, The rapid conversion of calcium aluminate cement hydrates, as revealed by synchrotron energy-dispersive diffraction, Advances in Cement Research, 4 (1992) 61-67.

[61] K.L. Scrivener, Historical and present day applications of calcium aluminate cements, in: R.J. Mangabhai, F.P. Glasser (Eds.) Proceedings of the International Conference on Calcium Aluminate Cements (CAC), IOM Communications, Heriot-Watt University, Edinburgh, Scotland, UK, 2001, pp. 3-23.

[62] H. Fryda, K.L. Scrivener, G. Chanvillard, C. Feron, Relevance of Laboratory Tests to Field Applications of Calcium Aluminate Cement Concretes, in: International Conference on Calcium Aluminate Cements (CAC), IOM Communications, Heriot-Watt University, Edinburgh, Scotland, UK, 2001, pp. 215-247.

[63] S. Rashid, P. Barnes, J. Bensted, X. Turrillas, Conversion of calcium aluminate cement hydrates re-examined with synchrotron energy-dispersive diffraction, Journal of materials science letters, 13 (1994) 1232-1234.

[64] C. Gosselin, K.L. Scrivener, Microstructure development of calcium alumiante cements accelerated by lithuium sulphate, in: C.H. Fentiman, R.J. Mangabhai, K.L. Scrivener (Eds.) Centenary Conference on Calcium Aluminate Cements, IHS BRE Press, Avignon, 2008, pp. 109-122.

[65] V.H.R. Lamour, P.J.M. Monteiro, K.L. Scrivener, H. Fryda, Microscopic studies of the early hydration of calcium aluminate cements, in: R.J. Mangabhai, F.P. Glasser (Eds.) International Conference on Calcium Aluminate Cements (CAC), IOM Communications, Edinburgh, Scotland, 2001, pp. 169-180.

[66] A. Capmas, D. Ménétrier-Sorrentino, D. Damidot, Effect of temperature on setting time of calcium aluminate cements, in: R.J. Mangbhai (Ed.) International Symposium on Calcium Aluminate Cements, E & F N Spon, London, 1990, pp. 65-80.

[67] S.R. Klaus, J. Neubauer, F. Goetz-Neunhoeffer, How to increase the hydration degree of CA - the influence of CA particle fineness, Cement and Concrete Research, 67 (2015) 11-20.

[68] K.L. Scrivener, H.F.W. Taylor, Microstructural development in pastes of a calcium aluminate cement, in: R.J. Mangabhai (Ed.) International Symposium on Calcium Aluminate Cements, E. & F. N. Spon, London, 1990, pp. 41-51.

[69] W. Gessner, S. Moehmel, T.A. Bier, Effects of the aluminat quality on hydration and thermal bahviour of calcium aluminate/alumina mixes, in: R.J. Mangabhai, F.P. Glasser (Eds.) International Conference on Calcium Aluminate Cements (CAC), IOM Communications Ltd., Edinburgh, Scotland, 2001, pp. 291-301.

[70] J.W. Bullard, H.M. Jennings, R.A. Livingston, A. Nonat, G.W. Scherer, J.S. Schweitzer, K.L. Scrivener, J.J. Thomas, Mechanisms of Cement Hydration, Cement and Concrete Research, 41 (2011) 1208-1223.

[71] P. Juilland, E. Gallucci, R. Flatt, K. Scrivener, Dissolution theory applied to the induction period in alite hydration, Cement and Concrete Research, 40 (2010) 831-844.

[72] K.L. Scrivener, A. Nonat, Hydration of cementitious materials, present and future, Cement and Concrete Research, 41 (2011) 651-665.

[73] B. Lothenbach, T. Matschei, G. Moschner, F.P. Glasser, Thermodynamic modelling of the effect of temperature on the hydration and porosity of Portland cement, Cement and Concrete Research, 38 (2008) 1-18.

[74] S. Klaus, J. Neubauer, F. Goetz-Neunhoeffer, Hydration kinetics of CA_2 and CA—Investigations performed on a synthetic calcium aluminate cement, Cement and Concrete Research, 43 (2013) 62-69.

[75] F. Goetz-Neunhoeffer, S.R. Klaus, J. Neubauer, Kinetics of CA and CA_2 dissolution by QXRD and corresponding enthalpies of reactions, in: C. Fentiman, R. Mangabhai, K. Scrivener (Eds.) International Conference on Calcium Aluminate Cements, IHS BRE, Avignon, FR, 2014, pp. 54-64.

[76] C. Gosselin, E. Gallucci, K. Scrivener, Influence of self heating and Li_2SO_4 addition on the microstructural development of calcium aluminate cement, Cement and Concrete Research, 40 (2010) 1555-1570.

[77] A. Bentivegna, Multi-scale characterization, implementation, and monitoring of calcium aluminate cement based systems, in: Civil Engineering, University of Texas at Austin, Austin, Texas, 2012.

[78] ASTM Standard C31, Standard practice for making and curing concrete test specimens in the field, in: ASTM International (Ed.), ASTM International, West Conshohocken, PA, 2012.

[79] A. Negro, A. Bachiorrini, M. Murat, Interaction, in aqueous medium, between calcium carbonate and monocalcium aluminate at 5°C, 20°C, and 40°C, Bulletin de minéralogie, 105 (1982) 284-290.

[80] C.H. Fentiman, Hydration of carbo-aluminous cement at different temperatures, Cement and concrete Research, 15 (1985) 622-630.

[81] H.-J. Kuzel, H. Baier, Hydration of calcium aluminate cements in the presence of calcium carbonate, European Journal of Mineralogy, 8 (1996) 129-141.

[82] C.H. Fentiman, Hydration of carbo-aluminous cement at different temperatures, Cement and Concrete Research, 15 (1985) 622-630.

[83] H.H.M. Darweesh, Limestone as an accelerator and filler in limestone-substituted alumina cement, Ceramics international, 30 (2004) 145-150.

[84] A. Bachiorrini, L. Cussino, Alumina cement hydration in pure water and in sulfate solution in the presence of siliceous or calcareous aggregate, in: 8th International Congress on the Cement of Chemistry, Rio de Janeiro, Brazil, 1986, pp. 383-388.

[85] F. Trivino, Aluminous cement: How to avoid degrading of mechanical resistance, in: 8th International Congress on the Chemistry of Cement, Rio de Janeiro, Brazil, 1986, pp. 417-422.

[86] W.G. Piasta, The Effect of Limestone Fillers on Sulphate Resistance of High Alumina Cement Compositers, in: R.J. Mangabhai (Ed.) Calcium Aluminate Cements, E. & F.N. Spon, London, UK, 1990, pp. 241-255.

[87] C.M. George, Aluminous cements, in: 7th International Congress on the Chemistry of Cement, Paris, France, 1980.

[88] H.G. Midgley, High alumina cement in construction - a future based on experience, in: R.J. Mangabhai (Ed.) Calcium Aluminate Cements, E. & F.N. Spon, London, UK, 1990, pp. 1-13.

[89] V. Lamour, P. Monteiro, K. Scrivener, H. Fryda, Mechanical properties of calcium aluminate cement concretes, in: International conference on calcium aluminate cements, 2001, pp. 199-213.

[90] F. Indelicato, On the correlation between porosity and strength in high-alumina cement mortars, Materials and Structures, 23 (1990) 289-295.

[91] L. Cussino, A. Negro, Hydration du ciment alumineux en présence d'agrégat siliceux et calcaire, in: 7th International Congress on the Chemistry of Cement, Paris, 1980.

[92] A.P. Luz, V.C. Pandolfelli, $CaCO_3$ addition effect on the hydration and mechanical strength evolution of calcium aluminate cement for endodontic applications, Ceramics International, 38 (2012) 1417-1425.

[93] H. Midgley, Measurement of high-alumina cement-calcium carbonate reactions using DTA, Clay Minerals, 19 (1984) 857-864.

[94] T. Matschei, Thermodynamics of Cement Hydration, in: Department of Chemistry, University of Aberdeen, 2007, pp. 222.

[95] T. Matschei, B. Lothenbach, F.P. Glasser, The role of calcium carbonate in cement hydration, Cement and Concrete Research, 37 (2007) 551-558.

[96] T. Matschei, B. Lothenbach, F.P. Glasser, Thermodynamic properties of Portland cement hydrates in the system CaO-Al_2O_3-SiO_2-$CaSO_4$-$CaCO_3$-H_2O, Cement and Concrete Research, 37 (2007) 1379-1410.

[97] E.T. Carlson, H.A. Berman, Some observations on the calcium aluminate carbonate hydrates, Journal of Research of the National Bureau of Standards, 64 (1960) 333-341.

[98] S.H. Kosmatka, M.L. Wilson, Design and control of concrete mixtures, 14 ed., Portland Cement Association, Skokie, Illinois, 2011.

[99] T. Fu, Autogenous deformation and chemical shrinkage of high performance cementitious systems, in: School of Civil and Construction Engineering, Oregon State University, Corvallis, OR, 2011.

[100] J.H. Ideker, Early-age behavior of Calcium Aluminate Cement Systems, in: Civil Engineering, The University of Texas at Austin, Austin, TX, 2008.

[101] J.H. Ideker, K.J. Folliard, M.D.A. Thomas, Early-age properties of calcium aluminate cement concrete with rigid cracking and free shrinkage frames: isothermal testing, in: C. Fentiman, R. Mangabhai, K. Scrivener (Eds.) Calcium Aluminate Cements: The Centenary Conference, IHS BRE Press, Avignon, FR, 2008.

[102] O. Jensen, P.F. Hansen, Autogenous deformation and change of relative humidity in silica fume modified cement paste, ACI materials Journal, 28 (1996) 539-543.

[103] P. Lura, K.v. Breugel, I. Maruyama, Effect of curing temperature and type of cement on early-age shrinkage of high-performance concrete, Cement and Concrete Research, 2001 (2001) 1967-1872.

[104] P. Lura, Autogenous deformation and internal curing of concrete, in: DUP Science, Delft University, Delft, NL, 2003.

[105] P.K. Mehta, P.J.M. Monteiro, Concrete: microstructure, properties, and materials, 3 ed., McGraw-Hill, New York, 2006.

[106] A.C. 209, Report on Factors Affecting Shrinkage and Creep of Hardened Concrete (ACI 209.1R-05), in, American Concrete Institute, Farmington Hills, Michigan, 2005.

[107] S.A. Rodger, D.D. Double, The chemistry of hydration of high alumina cement in the presence of accelerating and retarding admixtures, cement and Concrete Research, 14 (1984) 73-82.

[108] P. Barret, D. Bertrandie, Hydration of Aluminate Cements, in: M.W. Grutzeck, S.L. Sarkar (Eds.) Advances in Cement and Concrete, American Society of Civil Engineers, University of New Hampshire, Durham, NH, 1994, pp. 132-174.

[109] M.T. Gaztanaga, S. Goni, J.L. Sagrera, Reactivity of high-alumina cement in water: pore solution and solid phase characterization, Solid State Ionic, 63 (1993) 797-802.

[110] N. Ukrainczyk, T. Matusinović, Thermal properties of hydrating calcium aluminate cement pastes, Cement and Concrete Research, 40 (2010) 128-136.

[111] T. Chotard, N. Gimet-Breart, A. Smith, D. Fargeot, J.P. Bonnet, C. Gault, Application of ultrasonic testing to describe the hydration of calcium aluminate cement at the early age, Cement and Concrete Research, 31 (2001) 405-412.

[112] T. Chotard, J. Barthelemy, A. Smith, N. Gimet-Breart, M. Huger, D. Fargeot, C. Gault, Acoustic emission monitoring of calcium aluminate cement setting at the early age, Journal of materials science letters, 20 (2001) 667-669.

[113] H.G. Midgley, A. Midgley, The conversion of high alumina cement, Mag Concr Res, 27 (1975) 59-77.

[114] A. Bachiorrini, L. Montanaro, A. Delmastro, Microstructural disorder and calcium carbonate reactivity with monocalcium aluminate during hydration, Materials chemistry and physics, 14 (1986) 41-46.

[115] T. Matusinović, J. Šipušić, N. Vrbos, Porosity–strength relation in calcium aluminate cement pastes, Cement and concrete research, 33 (2003) 1801-1806.

[116] C. Gosselin, Microstructural development of calcium aluminate cement based systems with and without supplementary cementitious materials, in: Labratoire des Materiaux de Construction, Ecole Polytechnique Federale de Lausanne 2009, pp. 219.

[117] J.H. Ideker, Early-Age Behavior of Calcium Aluminate Cement Systems, in, Thesis(PhD), University of Texas, Austin, 2008, pp. 296.

[118] O. Kirca, I. Yaman, M. Tokyay, Strength Development of Calcium Aluminate Cement Blends at Different Temperatures, in: C. Fentiman, R.J. Mangabhai, K.L. Scrivener (Eds.) Calcium Aluminate Cements Proceedings of the Centenary Conference, IHS BRE Press, Palais des Papes, Avignon, France, 2008, pp. 487-499.

[119] M. Eglinton, Resistance of concrete to destructive agencies, in: P.C. Hewlett (Ed.) Lea's Chemistry of Cement and Concrete, Elsevier, Oxford, UK, 1998.

[120] R.C. Hibbeler, Mechanics of Materials, Fifth ed., Prentice Hall Pearson Education, Inc., Upper Saddle River, NJ, USA, 2003.

[121] T.C. Powers, Structure and physical properties of hardened portland cement paste, Journal of the American Ceramic Society, 41 (1958) 1-6.

[122] ASTM C31, Standard practice for making and curing concrete test specimens in the field, in: ASTM International (Ed.), ASTM International, West Conshohocken, PA, 2012.

[123] European Committee for Standardization, Calcium aluminate cement - Composition, specifications, and conformity criteria, in: EN 14647, European Committee for Standardization, Brussels, 2005.

[124] Texas Department of Transportation, TxDoT SS-4491 Class CAC Concrete, in, Texas Department of Transportation, Austin, TX, 2009.

[125] ASTM International, Form and style for ASTM Standards, ASTM International, West Conshohocken, PA, 2015.

[126] P. Picariello, Fact vs. fiction: The truth about precision and bias, in: ASTM Standardization News, ASTM International, West Conshohocken< PA, 2000, pp. 16-19.

[127] ASTM Standard E691 2014, Standard Practice for Conducting an Interlaboratory Study to Determine the Precision of a Test Method, in: A. International (Ed.), West Conshohocken, PA, 2015.

2 Experimental Methods

This section describes the experimental procedures used throughout the dissertation. In places where information is particular to a certain manuscript, the reader will be directed to see the individual manuscripts for more information

2.1 Materials

The materials used in testing are described in each individual manuscript. The reader should refer to each chapter individually for an explanation of the materials used in this research.

2.2 Mixture Design and Mixing Protocols

2.2.1 Mixture Designs

Cement, mortar, and concrete mixtures used in the research presented herein are described in detail in each individual manuscript. General guidelines for creation of CAC mixtures as discussed in Section 1.4.11 were followed for the initial mixture design parameters. The readers should refer to the manuscripts for this information.

2.2.2 Mixing Procedures

Mixing of cement pastes and mortars was performed according to ASTM C 305 [1]. When necessary for the paste and mortar mixtures, admixtures were incorporated by addition into the water for each mixture. Mortar cubes were cast according to ASTM C 109 [2].

A Gilson brand drum type mixer with a 0.17m^3 capacity that rotated at 25 RPM was used for all concrete mixtures. Cement paste and mortar mixtures were mixed in Hobart N50 paddle type mixer with a 4.7 dm^3 volume capacity.

All concrete mixtures made were done with the following procedure:

1. Added all aggregates and half of the mixing water to the mixer,
2. Covered the mixer and allow to mix for 1 minute,
3. While still mixing, added the retarder and the super plasticizer,
4. While still mixing, added the cement, and the remaining water over a 1 minute period,
5. Continued to mix for three more minutes,

6. Discharged and cast specimens.

The total mixing time from the time the mixer was first started was 4.5 minutes ± 10 seconds. Aggregates for both concrete and mortar systems were brought to near SSD conditions prior to mixing. Their moisture contents were then measured, and the total mixture water was adjusted to ensure that the w/cm was maintained.

Concrete mixtures were done in the laboratory with an ambient temperature of 23 ± 2 °C. The relative humidity in the laboratory was not controlled or monitored. Concrete specimens were cast according to ASTM C192 [3].

2.3 Sample Preparation and Handling

2.3.1 Concrete Fresh Properties Testing

Concrete temperature, unit weight, and slump were measured for each mixture directly after mixing. Unit weight was measured according to ASTM C 138 [4]. Slump was measured according to ASTM C 143 [5].

2.4 Curing Procedures

Curing procedures for each set of experiments varied depending on the work being done. Curing procedures are described individually in each manuscript.

2.4.1 Stopping of Hydration

Advanced microstructural analysis techniques often require dried samples in which hydration has been arrested. The most widely used technique to arrest hydration is oven or microwave drying [6, 7]. However, this method can induce damage in the system [6] as well as alter the structure of CAC hydrates, such as CAH_{10} which decomposes around 110°C [8]. An alternative method, which induces much less damage to the CAC system, is the solvent exchange method.

The solvent exchange method was described in detail in Zhang and Scherer [6], who found that isopropanol was the best organic solvent to use for this technique. For this method, thin slices of concrete or mortar were sliced using a diamond wafering-blade. The thin slices were then placed in isopropanol for 7 days, replacing the isopropanol once after 24 hours. During this soak period, the pore solution was replaced by the isopropanol through diffusion. The samples were then placed into

a desiccator for at least two days to evacuate the isopropanol from the system. This technique has been used to effectively study the microstructure of CAC samples in previous work [9, 10].

2.5 Mechanical Properties Testing

Mechanical properties testing was performed on 100 mm diameter x 200 mm height cylinders or 50 mm x 50 mm x 50 mm cubes. Exact specimens are described in each individual chapter of this dissertation. Curing conditions for specimens varied throughout the study and are presented individually within the dissertation.

Mechanical property testing presented in this dissertation was performed using a Forney FHS-700 testing machine pictured in Figure 2-1.

Figure 2-1: Forney FHS-700 used to measure mechanical properties

Compression testing for cylinders followed ASTM C 39. The precision and bias statement for this test method notes that the coefficient of variation for specimens according to this test method is 3.2% within-laboratory, and 5% between laboratories [11]. ASTM C 109 was followed for measuring the compressive strength of mortar cubes. The precision and bias statement for this test method notes that the coefficient of variation for specimens according to this test method is 3.7% within-laboratory

[2]. It is important to note, however, that these precision statements were developed for OPCconcrete systems, and therefore are not applicable to the CAC systems presented in this dissertation. This statement applies to all the precision and bias statements presented in this section. The values are useful for comparison, however.

Modulus of elasticity was measured according to ASTM C 469. The precision and bias statement for this test method notes that the coefficient of variation for specimens according to this test method is 4.25% within-laboratory, but only applies to the range of 17 – 28 GPa [12]. Tensile strength was measured according to ASTM C 496. The test method does not provide a precision statement for use with 100 mm diameter specimens [13].

2.6 Aggregate Property Testing

Aggregate properties were measured for all the aggregates used in this work. Properties including specific gravity, absorption capacity, dry rodded unit weight, fineness modulus, and grading were assessed. Sieve analyses were performed according to ASTM C 136 [14], except for one aggregate from Canada which was done according to CSA-A23.2-2A-14 [15]. Specific gravity and absorption capacity were measured according to ASTM C 128 for fine aggregates [16] and ASTM C 127 for coarse aggregates [17].

2.7 Volume Stability Measurement Procedures

2.7.1 Chemical Shrinkage

Chemical shrinkage is a measurement of the relative volume reduction observed during cement hydration and does not result in macroscopic volume change after setting, but instead relates to the amount of porosity that develops in the system during hydration [18, 19]. Chemical shrinkage measurements were performed according to ASTM C1608 [20] with some minor modifications. The paste sample was mixed in accordance with ASTM C305 [1]. Before mixing, the dry cement powder was sieved through a sieve with opening size of 0.8 mm. It was then mixed with deionized and deaired water at room temperature. The cement paste (~3 g per vial) was then placed into 25 mL hard plastic vials. The vial was filled with deionized and deaired water. The vial was closed using a rubber stopper that was pierced with a 1mL glass pipette. Care was taken during this process and during the placing of the cement paste to ensure that no air bubbles were entrapped in the system. The pipette was then filled with water, and a small amount of oil with coloured dye was placed into the pipette to prevent

water loss to the air. The vials and pipettes were then placed into a water bath to maintain a constant temperature of 20 ± 0.5 °C during the testing period. The pipette was then monitored over the test period to measure the amount of water sorbed into the system and the amount of chemical shrinkage was determined. An alternative system of monitoring than that described in the testing standard was used. Instead of manually monitoring the amount of water sorbed into the system, monitoring was automated through the use of a webcam and image analysis program as described in references [19, 21]. The chemical shrinkage set up was similar to that be seen below in Figure 2-2 [19].

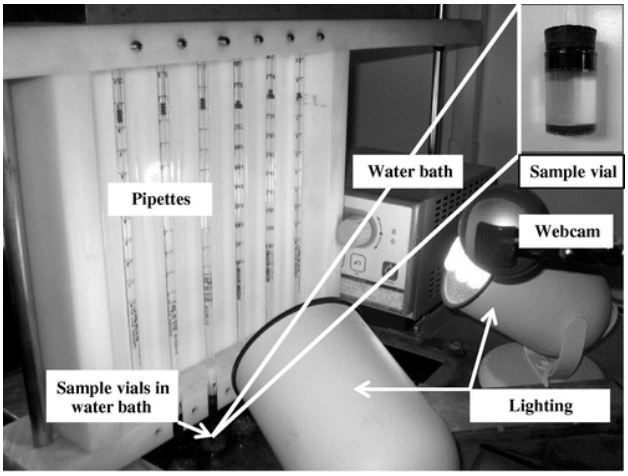

Figure 2-2: Automated chemical shrinkage monitoring apparatus [19]

Monitoring of chemical shrinkage began 30 ± 5 minutes after the cement powder contacted water in the mixer. The delay between mixing and monitoring was due to the time period required to cast the sample and place it in the chemical shrinkage apparatus.

2.7.2 Autogenous Shrinkage

Autogenous deformation is a measurement of the macroscopic volume change that occurs in a closed system due to hydration. Shrinkage may occur due to self-desiccation that causes water filled pores to collapse as the water is drawn out and consumed in hydration products [18]. Autogenous deformation was measured through the use of a small scale free deformation frame as described by Ideker et al. [22]. The free deformation frame measured the autogenous deformation of a 50.8 x 50.8 x 175 mm mortar bar that had an effective gage length of 135 mm. The frame can be seen below in Figure 2-3 and Figure 2-4.

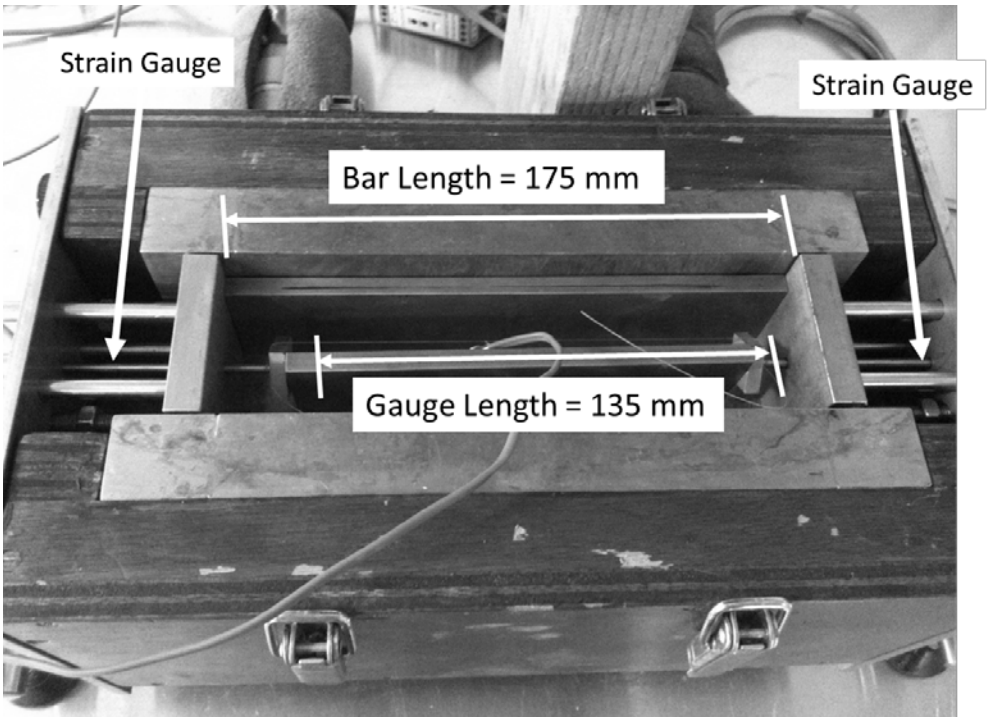

Figure 2-3: Interior of the free deformation frame

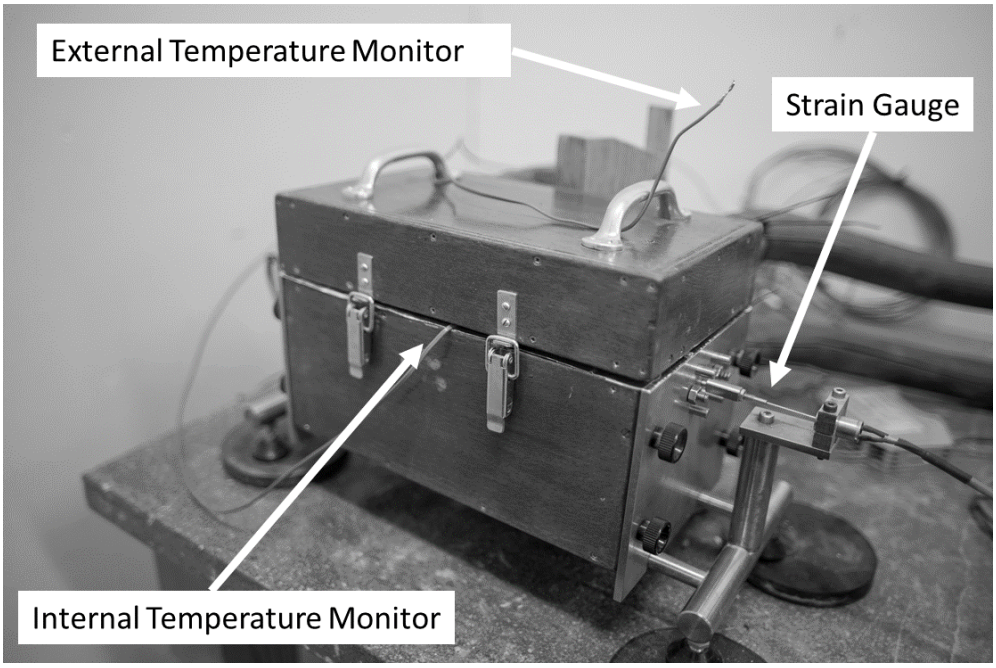

Figure 2-4: Exterior of closed and sealed free deformation frame

A mortar mixture was cast into the frame, and then sealed to prevent moisture loss to the outside environment. Mixing was performed according to ASTM C305 [1]. Setting time samples were matched

cured at 20 ± 3°C. Invar steel rods were embedded into the mortar bar with aluminium plates set at the gage length stated above. The other ends of the bars were attached to linear control potentiometers at either end of the frame. Initially the mortar was prevented from slumping by two moveable steel plates at either end of the specimen. These plates were released after final set, as determined by ASTM C403 [23] to allow free movement of the specimen for the remainder of the testing period.

Temperature of the specimen in the free shrinkage frame was regulated through the use of a cooling/heating water circulator. The circulator pumped water through the formwork of the free deformation frame to maintain a temperature of 20°C in the sample. Temperature was monitored through the use of a thermocouple embedded into the specimen when it was cast. Temperature of the setting time sample was not isothermally controlled. Due to the high heat of hydration of CAC and CSA cements, the standard size test specimen used for measuring setting time on mortars was too large to properly control isothermally. Therefore, the final set measured may not have matched exactly the final set time of the sample in the free deformation frame.

2.7.3 Free Drying Shrinkage

Drying shrinkage is caused when water in capillary pores is lost to the environment. This will occur when concrete is exposed to an environment that has less than 100% relative humidity and will continue to occur until the relative humidity inside the concrete equilibrates with external humidity conditions. As the water leaves these small pores, it creates pressures, which may cause the pores to collapse [18, 24]. Free drying shrinkage monitoring of specimens was implemented according to ASTM C157 [25]. Measurements were taken on hardened concrete prisms 75mm x 75 mm x 285mm. Specimens were cast in hard plastic moulds (3 prisms for each mixture), and then allowed to cure covered under wet burlap in ambient laboratory conditions (23 ± 4°C) for 10 hours or 24 hours according to the mixtures listed above. Specimens were then removed from their moulds and placed into an environmental chamber set to 23 ± 2°C and 50 ± 4% relative humidity. During drying, the length change and mass change were measured.

2.8 Analytical Methods

2.8.1 Pore Solution Analysis through ICP-OES

Concrete pore solutions were measured for several mixtures as a part of the study included in this work. Pore solution was expressed through mechanical methods. Samples from which pore solution

was obtained were removed from curing conditions and were cut into 25-50 mm thick discs, wrapped in plastic wrap, and stored in plastic freezer type bags and placed in a freezer to arrest hydration until pore solution extraction began. Samples were allowed to thaw for 12 hours at ambient temperatures in their plastic bags before being crushed for pore solution extraction. The pH was measured within three hours of extraction. Pore solution samples were stored at room temperature in capped vials between extraction and pH measurements. Solutions were analyzed within one week of extraction. Solutions were stored in capped vials wrapped in paraffin wax film in a refrigerator between pH measurements, and analysis through ICP.

After thawing, the samples were then crushed inside plastic freezer type bags with a hammer to particles smaller than 9.5 mm. As much aggregate as possible was removed from crushed concrete material by hand, to obtain as much of the mortar fraction as possible. The crushed mortar fraction or paste was then placed into the pore solution extraction dye system. The disassembled dye system can be seen in Figure 2-5 and the assembled dye system placed in the compression machine before applying load to express solution can be seen in Figure 2-6.

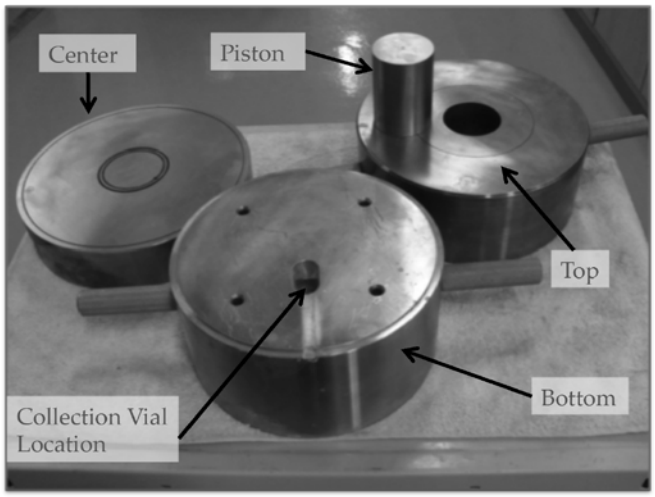

Figure 2-5: Disassembled pore solution extraction dye system

Figure 2-6: Assembled pore solution extraction dye system placed in compression machine

The crushed mortar fraction or paste (~250-300 g of material) was placed into the open hole in the top section of the dye system, resting on middle section of the dye system. A Teflon disc was then placed on top of the mortar to provide an even surface and protection for the piston during operation. Using the Forney compression machine shown above, the piston was then pushed into the dye, placing the crushed concrete under high pressures and forcing the pore solution to leave the system. The pore solution was collected in the grooves seen in the middle section, and then deposited into a vial placed in the bottom section of the dye. Paste samples were loaded to a maximum load of 890 kN, concrete samples were loaded to a maximum load of 2224 kN.

Samples from unconverted CAC systems (1 day samples) produced much less pore solution, ~0.5 - 1 ml per sample, compared converted samples (3-28 day samples) which produced ~ 2 – 4 ml per sample. This was expected because, as discussed above in Section 1.4.5, the metastable hydrate products produced during CAC hydration bind a significant amount water into their hydrate structures that is then released during conversion [26]. Therefore converted systems will have significantly higher amounts of pore solution. Consecutive samples from each test date and system processed in this manner until enough solution (5 ml) was obtained for testing.

The pH was measured using a pH electrode. Pore solution samples were diluted and acidified in a matrix of 2% HNO_3 prior to analysis in inductively coupled plasma-optical emission spectrometry (ICP-OES). Calcium, silicon, aluminium, potassium, and sodium concentrations were measured. Results presented represent actual concentrations in pore solution, calculated from the diluted

concentrations measured in the ICP-OES. The ICP-OES apparatus used was a Leeman Labs, Inc. Prodigy High Dispersion ICP seen below in Figure 2-7.

Figure 2-7: ICP-OES apparatus used in this work

2.8.2 Scanning Electron Microscopy, Energy Dispersive X-Ray Analysis, and Sample Preparation

Samples used for examination under the scanning electron microscope (SEM) were created from concrete specimens. Samples of around 20 mm x 20 mm x 3 mm were cut from the center of concrete cylinders and their hydration was arrested according to the solvent exchange method described above. After the solvent was removed via placement in a dessicator, the samples were mounted and impregnated with epoxy to stabilize the system. A 2-part transparent epoxy system, EpoTek – 301 was used for this work. Samples were mounted and impregnated using a Struers CitoVac vacuum impregnation device seen below in Figure 2-8.

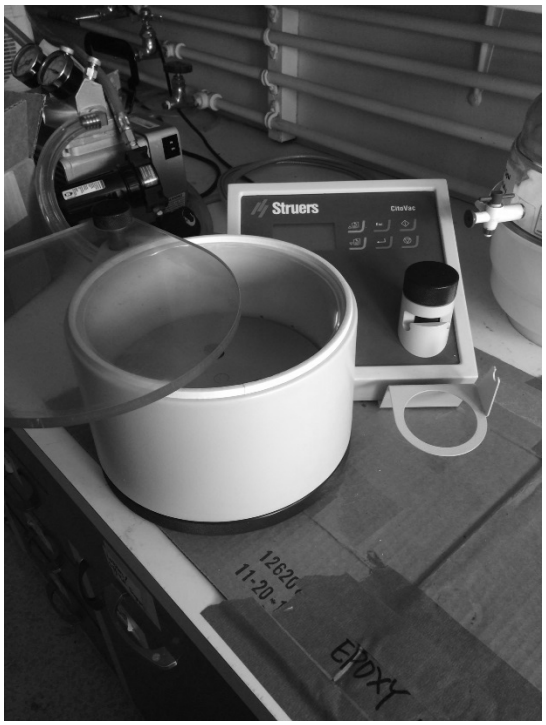

Figure 2-8: CitoVac epoxy impregnation system

After mounting and impregnation, the epoxy was allowed to cure for at least 48 hours. The epoxy was then removed down to the surface of the concrete sample using a Struers brand LaboPol-5. A 200 μm grit pad rotating at 300 rpm was used to grind off the epoxy from the surface of the concrete. Samples were held by hand during this polishing process. Isopropanol was used as a lubricating liquid during this portion of polishing. An image of this polishing device can be seen below in Figure 2-9.

Figure 2-9: LaboPol-5 polisher

After the epoxy was ground off of the sample, the samples were placed in isopropanol and cleaned in an ultrasonic cleaner. Then the samples were fine polished using a Struers LaboPol-35 polishing system with a LaboForce-1 counter-rotation sample holder seen below in Figure 2-10.

The polishing pad was rotated at 150 rpm during polishing, and the counter-rotation sample holder spun at 8 rpm. Diamond polishing sprays, sprayed onto a Struers MD-Largo polishing disc were used as the grit for fine polishing of the concrete samples. 9 μm grit, 3 μm grit, and a 1 μm grit were used in succession to create a smooth surface on the concrete sample for examination under the SEM. Samples were polished for six hours with the 9 μm grit, three hours with the 3 μm grit, and three hours with the 1 μm grit. Diamond grit was reapplied once every hour. Samples were cleaned in the ultrasonic cleaner every two hours or between grits. An oil-based polishing fluid from Logitech was used to lubricate and remove waste material from polishing plate during operation. Samples were placed into the dessicator after polishing for at least 48 hours to remove any remaining volatiles in the system prior to examination under the SEM. Also, samples were sputter coated with carbon prior to examination under the SEM.

Figure 2-10: LaboPol-35 polishing system with LaboForce-1 counter rotation sample holder

An FEI Quanta 600F environmental SEM was used under high vacuum with a BSE detector was used to image the samples. A beam acceleration voltage of 15kV was used to examine the samples. The SEM used in this study can be seen below in Figure 2-11.

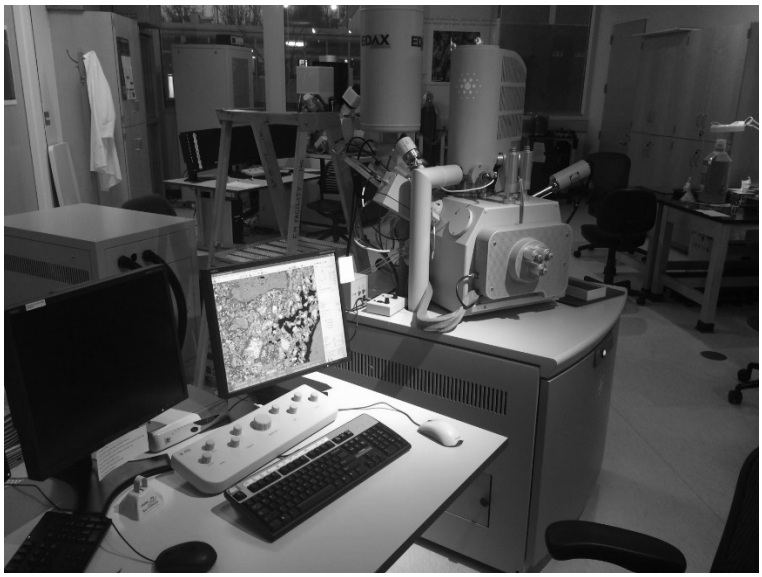

Figure 2-11: FEI Quanta 600F environmental SEM

An X-ray energy dispersive spectrometer (EDX) was used in the SEM to perform elemental spectra point and map analyses.

2.9 Works Cited

[1] ASTM C 305 2014, Standard practice for mechanical mixing of hydraulic cement pastes and mortars of plastic consistency, in: ASTM International (Ed.), ASTM International, West Conshocken, PA, 2015.

[2] ASTM C 109 2013, Standard test method for compressive strength of hydraulic cement mortars (using 2-in. or [50-mm] cube specimens, in: A. International (Ed.), ASTM International, West Conshohocken, PA, 2015.

[3] ASTM C 192 2014, Standard practice for making and curing concrete test specimens in the laboratory, in: A. International (Ed.), ASTM International, West Conshohocken, PA, 2015.

[4] ASTM C 138 2014, Standard test method for density (unit weight), yield, and air content (gravimetric) of concrete, in: A. International (Ed.), ASTM International, West Conshohocken, PA, 2015.

[5] ASTM C143 2012, Standard test method for slump of hydraulic-cement concrete, in: A. International (Ed.), ASTM International, West Conshohocken, PA, 2015.

[6] J. Zhang, G.W. Scherer, Comparison of methods for arresting hydration of cement, Cement and Concrete Research, 41 (2011) 1024-1036.

[7] C. Gosselin, Microstructural development of calcium aluminate cement based systems with and without supplementary cementitious materials, in: Faculte Sciences and Techniques de l'Ingenieur, Ecole Polytechnique Federale de Lausanne, Lausanne, Switzerland, 2008.

[8] H. Fryda, K.L. Scrivener, G. Chanvillard, C. Feron, Relevance of Laboratory Tests to Field Applications of Calcium Aluminate Cement Concretes, in: International Conference on Calcium Aluminate Cements (CAC), IOM Communications, Heriot-Watt University, Edinburgh, Scotland, UK, 2001, pp. 215-247.

[9] C. Gosselin, Microstructural development of calcium aluminate cement based systems with and without supplementary cementitious materials, in: Labratoire des Materiaux de Construction, Ecole Polytechnique Federale de Lausanne 2009, pp. 219.

[10] J. Bizzozero, Hydration and dimensional stability of calcium aluminate cement based systems, in: Materials Science and Engineering, Ecole Polytechnique Federal de Lausanne, Lausanne, Switzerland, 2014.

[11] ASTM C39 2012a, Standad test method for compressive strength of cylindrical concrete specimens, in: A. International (Ed.), ASTM International, West Conshohocken, PA, 2015.

[12] ASTM C 469 2014, Standard test method for static modulus of elasticity and poisson's ratio of concrete in compression, in: A. International (Ed.), ASTM International, West Conshohocken, PA, 2015.

[13] ASTM C 496 - 2011, Standard test method for splitting tensile strength of cylindrical concrete specimens, in: A. International (Ed.), ASTM International, West Conshohocken, PA, 2015.

[14] ASTM C 136 2014, Standard test method for sieve analysis of fine and coarse aggregates, in: A. International (Ed.), ASTM International, West Conshohocken, PA, 2015.

[15] CAN/CSA-A23.2-2a-14, Sieve analysis of fine and coarse aggregate, in: C.S. Association (Ed.), Canadian Standards Association, Toronto, Canada, 2014.

[16] ASTM C 128 2015, Standard test method for relative density (specific gravity) and absorption of fine aggregate, in: A. International (Ed.), ASTM International, West Conshohocken, PA, 2015.

[17] ASTM C 127 2015, Standard test method for relative density (specific gravity) and absorption capacity of coarse aggregate, in: A. International (Ed.), ASTM International, West Conshohocken, PA, 2015.

[18] P.K. Mehta, P.J.M. Monteiro, Concrete: microstructure, properties, and materials, 3 ed., McGraw-Hill, New York, 2006.

[19] T. Fu, T. Deboodt, J.H. Ideker, Simple procedure for determining long-term chemical shrinkage for cementitious systems using improved standard chemical shrinkage test, J Mater Civ Eng, 24 (2012) 989 - 995.

[20] ASTM Standard C1608 2012, Standard test method for chemical shrinkage of hydraulic cement paste, in: ASTM International (Ed.), West Conshohocken, PA, 2013.

[21] T. Fu, Shrinkage study of high performance concrete for bridge decks, in: School of Civil and Construction Engineering, Oregon State University, Corvallis, OR, 2013.

[22] J.H. Ideker, K.J. Folliard, M.D.A. Thomas, Early-age properties of calcium aluminate cement concrete with rigid cracking and free shrinkage frames: isothermal testing, in: C. Fentiman, R. Mangabhai, K. Scrivener (Eds.) Calcium Aluminate Cements: The Centenary Conference, IHS BRE Press, Avignon, FR, 2008.

[23] ASTM C 403 2008, Standard test method for time of setting of concrete mixtures by penetration resistance, in: ASTM International (Ed.), ASTM International, West Conshocken, Pennsylvania, 2015.

[24] S. Mindess, J.F. Young, D. Darwin, Concrete, 2 ed., Pearson Education, Inc., Upper Saddle River, NJ, 2003.

[25] ASTM C 157 2008 (2014e1), Standard test method for length change of hardened hydraulic-cment mortar and concrete, in: A. International (Ed.), ASTM International, West Conshohocken, PA, 2015.

[26] K.L. Scrivener, A. Capmas, Calcium Aluminate Cements, in: P.C. Hewitt (Ed.) Lea's Chemistry of Cement and Concrete, Elsevier - Butterworth-Heinemann, Oxford, UK, 1998, pp. 713-782.

Manuscript 1

Procedure for Determining the Converted Strength of Calcium Aluminate Cement Concrete

Matthew P. Adams and Jason H. Ideker

To be submitted to: ASTM Journal of Testing and Evaluation

3 Manuscript 1

Procedure for Determining the Converted Strength of Calcium Aluminate Cement Concrete

Matthew P. Adams[1], Jason H. Ideker[2]

Abstract: There is renewed interest in North America for use of calcium aluminate cement in infrastructure repair due to its ability to gain strength rapidly even at low temperatures, the ability to customize fresh workability, and durability in adverse environments. Conversion of the hydration products of concrete, where calcium aluminate cement is the only binder, is a well-known phenomenon which is typically accompanied by strength loss, the rate and extent of which is dependent on the temperature history of the sample, the w/cm, the cement content and the concrete mixture design. An accelerated method of determining the converted strength of calcium aluminate cement concrete that is convenient for use in the field is presented. This test allows the samples to be cast in the field and left at ambient field temperatures for the first 24 hours; then the specimens are moved to the laboratory and placed in a water bath at 50°C to promote conversion. Robustness testing results are presented for the test method. The effects of water to cement ratio, initial (first 24 hours) curing temperature, length of time before placing in the 50°C water bath, and aggregate type are examined. Also studied was the impact of low replacement rates (up to 10%) of FGLS for CAC in concrete mixtures on converted concrete strengths. Results from testing showed that the majority of mixtures converted 48 hours after submersion in the 50°C water bath, however differences in initial curing temperature or aggregate type can delay conversion by up to 11 days when specimens are cured following this procedure. Results also indicate that FGLS at replacement rates of 5% and below in CAC systems may help increase the converted strength observed without reducing initial early strength gain.

Keywords: calcium aluminate cement, conversion, aggregate, curing, finely ground limestone, test methods

[1] Corresponding Author, Ph.D. Candidate, School of Civil and Construction Engineering, Oregon State University
[2] Associate Professor, School of Civil and Construction Engineering, Oregon State University

3.1 Introduction

Calcium aluminate cement (CAC) concrete has been used in the construction industry for over 100 years [1]. Recently, there has been an increased interest in use of the material in cast-in-place rapid repair settings, particularly in North America. The interest in the material is due to its ability to gain strength rapidly, even at low temperatures [2-4]. However, other specialty properties such as scour resistance in dam spillways and wearing surfaces [5], and acid attack resistance for industrial floors and sewage applications [5-8] make it a useful alternative cement for specialty infrastructure applications. As with any other construction material, a robust quality assurance program is necessary to ensure that the material properties meet the design criteria.[9] The nature of CAC hydration, specifically conversion, precludes the use of existing standards to assess mechanical properties which were developed for use with portland cement concrete. Therefore, the development of a standard that is applicable for use where CAC is the only cementitious binder is necessary.

The main phase in CAC, monocalcium aluminate (CA), forms four main phases during the hydration process: CAH_{10}, C_2AH_8, C_3AH_6, and AH_3. The first two hydrates, CAH_{10}, C_2AH_8, are both metastable and will convert into the stable hydrate C_3AH_6. This reaction is known as conversion, and is accompanied by the formation of AH_3 gel, and the release of water [10-12]. The conversion process is driven by temperature as well as access to moisture [10, 13, 14]. At low curing temperatures ($T< 15°C$) the initial metastable hydrate favored to form is CAH_{10}. At higher temperatures ($T>30°C$) C_2AH_8 is favored to form initially. At curing temperatures between 15°C and 30°C, both CAH_{10}, C_2AH_8 will form, though neither is thermodynamically favored and formation will be slow [2-4, 15, 16]. CAH_{10} will convert into C_2AH_8, accompanied by the formation of AH_3 gel and water release. The C_2AH_8 will subsequently convert to the stable C_3AH_6, again accompanied by the formation of AH_3 gel and water release. This process is thermodynamically inevitable, and the rate at which it occurs is a function of the time and temperature history of the material during hydration. Increasing the curing temperature and exposure to moisture will result in faster conversion from the metastable hydrates to the stable hydrates [13, 14, 17]. The density of the metastable hydrates (density (g/cm^3): CAH_{10}=1.72, density of C_2AH_8=1.95) is lower than that of the stable hydrates (density (g/cm^3): C_3AH_6=2.52 AH_3=2.4) [10, 11, 18]. The increase in density as the hydrates undergo conversion causes porosity to form in the hydrated cement paste, thus causing compressive strength to drop. After

conversion occurs, and a minimum strength has been reached, the water released by conversion can continue to hydrate unhydrated cement grains resulting in continued long-term strength gain [10, 18].

A standard method used for sampling and curing concrete specimens for compressive strength testing, ASTM C31, states that cylinders should be cast on site, and allowed to be cured on site for a period up to 48 hours. The cylinders should then be moved to a moist cabinet where they are cured at 23 ± 2°C until tested [19]. This curing regime will not allow for obtaining the minimum strength of CAC concrete within a convenient time period because the metastable hydrates will not convert quickly to the stable hydrates. This is due to the typical small sample size of field cast cylinders (100 x 200 mm or 150 x 300 mm) which dissipate heat rather quickly and thus would not promote the full conversion of samples thereby resulting in a higher, unconverted strength at the time of testing. Consequently, one approach is to cure the cylinders at a higher temperature and in direct contact with water to ensure the conversion of the metastable hydrates [11].

There are two main methods that are currently used to promote accelerated conversion of CAC hydrates to obtain a minimum compressive strength of a given CAC concrete within a reasonable time. The method described in EN 14647 is used primarily in Europe. This method states that to achieve the minimum converted strength of CAC concrete rapidly, the test specimens should be placed in a 38°C water bath directly after being cast. According to this standard, the minimum converted strength will occur at five days after casting and subsequent submersion in the heated water bath [20]. The standard used by the Texas Department of Transportation, in Texas, U.S.A. that the specimens should be placed immediately in a heavily insulated box after casting. The insulated box takes advantage of the high heat of hydration produced during CAC hydration which is captured to encourage "self-heating" of the specimens [21].

These test methods, while useful for determining the converted strength of CAC concrete, are not convenient for use in the field due to the need for bulky equipment to be brought to each construction site. Fryda et al. [18] proposed a test method that overcomes these challenges by permitting the specimens to be cast and cured on site under ambient conditions, and then transported to the laboratory at a later time where they can be cured. This method allows for the specimens to be kept on site at ambient temperatures for up to 24 hours after casting; and then transported to the laboratory and placed in a heated water bath [18]. It is important to note, that this test method is only valid for use in 100% CAC mixtures. Inclusions of other cementitious materials or replacements will change

the structure of the hydrates formed and invalidate the test method. The following work examines the robustness of the test method proposed by Fryda et al. when performed with key mixture design and curing parameters changed. Additionally, inter-laboratory testing was performed between four laboratories to test the variation in results between laboratories. Finally, this work includes a study of the use of finely ground limestone (FGLS) at replacement rates for CAC of 1%, 2%, 5%, and 10% to understand if converted CAC concrete strengths can be increased through the use of low amounts of the materials.

3.2 Materials

3.2.1 Cement

A standard grade calcium aluminate cement for use in the repair market was used in all mixtures cast. The material had a G_s of 3.24, with a Blaine of 3600-4400 m^2/kg. The oxide composition of the CAC used is presented in Table 3-1

Table 3-1: Oxide composition of CAC

Oxide (% wt)	SiO_2	Al_2O_3	Fe_2O_3	CaO	MgO	Na_2O	K_2O	SO_3	TiO_2	Mn_2O_3	P_2O_5	SrO	LOSS
CAC	4.98	38.23	15.40	37.53	0.71	0.03	0.23	0.06	1.80	0.23	0.13	0.02	0.65

3.2.2 Finely Ground Limestone

A finely ground limestone was also used in this study as a partial replacement for CAC in some mixtures. The chemical analysis of the FGLS used showed that it was 98% pure $CaCO_3$. The material had a G_s of 2.7, with a Blaine of 9800 m^2/kg.

3.2.3 Aggregate

Three different aggregate types were used in this study. The KRC aggregate was a rounded river gravel and sand that contained mostly siliceous volcanic and igneous rocks along with quartzite and microsilica. The MM aggregate was a fractured stone with angular surfaces that comprised of limestone rock. The BLG aggregate was a fractured stone that had rough angular surfaces. This aggregate was composed mainly of granite and greywacke, with small amounts of quartz, basalt, and sandstone. Fine and coarse aggregates of each type were produced from the same sources to make the concrete mixtures.

3.2.4 Concrete Mixtures

The concrete mixtures used for this work are shown in Table 3-2.

Table 3-2: Concrete mixture designs

Mixture Label	Aggregate Type	w/cm	Fine Aggregate (kg/m^3)	Coarse Aggregate (kg/m^3)	Cement Content (kg/m^3)	FGLS Content (kg/m^3)
KRC - 0.35	KRC	0.35	760	920	440	0
KRC - 0.40	KRC	0.40	730	890	440	0
KRC - 0.45	KRC	0.45	730	840	440	0
MM - 0.40	MM	0.40	720	840	440	0
BLG - 0.40	BLG	0.40	730	890	440	0
FGLS - 1%	KRC	0.40	730	890	436	4
FGLS - 2%	KRC	0.40	730	890	431	9
FGLS - 5%	KRC	0.40	730	890	418	22
FGLS - 10%	KRC	0.40	730	890	396	44

The cement content remained constant between mixtures. Aggregate contents were modified according to the aggregate properties and water content to achieve the same unit mixture size of 0.77 m^3. Superplasticizer and a retarder were used to control the workability of each mixture. Dosage rates followed manufacturer's recommendations. The base mixture designs were developed from guidelines suggest that minimum cement content of 400 kg/m^3 be used in all mixtures with a maximum total w/cm of 0.40 [20, 22].

3.3 Experimental Methods

3.3.1 Mixing Techniques

Concrete mixtures were mixed using the following procedure:

1. Added all aggregates and half of the mixing water to the mixer,
2. Covered the mixer and allow to mix for 1 minute,
3. While still mixing, added the retarder and the super plasticizer,
4. While still mixing, added the cement, and the remaining water over a 1 minute period,
5. Continued to mix for three more minutes,

6. Discharged concrete and cast specimens.

The total mixing time from the time the mixer was first started was 4.5 minutes ± 10 seconds. Concrete mixtures were done in the laboratory with an ambient temperature of 23 ± 4 °C. The relative humidity in the laboratory was not controlled or monitored. Concrete specimens were cast according to ASTM C192 [23].

3.3.2 Curing Procedures

The proposed test method suggested by Fryda et al. suggests that the following curing procedure should be followed to obtain a minimum converted strength in CAC concrete within 3 days. The following procedure used as a part of this study is the suggested procedure for a future test method for accelerated determination of converted strength in CAC concrete systems.

Concrete specimens were cast into 100 mm diameter x 200 mm height cylindrical plastic molds. After casting the molds were capped to prevent moisture loss. Therefore, the samples were spaced with at least 75 mm between the outer edges of all samples to allow for dissipation of heat caused by the rapid and significant exotherm the accompanies hydration of CAC concrete [18]. Temperature was monitored for the initial 24 hour period. Concrete specimens reached peak temperatures between 50 - 55°C for less than one hour (unless otherwise noted). This temperature indicates that the specimens did not undergo conversion during the initial curing process. Previous work by Fryda et al. has shown that temperatures above 70°C during initial hydration will result in rapid conversion to stable hydrates [18].

Curing of specimens followed a three phase system, following the procedure designed by Fryda et al. [18].

- Phase 1: Samples were allowed to cure for 24 hours in the plastic molds.
- Phase 2: After 24 hours, the samples were removed from the plastic molds, labeled, and immediately placed into a 50 ±2 °C water bath. The samples were then cured in the 50°C water bath for an addition 27 days.
- Phase 3: On day 28 after casting, any remaining samples were removed from the heated water bath and placed into a moist curing room with a temperature of 23 ± 2 °C, and a > 95% RH until tested.

This curing regime was followed for all specimens except where otherwise indicated.

3.3.3 Compressive Strength Measurements

Compression testing for concrete cylinders followed ASTM C 39 [24]. ASTM C 109 was followed for measuring the compressive strength of the micro-concrete cubes [25]. Compressive strength was measured out to 56 days for most concrete mixtures and 28 days for the mixtures containing FGLS.

3.3.4 Scanning Electron Microscopy

A preliminary examination of the microstructure of some concrete specimens was done as a part of this work through the use of backscatter imaging with a scanning electron microscopy (SEM). Backscatter SEM (BSEM) images were taken using a FEI Quanta 600F SEM. An accelerating voltage of 15kV was employed and back scatter electron (BSE) images of concrete specimens were observed. Samples were taken from the center of concrete cylinders and had their hydration stopped. Observing concrete under the SEM requires dried samples in which hydration has been arrested. The solvent exchange method, as described in detail by Zhang and Scherer [26], was used to arrest hydration for this study. This technique has been used to effectively arrest hydration prior to studying the microstructure of CAC samples in previous work [14, 27]. After the samples' hydration was stopped, they were mounted in epoxy and polished prior to observation under the SEM.

Samples used for examination under the SEM were created from concrete specimens. Samples of around 20 mm x 20 mm x 3 mm were cut from the center of concrete cylinders and their hydration was arrested according to the solvent exchange method described above. After the solvent was removed via placement in a dessicator, the samples were mounted and impregnated with epoxy to stabilize the system. A 2-part transparent epoxy system, EpoTek – 301 was used for this work. Samples were mounted and impregnated using a Struers CitoVac vacuum impregnation device.

After mounting and impregnation, the epoxy was allowed to cure for at least 48 hours. The epoxy was then removed down to the surface of the concrete sample using a Struers brand LaboPol-5. A 200 μm grit pad rotating at 300 rpm was used to grind off the epoxy from the surface of the concrete. Samples were held by hand during this polishing process. Isopropanol was used as a lubricating liquid during this portion of polishing. After the epoxy was ground off of the sample, the samples were placed in isopropanol and cleaned in an ultrasonic cleaner. Then the samples were fine polished using a Struers LaboPol-35 polishing system with a LaboForce-1 counter-rotation sample holder.

The polishing pad was rotated at 150 rpm during polishing, and the counter-rotation sample holder spun at 8 rpm. Diamond polishing sprays, sprayed onto a Struers MD-Largo polishing disc were used as the grit for fine polishing of the concrete samples. 9 μm grit, 3 μm grit, and a 1 μm grit were used in succession to create a smooth surface on the concrete sample for examination under the SEM. Samples were polished for six hours with the 9 μm grit, three hours with the 3 μm grit, and three hours with the 1 μm grit. Diamond grit was reapplied once every hour. Samples were cleaned in the ultrasonic cleaner every two hours or between grits. An oil-based polishing fluid from Logitech was used to lubricate and remove waste material from polishing plate during operation. Samples were then placed into the dessicator after polishing for at least 48 hours to remove any remaining volatiles in the system. Samples were carbon coated prior to examination under the SEM.

3.4 Results and Discussion

3.4.1 Robustness Testing

Four main parameters were varied in this work to determine the robustness of the testing procedure described by Fryda et al. [18]. This involved varying mixture designs and curing procedures. The first parameter varied was the type of aggregate used. Three aggregates were examined, the KRC, BLG, and MM aggregates (coarse and fine portions from the same source).

The second parameter varied was the w/cm in the mixtures using the siliceous river gravel. A w/cm of 0.35, 0.40, and 0.45 were used.

The third parameter varied was the initial Phase 1 curing time prior to being placed in the 50 ±2 °C water bath. The KRC – 0.40 mixture was used for all specimens cast to examine this parameter. The standard procedure calls for the specimens to be removed from their molds at 24 hours, and placed directly into the 50°C water bath. This initial time was varied to 18 hours and 48 hours. These times represent variations in field activities in which the test specimens are returned to the laboratory early (after only 18 hours curing in the field) or delayed (after 48 hours curing in the field) and subsequently placed in the heated water bath.

The fourth parameter investigated was the temperature of curing during Phase 1 of the curing regime. The KRC – 0.40 mixture was used for all specimens cast to examine this parameter. Samples were cured for the initial 24 hours at temperatures of 5 ± 2°C, ambient laboratory temperature (23 ± 4°C), and 382 ± 2°C to simulate the extremes of temperatures that may be encountered on a construction

site. After the initial 24-hour cure, the procedure for Phase 2 and Phase 3 curing, as listed above, was followed. The materials used in these mixtures were placed in temperature controlled areas and allowed to equilibrate to the same temperature as the initial curing temperature to simulate stockpiled materials that were stored in non-temperature controlled situations.

3.4.1.1 Impact of Aggregate Type

Three different mixtures were used to examine the impact of aggregate source on conversion. These mixtures are listed in Table 1 as KRC – 0.40, MM - 0.40, and BLG - 0.40 using the KRC, MM, and BLG aggregates, respectively. The standard curing procedure described above was used for all three mixtures. Figure 3-1 presents the compressive strength of these concrete mixtures to 56 days.

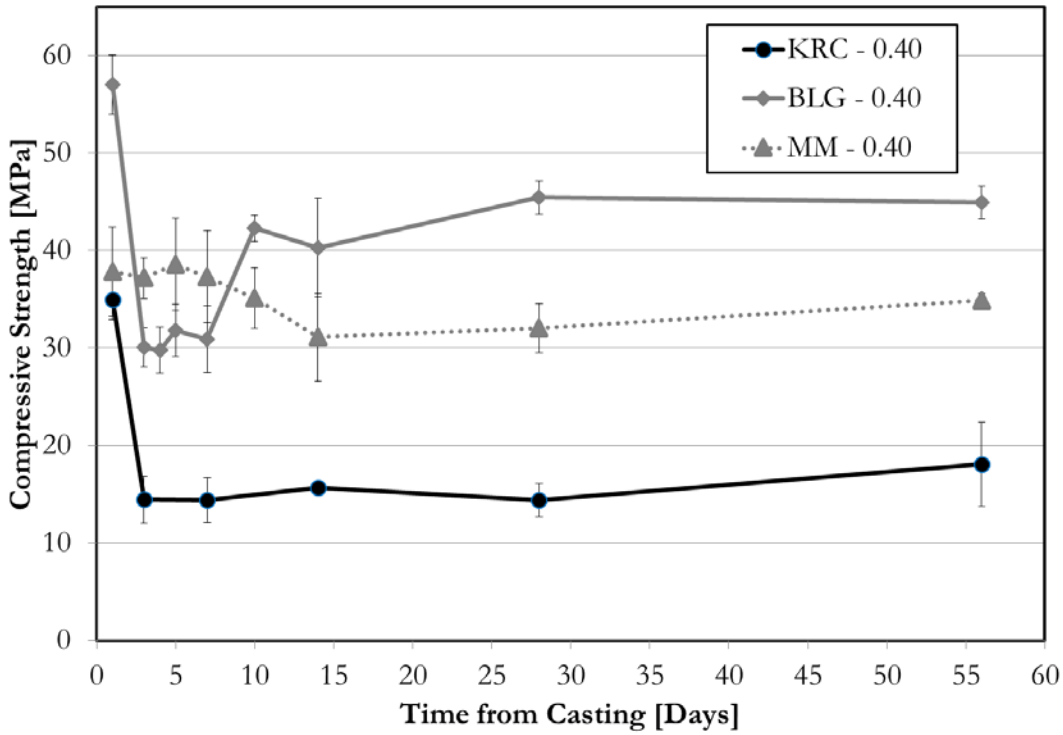

Figure 3-1: Aggregate impact on strength and conversion in CAC concrete

These results show that the source of aggregate had a significant effect on the strength at all ages and also the time to minimum converted strength. The mixture with the KRC aggregate and the mixture with the BLG aggregate both exhibited the same time to conversion: two days after the samples were immersed in the 50°C water bath. However, the mixture made with the BLG aggregate produced

significantly higher strength concrete: 58 MPa in the BLG – 0.40 mixture vs. 41 MPa in the KRC – 0.40 mixture at day one, and 30 MPa in the BLG – 0.40 mixture vs 15 MPa in the KRC – 0.40 mixture at day three (e.g. after conversion). This significant strength difference may be due to inherent strength differences between the aggregates. However, the strength gain due to continued hydration after conversion is significantly higher in the concrete made with BLG aggregates indicating a difference in hydration reactions after conversion between the two concrete mixtures.

The mixture that included the MM aggregate behaved quite differently from the other two mixtures in terms of both kinetics and strength. The initial one-day strength of MM – 0.40 mixture was similar to that of the KRC – 0.40. However, the MM – 0.40 mixture did not reach its minimum converted strength until day 14, despite having been placed in the 50°C water bath directly after the initial 24-hour curing period at ambient temperature per the procedure described above. Additionally, the converted strength of the M – 0.40 mixture did not reduce in strength as significantly (20% strength decrease) as the strength loss observed in both the KRC – 0.40 and the BLG – 0.40 mixtures (59% and 48% strength decreases, respectively).

Visual observations were made of the cracked cylinders after compression testing. When the samples were tested in compression on day one, or prior to conversion, the fractures in the sample continued directly through the aggregates in both the KRC -0.40 and MM 0.40 mixtures. However, after conversion occurred, fractures through the samples with the KRC aggregates propagated around the aggregates; the aggregates remained whole, and came loose from the mortar matrix. This was not observed in the mixtures made with MM aggregate after conversion. These observations may indicate that a change in the interfacial transition zone (ITZ) of the siliceous aggregates during conversion caused the sharper decrease in strength compared to the limestone type aggregates.

BSEM images were taken of samples from the KRC – 0.40 and MM – 0.40 mixtures. Figure 3-2 presents the BSEM images of CAC concrete made with the KRC aggregate at day 1, and day 14.

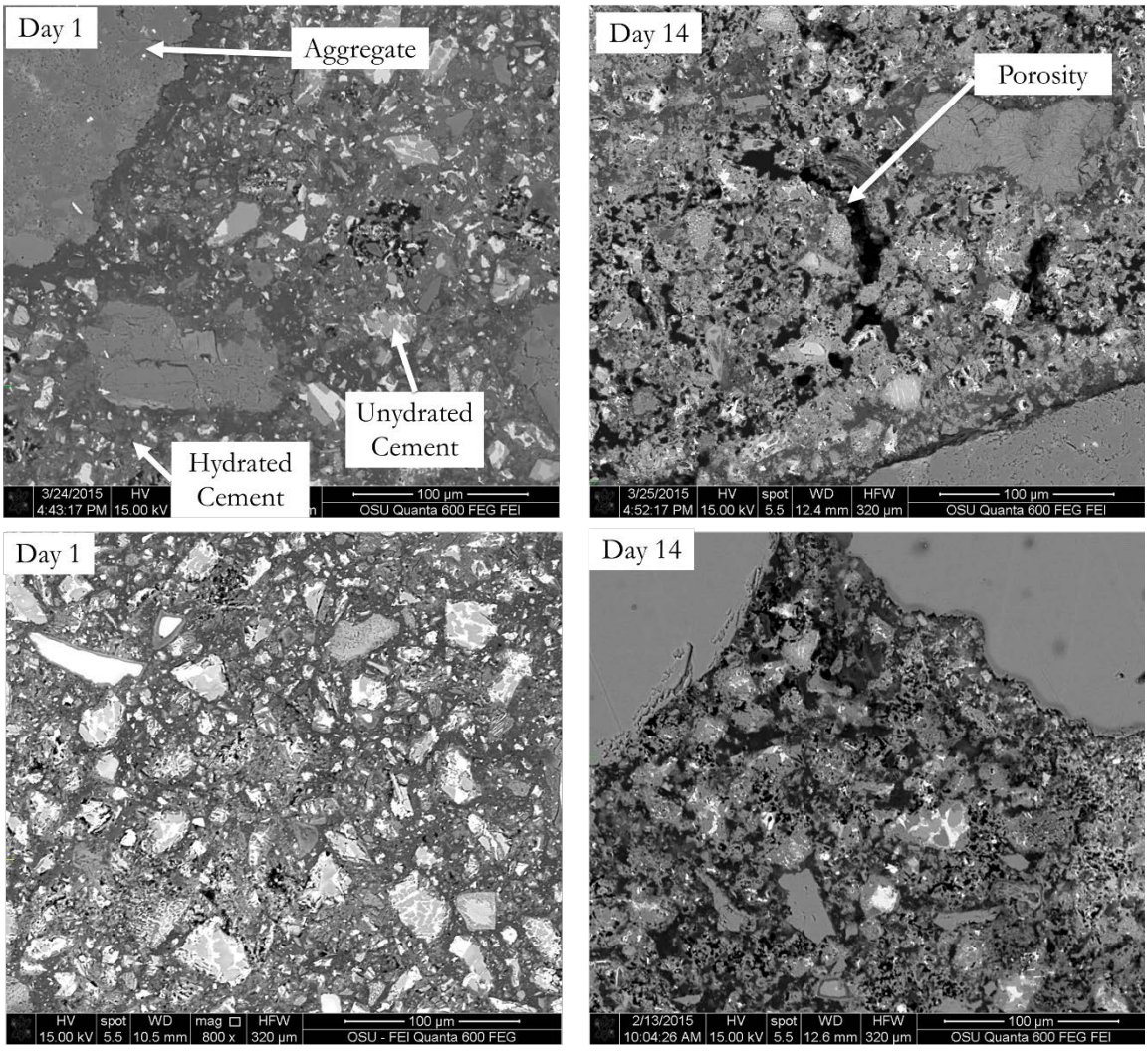

Figure 3-2: BSEM images of KRC - 0.40 sample at day 1 and day 14

In the images taken from the day 1 sample the ITZ around the aggregate was observed to be quite dense and well formed. Some porosity was observed in the bulk paste, however, the majority of the cement paste matrix was quite dense. The strength development curve indicated that this sample was fully converted by day 14, having reached its minimum strength already at day three. Comparatively higher levels of porosity were observed in the converted sample compared to the unconverted sample, both in the ITZ, and the bulk cement matrix.

Figure 3-3 presents the BSEM images of CAC concrete made with the KRC aggregate at day 1, and day 14.

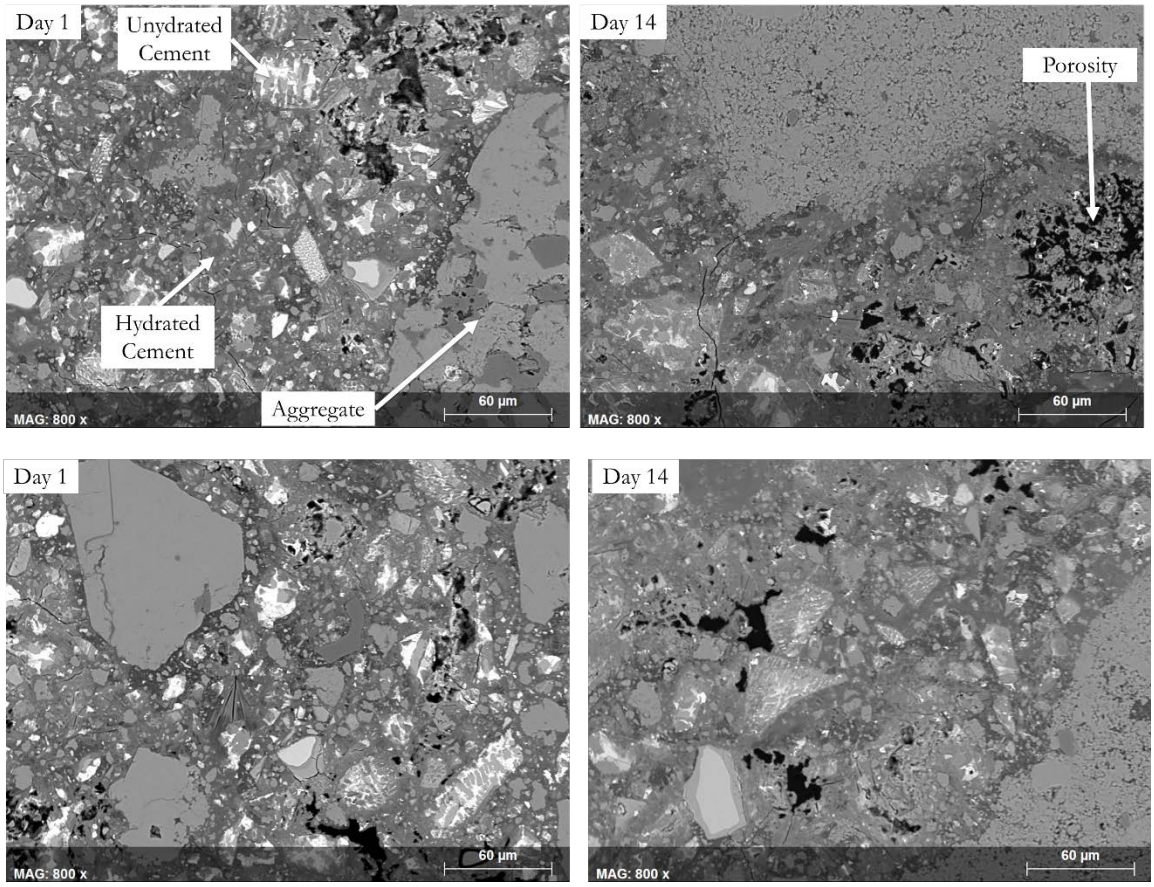

Figure 3-3: BSEM images of MM - 0.40 sample at day 1 and day 14

The day 1 sample showed a well formed and dense bulk cement matrix and ITZ, similar to what was observed in the day 1 KRC – 0.40 sample. The strength development curve indicated that this sample was fully converted by day 14 which was when these samples reached minimum converted strength. At day 14 some additional porosity was observed in the bulk cement paste compared to the day 1 sample, however the ITZ in the 14 day sample was still quite dense and very little porosity was observed around the aggregate. A relatively lower amount of porosity was also observed in the bulk cement paste of the MM – 0.40 system after conversion at day 14 compared to the KRC – 0.40 system at day 14.

The high level of porosity observed around the KRC aggregates after conversion compared to what was observed in the MM – 0.40 system suggests that a less well-formed ITZ may be forming around the KRC aggregates. These results corroborate the visually observed cracking patterns observed in the compressive strength samples. Additionally the relative levels of porosity observed in bulk cement matrix the MM – 0.40 mixture compared to the KRC – 0.40 mixture indicate that the limestone system

may develop less porosity overall. The difference in porosity correlates well with the difference in strength reduction due to conversion observed between the two systems. Further work is suggested to quantify the total amount of porosity observed in each system at each day, as well as the amount of porosity in just the ITZ.

The difference in converted strength between mixtures containing limestone aggregates and siliceous aggregates has been observed previous to this study. Cussino and Negro showed that specimens containing limestone aggregates steadily gained strength over a 5 year period, even when similar specimens made with siliceous aggregates lost strength due to conversion [28]. Scrivener and Capmas also noted that CAC concrete made with limestone typically showed strengths about 20% higher than those made with siliceous aggregates, ascribing the difference to bond strengths between the cement paste and aggregates [10]. Lamour et al. observed similar findings in concrete and mortars made with siliceous and limestone aggregates [29].

As discussed above, the use of FGLS in concrete mixtures in high enough dosage rates will result in the formation of calcium monocarboaluminate [28-39]. Cussino and Negro [28] and Lamour et al. [29] assumed that analogous reactions were occurring in the systems containing limestone aggregates, however they did not confirm the existence of calcium monocarboaluminates in the concrete systems containing 100% CAC and limestone aggregates. The use of studies observing cement hydration in the presence of a high surface area material such as FGLS to explain how a larger limestone aggregate, with significantly less surface area on which topochemical reactions may occur may not provide an accurate answer to the results discussed above. Previous researchers have suggested mechanistic work be performed to further understand the differences between CAC concrete made with limestone and CAC concrete made with siliceous aggregates [29].

In the work presented here, the concrete made with KRC aggregates had a minimum converted strength 15 MPa lower than the concrete made with MM aggregates. The difference in strength, and time to conversion seen between the concrete made with MMe aggregates, and concrete made with KRC aggregates may have been caused by a combination of effects. The strength difference may be attributed to the change in ITZ around the KRC aggregates as was observed in the SEM images. The formation of a more porous band around the aggregates may have weakened the ITZ, and reduced the strength of the concrete. There may also be a chemical affect in the ITZ based on the aggregate

type chosen. Further detailed work examining the differences in microstructure and chemistry between these two systems can be seen in Chapter 4 and Chapter 5 of this dissertation.

The difference in shape and surface texture may have provided extra strength in the mixtures with the limestone aggregates. The angularity of the limestone aggregates allowed for more mechanical bonding between the cement paste and the aggregates [40, 41]. Aggregate particle shape impacts are typically associated with high strength concrete however, and are typically not as prominent in low and normal strength concrete mixtures where the strength of the cement paste is the controlling factor [42-44]. This relationship has not been well defined for CAC mixtures however.

The delay in converted strength, may be attributed to the formation of calcium monocarboaluminate at early ages. Fentiman observed the formation of calcium monocarboaluminate as a secondary metastable hydrate in systems that contained 25% FGLS as a replacement for CAC. In Fentiman's study, the calcium monocarboaluminate eventually converted to the stable C_3AH_6, though at a slower rate compared CAH_{10} and C_2AH_8 [45] resulting in similar strength loss as the systems not containing FGLS. However, given the difference in surface area between these concrete aggregates and FGLS, the formation of calcium monocarboaluminate needs to be confirmed through further chemical analysis of the hydrated systems.

3.4.1.2 Impact of w/cm

The impact of varying w/cm on the time to conversion and converted concrete strength was examined as a part of this study. Figure 3-4 presents the compressive strength development of mixtures using the KRC aggregate with a w/cm ratio of 0.35. 0.40, and 0.45.

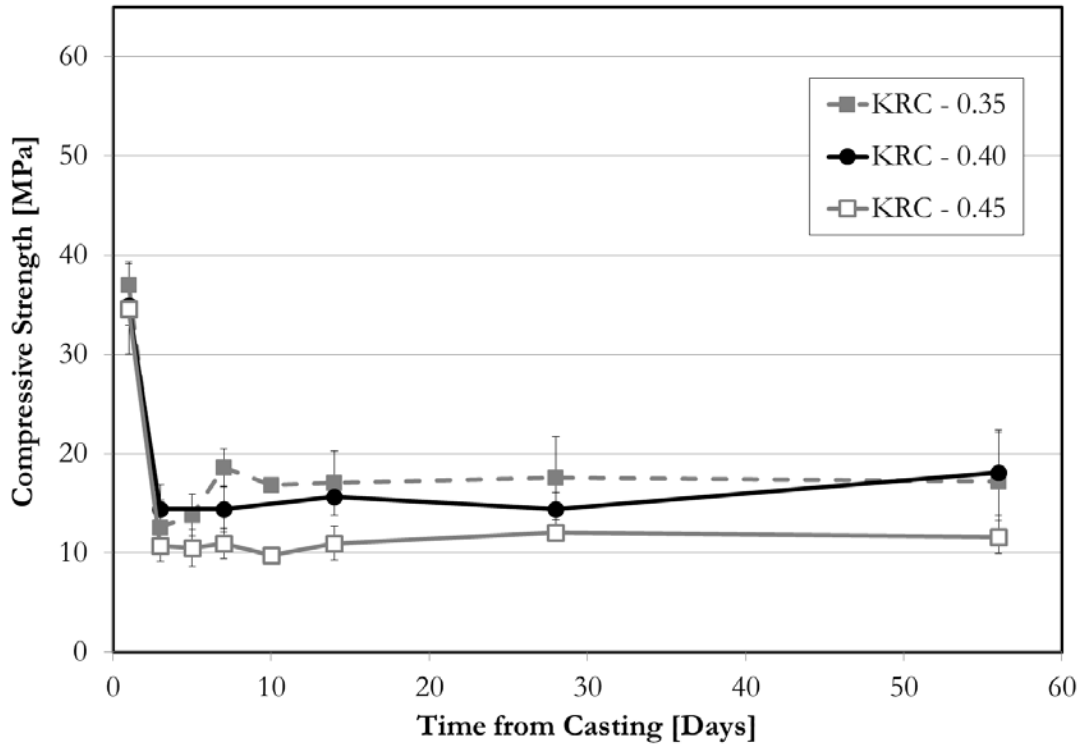

Figure 3-3: Effect of w/cm on time to minimum strength

These results indicate that the w/cm used in mixtures had no impact on conversion time when the standard curing procedures outlined above are followed. The minimum converted strength of all three mixtures was reached at three days after casting, two days after being immersed in the 50°C water bath.

Current standards suggest that a w/cm of 0.40 or lower is necessary to achieve appropriate converted strengths for CAC concrete [20, 22]. The work presented here indicates that while the converted strength was lower at higher w/cm the percent decrease in strength from the maximum strength was similar for all w/cm tested. The low impact of w/cm on converted strength may be due to the already low strength observed in this system due to aggregate choice. Further work is suggested in the future to examine w/cm impact on high strength CAC concrete systems. Continued strength development after conversion due to hydration was observed to be lower for the 0.45 w/cm mixture, however, while being similar in both the 0.35 and 0.40 w/cm mixtures. Therefore, the long-term strength increase was reduced at higher w/cm.

3.4.1.3 Impact of Changes in Phase 1 Curing Time

Figure 3-5 shows the compressive strength development over time for the mixtures examining the impact of changes in the initial curing length observed during Phase 1 of curing. These times were 24 hours, 18 hours, and 48 hours.

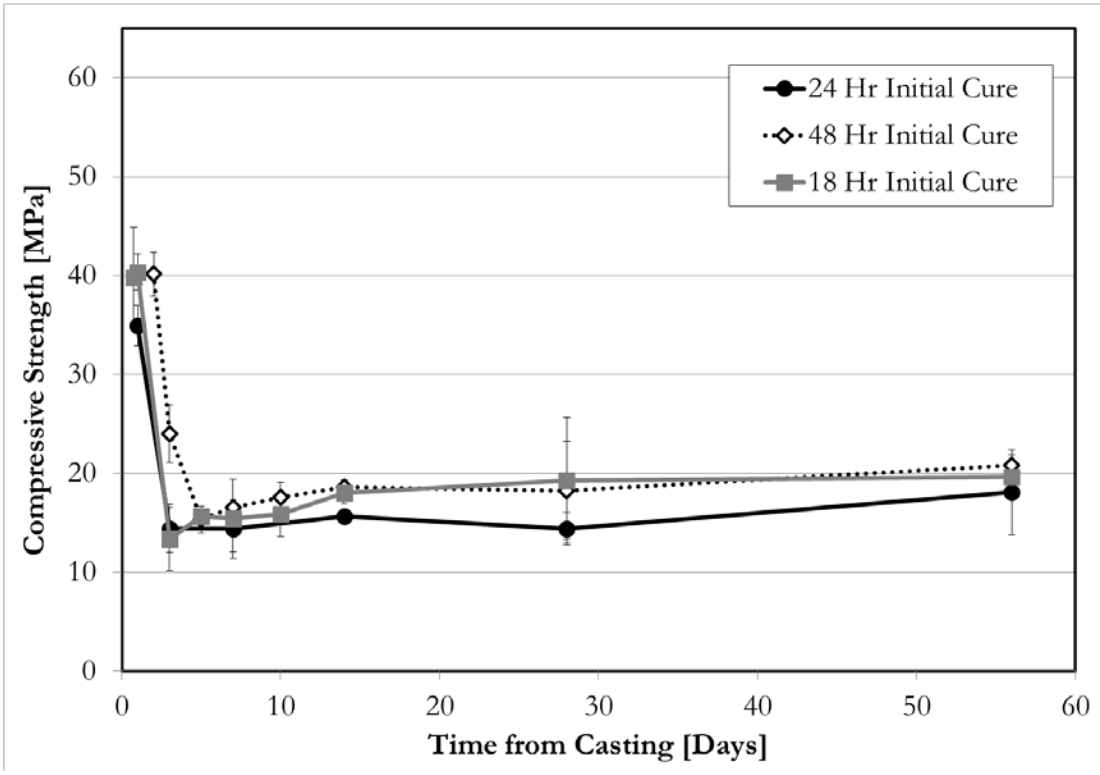

Figure 3-4: Compressive strengths of systems examining length of Phase 1 curing

Samples cast from mixtures using the KRC aggregate at a 0.40 w/cm were cured at ambient laboratory temperatures for 18, 24, or 48 hours, then immersed in a 50°C water bath. Compression testing results showed that minimum strength for the samples cured for 18 and 24 hours prior to submersion occurred 48 hours after submersion in the 50°C water bath. The samples initially cured for 48 hours reached minimum strength 72 hours after submersion in the 50°C water bath.

Previous work by Fryda et al. reported that cylinders placed in a 38°C water bath 24 hours after casting took three months to reach minimum converted strength. However, when that same mixture was submerged in a 38°C water bath directly after being cast, the minimum converted strength occurred after only five days [11], indicating that earlier exposure to elevated temperatures can accelerate the conversion process. When examining the strength development of the 48-hour initial cure sample in

this work, it was observed that the strength had dropped by 40 percent 24 hours after submersion. The next test was not performed until 72 hours after submersion. If testing was performed 48 hours after submersion, the minimum strength may have been observed at that time. Future robustness testing for this procedure should include more frequent testing of specimens at early ages to achieve a more precise determination of this parameter's effect on time to conversion.

3.4.1.4 Impact of Curing Temperature During Phase 1

Figure 3-6 presents the compressive strength development the KRC – 0.40 mixture cured at 5°C, ambient laboratory temperature, and 38°C during Phase 1 curing. Phase 2 and Phase 3 curing were procedures were unchanged.

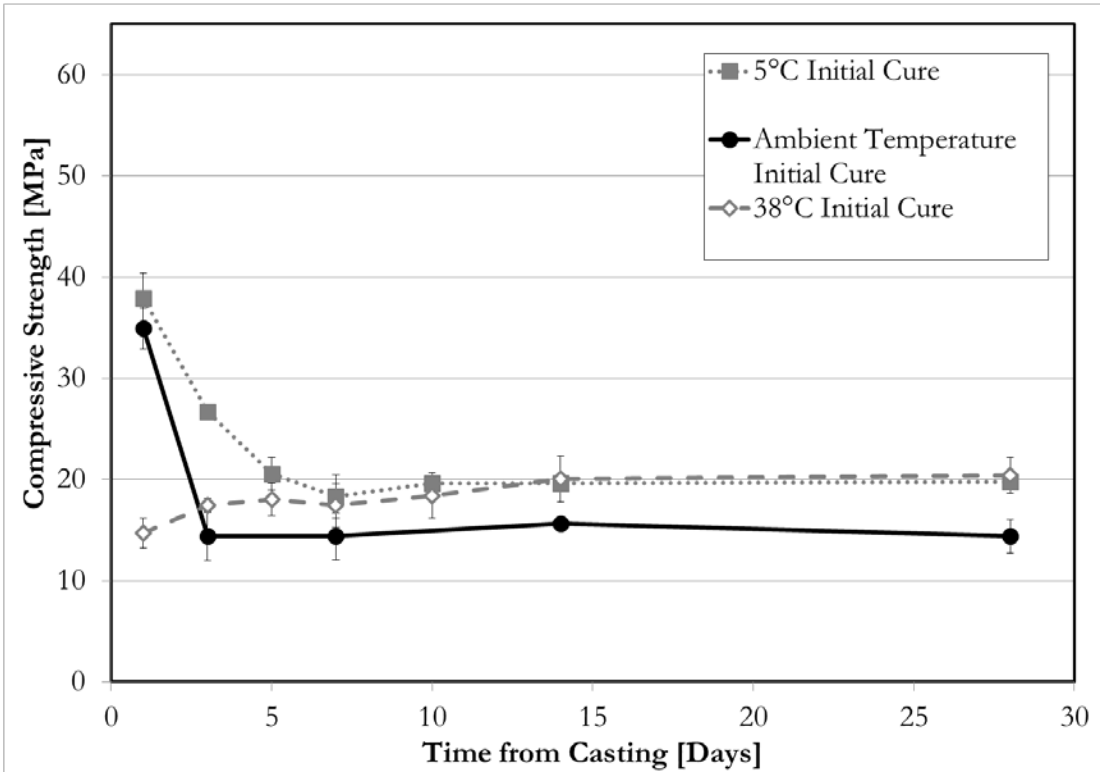

Figure 3-5: Compressive strengths of systems examining temperature of Phase 1 curing

It is important to note that while the samples were cured in environments at set temperatures, the specimens were not kept isothermal. The temperature in each set of specimens was monitored via embedded thermocouple during Phase 1 curing. Figure 3-7 presents the temperature profiles of the

KRC – 0.40 specimens during the initial Phase 1 (initial 24 hours) curing period when cured at 5°C, ambient laboratory temperature, and 38°C.

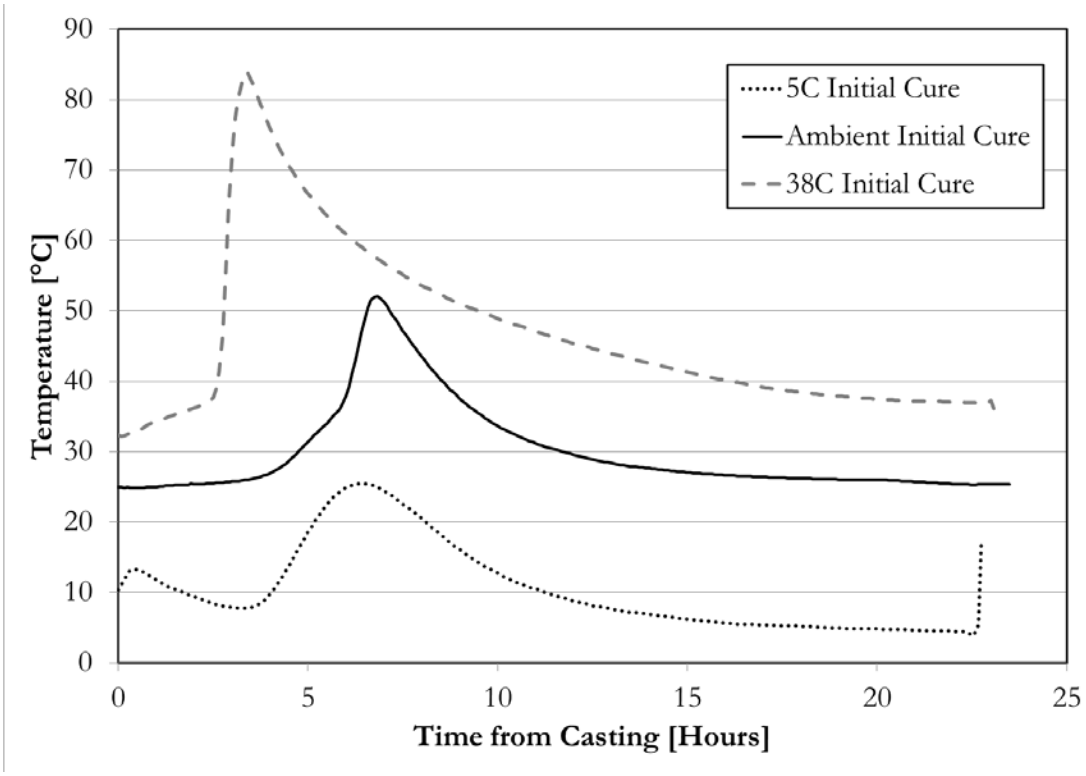

Figure 3-6: Temperature profile for KRC - 0.40 cured at different temperatures during Phase 1

The spikes observed in temperature in Figure 3-7 show that the samples cured at 38°C reached temperatures of 84°C, which was above the 70°C required to cause conversion of the hydrates while the concrete was still in a plastic state [11]. The samples cured at ambient temperatures reached a maximum temperature of 53°C, and samples cured at 5°C reached a maximum temperature of 25°C. Figure 3-6 shows that the mixture that was cured for 24 hours at 38°C then submerged in the 50°C water bath experienced continuous strength gain over the observed period. This is due to the immediate conversion of the metastable hydrates to stable hydrates while the concrete was still in a plastic state. As stated earlier, Fryda et al. showed that specimens placed directly in 38°C after casting did not experience immediate conversion of the metastable hydrates until 5 days after casting. However, they also showed that specimens that reached temperatures higher than 70°C while setting converted immediately to the stable C_3AH_6 and AH_3 hydrates [11]. The long-term strength in the specimens cured at 38°C were higher than those of the specimens cured at ambient laboratory temperatures. This indicates that the test method proposed may be more conservative in strength

estimation compared to existing test methods which suggest immediate submersion in 38°C water baths, or using self-heating to rapidly convert the systems.

The specimens cured at 5°C did not reach the minimum converted strength until day 7, or 6 days after immersion in the 50°C water bath. These specimens reached a maximum internal temperature of 25°C while hardening, whereas the specimens cured at ambient laboratory temperatures reached a maximum temperature of 53°C. Research has shown that CAC paste cured isothermally at 20°C formed mostly CAH_{10}. However, when the CAC paste was submitted to a realistic time-temperature history with a maximum temperature peak of 50°C during the first 24 hours, C_2AH_8 was observed with no CAH_{10} [14]. This indicates that the higher temperature reached during self-heating at ambient curing temperatures allows for the conversion process to begin during hardening. The low maximum temperature observed in the specimens cured at 5°C would have resulted in, primarily, the formation of CAH_{10}. The higher temperature observed during ambient curing allowed for faster conversion from the metastable hydrates to stable hydrates once the specimens were placed in the 50°C water bath. The system cured at 5°C also developed higher minimum converted and long-term strengths compared to the specimens cured at ambient temperatures. This suggest that 23°C curing may result in the most conservative minimum converted strength values.

The results from the variation in initial curing temperatures imply the importance of understanding the internal temperature reached by the concrete specimens that would be cured in a realistic field condition. The initial temperature can have a significant effect on the time to converted strength. Therefore, a standard procedure written based off of the methods presented here will need to indicate that the time to conversion will vary depending on the maximum temperature reached during curing.

3.4.2 Inter-laboratory Variability

Testing was performed in four laboratories to study the inter-laboratory variability within this proposed test method. The KRC – 0.40 mixture design was cast by all laboratories for this testing. All four laboratories used aggregate that was sampled from the same stockpiles (KRC aggregate) at the same time and cement from the same production lot. The same mixing, casting and curing procedures were used by all laboratories. Curing tank set-ups varied between laboratories, but the correct curing temperatures were maintained. This was verified with thermocouples to record temperatures in the center of selected cylinders and in the water baths themselves.

Table 3-3 presents results from the inter-laboratory testing program. Compressive strength averages, standard deviations, coefficients of variation between laboratories and the reproducibility limits between laboratories (d2s value) are presented.

Table 3-3: Inter-laboratory compressive strength averages, standard deviations, coefficients of variation, and reproducibility limits

Time From Casting [Days]	Number of Specimens Tested	Average Compressive Strength [MPa]	Standard Deviation [MPa]	Coefficient of Variation [%]	Reproducibility Limit , d2s, [%]
1	21	37.72	3.1	8.3	23
3	21	16.18	2.1	13.2	36
5	21	17.98	2.2	12.4	34
7	21	19.44	2.1	10.9	30
10	21	19.36	2.3	12.0	33
14	21	21.02	3.3	15.5	43
28	21	23.09	2.7	11.5	32
56	21	23.53	3.2	13.8	38

These results indicate that time to minimum converted strength for all laboratories was three days. Standard deviations between laboratories ranged between 2.09 to 4.20 MPa. Coefficients of variation ranged from 8.3% to 21.2%. The reproducibility limit varied from 23.0% to 58.9%. ASTM C39, the standard followed for performing compression tests in this study, states that the multi-laboratory coefficient of variation for portland cement concrete specimens is 5.0%, and the reproducibility limit is 14% [46]. The values produced as a part of this multi-laboratory study are higher than those suggested in ASTM C39, however, the variation seen in concrete made with CAC may be higher, owing to the conversion process, than what is seen for OPC concrete, for which the standard was developed. These statements were developed based on testing for OPC systems through a testing program in which test specimens were all cast in the same laboratory, and then transported to the testing laboratories separately [46, 47]. The specimens cast as a part of this study were made with CAC, cast at four different laboratories, and tested at four different laboratories. For these reasons the values reported by ASTM C39 are not applicable.

The results presented here form the basis for a preliminary precision statement. A precision and bias statement must also be developed for this test method before it can gain wide acceptance within the

U.S. [48]. Precision is "the closeness of agreement among test results obtained under prescribed conditions," and bias is "a systematic error that contributes to the difference between the mean of a large number of test results and an accepted reference value" [48]. Data for the precision and bias statement can be developed through an interlaboratory study such as the one presented here [48]. However, ASTM Standard E 691, "Standard Practice for Conducting and Inter-laboratory Study to Determine the Precision of a Test Method" suggests that at least six laboratories be included in any inter-laboratory study to ensure an adequate sampling of different laboratories [49]. Therefore it is suggested that a wider study involving at least six laboratories be done to confirm the results presented here. A within-laboratory study examining the same mixture will need to be completed to determine the within-laboratory variability, which is also required for test method acceptance.

3.4.3 Impact of Finely Ground Limestone

Several researchers have examined the impact of additions of FGLS on CAC hydration, though mostly at significantly higher dosage rates (20-30% FGLS). These results have shown, however that the use of FGLS will increase the rate of hydration in CAC systems [30]. Further research observed the formation of calcium monocarboaluminate as an intermediary metastable hydrate, which delayed conversion [28, 29, 31-39, 45]. However it was shown that the calcium monocarboaluminate may later converted to C_3AH_6 resulting in the typical strength loss observed due to conversion [45]. The stability of calcium monocarboaluminate in CAC systems has not been well defined, however, along with the replacement level at which calcium monocarboaluminate begins to form. As a part of this study, low dosage rates were examined to determine if FGLS could be used to increase strength without delaying time to conversion while using the test method dedcribed above. CAC was replaced with 1%, 2%, 5% and 10% FGLS in the KRC – 0.40 concrete mixture. Concrete for the FGLS study was mixed, cast, and cured according to the procedure outlined in Section 3.3.1.

Compressive strength of the KRC – 0.40 (0% FGLS), 1% FGLS, 2% FGLS, 5% FGLS, and 10% FGLS out to 28 days can be seen in Figure 3-8.

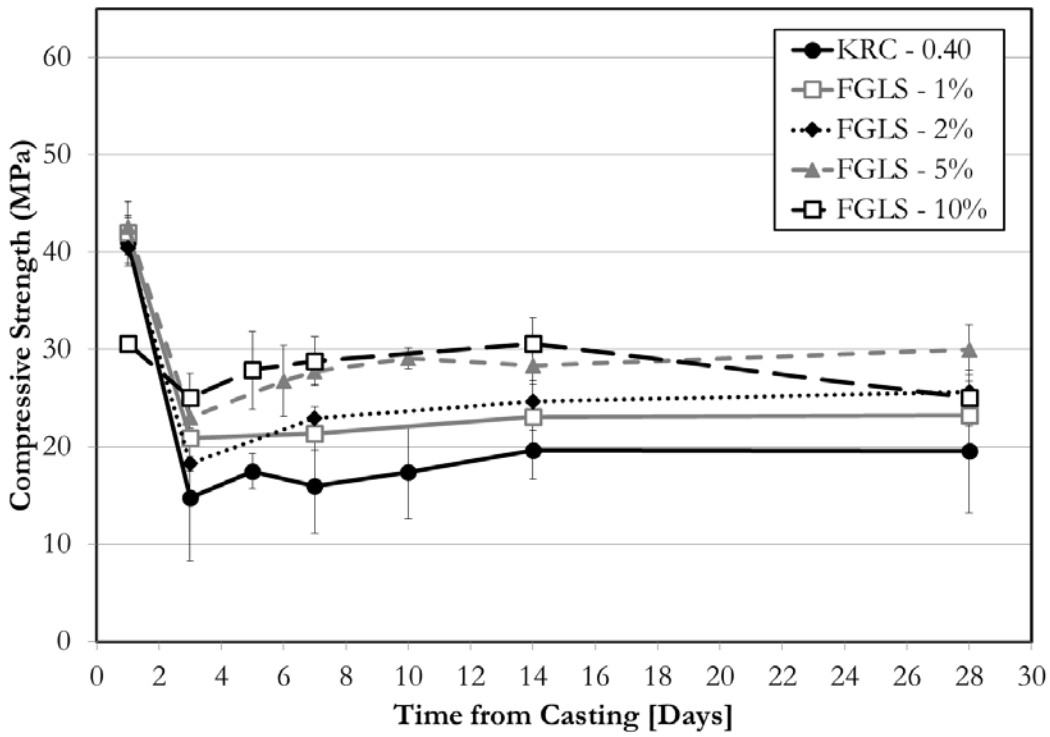

Figure 3-7: Compressive strength of CAC systems incorporating FGLS

These results show that replacement rates of up to 5% FGLS had little impact on day 1, unconverted strengths. A 10% replacement of CAC with FGLS resulted in significantly lower strengths compared to all other mixtures containing FGLS. Fentiman also observed lower day 1 strengths in systems containing 30% FGLS compared to pure CAC systems. This was determined to be because of the relatively lower amount of CAC which provided rapid strength gain to the system [45]. The results presented here indicate that even at 10% replacement levels, the system is altered significantly enough to reduce the early age strength provided from CAC systems. The reduced strength observed at Day 1 in the 10% system is likely due to the formation of alternate hydrates, and not simply a dilution effect of reducing the amount of CAC in the system. As shown in previous literature [28, 29, 31-39, 45], the addition of FGLS to CAC systems in sufficient amounts can alter the hydrates formed significantly.

All systems exhibited strength drops associated with conversion at Day 3. Day 3 converted strengths increased with increasing replacement rates of FGLS. An 8.2 MPa strength increase was observed with a replacement rate of 5% FGLS and a 10.2 MPa strength increase observed with a replacement rate of 10% FGLS at Day 3. Long-term strengths out to 28 days (27 days submerged in the 50°C)

water bath shows that the converted strengths in the systems up to 5% FGLS replacement are stable, increasing as further hydration occurs. However, the system with 10% FGLS experience a second drop in strength at 28 days. This second drop may have been due to the conversion of calcium monocarboaluminate to C_3AH_6. Secondary strength reductions were not observed in systems with lower replacement levels of FGLS, however, indicating that those systems were stable.

These results indicate that replacement rate of 10% resulted in reduced early strength gain, and secondary strength reductions caused by the conversion of calcium monocarboaluminate. Further investigation of systems containing low dosage rates of FGLS is suggested to determine the hydrate structure in each system, and confirm the stability of the strength increase observed in long-term testing. Systems ranging between 5% and 10% replacement of FGLS should also be investigated to determine the optimum replacement ratio to maximize converted strength and minimize impact on day 1 strengths. However, these results indicate that a 5% replacement of FGLS will result in an increased converted strength without compromising early age strength gains. Therefor use of FGLS may be one tool to increase the converted strength in systems where the strength reduction due to conversion is too high.

3.4.4 Future Work

The next steps for this study include completing some additional robustness testing not yet completed as part of the work presented here. The impact of aggregate sources indicates that aggregates can have significant impacts on the time to conversion observed using this test method. Additional aggregate sources need to be studied to understand if the delay applies only to high carbonate limestones, or if the impact is observed with other aggregate types as well. Additionally, further examinations on the cause of the behavior observed in the system containing the limestone aggregate needs to be carried out. It is suggested that a study of porosity in each system, along with a full hydrate analysis be performed.

Additional investigations into test method variability are also suggested. Specifically, a larger inter-laboratory investigation will be required to provide enough variability data to create inter-laboratory precision and bias statements for a standardized test method. Similar testing needs to be completed to determine within-laboratory variability as well. Finally additional work needs to be completed to understand the impact of FGLS on CAC systems, particularly at lower dosage rates. In particular, the stability of long-term strength in these systems needs to be confirmed, along with the presence or

absence of calcium monocarboaluminate. Systems should also be examined that contain replacement rates of FGLS for CAC between 5% and 10% to better understand the optimum dosage rate of FGLS to increase converted CAC strength.

3.5 Conclusion

The work presented herein provides information on repeatability and robustness testing for a new test method to determine the converted strength of CAC concrete. The test method examined as a part of this work establishes a convenient and field friendly test method for the converted strength of CAC concrete that can be used in a wide range of environmental conditions. It is important to note that this test should only be applied to concrete where CAC was the sole binder. This method allowed for the samples to be cured at ambient construction site temperatures, and then moved to the laboratory where they are then submerged in 50°C water. The elevated temperature cure promotes conversion to occur at an accelerated rate, and the minimum converted strength can be observed within approximately three days for non-limestone systems and within 14 days for limestone systems. Additional work on systems containing low dosage rates of FGLS were also done. The material showed promise for use as a tool to increase converted strength in CAC systems at replacement rates up to 5% however the stability of increased converted strength in these systems was not determined.

Several conclusions can be drawn from the work presented here:

- Variation in compressive strength for concrete made with CAC may be inherently higher than for concrete made with portland cement. A larger inter-laboratory study is required, however, to verify these results with a recommendation of at least 6 participating qualified laboratories.

- Initial ambient curing temperature can significantly affect the time to conversion. Samples cured at 38°C for the initial 24 hours experience conversion during the first 24 hours. Samples cured at 5°C for the initial curing period did not convert until they had been submerged in the 50°C water bath for six days. Any standard written should therefore consider including a temperature range in which the samples must be maintained in the field to prevent this variation.

- Aggregate mineralogy has a significant impact on the time to conversion, and final converted strength. CAC concrete made with limestone aggregate experienced a delayed conversion, as well as higher converted strengths compared to CAC concrete made with siliceous aggregates.

- FGLS replacements at rates up to 5% in CAC systems can increase the converted strength in CAC concrete without compromising early strength gain.

Further work is necessary as suggested above is necessary to better understand the differences observed between limestone and siliceous aggregate systems, as well as to determine the variability inherent within the test method. However this test method shows significant promise for use as a field friendly way of determining the minimum converted strength of CAC concrete in an accelerated manner.

3.6 Acknowledgements

The authors would like to acknowledge the support of the Microscopy Center at Oregon State University. Undergraduate research assistants Aaron Strand and Travis Moore were also very helpful in collecting some of the data presented in this paper. Additionally, we would like to thank the Michael D. A. Thomas of University of New Brunswick, Kevin Folliard of University of Texas at Austin and Charles Alt of Kerneos Aluminate Technologies for participating in the inter-laboratory study. Finally, the authors would like to thank Kerneos Aluminate Technologies for financial support.

3.7 Works Cited

[1] K.L. Scrivener, 100 years of calcium aluminate cements, in: C.H. Fentiman, R.J. Mangabhai, K.L. Scrivener (Eds.) Calcium aluminate cements : Proceedings of the centenary conference, IHS BRE Press, Avignon, France, 2008, pp. 3-6.

[2] S.M. Bushnell-Watson, J. Sharp, The effect of temperature upon the setting behavior of refractory calcium aluminate cements, Cement and Concrete Research, 16 (1986) 875-884.

[3] S.M. Bushnell-Watson, J.H. Sharp, Further studies of the effect of temperature upon the setting behavior of refractory calcium aluminate cements, cement and Concrete Research, 20 (1990) 623-635.

[4] S.M. Bushnell-Watson, J.H. Sharp, On the cause of the anomalous setting bahavior with respect to temperature of calcium aluminate cement, Cement and Concrete Research, 20 (1990).

[5] K.L. Scrivener, J.-L. Cabiron, R. Letourneux, High-performance concretes from calcium aluminate cements, Cement and Concrete Research, 29 (1999) 1215-1223.

[6] J.P. Bayoux, J.P. Letourneux, S. Marcdargent, M. Vershaeve, Acidic corrosion of high alumina cement, in: R.J. Mangabhai (Ed.) International Symposium on Calcium Aluminate Cements, E. & F. N. Spon, London, UK, 2014, pp. 230-240.

[7] A. Goyns, Calcium aluminate cement linings for cost-effective sewers, in: R.J. Mangabhai, F.P. Glasser (Eds.) International Conference on Calcium Aluminate Cements, IOM Communications, Edinburgh, UK, 2001, pp. 617-631.

[8] A.M. Goyns, M.G. Alexander, Performance of various concretes in the Virginia experimental sewer over 20 years, in: C. Fentiman, R. Mangabhai, K. Scrivener (Eds.) International Conference on Calcium Aluminate Cements, IHS BRE Press, Avignon, FR, 2014, pp. 573-584.

[9] J.L. Burati, R.M. Weed, C.S. Hughes, H.S. Hill, Optimal procedures for quality assurance specifications, in, Federal Highway Administration, McLean, VA, 2003.

[10] K.L. Scrivener, A. Capmas, Calcium Aluminate Cements, in: P.C. Hewitt (Ed.) Lea's Chemistry of Cement and Concrete, Elsevier - Butterworth-Heinemann, Oxford, UK, 1998, pp. 713-782.

[11] H. Fryda, K.L. Scrivener, G. Chanvillard, C. Feron, Relevance of Laboratory Tests to Field Applications of Calcium Aluminate Cement Concretes, in: International Conference on Calcium Aluminate Cements (CAC), IOM Communications, Heriot-Watt University, Edinburgh, Scotland, UK, 2001, pp. 215-247.

[12] K.L. Scrivener, Historical and present day applications of calcium aluminate cements, in: R.J. Mangabhai, F.P. Glasser (Eds.) Proceedings of the International Conference on Calcium Aluminate Cements (CAC), IOM Communications, Heriot-Watt University, Edinburgh, Scotland, UK, 2001, pp. 3-23.

[13] H. Pöllman, Calcium alumiante cements- Raw materials, differences, hydration and properties, in: M.A.T.M. Broekmans, H. Pöllmann (Eds.) Applied mineralogy of cement & concrete, The Mineralogical Society of Virginia, Chantilly, Virginia, USA, 2012, pp. 1-82.

[14] C. Gosselin, Microstructural development of calcium aluminate cement based systems with and without supplementary cementitious materials, in: Faculte sciences et techniques de l'ingenieur, Ecole Polytechniqe Federale de Lausanne, Lausanne, CH, 2009.

[15] S.M. Bushnell-Watson, J.H. Sharp, The application of thermal analysis to the hydration of conversion reactions of calcium aluminate cements, Materiales De Construccion, 42 (1992) 13-32.

[16] V. Antonovič, J. Keriene, R. Boris, M. Aleknevičius, The effect of temperature on the formation of the hydrated calcium aluminate cement structure, Procedia Engineering, 57 (2013) 99-106.

[17] A. Muller, Conversion & résistance en compression des ciments cT a lu m in a tes de calcium, in: DEPARTEMENT GENIE CIVIL, UNIVERSITE LAVAL, Quebec City, 2010.

[18] H. Fryda, E. Charpentier, J.M. Bertino, Accelerated test for conversion of calcium aluminate cement concrete, in: C.H. Fentiman, R.J. Mangabhai, K.L. Scrivener (Eds.) Calcium Aluminate Cements: The Centenary Conference, IHS BRE Press, Avignon, FR, 2008.

[19] ASTM C31, Standard practice for making and curing concrete test specimens in the field, in: ASTM International (Ed.), ASTM International, West Conshohocken, PA, 2012.

[20] European Committee for Standardization, Calcium aluminate cement - Composition, specifications, and conformity criteria, in: EN 14647, European Committee for Standardization, Brussels, 2005.

[21] Texas Department of Transportation, TxDoT SS-4491 Class CAC Concrete, in, Texas Department of Transportation, Austin, TX, 2009.

[22] Concrete Society Technical Report, Calcium Aluminate Cements in Construction: A Reassessment, in, Concrete Society, 1997, pp. 63.

[23] ASTM C 192 2014, Standard practice for making and curing concrete test specimens in the laboratory, in: A. International (Ed.), ASTM International, West Conshohocken, PA, 2015.

[24] ASTM C39 2012a, Standad test method for compressive strength of cylindrical concrete specimens, in: A. International (Ed.), ASTM International, West Conshohocken, PA, 2015.

[25] ASTM C109-11b, ASTM C109-11b: Standard test method for compressive strength of hydraulic cement mortars (using 2 in. or [50mm] cube specimens), in: ASTM International (Ed.) ASTM C109-11b, ASTM International, West Conshocken, Pennsylvania, 2011, pp. 10.

[26] J. Zhang, G.W. Scherer, Comparison of methods for arresting hydration of cement, Cement and Concrete Research, 41 (2011) 1024-1036.

[27] J. Bizzozero, Hydration and dimensional stability of calcium aluminate cement based systems, in: Materials Science and Engineering, Ecole Polytechnique Federal de Lausanne, Lausanne, Switzerland, 2014.

[28] L. Cussino, A. Negro, Hydration du ciment alumineux en présence d'agrégat siliceux et calcaire, in: 7th International Congress on the Chemistry of Cement, Paris, 1980.

[29] V. Lamour, P. Monteiro, K. Scrivener, H. Fryda, Mechanical properties of calcium aluminate cement concretes, in: International conference on calcium aluminate cements, 2001, pp. 199-213.

[30] A. Negro, A. Bachiorrini, M. Murat, Interaction, in aqueous medium, between calcium carbonate and monocalcium aluminate at 5°C, 20°C, and 40°C, Bulletin de minéralogie, 105 (1982) 284-290.

[31] H.H.M. Darweesh, Limestone as an accelerator and filler in limestone-substituted alumina cement, Ceramics international, 30 (2004) 145-150.

[32] A. Bachiorrini, L. Cussino, Alumina cement hydration in pure water and in sulfate solution in the presence of siliceous or calcareous aggregate, in: 8th International Congress on the Cement of Chemistry, Rio de Janeiro, Brazil, 1986, pp. 383-388.

[33] F. Trivino, Aluminous cement: How to avoid degrading of mechanical resistance, in: 8th International Congress on the Chemistry of Cement, Rio de Janeiro, Brazil, 1986, pp. 417-422.

[34] W.G. Piasta, The Effect of Limestone Fillers on Sulphate Resistance of High Alumina Cement Compositers, in: R.J. Mangabhai (Ed.) Calcium Aluminate Cements, E. & F.N. Spon, London, UK, 1990, pp. 241-255.

[35] C.M. George, Aluminous cements, in: 7th International Congress on the Chemistry of Cement, Paris, France, 1980.

[36] C.M. George, Manufacture and performance of aluminous cement, in: R.J. Mangabhai (Ed.) Calcium Aluminate Cements, E. & F.N. Spon, London, UK, 1990, pp. 181-207.

[37] H.G. Midgley, High alumina cement in construction - a future based on experience, in: R.J. Mangabhai (Ed.) Calcium Aluminate Cements, E. & F.N. Spon, London, UK, 1990, pp. 1-13.

[38] F. Indelicato, On the correlation between porosity and strength in high-alumina cement mortars, Materials and Structures, 23 (1990) 289-295.

[39] A.P. Luz, V.C. Pandolfelli, $CaCO_3$ addition effect on the hydration and mechanical strength evolution of calcium aluminate cement for endodontic applications, Ceramics International, 38 (2012) 1417-1425.

[40] W.A. Cordon, H.A. Gillespie, Variables in concrete aggregates and portland cement paste which influence the strength of concrete, Journal Proceedings of the American Concrete Institute, 60 (1963) 1029-1052.

[41] A.M. Neville, Aggregate Bond and Modulus of Elasticity of Concrete, ACI Materials Journal, 94 (1994) 71-75.

[42] P.K. Mehta, P.J.M. Monteiro, Concrete: microstructure, properties, and materials, 3 ed., McGraw-Hill, New York, 2006.

[43] P.C. Aitcin, P.K. Mehta, Effect of Coarse Aggregate Characteristics on Mechanical Properties of High-Strength Concrete, Materials Journal, 87.

[44] S.H. Kosmatka, M.L. Wilson, Design and control of concrete mixtures, 14 ed., Portland Cement Association, Skokie, Illinois, 2011.

[45] C.H. Fentiman, Hydration of carbo-aluminous cement at different temperatures, Cement and concrete Research, 15 (1985) 622-630.

[46] J.M. Khatib, Properties of concrete incorporating fine recycled aggregate, Cement and Concrete Research, 35 (2005) 763-769.

[47] S. Kennedy, R. Detwiler, J. Bickley, M. Thomas, Results of an interlaboratory test program: compressive strength of concrete, Cement, Concrete, and Aggregates, 17 (1995) 3-10.

[48] P. Picariello, Fact vs. fiction: The truth about precision and bias, in: ASTM Standardization News, ASTM International, West Conshohocken< PA, 2000, pp. 16-19.

[49] ASTM Standard E691 2014, Standard Practice for Conducting an Interlaboratory Study to Determine the Precision of a Test Method, in: A. International (Ed.), West Conshohocken, PA, 2015.

Manuscript 2

Pore Solution Chemistry of Calcium Aluminate Cement Concrete Systems Undergoing Accelerated Conversion

Matthew P. Adams and Jason H. Ideker

Submitted and Under Review for the Proceedings of The 14th International Congress on Cement Chemistry

To be held in Beijing, China in October 2015

4 Manuscript 2

Pore Solution Chemistry of Calcium Aluminate Cement Systems Undergoing Accelerated Conversion

Matthew P. Adams[1], Jason H. Ideker[2]

Abstract: The use of calcium aluminate cement (CAC) concrete in construction is increasing as the need for rapid repair solutions for deteriorating infrastructure rises. CAC is particularly useful because of its rapid strength gain property, even at low temperatures. However, the use of CAC in construction has been limited by a lack of understanding of the process of conversion, in which metastable hydrates convert to stable hydrates. This study examined two concrete mixtures, one containing a limestone aggregate and one containing a siliceous aggregate. The pore solution chemistry of each concrete system was determined, along with that of a CAC cement paste to determine the impact of aggregates. Pore solution chemistry of siliceous and limestone CAC concrete systems, as well as CAC paste was observed prior to and after conversion. Pore solution was expressed using mechanical methods, and the pore solution was analysed using inductively couple plasma optical emission spectrometry (ICP-OES). Results have shown that aluminium concentrations decreased and calcium concentrations increased in the limestone aggregate system and CAC paste system. Concentrations of aluminium and calcium remained constant prior to and after conversion in the siliceous aggregate system. These results indicate aggregate mineralogy does have a significant impact on pore solution chemistry and phase dissolution in CAC systems.

Keywords: Calcium aluminate cement; pore solution; Calcium aluminate cement concrete, aggregates; mineralogy

[1] Corresponding Author: Ph.D. Candidate, School of Civil and Construction Engineering, Oregon State University. matthewpadams@gmail.com
[2] Associate professor, School of Civil and Construction Engineering, Oregon State University

4.1 Introduction

Calcium aluminate cement (CAC) concrete has been used in the construction industry for over 100 years. Recently, there has been an increased interest in use of the material in cast-in-place rapid repair settings, particularly in North America. This interest has been spurred by the material's rapid strength gain properties, particularly at low temperatures. However, use of this cement in construction has been limited since the 1970s due to a lack of understanding of the conversion process, in which metastable hydrates convert to stable hydrates resulting in a subsequent loss of strength. Several high profile collapses attributed to conversion in the U.K. in the 1970s lead to significant limitations on the use of the material in structural applications [1]. Later investigations found that the limitations put in place were primarily due to a lack of understanding concerning the conversion process and hydration in CAC systems within the construction industry [1-3], a problem that still exists today in the general construction community. This work seeks to increase understanding of CAC hydration, particularly in concrete systems where aggregates are present, through an examination of the pore solution chemistry as CAC concrete systems undergo conversion. Presented is the pore solution chemistry for two concrete systems (one containing siliceous aggregate, one containing a limestone aggregate). These results are compared to a pure CAC paste system. Pore solution is monitored in each system prior to and after conversion to determine the effect of conversion on pore solution chemistry.

The main phase in CAC, monocalcium aluminate (CA), forms four main phases during its hydration process: CAH_{10}, C_2AH_8, C_3AH_6, and AH_3. When placed in contact with water the hydration of CA is characterized by rapid dissolution of Ca^{2+} and Al^{3+} followed by a rapid precipitation of hydration products. This results in an exothermic reaction that is concentrated in a short time and can lead to a resulting significant temperature rise, even in relatively small volumes [2, 4]. This is important to note, because temperatures during hydration can affect the hydrate structures formed. Two hydrates that are formed, CAH_{10} and C_2AH_8, are both metastable and will convert into the stable hydrate C_3AH_6. This reaction is known as conversion, and is accompanied by the formation of AH_3 gel, and the release of water [2]. The conversion process is driven by temperature as well as access to moisture. At low curing temperatures ($T< 15°C$) the initial metastable hydrate favored to form is CAH_{10}. At higher temperatures ($T>30°C$) C_2AH_8 is favored to form initially. At curing temperatures between 15°C and 30°C, both CAH_{10}, C_2AH_8 will form, though neither is thermodynamically favored and formation will be slow [5]. CAH_{10} will convert into C_2AH_8, accompanied by the formation of AH_3 gel and water release. The C_2AH_8 will subsequently convert to the stable C_3AH_6, again accompanied by the

formation of AH_3 gel and water release. This process is thermodynamically inevitable, and the rate at which it occurs is a function of the temperature history of the material during hydration. Increasing the curing temperature and exposure to moisture will result in faster conversion from the metastable hydrates to the stable hydrates [6-8].

The density of the metastable hydrates (density (g/cm^3): CAH_{10}=1.72, C_2AH_8=1.95) is lower than that of the stable hydrates (density (g/cm^3): C_3AH_6=2.52, AH_3=2.4) [7]. The increase in density as the hydrates undergo conversion causes porosity to form in the hydrated cement paste, thus causing compressive strength to drop. After conversion occurs, and a minimum strength has been reached, the water released by conversion can continue to hydrate unhydrated cement grains resulting in continued long-term strength gain [2, 7]. It is important to note that conversion is a process that occurs only in pure CAC systems. The testing outlined in this manuscript does not apply to systems where CAC is a component of a blended binder system. In these systems the hydration products are typically not subject to conversion as they are stable in the long-term. Much of the research concerning CAC conversion has been performed on pastes, mortars and to only a small extent on concrete [8-20].

In addition to the impact that temperature history has on conversion, previous research has alluded that aggregate mineralogy has an impact on the conversion process in CAC concrete [20, 21]. In a study by Cussino and Negro, it was observed that the specimens containing siliceous aggregate experienced strength reductions due to conversion beginning after 90 days; however mixtures containing either limestone aggregates or limestone powder used as a partial replacement for CAC were still steadily gaining strength in the same time period [20]. Analysis of the samples containing just limestone powder showed the formation of calcium monocarboaluminate. Further studies confirmed that when CAC was mixed with finely ground limestone powder, calcium monocarboaluminate was formed, which improved the strength in these systems, even after conversion [13, 21]. The formation of calcium monocarboaluminate was only confirmed in systems containing finely ground limestone powder, not systems containing larger-size concrete aggregates. Systematic scientific studies have not been conducted to fully elucidate the role that aggregate mineralogy plays on the conversion process, chemistry, and hydration within CAC systems.

Work has been completed to examine the pore solution chemistry in CAC paste systems. Barrett et al. performed experiments where they placed a standard grade CAC in a dilute lime solution and monitored ionic concentrations in the solution over 10 hours [22]. Results from this work indicated

that during hydration, as hydrates precipitate from solution, the concentrations of calcium and aluminum in solution decreased significantly. Gaztanaga et al. examined the pore solution chemistry in a CAC paste cured at 20°C using a standard grade CAC out to 30 days [23]. The authors reported that calcium concentrations continued to decreased after initial hydration from 20 ppm at 1 day after casting to 1 ppm at 30 days. Aluminum concentrations also decreased significantly over the curing period. The pH ranged from 12.53 to 12.69 in that same time period. This analysis was performed on systems that had been cured at 20°C over their lifespan, and therefore examined only unconverted CAC concrete systems [23]. Neither of these works examined how the pore solution chemistry in hardened systems changed during the conversion process, and therefore it is still not well understood how elemental composition of the pore solution is affected by conversion in hardened systems. Additionally, these authors examined cement paste systems specifically, and the impact of aggregate mineralogy was not observed. As described above, changes in mineralogy in CAC concrete systems can have significant impacts on strength, particularly after conversion. Therefore, understanding the influence of mineralogy on pore solution chemistry will explain some of the differences occuring in these systems when different aggregate types are employed.

4.2 Experimental

4.2.1 Materials

4.2.1.1 Cement

A standard grade CAC was used for all mixtures presented in this study. The oxide composition of the CAC used in this study is presented in Table 4-1.

Table 4-1: Cement Oxide Analysis

Oxide (% wt)	SiO_2	Al_2O_3	Fe_2O_3	CaO	MgO	Na_2O	K_2O	SO_3	TiO_2	Mn_2O_3	P_2O_5	SrO	LOSS
CAC	4.98	38.23	15.40	37.53	0.71	0.03	0.23	0.06	1.80	0.23	0.13	0.02	0.65

4.2.1.2 Aggregates

Two different aggregates were used in the concrete mixtures produced in this study. A siliceous river gravel from Oregon in the United States and a limestone from Washington state in the United States. The siliceous aggregate was predominantly composed of SiO_2 and Al_2O_3.The limestone was

composed of $CaCO_3$. Both fine and coarse aggregates were created from the same source for each type. A summary of information about these aggregates can be found in Table3. 2.

Table 4-2: Aggregate Description and Properties

Aggregate Type	Absorption Capacity (%)	$G_{sb, OD}$	Source	Composition	Particle Shape and Texture
Siliceous	2.58	2.44	Oregon, USA	SiO_2 and Al_2O_3	Smooth, Rounded
Limestone	0.67	2.68	Washington, USA	$CaCO_3$	Coarse, Angular

4.2.1.3 Concrete and Cement Paste Mixtures

Table 4-3 shows the concrete and paste mixtures used for this study.

Table 4-3: Concrete and cement paste mixture designs

Mixture Label	Aggregate Type	w/cm	Fine Aggregate (kg/m^3)	Coarse Aggregate (kg/m^3)	Cement Content (kg/m^3)
Siliceous System	Siliceous	0.40	730	890	440
Limestone System	Limestone	0.40	855	938	440
CAC Paste	-	0.40	0	0	440

The cement content and w/cm remained constant between mixtures. Aggregate contents were modified according to the aggregate properties to achieve the same unit mixture size of 0.77 m^3. A set retarding agent (Chryso brand Fondu Retard) and a super plasticizer (Chryso brand Optima 203) were both used to achieve acceptable working time and workability in the mixtures. Aggregates were premixed to achieve consistent, near-saturated surface dry conditions prior to being used in concrete mixtures. Aggregate moisture contents were measured prior to mixing, and total water content was adjusted for each mixture to maintain an effective w/cm of 0.4.

Concrete samples were cast into 100 mm (diameter) x 200 mm (height) plastic cylinders and sealed with plastic caps to prevent moisture loss. The cement paste samples were cast in 75 mm (diameter) x 150 mm (height) plastic cylinders and sealed with plastic caps to prevent moisture loss. Specimens

were organized to have at least 75mm of space around them in all directions to allow for adequate air flow and prevent self-heating. Fryda et al. noted that specimens that reached temperatures higher than 70°C while setting converted immediately to the stable C_3AH_6 and AH_3 hydrates [8]. Self-heating for samples during initial hydration prior to 24 hours was monitored. Temperatures remained below 60°C in all three systems, and therefore these samples were still unconverted.

4.2.2 Experimental Process

4.2.2.1 Curing Regime

Standard curing procedures for this method involved two phases of curing: phase 1, the initial 24 hour period after casting, and phase 2, the period between 24 hours and 28 days. During phase 1 curing, after being cast, samples were kept at ambient temperature and humidity conditions in the laboratory in the capped sample molds. Ambient temperature in the laboratory was 23 ± 3 °C. During phase 2 curing period, the samples were removed from the molds and placed immediately into a 50 ± 2 °C water bath. This procedure followed the procedure laid out by Fryda et al. [7]. This curing regime accelerates the conversion of the metastable hydrates to stable hydrates by placing the specimens in the heated water bath. The elevated temperature of 50°C accelerates the conversion process, allowing for full conversion within two days after submersion in the water bath [6, 7]. Conversion was monitored through compressive strength testing. All samples were fully converted by Day 3, after casting. The specimens remained in the heated water bath until tested. This curing regime was followed for all specimens.

4.2.2.2 Pore Solution Extraction and Measurement

Pore solution was extracted from the samples at 24 hours, 3, 7, 14, and 28 days. Measurements from Day 1 were on unconverted samples, and later age measurements (Day 3-28) were on converted samples. Concrete or paste slices, 25-50 mm slices thick, were obtained from the sample cylinders using a diamond saw. The slices were placed into plastic freezer type bags and crushed into small fragments using a hammer. (< 9.5mm). Aggregates were removed by hand from the concrete samples. The remaining crushed material was then placed into a pore solution extraction device that expressed the pore solution from the sample under a high pressure (450 MPa for paste samples, 1130 MPa for concrete samples). Each sample produced 1 ml to 5 ml of pore solution. Samples from unconverted systems (1 day samples) produced much less pore solution, ~0.5 - 1 ml per sample, compared to

converted samples (3-28 day samples) which produced ~ 2 – 4 ml per sample. This was expected as the metastable hydrate products produced during CAC hydration bind a significant amount of water into their hydrate structures that is then released during conversion [2]. Consecutive samples from each test date and system had their pore solution expressed until enough solution (5 ml) was obtained for testing.

The pH was measured within several hours of pore solution expression using a pH electrode. Pore solution samples were then acidified in a matrix of 2% HNO_3 prior to analysis in inductively coupled plasma-optical emission spectrometry (ICP-OES). The ICP-OES apparatus used was a Leeman Labs, Inc. Prodigy High Dispersion ICP.

4.3 Results and Discussion

4.3.1 Pore solution chemistry

Figure 4-1 shows the elemental concentrations of sodium (Na), potassium (K), aluminum (Al), and calcium (Ca) in the pore solution for the Limestone System, the Siliceous System and the CAC paste over time. The pH evolution in these systems is also presented in Figure 4-2.

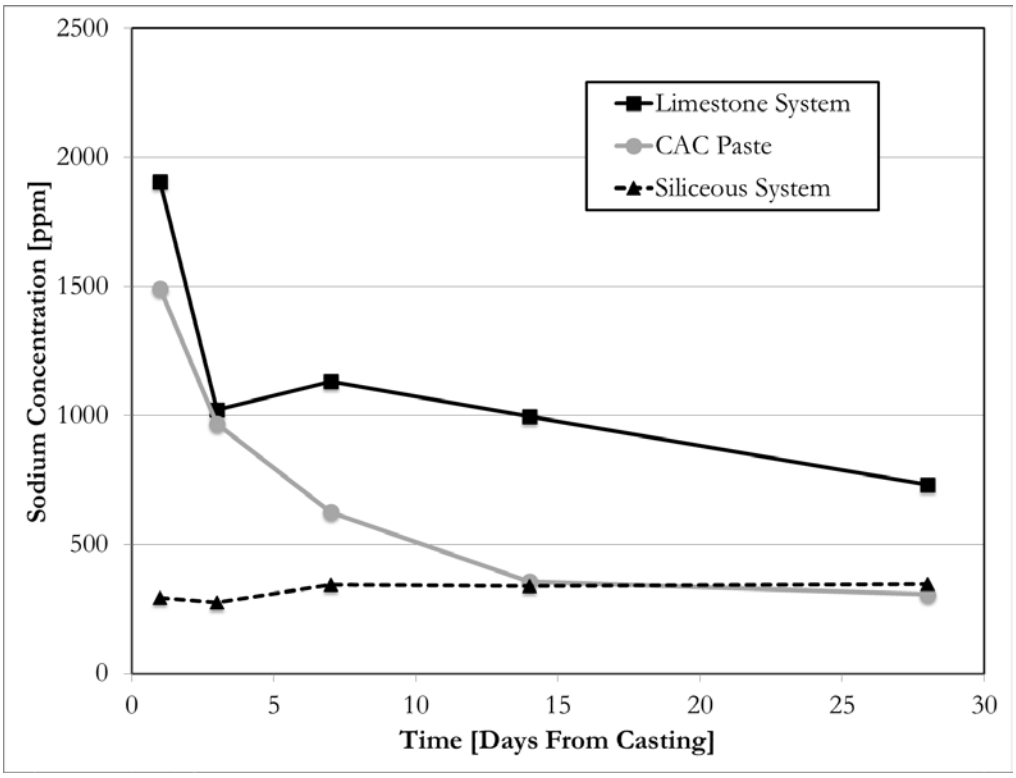

a) Sodium Concentration

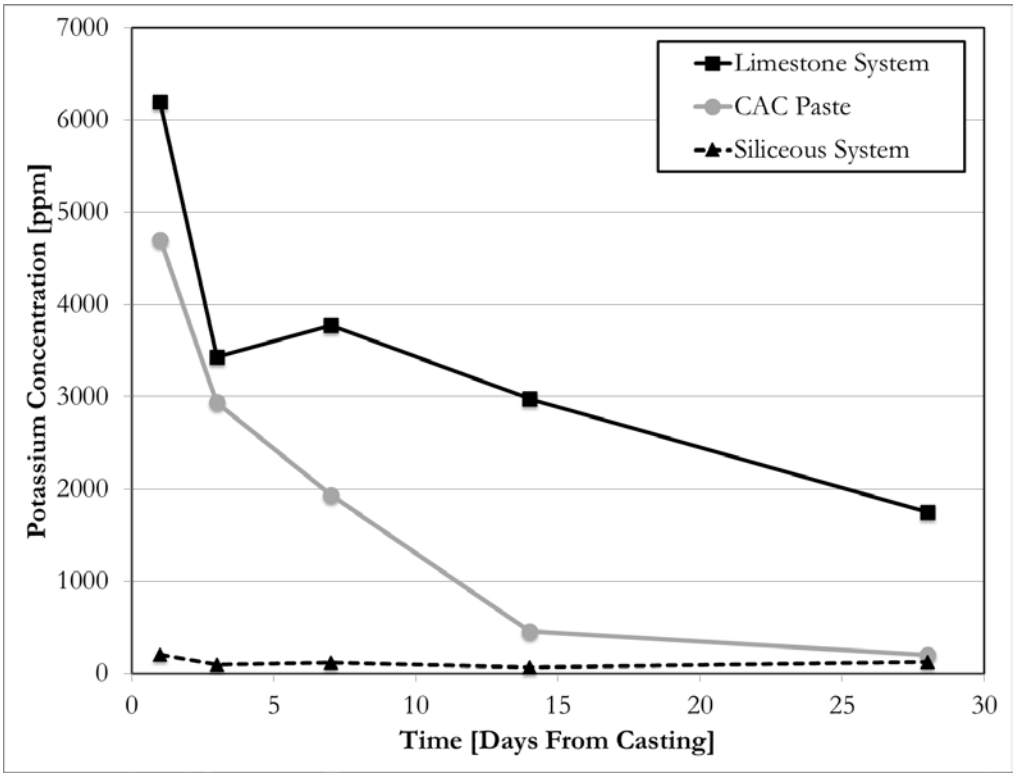

b) Potassium Concentration

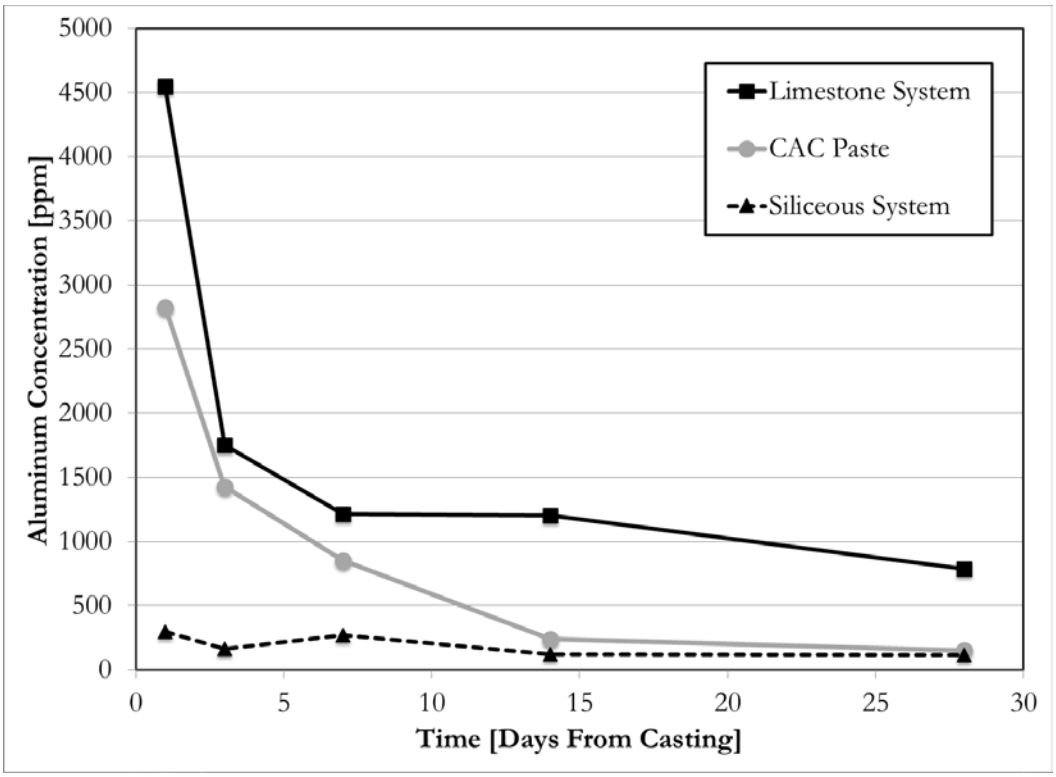

c) Aluminum Concentration

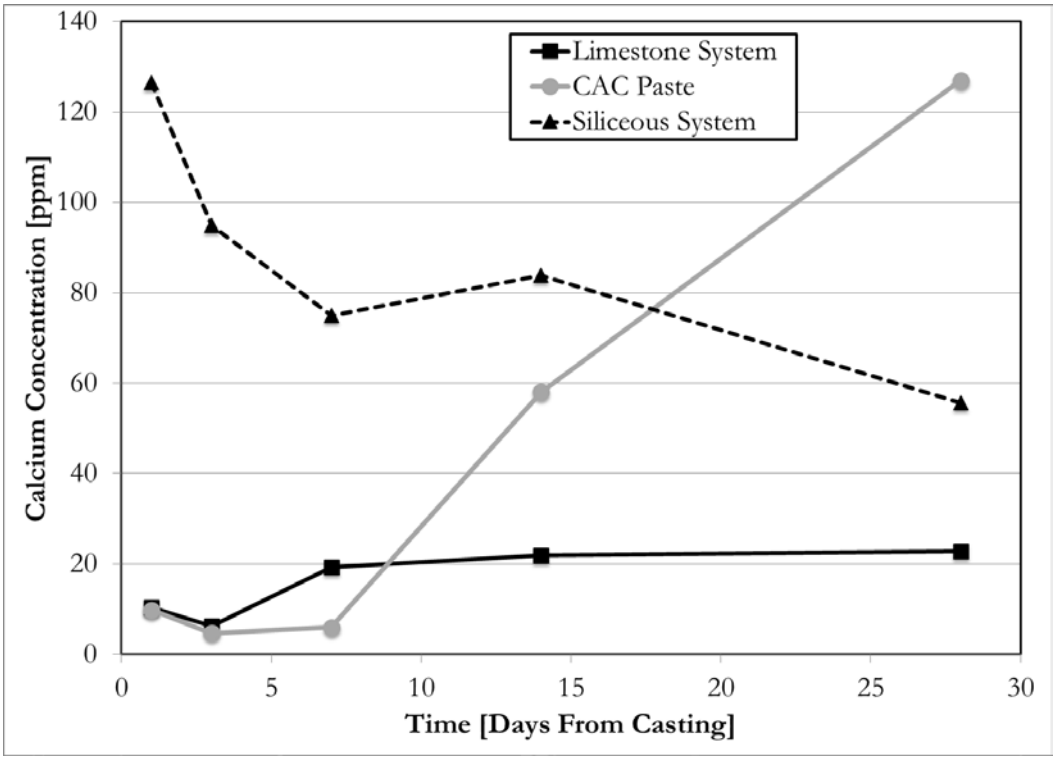

d) Calcium Concentration

Figure 4-1: Elemental concentration (1a-1d) of CAC concrete and paste systems over time when subjected to accelerated conversion curing regime

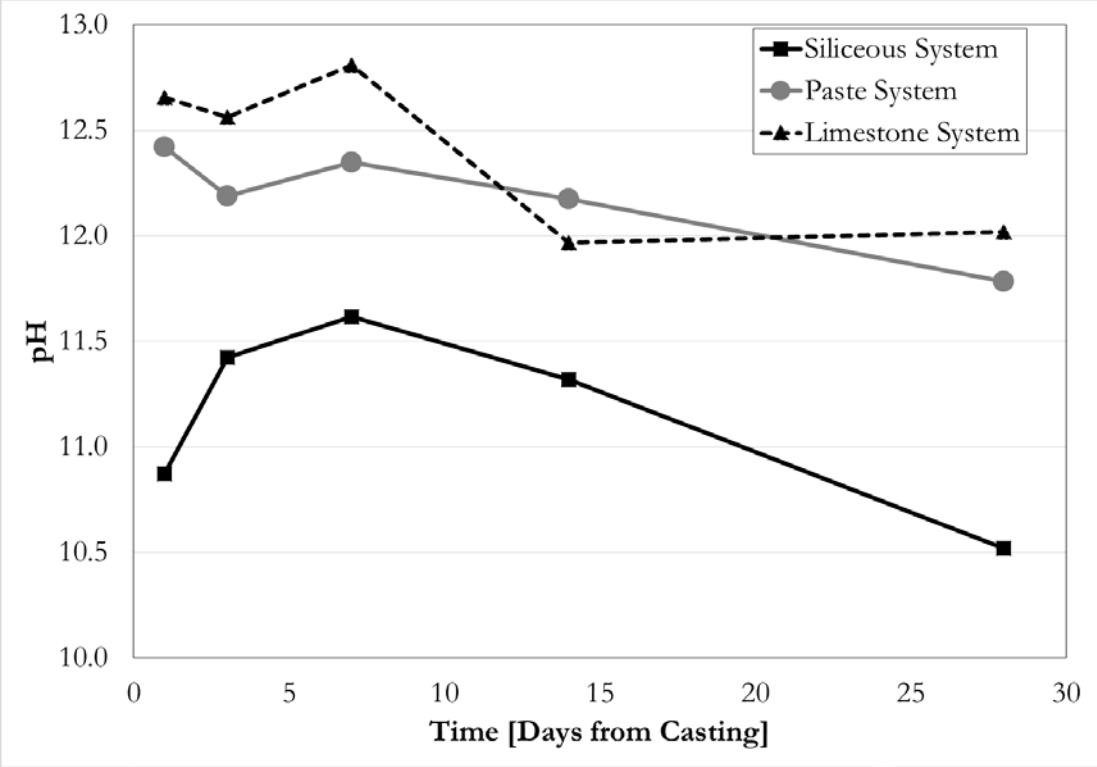

Figure 4-2: pH evolution of CAC concrete and paste systems over time when subjected to accelerated conversion curing regime

Silicon concentrations were also measured, however the concentration for all systems was below detection limits for each test date. Figure 4-1a and Figure 4-1b Show the concentration for the alkalis in each system, sodium (Na) and potassium (K). The trend is similar for both elements. Alkali concentrations in the Siliceous System were low (less than 350 ppm Na and less than 200 ppm K) and remained relatively constant at all ages. In the CAC Paste system the alkali concentrations at Day 1 were 1490 ppm Na and 4700ppm K. The alkali concentration then dropped continuously until day 14, where it stayed relatively constant through day 28 at 300 ppm Na and 200 ppm K. Alkalis in the Limestone System also were high prior to conversion at 1900 ppm Na and 6200 ppm K and dropped significantly after conversion to a concentration of 1000 ppm Na and 3400ppm K at day three. This initial reduction in concentration was followed by a continuous, longer-term decrease through 28 days. Earlier research by Gaztanaga et al. observed that alkali concentrations increased slightly over time in an unconverted system [23]. These results indicate that the conversion process, and subsequent continued hydration of unhydrated cement grains may actually bind some alkalis into the converted hydrate structures.

Aluminum concentrations followed similar trends as were seen for the alkali concentrations. The Siliceous System's aluminum concentration was low (below 300 ppm Al) and remained relatively constant at all ages. The Limestone System, however, experienced an decrease in aluminum concentration from Day 1 (unconverted) at 4550 ppm Al to Day 3 (converted) at 1750 ppm Al. The aluminum concentration in the Limestone system then continued to decrease through 28 days to 790 ppm Al. The CAC Paste system also saw a decrease in aluminum concentration, decreasing from Day 1 (unconverted) at 2820 ppm Al to Day 3 (converted) at 1430 ppm Al, eventually decreasing to 150 ppm of Al at Day 28. The Siliceous System's aluminum concentration remained relatively constant and low compared to the Limestone System and CAC Paste Al concentrations, and did not experience a similar decrease in concentration after conversion. These results show that there was relatively little activity in the Siliceous System compared to the Limestone System and Paste System, nor did the Siliceous System did not experience reductions in concentration of Al, Na, and K as was seen in the Limestone System and Paste System during conversion. These results indicate that the siliceous aggregates reduced overall reactivity in the CAC system.

The pH evolution between systems was quite different, as can be observed in Figure 4.2. The pH in both the Limestone System and CAC Paste pore solutions were significantly higher than the pH in the siliceous system. It has been shown that Al_2O_3 becomes more soluble as pH rises in cement systems [24]. Therefore, the higher pH observed in the Limestone System and the CAC Paste system may have allowed for increase dissolution of cement grains during the initial hydration period. This is supported by the high concentrations of aluminum in the pore solution of the Limestone System and the CAC Paste at early ages. The relatively lower pH observed in the Siliceous System may have reduced the overall degree of hydration in the Siliceous System compared to the Limestone System. The lower pH indicates that there may not be as high of a degree of hydration occurring in the Siliceous System, early on, as is occurring in the Limestone System. Therefore, as conversion occurs in the Limestone System and CAC Paste, porosity will form due to the densification of metastable hydrates in the system and additional stable hydrates (AH_3 and C_3AH_6) will be able to precipitate out of solution due to the high level of ionic activity in the solution compared to the Siliceous System. The formation of these additional hydrates may explain why higher strengths were observed in systems containing limestone aggregates compared to those containing siliceous aggregates [20]. The effect of conversion on pH in CAC systems was varied. Both the Limestone System's and CAC Paste's pH decreased from Day 1 (unconverted) to Day 3 (Converted). However, an increase of 0.5 pH was observed in the

Siliceous System during conversion. This indicates pH changes during conversion are significantly affected by aggregate mineralogy in CAC systems.

Calcium concentrations, as shown in Figure 1d indicate that over time, and after conversion, calcium concentrations in the pore solutions in the Limestone System stayed relatively constant, whereas calcium concentrations in the CAC Paste systems started low, decreased slightly directly after conversion, and then increased significantly after 28 days. Calcium concentrations in the Siliceous System, however, started high with a subsequent decreased after conversion. The level of calcium concentrations in all systems were generally less than those observed for potassium, sodium, or aluminum indicating that a low amount of calcium is released into the pore solution during conversion, and that much of the calcium that does dissolve during initial hydration is quickly bound into the initial hydrates formed. Previous work, as described above, has stated that the strength differences observed between siliceous and limestone aggregate CAC concrete systems was due to the formation of calcium monocarboaluminate due to dissolution of the limestone and resultant release of calcium into the pore solution [13, 15, 20, 21]. The reaction between the cement and aggregates in the concrete system was assumed to be analogous to that observed when finely ground limestone powder was included in CAC paste systems [13, 20, 21]. The low level of calcium in the pore solution in the Limestone System indicates that the limestone aggregates were not going into solution to help form calcium monocarboaluminate, contradicting the assumptions of the studies mentioned previously. Further studies using alternative analysis techniques need to be performed, however, to confirm whether calcium monocarboaluminate forms in these systems containing limestone aggregates.

It is important to note that comparisons between absolute elemental concentration values should not be made between concrete and paste systems when examining the pore solution. Only comparisons of trends between concrete and paste systems should be examined. This is because the relative amount of porosity, hydrates, and pore solution in each system will be significantly different, resulting in differences in concentration due to the amount of free water in each specimen. Additionally, there is some concern that the release of water caused by the conversion of hydrates from metastable hydrates to stable hydrates may result in significantly reduced concentrations after conversion [23]. This may explain the drop in concentration in the alkalis and aluminum in the Limestone Aggregate and CAC Paste samples. However, similar decreases in concentration were not observed in the Siliceous System for the aluminum and alkali concentrations, indicating that this may not actually have a significant

effect. A further examination of the amount of pore solution that is released during conversion for each system, and the effect on concentrations should be done to clarify this possible source of error.

4.3.2 Leaching Study

An additional study was done to understand the amount of leaching that occurred in the systems. Specifically to determine if the significant drop in concentration of the aluminum, potassium, and sodium from Day 1 (unconverted) to Day 3 (converted) in the Limestone System and CAC Paste was caused by leaching of these elements into the water bath in which they were stored. In order to examine this concrete cylinders from the Limestone System were soaked in water at 50°C, and then concentrations of potassium, sodium, aluminum, silicon, and calcium, as well as pH of the soak water were monitored over time.

Plastic cylinders measuring 150 mm in diameter and 300 mm in height were filled with 3000 cm^3 of tap water and placed in a heated oven at 50°C. Cylinders made from the Limestone System mixture were submerged in the water after 24 hours of curing at ambient laboratory temperatures (similar to the curing regime described above). The volume of water used kept the cylinders submerged with a 25 mm depth of water over the concrete cylinder, as well as 25 mm of water surrounding the cylinder's circumference. The cylinders were capped and wrapped in plastic paraffin film to prevent moisture loss to the environment. Samples were taken from the water prior to submersion of the concrete cylinders, as well as at 3, 7, 14, and 28 days after the concrete was cast. These samples were then analyzed in the same method as those above through the use of the ICP-OES and pH meter. Three specimens were maintained and the results were averaged and are presented in Table 3.4.

Table 3.4: Elemental concentration and pH evolution of concrete cylinder curing water over time

Time	Elemental Concentration of Curing Water [ppm]					pH
[Days From Casting]	K	Na	Al	Si	Ca	
1**	20	237	*	*	*	7.6
3	172	247	150	*	174	10.9
7	334	256	127	*	130	11.0
14	175	263	127	*	97	11.1
28	335	278	138	*	50	11.4

* - Indicates that concentration was below detection limits.

** - Sample was taken prior to introduction of concrete samples

These results indicate that very little leaching occurred in these systems. As with the concrete and paste systems, silicon concentrations were below detection limits. Potassium, aluminum, and calcium concentrations increased after submersion of the samples in the water, indicating that there was some leaching initially, however the increase in concentration was very low (~ 150 ppm) for each element. While some leaching may have occurred in these systems, it would not have been significant enough to explain the total decrease in concentration observed in the Limestone System and CAC Paste system pore solutions. Therefore the decrease in aluminum, potassium, and sodium concentrations observed in the Limestone System and CAC Paste were most likely due to the precipitation of hydrates from solution. The small amount of leaching that did occur in this system, did result in a significant increase in pH, however, after the concrete cylinders were submerged in the water.

4.4 Conclusions

The study presented in this paper examined the pore solution chemistry in CAC concrete and paste systems. This work has shown that the pore solution chemistry evolution during the conversion of CAC concrete can be significantly affected by the mineralogy of the aggregates used in the system. The pH of the Limestone Aggregate was significantly higher than that of the Siliceous Aggregate system at all ages. The concentrations of aluminum, potassium, and sodium were low (around 320 ppm Na, 120 ppm K, and 200 ppm Al) and stayed relatively constant before and after conversion in the Siliceous System, whereas a significant decrease in the concentration of these elements was observed in the Limestone System (1900 ppm to 1000 ppm Na, 6000 ppm to 3500 ppm K, and 4500 to 1800 ppm Al). Concentration trends in the CAC Paste system were similar to those observed in the Limestone system.

These results indicated that the addition of siliceous aggregates into a hydrating CAC system significantly reduce the overall pH and activity of the system. The reason for this drop in pH is still not well understood and further work needs to be completed to better understand these results. The drop in pH may have caused a reduction in the dissolution of cement grains prior to conversion. Subsequently, less material is available to precipitate out of solution during conversion. This may have been the cause for the significantly lower strengths in CAC concrete made with siliceous aggregates compared to limestone aggregates observed by previous studies. Further work needs to be completed to understand the phases present in each of these systems, overall porosity differences, as well as the rate at which they form during hydration and conversion.

4.5 Acknowledgements

Generous financial support for this work from Kerneos Aluminate Technologies is greatly appreciated. We also value the help of Andy Ungerer and the W. M. Keck Collaboratory for Plasma Spectrometry at Oregon State University. Finally, thank you to our undergraduate research assistant, Aaron Strand, for his help with sample preparation.

4.6 Works Cited

[1] Concrete Society Technical Report, Calcium Aluminate Cements in Construction: A Reassessment, in, Concrete Society, 1997, pp. 63.

[2] K.L. Scrivener, A. Capmas, Calcium Aluminate Cements, in: P.C. Hewitt (Ed.) Lea's Chemistry of Cement and Concrete, Elsevier - Butterworth-Heinemann, Oxford, UK, 1998, pp. 713-782.

[3] H.G. Midgley, High alumina cement in construction - A future based on experience, in: R.J. Mangabhai (Ed.) International Symposium on Calcium Aluminate Cements, E & F. N. Spon, London, 1990, pp. 1-13.

[4] K.L. Scrivener, Calcium Aluminate Cements, in: J. Newman, B.S. Choo (Eds.) Advanced Concrete Technology, Butterworth-Heinemann, 2003, pp. 2-30.

[5] S.M. Bushnell-Watson, J.H. Sharp, On the cause of the anomalous setting bahavior with respect to temperature of calcium aluminate cement, Cement and Concrete Research, 20 (1990).

[6] A. Muller, Conversion & résistance en compression des ciments aluminates de calcium, in: Department Genie Civil, Universite Laval, Quebec City, 2010.

[7] H. Fryda, E. Charpentier, J.M. Bertino, Accelerated test for conversion of calcium aluminate cement concrete, in: C.H. Fentiman, R.J. Mangabhai, K.L. Scrivener (Eds.) Calcium Aluminate Cements: The Centenary Conference, IHS BRE Press, Avignon, FR, 2008.

[8] H. Fryda, K.L. Scrivener, G. Chanvillard, C. Feron, Relevance of Laboratory Tests to Field Applications of Calcium Aluminate Cement Concretes, in: International Conference on Calcium Aluminate Cements (CAC), IOM Communications, Heriot-Watt University, Edinburgh, Scotland, UK, 2001, pp. 215-247.

[9] F. Indelicato, On the correlation between porosity and strength in high-alumina cement mortars, Materials and Structures, 23 (1990) 289-295.

[10] N. Ukrainczyk, T. Matusinović, Thermal properties of hydrating calcium aluminate cement pastes, Cement and Concrete Research, 40 (2010) 128-136.

[11] S. Klaus, J. Neubauer, F. Goetz-Neunhoeffer, Hydration kinetics of CA_2 and CA—Investigations performed on a synthetic calcium aluminate cement, Cement and Concrete Research, 43 (2013) 62-69.

[12] H.H.M. Darweesh, Limestone as an accelerator and filler in limestone-substituted alumina cement, Ceramics international, 30 (2004) 145-150.

[13] C.H. Fentiman, Hydration of carbo-aluminous cement at different temperatures, Cement and Concrete Research, 15 (1985) 622-630.

[14] H.-J. Kuzel, H. Baier, Hydration of calcium aluminate cements in the presence of calcium carbonate, European Journal of Mineralogy, 8 (1996) 129-141.

[15] V. Lamour, P. Monteiro, K. Scrivener, H. Fryda, Mechanical properties of calcium aluminate cement concretes, in: International conference on calcium aluminate cements, 2001, pp. 199-213.

[16] H. Midgley, Measurement of high-alumina cement-calcium carbonate reactions using DTA, Clay Minerals, 19 (1984) 857-864.

[17] H.G. Midgley, A. Midgley, The conversion of high alumina cement, Mag Concr Res, 27 (1975) 59-77.

[18] A. Bachiorrini, L. Montanaro, A. Delmastro, Microstructural disorder and calcium carbonate reactivity with monocalcium aluminate during hydration, Materials chemistry and physics, 14 (1986) 41-46.

[19] C. Gosselin, Microstructural development of calcium aluminate cement based systems with and without supplementary cementitious materials, in: Labratoire des Materiaux de Construction, Ecole Polytechnique Federale de Lausanne 2009, pp. 219.

[20] L. Cussino, A. Negro, Hydration du ciment alumineux en présence d'agrégat siliceux et calcaire, in: 7th International Congress on the Chemistry of Cement, Paris, 1980.

[21] A. Negro, A. Bachiorrini, M. Murat, Interaction, in aqueous medium, between calcium carbonate and monocalcium aluminate at 5°C, 20°C, and 40°C, Bulletin de minéralogie, 105 (1982) 284-290.

[22] P. Barret, D. Bertrandie, Hydration of Aluminate Cements, in: M.W. Grutzeck, S.L. Sarkar (Eds.) Advances in Cement and Concrete, American Society of Civil Engineers, University of New Hampshire, Durham, NH, 1994, pp. 132-174.

[23] M.T. Gaztanaga, S. Goni, J.L. Sagrera, Reactivity of high-alumina cement in water: pore solution and solid phase characterization, Solid State Ionic, 63 (1993) 797-802.

[24] F. Winnefeld, B. Lothenbach, Hydration of calcium sulfoaluminate cements — Experimental findings and thermodynamic modelling, Cement and Concrete Research, 40 (2010) 1239-1247.

Manuscript 3

Influence of Aggregate Type on Conversion and Strength in Calcium Aluminate Cement Concrete

Matthew P. Adams and Jason H. Ideker

To be submitted to: Cement and Concrete Research

5 Manuscript 3

Influence of Aggregate Type on Conversion and Strength in Calcium Aluminate Cement Concrete

Matthew P. Adams[1,2] and Jason H. Ideker[2]

Abstract: Calcium aluminate cement (CAC) is gaining popularity in North America as a rapid repair material due to its ability to quickly gain strength, even at low curing temperatures. Use of CAC has been limited, however, due to a lack of understanding of the process of conversion generally, and the role of aggregates in CAC concrete in particular. Conversion, which occurs only in 100% CAC systems, is a chemical process in which metastable hydrates (CAH10 and C2AH8) convert into denser, stable hydrates (C3AH6 and AH3). The conversion of hydrates is accompanied by the formation of porosity and a subsequent strength reduction. Presented is an examination of aggregate source impacts on this conversion process and converted CAC concrete strengths. Nine different concrete systems with fifteen varying aggregate sources were examined. Results indicated that the carbonate limestone and siliceous limestone aggregate systems had significantly less strength reduction due to conversion compared to siliceous aggregate systems. Microstructural analysis of one carbonate limestone system and one siliceous river gravel system suggested that the limestone system had less porosity and better-formed aggregate/paste interfacial transition zones compared to the carbonate limestone system. Chemical analysis of the concrete pore solution indicated that the carbonate limestone system's pH and ionic concentrations of aluminum, sodium, and potassium were significantly higher than that of a siliceous river gravel system indicating more dissolution on unhydrated cement in the carbonate limestone system. These studies are presented along with a proposed theory explaining the cause of the significant converted strength differences in CAC concrete systems made with limestone aggregates compared to siliceous aggregates.

Keywords: calcium aluminate cement, calcium aluminate cement conversion, aggregate porosity, pore solution

[1] Corresponding Author: matthewpadams@gmail.com
[2] School of Civil and Construction Engineering, 101 Kearney Hall, Oregon State University, Corvallis, OR 97333

5.1 Introduction

Calcium aluminate cement (CAC) concrete has been used in the construction industry for over one hundred years, first gaining popularity as a rapid strength gain material to produce gun emplacements during WWI in France [1]. Today the material has a wide range of uses including as a temperature resistant material in refractory applications [2, 3], scour resistance in dam spillways and wearing surfaces [4], and acid attack resistance for industrial floors and sewage applications [4-7]. More recently there has been significant interest in North America concerning the use of CAC concrete as a rapid repair material [8, 9]. Due to its ability to gain strength rapidly, even at low temperatures, CAC will continue to be an important material for use in construction and repairing deteriorating infrastructure.

Despite the fact that CAC hydration has been studied significantly, it is still not well understood within the general construction industry. Furthermore, much of the research into CAC systems has focused on cement pastes and mortars and as a result, the impact of aggregates on CAC hydration and concrete properties is not well understood. Limited previous work has shown that aggregate mineralogy can significantly alter the strength development and hydration in CAC concrete [10, 11]. Despite these findings, however, no systematic study of the impact of different aggregate types on CAC concrete has been done. Of particular concern is the impact that aggregates have on strength development and conversion, a chemical process which causes porosity to form in the system over time.

5.1.1 Hydration and Conversion in CAC Systems

The following section discusses hydration in standard grade CACs, which are the focus of this research, and applies only to pure CAC systems. Additions of other cementitious products will alter the hydration products and change the overall chemistry of the system. Monocalcium aluminate (CA) is the main unhydrated cement phase in CAC and makes up more than 40% of the phase composition of standard grade CAC systems [12]. CA will hydrate to form four main phases: CAH_{10}, C_2AH_8, C_3AH_6, and AH_3. These hydrates fall into two main categories, metastable (CAH_{10}, C_2AH_8) and stable hydrates (C_3AH_6, and AH_3) [12-14]. Which hydrate is initially formed depends on the temperature history of the system. When cured isothermally at temperatures below 15°C, CAH_{10} is primarily formed during initial hydration. When cured isothermally at temperatures between 15°C and 27°C, both CAH_{10} and C_2AH_8 are formed during initial hydration [12, 13], however as the temperature approaches 27°C, formation of neither hydrate is favored, slowing setting time at this temperature [15-19]. When cured isothermally at temperatures above 27°C, C_2AH_8 is the primary hydrate formed

during initial hydration along with AH_3, a stable gel hydrate. CAH_{10} and C_2AH_8 are both metastable hydrates and will undergo transitions to form the stable hydrate C_3AH_6 along with additional AH_3 gel. The speed at which this transition reaction occurs is dependent on the temperature and moisture state of the system [12-14] as well as w/cm [13]. As temperatures increase above 27°C, the conversion of C_2AH_8 to C_3AH_6 occurs with increasing rapidity, therefore, higher curing temperatures result in faster conversion from metastable to stable hydrates. However, it is important to note that this reaction is thermodynamically inevitable and will occur at all temperatures [12, 14].

The conversion reaction has significant impacts on porosity, and consequently strength, in the CAC system. Long-term the strength is based on the stable hydrates C_3AH_6 and AH_3, whereas early-age strength is dependent on the metastable hydrates CAH_{10} and C_2AH_8. The rapid strength gain observed in calcium aluminate cements is a byproduct of the rapid precipitation observed during hydration of CAC cement. Lamour et al. observed through transmission soft X-ray microscopy that as the induction period ends, there is a rapid formation of metastable hydrates resulting in a significant binding of water and filling of space [13, 20]. The rapid space filling due to the formation of the metastable hydrates provides high early strength in these systems [13]. The strength developed from the metastable hydrates is transitory, however, as conversion occurs strength loss is observed in CAC systems. Converted CA hydrates (density (g/cm^3): C_3AH_6=2.52 AH_3=2.4) are denser than unconverted hydrates (density (g/cm^3): CAH_{10}=1.72, density of C_2AH_8=1.95) [21, 22]. As the hydrates densify during conversion, they release water into the system and porosity is formed. The formation of porosity in the system results in a significant loss of strength. After conversion occurs, and a minimum strength has been reached, the water released by conversion can continue to hydrate unhydrated cement grains resulting in continued long-term strength gain [13, 22]. After conversion occurs, long-term strength gain will be stable because once C_3AH_6 has nucleated, direct formation of C_3AH_6 from CA becomes favorable [23, 24].

5.1.2 Impact of Aggregate Mineralogy on CAC Strength and Conversion

Previous work has observed that aggregate mineralogy can have a significant impact on concrete strength and conversion in CAC systems. Cussino and Negro showed that specimens containing limestone aggregates steadily gained strength over a 5-year period, even when similar specimens made with siliceous aggregates lost strength due to conversion [10]. Scrivener and Capmas also noted that CAC concrete made with limestone typically showed strengths about 20% higher than those made

with siliceous aggregates, ascribing the difference to bond strengths between the cement paste and aggregates [13]. Lamour et al. observed similar findings in concrete and mortars made with siliceous and limestone aggregates [11].

Cussino and Negro's preliminary analysis observed the formation of calcium monocarboaluminate in the samples containing finely ground limestone (FGLS) (15 μm to 150 μm particle size diameter) as opposed to limestone aggregates (150 μm to 4.75 mm particle size diameter for fine aggregates, 4.75 mm and greater particle size diameter for coarse aggregates) [10, 25]. Additional work has confirmed that the use of FGLS as a partial replacement for CAC results in the formation of calcium monocarboaluminate [10, 11, 26-34]. However, using a high surface area material such as FGLS to explain how a larger limestone aggregate, with significantly less surface area on which topochemical reactions may occur may not provide an accurate answer to the results discussed above. Cussino and Negro [10] and Lamour et al. [11] assumed that analogous reactions were occurring in the systems containing limestone aggregates, however they did not confirm the existence of calcium monocarboaluminates in the concrete systems containing 100% CAC. Previous researchers have suggested mechanistic work be performed to further understand the differences between CAC concrete made with limestone and CAC concrete made with siliceous aggregates [11]. It is important to note, however, that the literature discussed above did not clearly distinguish the mineralogy of the limestone aggregates.

The work presented in this paper seek to addresses the gaps in literature concerning the impact of aggregate source on CAC concrete; and to address the aforementioned call for mechanistic work examining the impact of limestone aggregate on CAC conversion and strength. Presented are the results of a study that examined compressive strength of CAC concrete prepared with 15 different aggregate sources (nine coarse aggregate, six fine aggregate) prior to and after conversion. Eight aggregate sources (four coarse aggregate, four fine aggregate) were examined in depth to determine the impact of aggregate gradation on CAC concrete. Pore solution chemistry, scanning electron microscope imaging with elemental mapping, and porosity development were also examined for two of the concrete mixture: one containing carbonate limestone aggregates and one containing siliceous river gravel aggregates.

5.2 Materials

5.2.1 Cement

A standard grade CAC was used for all concrete and mortar mixtures examined in this study. The oxide composition of the CAC used in this study is presented below in Table 5-1.

Table 5-1: Oxide composition for CAC used in this study

Oxide (% wt)	SiO_2	Al_2O_3	Fe_2O_3	CaO	MgO	Na_2O	K_2O	SO_3	TiO_2	Mn_2O_3	P_2O_5	SrO	LOSS
CAC	4.98	38.23	15.40	37.53	0.71	0.03	0.23	0.06	1.80	0.23	0.13	0.02	0.65

5.2.2 Aggregates

A wide range of aggregates were used through this study in concrete and mortar mixtures. Nine coarse aggregates and six fine aggregates from around North America were used. Absorption capacities and specific gravities (G_S) were measured according to ASTM C127 for coarse aggregates and ASTM C128 for fine aggregates [35, 36]. A description of the aggregates including name, absorption capacity, G_S, source location, mineralogical description and particle shape description can be found in Table 5-2 for the coarse fraction Table 5-3 for the fine fraction.

Table 5-2: Coarse aggregate description

Aggregate Name	Absorption Capacity (%)	$G_{sb, OD}$	Source	Mineralogical Description	Particle Shape and Texture
KRCC	2.58	2.44	Oregon, USA	Siliceous	Smooth, Rounded
KQGC	1.71	2.66	Proprietary	Siliceous	Smooth, Rounded
TXIC	1.31	2.56	Texas, USA	Siliceous	Smooth, Rounded
STRC	0.73	2.62	Wyoming, USA	Siliceous	Smooth, Rounded
PLTC	1.55	2.55	New Mexico, USA	Siliceous	Smooth, Rounded
BLGC	0.83	2.72	New Brunswick, Canada	Siliceous	Smooth, Rounded
MMC	2.73	2.49	Texas, USA	Carbonate Limestone	Coarse, Angular
CRCC	0.67	2.68	Washington, USA	Carbonate Limestone	Coarse, Angular
SPTC	0.96	2.64	Ontario, Canada	Siliceous Limestone	Coarse, Angular

Table 5-3: Fine aggregate description

Aggregate Name	Absorption Capacity (%)	$G_{sb, OD}$	Source	Mineralogical Description
KRCF	3.08	2.41	Oregon, USA	Siliceous
KQGF	2.08	2.66	Proprietary	Siliceous
TXIF	0.56	2.55	Texas, USA	Siliceous
BLGF	0.99	2.67	New Brunswick, Canada	Siliceous
MMF	2.5	2.95	Texas, USA	Carbonate Limestone
CRCF	0.71	2.69	Washington, USA	Carbonate Limestone

Four aggregate sources were chosen for further analysis to examine grading differences between the aggregates. The coarse (C) and fine (F) portions of the KRC, BLG, MM, and CRC aggregates were examined. These aggregates are coarse and fine portions produced from the same aggregate source.

A sieve analysis was completed for the MM, CRC, KRC aggregates according to ASTM C136 [37] for both coarse and fine fractions. Sieve analysis for the BLG aggregates, which were from Canada, was done according to CAN/CSA-A23.2-2a-14 [38]. These methods are similar, differing slightly in the opening size of the sieves used as can be observed in the sieve analysis results. Results from the sieve analyses are presented in Figure 5-1.

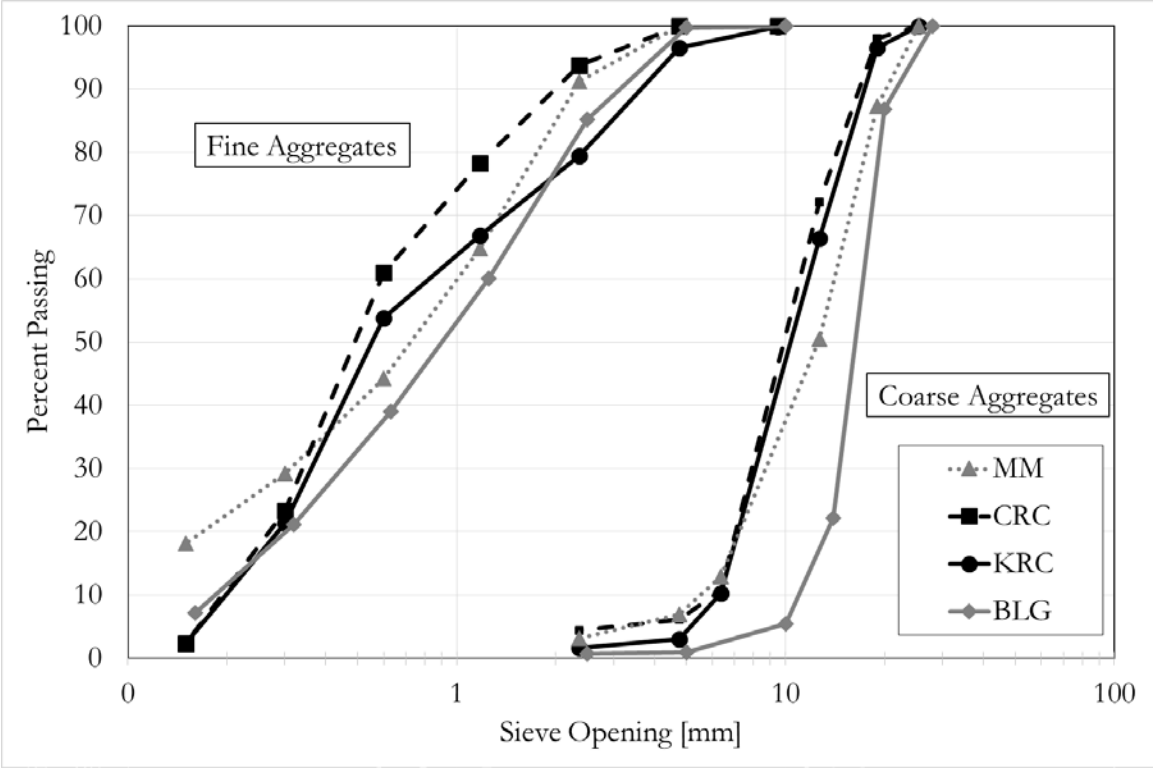

Figure 5-1: Sieve analysis results for selected coarse and fine aggregates

Figure 5-1 indicates that the coarse aggregates were of similar grading. The BLG coarse aggregate was measured using slightly larger sieve sizes, as discussed above, compared to the CRC, KRC, and MM mixtures which accounts for some of the difference in the curve. The fine aggregate grading had more scatter between the different aggregate sources. However, no significant differences were observed between the siliceous and limestone aggregate grading overall.

The D50 number is a particle size measurement that describes median diameter of a particular aggregate by noting the particle size at which 50% of the material is larger than the D50 number and 50% of the material is smaller than the D50 number. This is a useful tool for comparing grading between different aggregate sources [39]. The fineness modulus (FM) is a semi-quantitative index that is useful for comparing the grading between two aggregate sources. It can be used to evaluate the fineness of aggregates in a concrete mixture. A higher FM indicates a coarser graded aggregate [40]. The fineness modulus was calculated according to Equation 5-1 [41]:

$$FM = \frac{(\sum S_x)}{100} \qquad \text{Equation 5-1}$$

Where FM is the fineness modulus, and S is the percent mass retained on sieve size x, and x is the sieves with the following openings: 150μm, 300μm, 600μm, 1.18 mm, 2.36 mm, 4.75 mm, 9.5 mm, 19 mm, 37.5 mm, 75 mm, and 150 mm [41]. For this study, only the FM of the fine aggregate was calculated. The D50 of the coarse and fine portions and FM for the fine portion of the MM, BLG, KRC, and CRC aggregates can be observed in Table 5-4.

Table 5-4: D50 and fineness modulus of MM, BLG, KRC, and CRC aggregates

Aggregate Name	Coarse D50 (mm)	Fine D50 (mm)	Fine FM
KRCF/KRCC	12.73	0.56	2.8
BLGF/BLGC	16.58	0.95	2.9
MMF/MMC	12.61	0.76	2.5
CRCF/CRCC	10.4	0.51	2.4

The D50 and FM values indicate that the BLG aggregate had a coarser grading than all other aggregates. The KRC aggregates also show relatively high FM and Coarse D50 number. However, the fine D50 number of the KRC aggregates is low compared to the BLG and MM aggregates. Overall, the CRC aggregate had the finest material in both the coarse and fine fractions compared to the BLG, MM, and KRC aggregates.

5.2.3 Concrete and Micro-concrete Mixture Designs

The concrete mixtures prepared for use in this study are described in Table 5-5.

Table 5-5: Concrete mixture designs

Mixture Designation	Fine Aggregate Type	Fine Aggregate Content (kg/m^3)	Coarse Aggregate Type	Coarse Aggregate Content (kg/m^3)	Cement Content (kg/m^3)	w/cm	Fresh Concrete Unit Weight (kg/m^3)
KRC	KRCF	730	KRCC	890	440	0.40	2360
BLG	BLGF	730	BLGC	890	440	0.40	2350
KQG	KQGF	810	KQGC	810	440	0.40	2370
TXI	TXIF	780	TXIC	954	440	0.40	2340
PLT	TXIF	774	PLTC	948	440	0.40	2330
STR	TXIF	786	STRC	960	440	0.40	2330
SPT	TXIF	786	SPTC	969	440	0.40	2350
MM	MMF	720	MMC	840	440	0.40	2320
CRC	CRCF	855	CRCC	938	440	0.40	2400

The cement content of 440 kg/m^3 and w/cm of 0.40 remained constant between all mixtures. These values were chosen based off of long-standing mixture design recommendations for CAC concrete mixtures [42, 43] that have been used to provide good quality CAC concrete after conversion. Aggregate contents were modified according to the aggregate properties to achieve the same unit mixture size of 0.77 m^3. Aggregates were premixed to achieve consistent, near-saturated surface dry conditions prior to being used in concrete mixtures. Aggregate moisture contents were measured prior to mixing, and total water content was adjusted for each mixture to maintain an effective w/cm of 0.40.

Three micro-concrete mixtures were also used as a part of this study, these mixture designs are described in Table 5-6.

Table 5-6: Micro-concrete mixtures

Mixture Designation	Fine Aggregate Type	Fine Aggregate Content (kg/m^3)	Cement Content (kg/m^3)	w/cm
CRCM	CRC	1300	730	0.40
KRCM	KRC	1215	730	0.40
Mod-KRCM	KRC (Grading Modified)	1300	730	0.40

The Mod-KRCM micro-concrete mixture used KRCF aggregate with its grading modified to match that of the CRCF aggregate. This was done in order to examine the impact of grading on strength in these systems. These two systems were chosen because they were of different mineralogies (siliceous and carbonate limestone), and as seen above in Figure 5-1 and Table 5-4 the CRCF was a much finer grading compared to the KRCF.

5.3 Experimental Methods

5.3.1 Mixing Technique

All concrete mixtures made were mixed according to the following procedure:

1. Added all aggregates and half of the mixing water to the mixer,
2. Covered the mixer and allowed to mix for 1 minute,
3. While still mixing, added the retarder and the super plasticizer,
4. While still mixing, added the cement, and the remaining water over a 1 minute period,
5. Continued to mix for three more minutes,
6. Discharged and cast specimens.

The total mixing time from the time the mixer was first started was 4.5 minutes ± 10 seconds. Concrete mixtures were done in the laboratory with an ambient temperature of 23 ± 4 °C. The relative humidity in the laboratory was not controlled or monitored.. Mixing of micro-concrete mixtures was done according to ASTM C 305 [44] standard procedure for mixing mortars.

5.3.2 Curing Regime to Promote Accelerated Conversion

Concrete specimens were cast according to ASTM C192 [45]. Concrete specimens were cast into 100 mm diameter x 200 mm height cylindrical plastic molds. After casting the molds were capped to prevent moisture loss. Hydration of CAC concrete results in a rapid and extreme exotherm [22]. Therefore, the samples were spaced with at least 75 mm between the outer edges of all samples to allow for heat dissipation. Temperature was monitored for the initial 24 hour period. Concrete specimens reached peak temperatures between 50 - 55°C for less than one hour. This temperature indicates that the specimens did not undergo full conversion during the initial curing process. Previous work by Fryda et al. has shown that temperatures above 70°C during initial hydration will result in rapid conversion to stable hydrates [22]. However, since the samples did reach elevated temperatures for a short period of time, minor amounts of conversion during the initial cure may have occurred.

Samples were allowed to cure for 24 hours in the plastic molds. After 24 hours, the samples were removed from the plastic molds, labeled, and immediately placed into a 50 ±2 °C water bath. The samples were then cured in the 50°C water bath for an additional 27 days. On day 28 after casting, any remaining samples were removed from the heated water bath and placed into a moist curing room with a temperature of 23 ± 2 °C, and > 95% RH until tested. One set of cylinders from the CRC mixture were maintained in the 50 ±2 °C water bath to measure long-term strength stability at elevated temperatures in that system. This curing regime promotes conversion due to the elevated temperature. Work has shown that at 50°C, the samples should reach minimum converted strength within two days after immersion in the water bath [22], however the length of time to minimum converted strength may be affected by aggregate type (see Chapter 3).

The micro-concrete was cast into 50mm x 50mm x 50mm steel cube molds, three cubes to one mold. Similarly to the concrete specimens, after being cast, the cubes were spaced out with at least 75 mm between each mold to allow for heat dissipation. After 24 hours, the samples were removed from the steel cube molds, labeled, and immediately placed into a 50 ±2 °C water bath to promote conversion until they were tested.

5.3.3 Compressive Strength Measurements

Compression testing for concrete cylinders followed ASTM C 39 [46]. ASTM C 109 was followed for measuring the compressive strength of the micro-concrete cubes [47]. Compressive strength was measured out to 56 days for most concrete mixtures and 28 days for the micro-concrete mixtures. Compressive strength was measured out to 180 days for the KRC and CRC concrete mixtures to determine long-term strength gain, and stability of strength in these systems.

5.3.4 Stopping of Hydration

Advanced microstructural analysis techniques such as scanning electron microscopic (SEM) analysis and mercury intrusion porosimetry (MIP) require dried samples in which hydration has been arrested. The most widely used technique to arrest hydration is oven or microwave drying [14, 48]. However, this method can induce damage in the system [48] as well as alter the structure of CAC hydrates, such as CAH_{10} which decomposes around 110°C [21]. An alternative method, which induces much less damage to the CAC system, is the solvent exchange method.

The solvent exchange method was described in detail in Zhang and Scherer [48], who found that isopropanol was the best organic solvent to use for this technique and induced very little damage to the surrounding microstructure. This technique has been used to effectively arrest hydration prior to studying the microstructure of CAC samples in previous work [49, 50].

5.3.5 Scanning Electron Microscopy and Image Analysis

The microstructure of concrete specimens was studied through the use an FEI Quanta 600F SEM with an energy dispersive X-ray analyser was used. An accelerating voltage of 15kV was employed. Back scatter electron (BSE) image analysis was done on images taken of polished concrete samples impregnated with epoxy.

5.3.5.1 SEM Sample Preparation

Samples used for examination under the scanning electron microscope (SEM) were created from concrete specimens. Samples of around 20mm x 20 mm x 3 mm were cut from the center of concrete cylinders and their hydration was arrested according to the solvent exchange method described above. After the solvent was removed via placement in a dessicator, the samples were mounted and impregnated with epoxy to stabilize the system. A 2-part transparent epoxy system, EpoTek – 301 was used for this work. Samples were mounted and impregnated using a Struers CitoVac vacuum impregnation device.

After mounting and impregnation, the epoxy was allowed to cure for at least 48 hours. The epoxy was then removed down to the surface of the concrete sample using a Struers brand LaboPol-5. A 200 μm grit pad rotating at 300 rpm was used to grind off the epoxy from the surface of the concrete. Samples were held by hand during this polishing process. Isopropanol was used as a lubricating liquid during this portion of polishing. After the epoxy was ground off of the sample, the samples were placed in isopropanol and cleaned in an ultrasonic cleaner. Then the samples were fine polished using a Struers LaboPol-35 polishing system with a LaboForce-1 counter-rotation sample holder.

The polishing pad was rotated at 150 rpm during polishing, and the counter-rotation sample holder spun at 8 rpm. Diamond polishing sprays, sprayed onto a Struers MD-Largo polishing disc were used as the grit for fine polishing of the concrete samples. 9 μm grit, 3 μm grit, and a 1 μm grit were used in succession to create a smooth surface on the concrete sample for examination under the SEM.

Samples were polished for six hours with the 9 μm grit, three hours with the 3 μm grit, and three hours with the 1 μm grit. Diamond grit was reapplied once every hour. Samples were cleaned in the ultrasonic cleaner every two hours or between grits. An oil-based polishing fluid from Logitech was used to lubricate and remove waste material from polishing plate during operation. Samples were then placed into the dessicator after polishing for at least 48 hours to remove any remaining volatiles in the system. Samples were carbon coated prior to examination under the SEM.

5.3.5.2 Porosity Measurement through Image Analysis

Porosity was quantified through the use of image segmentation and quantification of the grey levels in each of the BSE images. The grey levels of the pores were determined in each image, and then the image was segmented into two sections: (1) porosity, and (2) hydrated cement paste, unhydrated cement, and aggregates. Porosity was then measured as a percent of each image. Examples of original images with their binary segmented image counterparts from the KRC and CRC concrete mixtures are shown in Figure 5-2, the original image is on the left, and the segmented image is on the right. Additional BSE-SEM images can be seen in Appendix B, Sections B.1.2 and B.1.3.

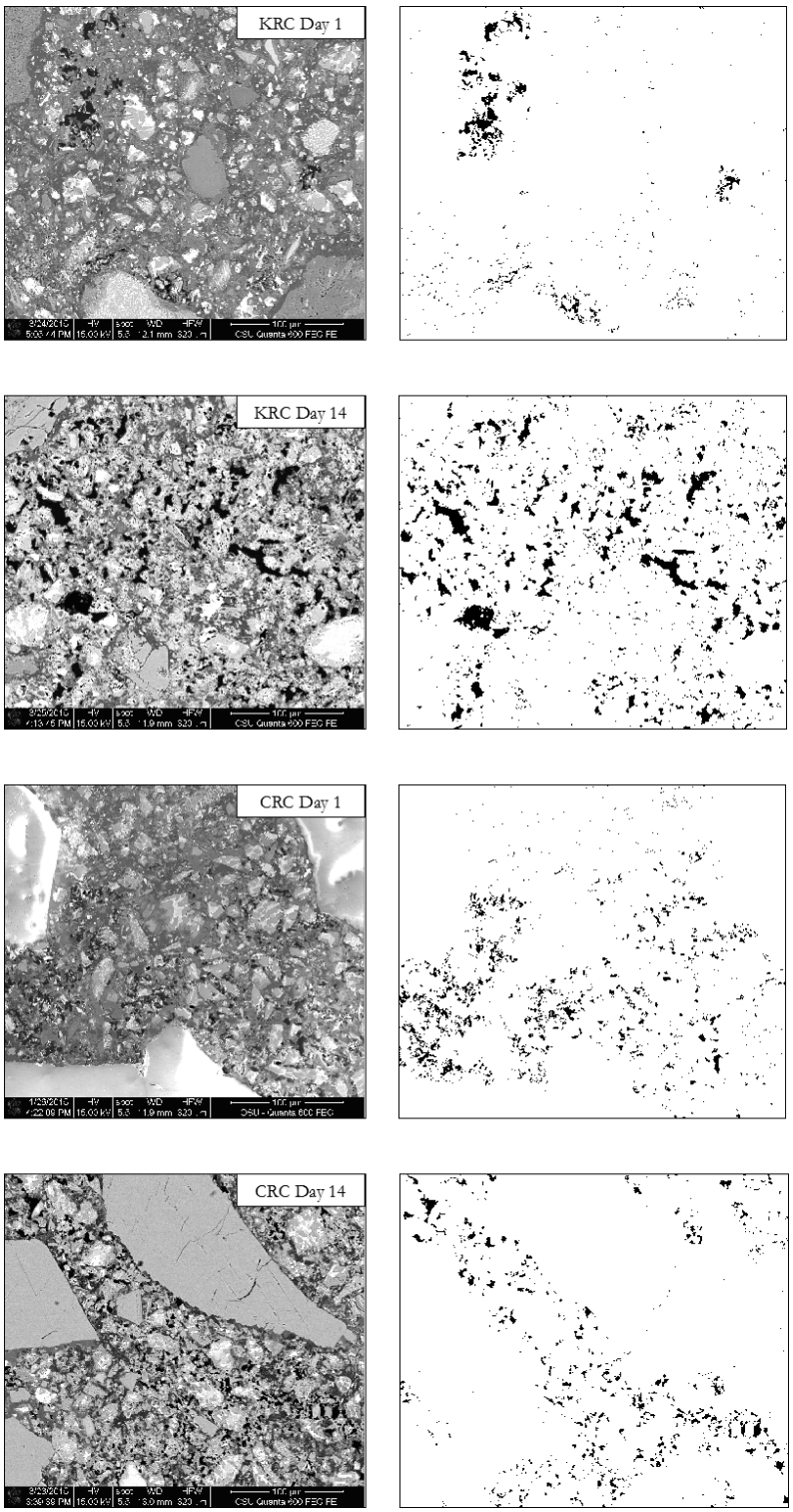

Figure 5-2: Example original SEM image (left) and segmented image (right) from KRC and CRC mixtures at 1 and 14 days

As can be observed, it is quite difficult to differentiate between aggregate, hydrated cement, and unhydrated cement through the use of gray levels in these images, as many of these phases share

similar gray levels. Therefore, individual phases and degree of hydration were not quantified. However, the porosity was easily separated through thresholding of the histogram and segmentation. For each age and concrete mixture two to three slices of concrete were analyzed, each from the same concrete cylinder. Fifty images were examined for each system at each age. The standard error of measurement for the porosity was determined by Equation 5-2 [51].

$$sem(\%) = \frac{\sigma}{\sqrt{N}} \qquad \text{Equation 5-2}$$

Where σ is the standard deviation over all images in a set, and N is the number of images for each age.

It is important to note that the SEM used for this study did not have an automatic image navigation option that took images over the area of a larger sample. Therefore, some bias was introduced into these results as all image locations were selected by the user. Future work should be sure to use SEMs which can automatically take images across a sample to avoid image location bias introduced by the user. Additionally, the locations for images were taken at points avoiding entrapped air voids and generally only examined pores below 100μm.

5.3.6 Mercury Intrusion Porosimetry

Very few studies have applied mercury intrusion porosimetry (MIP) to studying the porosity of CAC [51-54] and therefore the method is not well developed for use with the material [54]. System parameter such as the contact angle of the mercury have not been optimized. Also, despite the fact that the technique is regularly used to characterize the porosity of cementitious materials [55] the use of MIP for characterizing pore distribution in cement-based materials is controversial [56-58]. It has been shown to be useful as a comparative tool to analyse total porosity differences between mixtures [56]. For the work presented here, an MIP device from Porotec was used. The contact angle was taken as 140° with a model of cylindrical pores. A 3.5 g mortar specimen was used from each sample day for testing. MIP was done on samples from the KRCM and CRCM microconcrete mixtures. The small sample size required for MIP precluded the use of concrete samples.

5.4 Results

5.4.1 Concrete Compressive Strength Study

Nine separate concrete mixtures were cast and their compressive strength was measured to determine the impact of aggregate type on strength development following the accelerated conversion curing regime described above. Six mixtures contained both siliceous fine and coarse aggregates. Compressive strength through 56 days from the six siliceous aggregate mixtures can be seen in Figure 5-3, error bars indicate standard deviation of samples tested.

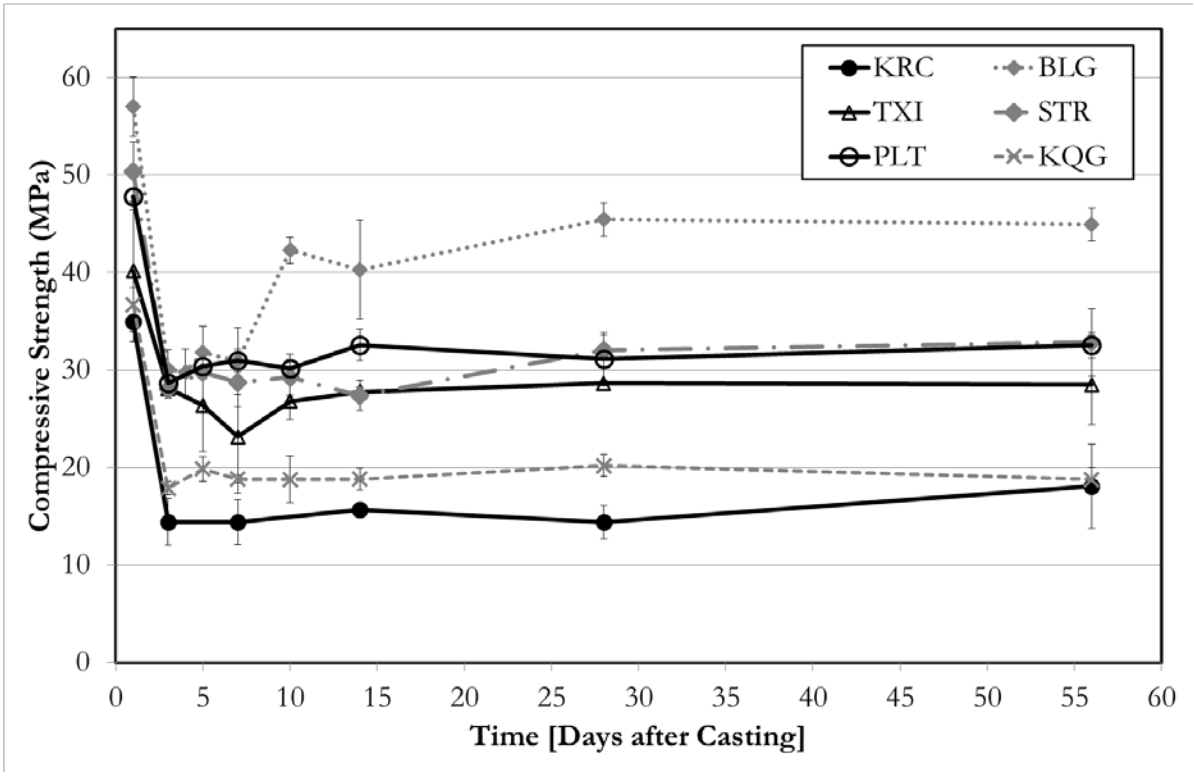

Figure 5-3: Compressive strength of concrete mixtures containing siliceous aggregates

Strengths measured at 24 hours were unconverted strengths, and strengths measured at day 3 and after were converted strengths. Conversion resulted in significantly reduced strengths in all mixtures containing siliceous aggregates. The one day strengths ranged from 34.9 MPa for the KRC mixture to 57.0 MPa for the BLG mixture. The mixtures containing the KRC and KQG aggregates exhibited the lowest converted strengths. Converted, 3-day strengths ranged from 14.4 MPa in the KRC mixture to 30.1 MPa in the BLG mixture. Percent strength reduction due to conversion between day 1 and minimum converted strength ranged from 59% strength reduction in the KRC mixture and 40%

strength reduction in the PLT system. The BLG, TXI, STR, and PLT mixtures all had similar converted strengths at day 3. The TXI mixture exhibited its minimum strength at day 7 (23.2 MPa), however the standard deviation at day 7 was quite large (5.8 MPa) and so the difference may not be significant compared to day 3 strength (28.1 MPa). All mixtures experienced strength gain between day 3 and day 28. The BLG mixture gained 15.6 MPa of strength, significantly higher than any other mixture.

Two mixtures were examined that were composed of carbonate limestone fine and coarse aggregates (MM and CRC), and one mixture was examined that had a siliceous limestone coarse aggregate with a siliceous fine aggregate (SPR). Compressive strengths through 56 days from the three mixtures containing limestone aggregates is shown in Figure 5-4, error bars indicate standard deviation of samples tested.

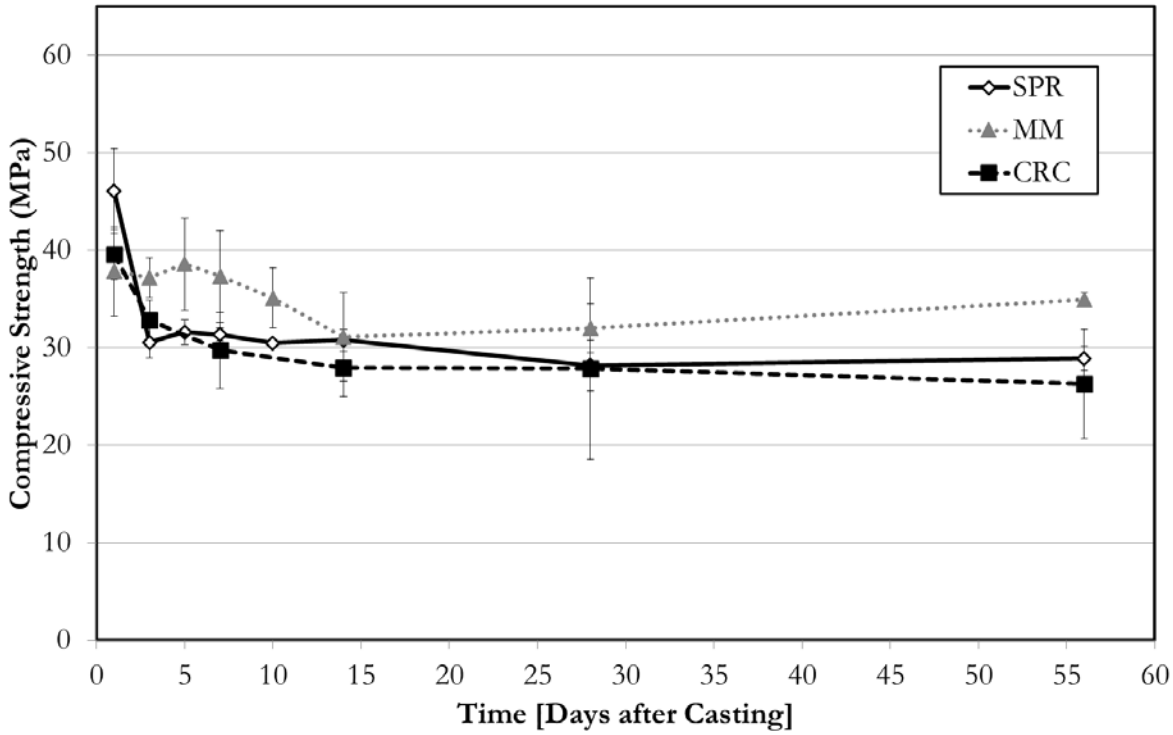

Figure 5-4: Compressive strength of concrete mixtures containing limestone aggregates

Strengths measured at 24 hours were unconverted strengths, and strengths measured at day 3 and after were converted strengths. The SPR samples experienced a significant strength reduction during conversion (15.5 MPa, or 34% strength reduction between day 1 and day 3). The MM and CRC

mixtures experienced much less strength loss due to conversion compared to the SPR and siliceous river gravel aggregate mixtures - 18% strength reduction in the MM mixture and 34% strength reduction in the CRC mixture. Average minimum converted strength for the MM system was observed at day 14, and at day 28 for the CRC. However, given the large standard deviation observed in all CAC mixtures (Chapter 1) [59], it is difficult to determine the exact date of minimum converted strength for the CRC mixture in particular without additional testing to verify variability within CAC systems.

Compressive strengths of the KRC and CRC mixtures were also measured out to 180 days. Additionally, a separate set of three CRC cylinders (labeled as CRC – Heated) were cured for the full 180 day duration in the 50°C water bath, instead of being moved to the 23°C moist curing room at 28 days. Compressive strengths to 180 days for the KRC, CRC, and CRC-Heated samples are presented in Figure 5-5, error bars indicate standard deviation for sample tested.

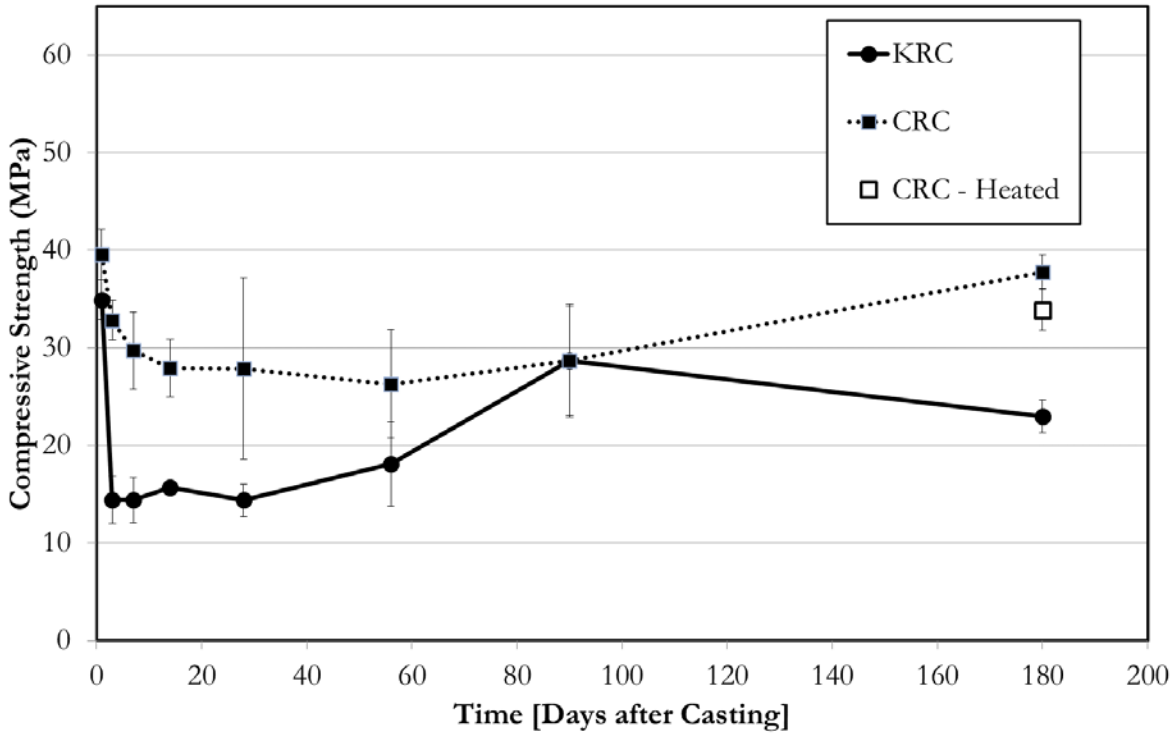

Figure 5-5: Long-term compressive strength of KRC and CRC mixtures

Long-term strength results indicate that both the CRC and KRC mixtures continued to gain strength over the full curing period, which resulted in significant strength increases from the minimum converted strengths. The 180 day strength of the CRC system was only slightly lower (1.8 MPa

difference) than that system's strength prior to conversion (1 day). The 180 day strength of the KRC system was still significantly lower (11.9 MPa difference) than the system's strength prior to conversion (1 day). The 180 day strength of the CRC-heated cylinders was 5 MPa less than the 180 day strength cylinders placed into the 23°C moist curing room after 28 days.

Two aggregate systems were examined in micro-concrete mixtures to determine the impact of coarse aggregate converted strengths in CAC systems. The microconcrete mixtures were developed total percentage of aggregate in the concrete mixtures, and then scaled to use only fine aggregate. By doing this, a comparison can be made to understand if similar behaviour was observed in systems containing only fine aggregate. Additionally, the microconcrete mixtures allowed for an examination of the impact of the fine aggregate gradation differences between systems on strength. Compressive strengths through 28 days for the KRCM, CRCM, and Mod-KRCM micro-concrete are presented in Figure 5-6, error bars indicate standard deviation for samples tested.

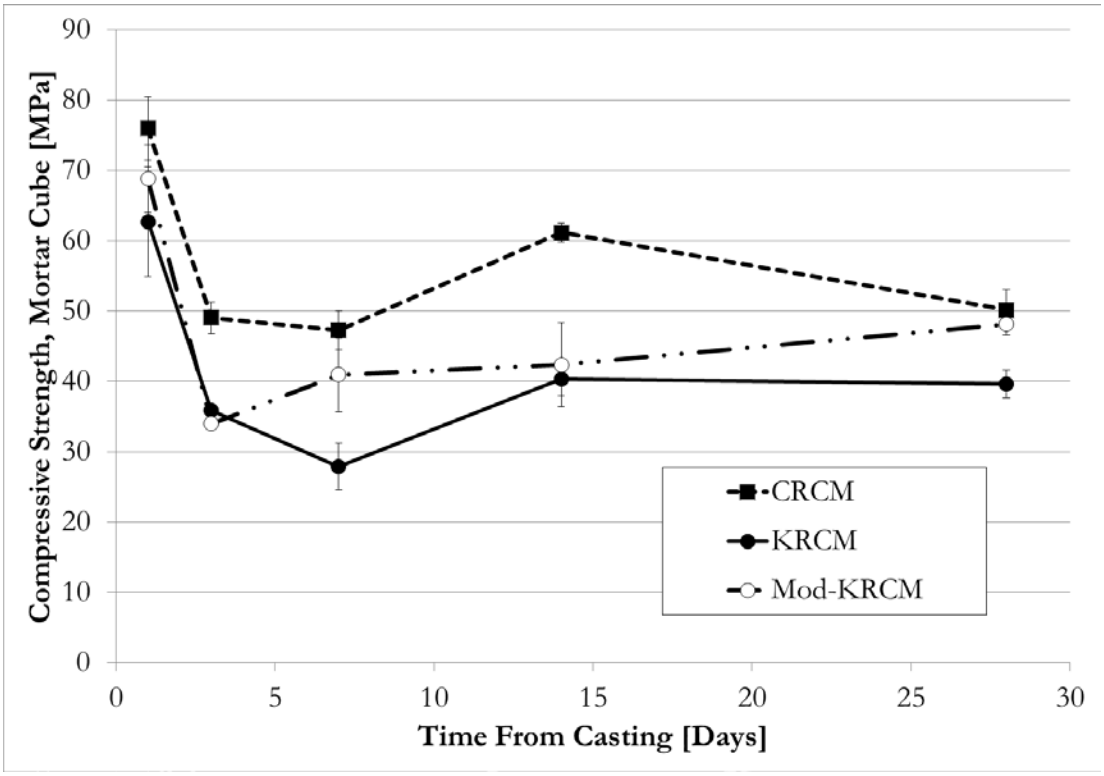

Figure 5-6: Compressive strengths in micro-concrete mixtures

Strengths measured at 24 hours are unconverted strengths, and strengths measured at day 3 and after are converted strengths. Day one strengths varied from 62.7 MPa in the KRCM mixture to 76.0 MPa

in the CRCM Mixture. Minimum converted strengths varied from 27.9 MPa in the KRCM mixture at 7 days, to 47.3 MPa in the CRCM mixture at 7 days. The Mod-KRCM experienced its minimum converted strength at 3 days. The strength reduction due to conversion was significantly higher for the KRCM and Mod-KRCM mixtures (55.5% and 50.6%, respectively) compared to the CRCM mixture (37.8%).

5.4.2 Aggregate Properties

A comparison of 1-day, 3-day, and 28-day strengths with aggregate properties (D50, G_s, absorption capacity, and fineness modulus) was done for the KRC, BLG, CRC, and MM aggregates to determine if aggregate property trends correlated with 1 day, converted, or longterm strengths. Figures examining the compressive strength, and strength loss due to conversion vs. the aforementioned aggregate properties can be found in Appendix B, Section B.1.1. These results indicated that higher D50 numbers and G_s correlated with higher day 1 concrete strengths for the mixtures examined, however this same correlation did not hold true when examining converted concrete strengths.

5.4.3 Elemental Analysis

5.4.3.1 Examination of Concrete Pore Solution

Additional chemical and microstructural analysis was done to study the CRC and KRC concrete systems. These systems were chosen for examination in particular because of differences in converted strength and strength evolution after conversion, as well as the availability of the aggregates for use in research.

Concrete pore solution was expressed and analysed for the CRC, KRC concrete mixtures. Additionally, the pore solution was expressed and analysed from a hardened CAC paste with a w/cm of 0.40 for comparison. Sodium (Na), potassium (K), aluminum (Al), silicon (Si), and calcium (Ca) concentrations were measured through inductively coupled plasma-optical emission spectrometry (ICP-OES). The pore solution work is discussed in full in Adams and Ideker [60], also seen as Chapter 4 in this dissertation. A summary of the pore solution analysis as it relates to this work is presented. Concentrations of Na, K, and Al for the CRC, KRC and Paste mixtures are presented in Figure 5-7.

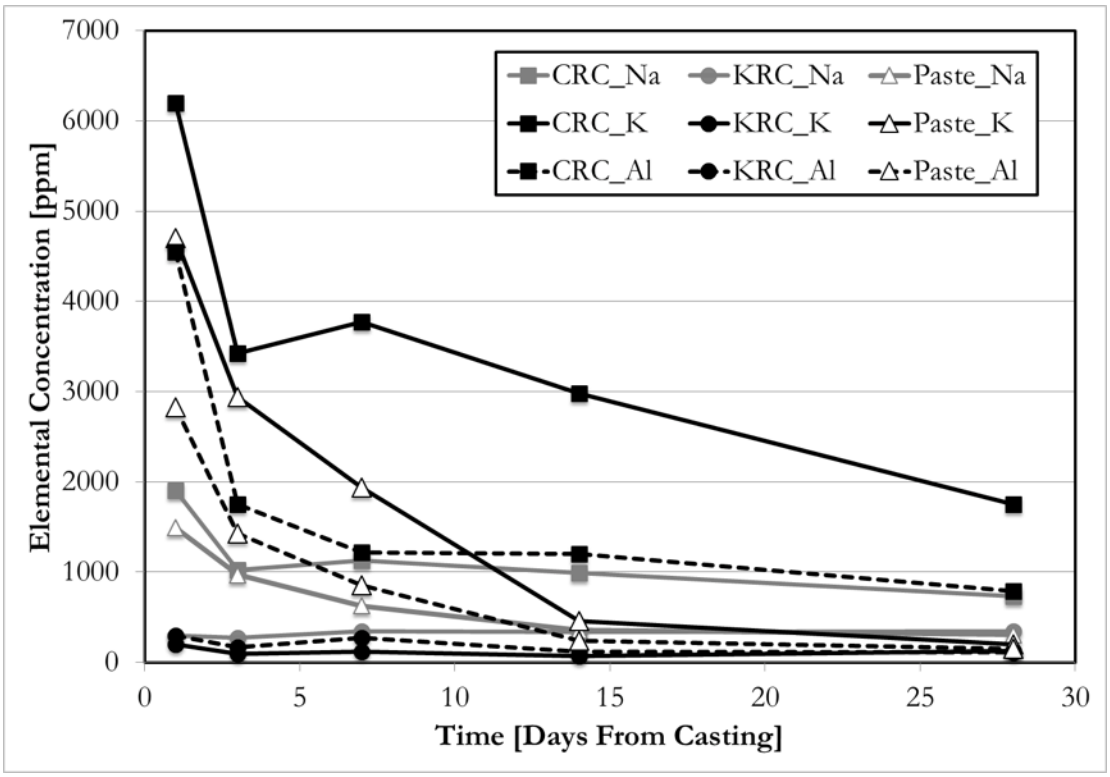

Figure 5-7: Elemental concentration of Na, K, and Al in pore solution of CRC, KRC, and Paste mixtures

Silicon concentrations were below detection limits, and calcium concentrations were below 150 ppm for all systems [60]. The trend in concentration amounts is similar for all three elements Na, K, and Al. The Paste and CRC system Na and K concentrations at day 1 were relatively high initially and showed significant decrease in concentration commensurate with conversion. The alkali concentrations continued to decrease through 14 days, and stayed relatively constant until day 28. Alkali concentrations in the CRC pore solution then dropped significantly after conversion at day 3. This initial reduction in concentration was also followed by a continuous, longer-term decrease through 28 days. Alkali concentrations in the KRC system remained relatively low (below 350 ppm for both Na and K) compared to CRC and Paste systems at all dates tested. Additionally, The KRC system did not experience a significant decrease in concentration of Na or Kt commensurate with conversion at day 3 as was observed in the CRC and Paste systems.

The Al concentration followed similar trends as seen in the K and Na concentrations. The CRC system experienced a significant decrease in Al concentration between day 1 and day 3 during conversion, even larger than that was observed in the alkali systems, and then continued to decrease at a slower rate through 28 days. Al concentrations in the paste system also started relatively high, and dropped

at a significant rate through day 14, and then remained constant through day 28. Al concentrations in the KRC system remained low at all testing days (below 300 ppm) and did not experience the significant decrease in concentration observed in the CRC and Paste systems.

The pH of the pore solutions was measured for each testing date and is shown in Figure 5-8.

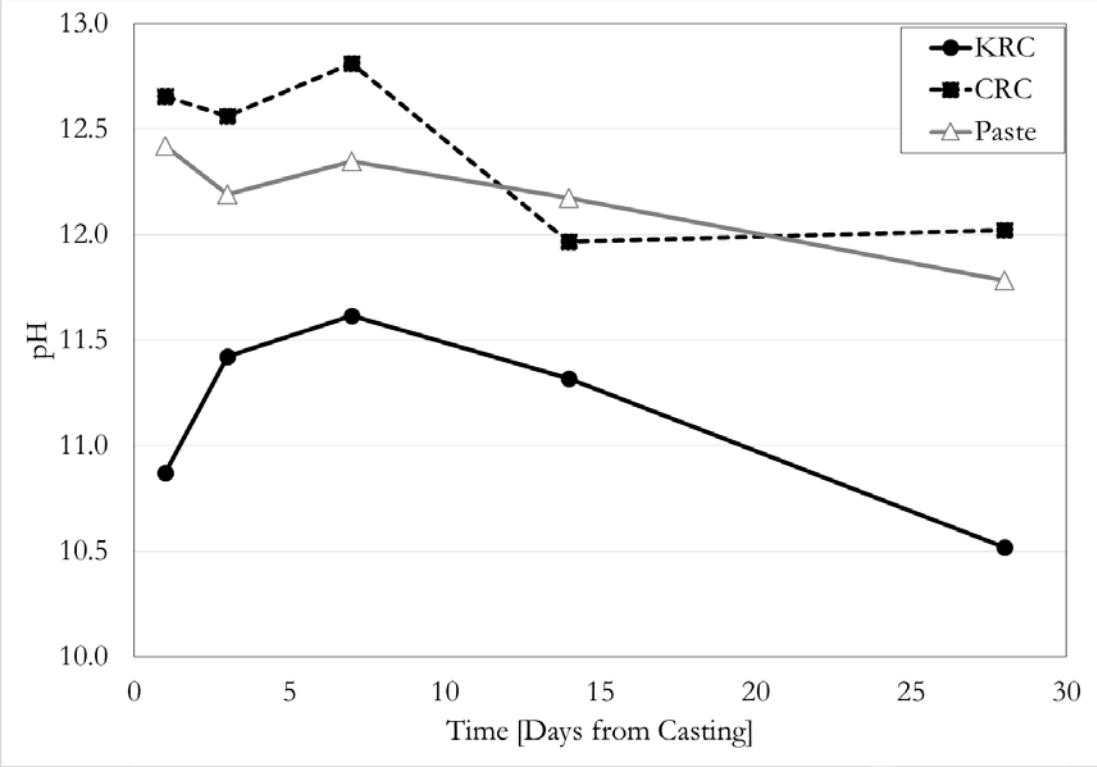

Figure 5-8: pH of pore solution of CRC, KRC, and Paste mixtures

This figure shows that the pH was significantly different between the CRC and Paste systems compared to the KRC system. The CRC and Paste system's pH were significantly higher than the KRC system at all dates. Additionally the pH of the KRC system started off low, peaking at 7 days, and then continuously dropping afterwards. Both the CRC and Paste systems experienced a slight decrease in pH during conversion (day 1 to day 3). Conversely, the KRC system experienced a 0.5 increase in pH. All three systems experienced continuous decreases in pH after day 7, however.

5.4.3.2 Elemental Analysis from EDX

Elemental maps were produced through energy dispersive X-ray analysis in the SEM. Figures 5-9 A and B show an example of the SEM image and elemental maps for aluminium, silicon, calcium, and

iron for a day 1 unconverted sample and a day 14 converted sample from the KRC mixture. Maps were also produced for day 3 and day 7 samples but are not shown here. Additional elemental maps from the KRC concrete samples can be found in Appendix B, Section B.1.4.

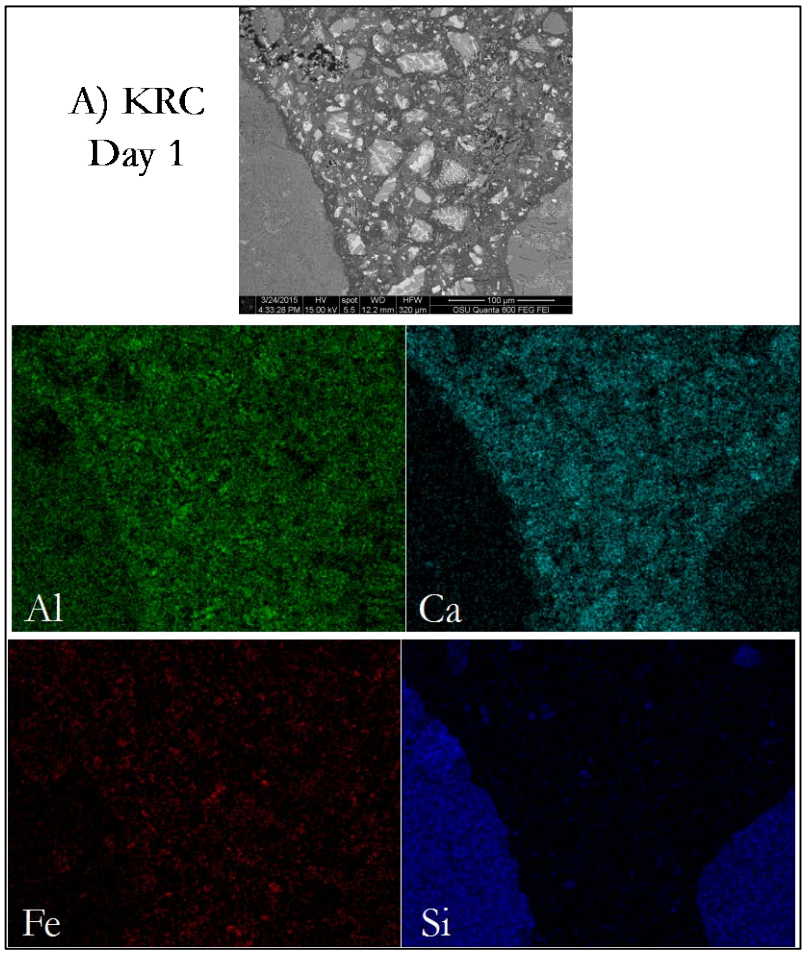

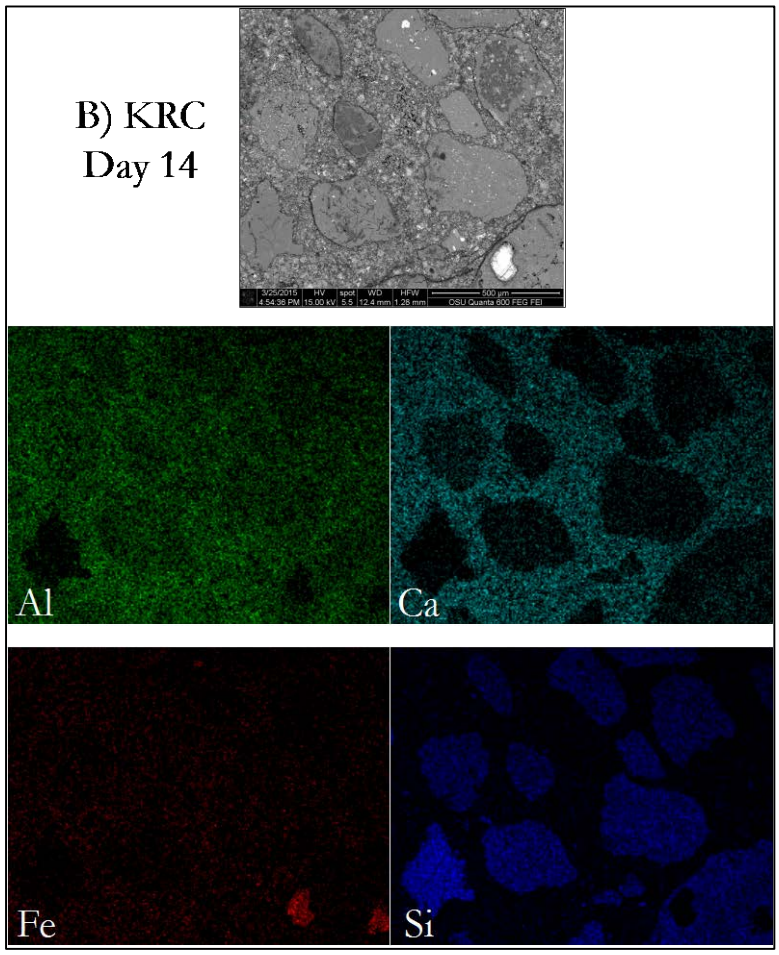

Figure 5-9: SEM image and elemental map of Al, Ca, Fe, and Si from EDX for KRC mixture day A) 1 and B) 14

Figure 5-A, from an unconverted sample, shows a well formed, dense microstructure in the SEM image. The aggregates visible in the image are mainly siliceous but also contain some calcium and aluminum. From the SEM image, it can be observed that there is hydrated phases near the interface with the aggregates with very little porosity around the aggregates. Figure 5-9B, from a converted sample of the KRC concrete shows more open porosity in the system. Additionally we can see most of the aggregates in this sample are also a blend of aluminum, silica, and calcium. One aggregate towards the lower left of the image was mainly siliceous however. In the SEM image, a ring of porosity was observed around the aluminum bearing aggregates that was not present around the siliceous aggregates. This ring of porosity around aluminum bearing aggregates was consistent throughout the elemental maps taken in converted KRC system. Bright areas were observed in the images, mainly from unhydrated ferrite phases present both at day 1 and day 14. Additional iron was observed in

hydrated phases, but at a relatively lower amount than what can be observed in the slowly hydrating ferrite phases. Aluminum and calcium was well dispersed throughout the cement matrix at all ages.

Figures 5-10A and 5-10B show an example of the SEM image and elemental maps for aluminium, silicon, calcium, and iron for a day 1 unconverted samples and a day 14 converted samples from the CRC mixture. Maps were also produced for day 3 and day 7 samples but are not shown here. Additional elemental maps from the CRC concrete samples can be found in Appendix B, B.1.5

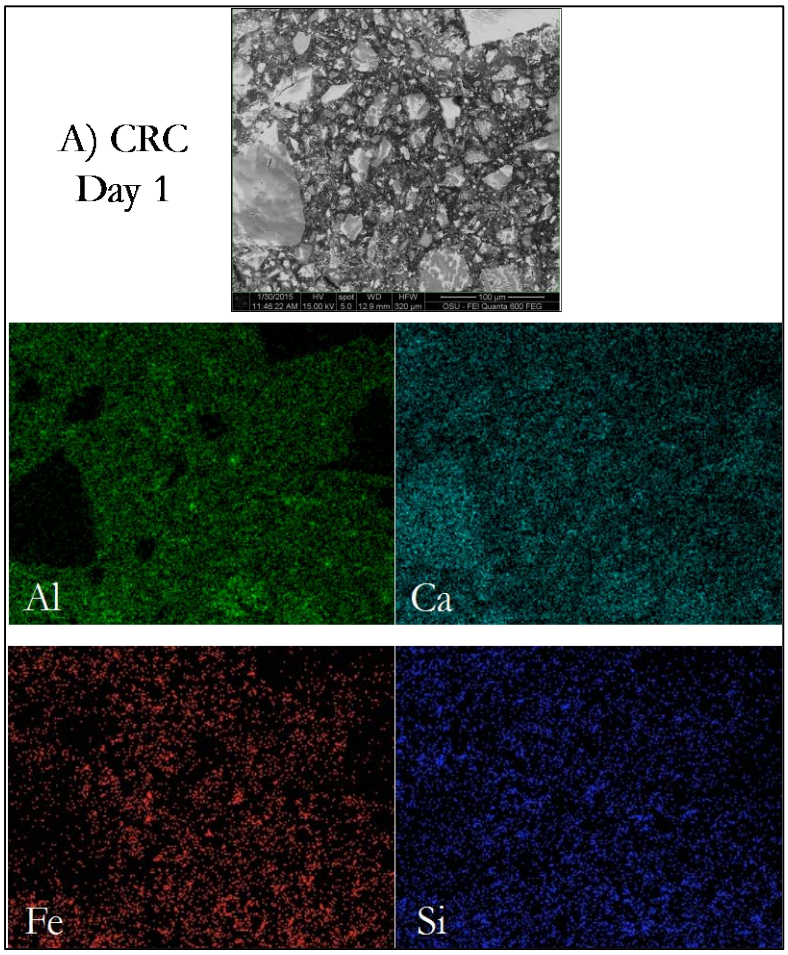

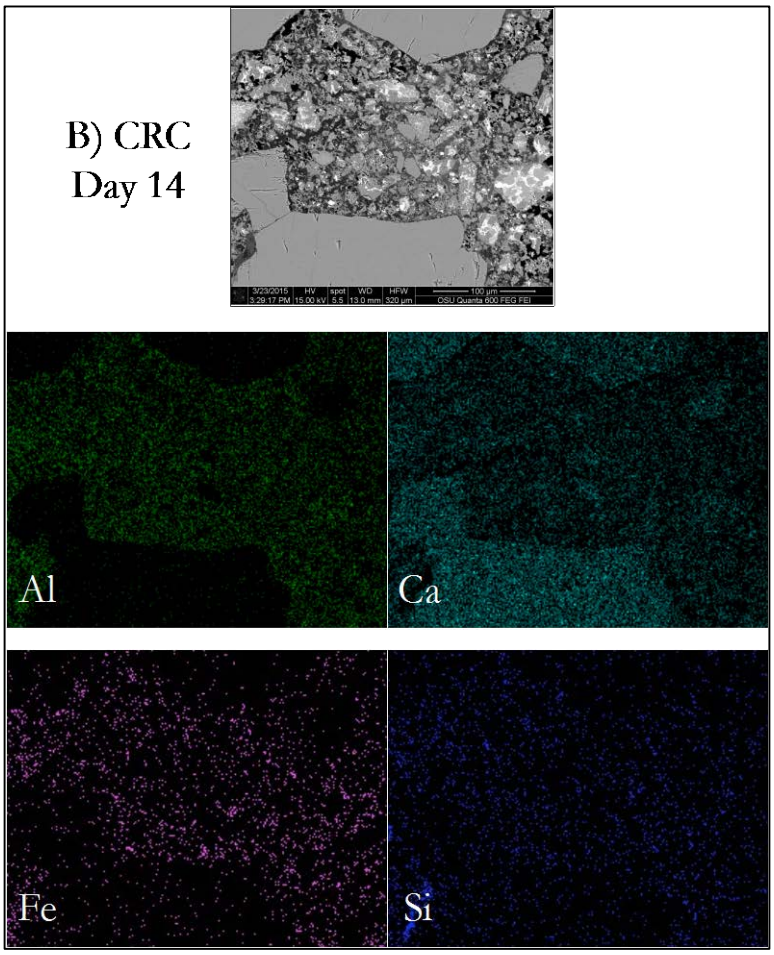

Figure 5-10: SEM image and elemental map of Al, Ca, Fe, and Si from EDX for CRC mixture day A) 1 and B) 14

Figure 5-1A, from an unconverted sample, shows a well-formed, dense microstructure in the SEM image. The aggregates visible both in Figure 5-10A and 5-10B are mainly calcium bearing, with small amounts of iron and silicon. Little to no aluminum was observed in the CRC aggregates through EDX analysis. Interfacial transition zones (ITZ) were well formed with very little porosity around the aggregates at both day 1 and day 14 for the CRC system, though additional porosity was observed in the system overall at day 14 compared to day 1. As with the KRC sample, bright areas were observed in the system, mainly in unhydrated ferrite phases present both at day 1 and day 14. Additional iron is scattered in hydrated phases, but at a relatively lower amount than what can be observed in the slowly hydrating ferrite phases. Aluminum and calcium were dispersed throughout the cement matrix at all days. It appeared that there was more silicon in the cement matrix in the CRC system compared to the KRC system however, this is an artefact of the technique. Brightness in elemental maps from EDX is relative to each particular map. Since the aggregates were mainly siliceous in the KRC samples,

it appeared that there was very little silicon in the cement matrix. In the CRC sample, however, there was very little silicon in the aggregates, which made the silicon in the cement paste more apparent.

5.4.4 Porosity Development

5.4.4.1 Porosity Measurement through Image Analysis

Porosity was measured from SEM images taken of the CRC and KRC concrete systems from day 1 to day 14. The procedure for determining porosity was described above in Section 5.3.5.2. The results of this image analysis are presented in Figure 5-11.

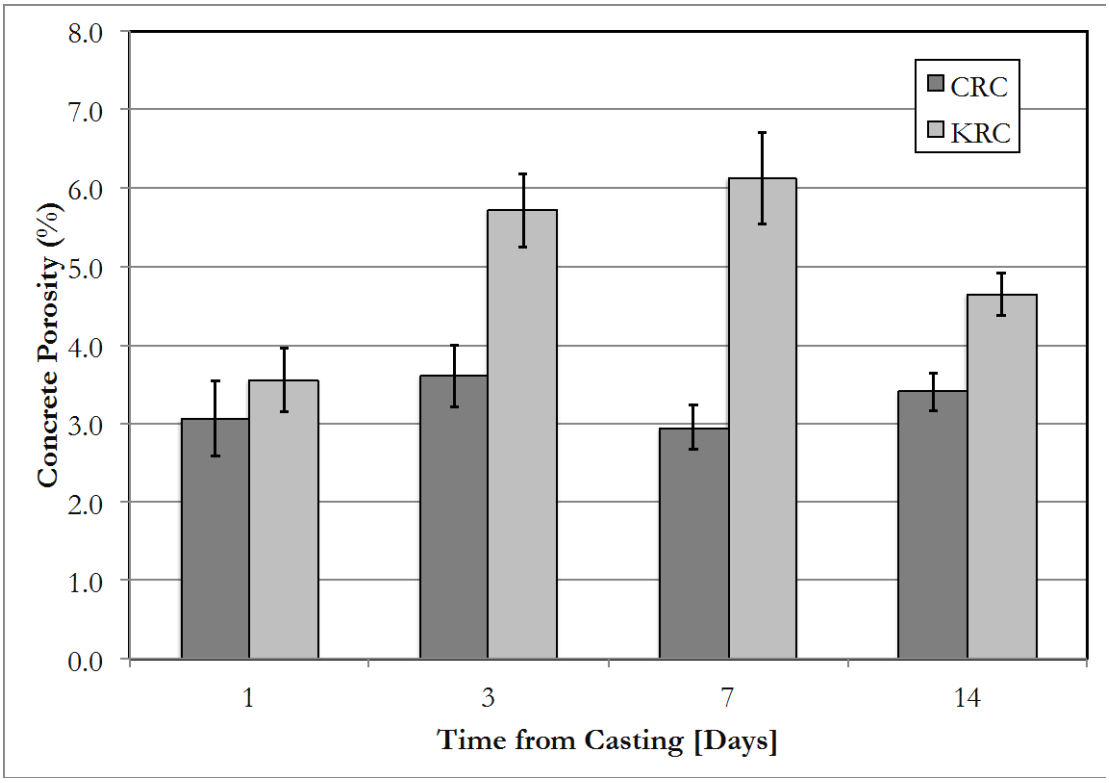

Figure 5-11: Concrete porosity of CRC and KRC mixtures as measured by image analysis

Porosity as measured by image analysis was higher in the KRC concrete compared to the CRC concrete at all days. Day 1 porosity was only slightly higher in the KRC concrete than the CRC concrete. After conversion, porosity in the KRC concrete increased significantly, and was more than twice the porosity of the CRC concrete by day 7. Porosity in the KRC concrete decreased at day 14. Porosity in the CRC concrete remained relatively constant from day 1 to day 14.

5.4.4.2 Mercury Intrusion Porosimetry

Porosity was also measured through MIP on micro-concrete samples created from the KRCM and CRCM mixtures at days 1, 3, and 14. The results from the MIP analysis are shown in Figure 5-12.

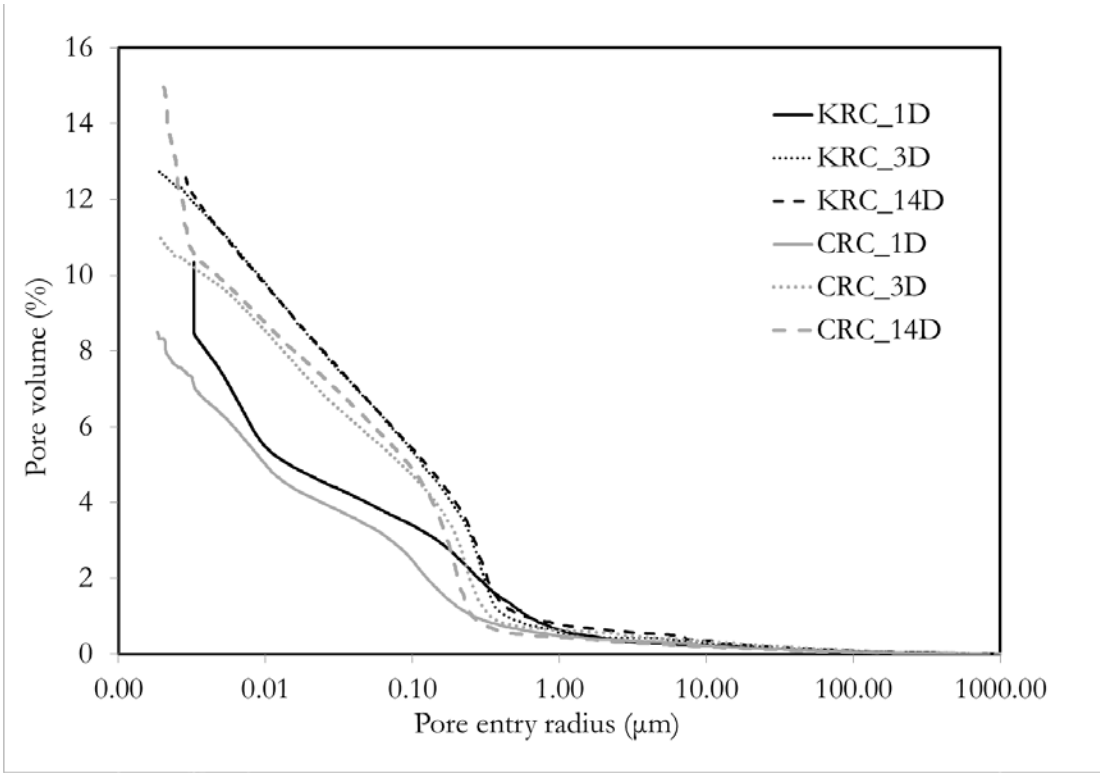

Figure 5-12: Porosity development as determined by MIP

Overall porosity as measured by MIP was higher in the KRCM sample than in the CRCM sample system at all days. Significant increases in porosity from day 1 to day 3 were observed for both the KRCM and CRCM system, but the porosity remained relatively constant between day 3 and day 14 for both systems. MIP results indicate that much of the porosity that formed due to conversion was at pore entry sizes of less than 0.5 μm. The converted KRCM system had higher converted porosity (day 3 and day 14) compared to the CRCM system and this gap increased below 0.10 μm pore entry radius. Porosity values above 1 μm pore entry radius were similar for all systems at all dates.

5.5 Discussion

Aggregate source was shown to have a significant impact on strength in both 100% CAC concrete and mortar systems. As seen in Figure 5-3, the source of the siliceous aggregates had a significant

impact on day 1 strength, converted strength, and long-term strength development after conversion. All siliceous systems experienced significant strength loss due to conversion (average strength loss 48%), however; and all but one siliceous system experienced minimum strength at day 3, two days after being submerged in the 50°C water bath. The systems made with both carbonate limestone fine and coarse aggregate experienced significantly less strength reduction (average strength loss 26%) due to conversion compared to the siliceous aggregate systems. The system with the siliceous limestone (SPT) lost 39% of strength due to conversion. Additionally the CRC system experienced minimum converted strength at day 28, and the MM system experienced minimum converted strength at day 14, indicating that there is a significant kinetic difference as well as mechanical interaction. The SPT system reached minimum strength at 3 days similar to the siliceous river gravel systems. These results indicate that the siliceous limestone system behaved similarly in kinetics to the siliceous river gravel systems, but saw reduced strength reductions as observed in the carbonate limestone systems. This suggests that the high carbonate content in the CRC and MM systems was the cause of the difference conversion kinetics and reduced the strength loss due to conversion, since the effect was not as pronounced in the siliceous limestone SPT system.

Long-term strengths (180 days) were measured for both the KRC (siliceous river gravel) and CRC (carbonate limestone) systems. The results indicated that CAC concrete can regain a significant portion of strength lost due to conversion after minimum converted strength is reached as further hydration of unhydrated cement grains occurs. Previous work has indicated that long-term strength in carbonate limestone systems may not be stable, particularly at higher temperatures. This was shown to be caused by calcium monocarboaluminate decomposing into C_3AH_6 [29, 34, 61-63]. As discussed earlier, however, this work relied on the results of mortar and paste systems created with finely ground limestone, and not limestone aggregates, so the results do not necessarily apply to these systems. It was deemed important, however, to determine if the strength in the CRC system was maintained even in the long-term at elevated temperatures. Results show here indicated that after 179 days of being stored at 50°C, the CRC system still maintained higher strengths compared to the KRC system, and continued to gain strength. Therefore, the high strength observed in the carbonate limestone CAC systems appears to be stable even long-term. These results indicate that limestone (carbonate or siliceous) may be a useful material solution for increasing the converted strength in CAC systems and providing a higher design strengths for particular applications where that is necessary.

The micro-concrete systems were also cast to examine differences between a siliceous system and a carbonate limestone system using only fine aggregate material. The CRCM, carbonate limestone system, also behaved similarly to the siliceous systems with a significant strength reduction due to conversion, and minimum converted strength at day 3. These results indicate that the difference in conversion kinetics and strength reduction may be more pronounced in the presence of coarse aggregate.

5.5.1 Influence of Aggregate Properties

No significant correlation between aggregate properties and strength reduction due to conversion were observed. Higher 1 day strengths were observed in aggregates with higher D50 numbers and higher G_s. Particle shape and surface roughness may also have played a role in strength differences between concrete mixtures. The limestone aggregates used were crushed material, with rough angular surfaces, whereas the siliceous material was river gravel with rounded smooth surfaces. It has shown that substituting a crushed material with a higher angularity and surface roughness can increase the strength of the concrete compared to concrete made with smoother aggregates by increasing mechanical interlocking of the aggregate with the paste [64, 65]. The impact of aggregate angularity on strength is generally more prominent in high strength concrete, however, and typically does not affect normal or low strength concrete mixtures as significantly because at these strengths the strength of the paste becomes the limiting factor [40, 66, 67]. This correlation has not been studied for CAC concrete however, and may not necessarily hold true. Despite this, increases in strength due to aggregate properties would result in overall strength increases prior to and after conversion, and relative strength reduction due to conversion should remain the same. In the work presented here, the concrete experienced significantly less strength loss due to conversion, and also experienced minimum converted strengths at later dates than observed in the siliceous mixtures.

Aggregate grading had little impact on the strength reduction due to conversion. The Mod-KRCM system used the KRCF aggregate with a modified grading to match the grading of the CRCM aggregate. This was done to determine if aggregate grading affected the overall strength loss due to conversion that was seen with the CRC systems. While this modification in grading resulted in a moderately higher 1 day strength, the strength loss due to conversion was still similar to the KRCM system.

Particle roughness of the limestone aggregates may allow for further nucleation of hydrated material during conversion in the limestone systems compared to the siliceous system. It has been shown that CAC hydrates will more easily nucleate in the presence of aggregates and the rougher surface of the crushed limestone aggregates may provide more available locations for hydrate nucleation [68]. This theory is supported by the better formed ITZ in the CRC system observed in the SEM images discussed above. However, the delay in time to minimum converted strength in the carbonate limestone systems suggests that this was not the only change to the system. Additionally differences in particle shape do not account for the differences observed in system chemistry and bulk paste porosity observed between systems.

In addition to particle shape, elemental composition of aggregates seemed to have a significant impact on the ITZ observed around the aggregates. As indicated by the EDX maps in Figure 5-9, some of areas around the KRC aggregates containing aluminum showed porosity in the ITZ. Conversely, poor ITZs were not observed around the purely siliceous aggregates in the KRC mixture nor around the carbonate limestone aggregates in the CRC system. This indicates that CAC hydrates may have difficulty nucleating around aluminum bearing aggregates, creating poor ITZs and weakening the overall system.

5.5.2 System Chemistry

Significant differences in system chemistry were observed when the pore solution of the CRC and KRC concrete systems was examined as described above. Previous work has examined the pore solution chemistry in CAC systems, however this work focused on pore solution chemistry prior to conversion and only paste systems [69-71]; and are therefore not comparable to the systems presented here. Results indicated that in the CRC and CAC Paste systems sodium, potassium, and aluminium are present in the pore solution in large concentrations, but are then bound into hydrates during the conversion process reducing the overall concentration of these elements in solution. The concentration of these elements in the KRC system (siliceous) remained relatively constant and were significantly lower than the CRC (carbonate limestone) and paste systems even at day 1 prior to conversion.

The pH in the CRC and Paste pore solutions was significantly higher than the pH in KRC system. Work by Winnefeld and Lothenbach has shown that Al_2O_3 becomes more soluble as pH rises in cement systems [72]. This indicates that the relatively high pH in the CRC and Paste system caused

further dissolution of the unhydrated CAC grains compared to the KRC system. Subsequently, the relatively low pH observed in the KRC system suggests a reduced degree of hydration compared to the CRC and Paste systems.

Previous work has shown that nucleation of hydrates in CAC systems prior to conversion happens rapidly, and quickly fills space preventing further nucleation of hydrates [14, 20, 24, 73]. Conversion results in the densification of hydrates and the opening of porosity in the system. As porosity forms during conversion space is created for further precipitation of hydrates from solution [13, 14, 24]. These results suggest that as conversion occurred in the CRC system, porosity formed and additional stable hydrates (AH_3 and C_3AH_6) precipitated out of solution due to the high level of ionic activity in the solution compared to the KRC System. Additional formation of hydrates (and subsequently less porosity formation) during conversion may explain why less strength reduction due to conversion was observed in the CRC system compared to the KRC system.

5.5.3 Porosity Development

Porosity amounts differed significantly between the MIP analysis and the SEM image analysis techniques. It is important to note that the SEM images used to measure porosity through image analysis were taken at points avoiding entrapped air voids, and generally only examined pores below 100 μm. The MIP analysis examined pores at all sizes. Additionally the MIP was done on micro-concrete samples and not concrete samples. These differences in analysis techniques and mixtures explain why there were significant differences in the amount of porosity measured by each technique. However, the trends observed were similar and explain the difference in strength observed between carbonate limestone and siliceous river gravel systems.

Porosity results from both the image analysis and MIP analysis indicate that the systems with KRC (siliceous) aggregate had significantly more porosity in the system after conversion than the systems with CRC (carbonate limestone) aggregates. Image analysis showed that the porosity formed by 24 hours was similar in both the KRC and CRC system. The MIP results indicated that the porosity remained relatively unchanged between 3 and 14 days in both systems. The image analysis results showed that porosity decreased at 14 days in both systems. The decrease in the image analysis results was due to further hydration of unhydrated cement filling the smaller size pores measured in image analysis. In the image analysis technique, only pores less than 100μm were measured, therefore the

further hydration resulted in a larger percentage of observed pore being filled with hydrates, which accounts for this difference.

Strength is inversely proportional to porosity in solids. Consequently, strength of cement paste is dependent on the w/cm and the degree of cement hydration which both influence the porosity. The effect of porosity on strength is typically associated with the macropores and air voids (50 nm and greater) [66]. Pores of this size cause significant stress concentrations to form within the concrete at the site of the pore. Stress concentrations are caused where there is a change in a material's cross sectional area (such as a void). At these points the stresses do not redistribute equally, and higher stresses occur closer to the defect [74]. Therefore, the relatively high porosity present in the KRC aggregate systems resulted in larger strength reductions due to conversion conversion compared to the CRC systems.

5.5.4 Further Work

This work presented results examining the differences present between limestone and siliceous aggregate CAC systems. While several theories have been developed regarding the cause of the differences, additional work is suggested to elucidate and verify these theories. Further suggested research includes:

- An investigation to determine why pH levels were so low in the KRC system, and if the low pH is consistent across siliceous aggregates;
- An in-depth examination of the hydrate phases formed in each aggregate system, particularly to confirm or deny existence of calcium monocarboaluminate in limestone systems.
- A measurement of the degree of hydration in each system.
- Further work to examine a broader range of aggregates, including crushed siliceous aggregates and other aggregate mineralogies.
- Further examination of aggregates to determine exact mineralogy of each system.

5.6 Conclusion

This work has shown that aggregate mineralogy and source can result in significantly different strengths both prior to and after conversion in CAC systems. Particular differences were observed between siliceous aggregate systems and carbonate limestone aggregate systems. Further examinations of a siliceous system and a carbonate limestone system were done and showed that the carbonate

limestone system had higher pore solution pH values and higher levels of ionic activity in its pore solution. In particular, the concentration of aluminum at 24 hours after casting showed high concentrations of Al in the pore solution of the carbonate limestone system and the CAC paste system compared to the siliceous aggregate system indicating a higher level dissolution of unhydrated cement in the carbonate limestone system. Additionally the siliceous system had higher porosities and less well-formed interfacial transition zones than the limestone systems. Several theories are proposed below, that when considered together, can explain the differences observed between these systems:

- The relatively low pH in the siliceous system may have reduced the degree of hydration resulted in higher porosity after conversion compared to the carbonate limestone system; and
- Aluminum bearing aggregates in the siliceous system developed poor interfacial transition zones reducing overall concrete strength in that system; and
- Surface roughness of the limestone aggregates may provide additional sites for nucleation of CAC hydrates creating increased bond strength between carbonate limestone aggregates and cement paste matrix.

Further work is necessary to confirm the validity of these theories. Long-term strength results confirmed, however, that the increased strength observed in the limestone system was stable. Therefore, limestone aggregates may be a viable material alternative for increasing the converted strength of CAC concrete.

5.7 Acknowledgements

The authors would like to acknowledge the support of the Microscopy Center and the W. M. Keck Collaboratory for Plasma Spectroscopy, at Oregon State University. Undergraduate research assistants Aaron Strand and Travis Moore were also very helpful in collecting some of the data presented in this paper. We also acknowledge the help of Karen Scrivener and Elise Berodier of Ecole Polytechnique Federale de Lausanne for their help in obtaining the MIP measurements. Additionally, we would like to thank Thano Drimalas, Racheal Lute and Kevin Folliard of the University of Texas and Edward G. Moffatt and Michael D. A. Thomas of the University of New Brusnwick for helping test concrete with a variety of aggregates. Finally, the authors would like to thank Kerneos Aluminate Technologies for Financial Support

5.8 Works Cited

[1] H.G. Midgley, High alumina cement in construction - A future based on experience, in: R.J. Mangabhai (Ed.) International Symposium on Calcium Aluminate Cements, E & F. N. Spon, London, 1990, pp. 1-13.

[2] C. Parr, D. Verat, C. Wohrmeyer, J.P. Letourneux, High purity calcium aluminate binders for demanding high temperature applications, in: C. Fentiman, R. Mangabhai, K. Scrivener (Eds.) Centenary Conference on Calcium Alumiante Cements, IHS BRE Press, Avignon, FR, 2008.

[3] P. Boch, S. Masse, N. Lequeux, CAC in refractory applications: from LCCs to ZCCs, in: R.J. Mangabhai, F.P. Glasser (Eds.) International Conference on Calcium Aluminate Cements, IOM Communications, Edinburgh, UK, 2001.

[4] K.L. Scrivener, J.-L. Cabiron, R. Letourneux, High-performance concretes from calcium aluminate cements, Cement and Concrete Research, 29 (1999) 1215-1223.

[5] J.P. Bayoux, J.P. Letourneux, S. Marcdargent, M. Vershaeve, Acidic corrosion of high alumina cement, in: R.J. Mangabhai (Ed.) International Symposium on Calcium Aluminate Cements, E. & F. N. Spon, London, UK, 2014, pp. 230-240.

[6] A. Goyns, Calcium aluminate cement linings for cost-effective sewers, in: R.J. Mangabhai, F.P. Glasser (Eds.) International Conference on Calcium Aluminate Cements, IOM Communications, Edinburgh, UK, 2001, pp. 617-631.

[7] A.M. Goyns, M.G. Alexander, Performance of various concretes in the Virginia experimental sewer over 20 years, in: C. Fentiman, R. Mangabhai, K. Scrivener (Eds.) International Conference on Calcium Aluminate Cements, IHS BRE Press, Avignon, FR, 2014, pp. 573-584.

[8] C.M. Williams, F. Garrott, Recycling/Reclaiming a savings spree: Chicago reuses to the max on famous shopping mile, in: Illinois Interchange, Illinois Department of Transportation, Springfield, IL, 2012.

[9] Texas Department of Transportation, TxDoT SS-4491 Class CAC Concrete, in, Texas Department of Transportation, Austin, TX, 2009.

[10] L. Cussino, A. Negro, Hydration du ciment alumineux en présence d'agrégat siliceux et calcaire, in: 7th International Congress on the Chemistry of Cement, Paris, 1980.

[11] V. Lamour, P. Monteiro, K. Scrivener, H. Fryda, Mechanical properties of calcium aluminate cement concretes, in: International conference on calcium aluminate cements, 2001, pp. 199-213.

[12] H. Pöllman, Calcium alumiante cements- Raw materials, differences, hydration and properties, in: M.A.T.M. Broekmans, H. Pöllmann (Eds.) Applied mineralogy of cement & concrete, The Mineralogical Society of Virginia, Chantilly, Virginia, USA, 2012, pp. 1-82.

[13] K.L. Scrivener, A. Capmas, Calcium Aluminate Cements, in: P.C. Hewitt (Ed.) Lea's Chemistry of Cement and Concrete, Elsevier - Butterworth-Heinemann, Oxford, UK, 1998, pp. 713-782.

[14] C. Gosselin, Microstructural development of calcium aluminate cement based systems with and without supplementary cementitious materials, in: Faculte sciences et techniques de l'ingenieur, Ecole Polytechniqe Federale de Lausanne, Lausanne, CH, 2009.

[15] S.M. Bushnell-Watson, On the Cause of the Anomalous Setting Behaviour With Respect to Temperature of Calcum Aluminate Cements, Cement and Concrete Research, 20 (1990) 677-686.

[16] S.M. Bushnell-Watson, J.H. Sharp, The application of thermal analysis to the hydration of conversion reactions of calcium aluminate cements, Materiales De Construccion, 42 (1992) 13-32.

[17] S.M. Bushnell-Watson, J. Sharp, The effect of temperature upon the setting behavior of refractory calcium aluminate cements, Cement and Concrete Research, 16 (1986) 875-884.

[18] S.M. Bushnell-Watson, J.H. Sharp, Further studies of the effect of temperature upon the setting behavior of refractory calcium aluminate cements, cement and Concrete Research, 20 (1990) 623-635.

[19] V. Antonovič, J. Keriene, R. Boris, M. Aleknevičius, The effect of temperature on the formation of the hydrated calcium aluminate cement structure, Procedia Engineering, 57 (2013) 99-106.

[20] V.H.R. Lamour, P.J.M. Monteiro, K.L. Scrivener, H. Fryda, Microscopic studies of the early hydration of calcium aluminate cements, in: R.J. Mangabhai, F.P. Glasser (Eds.) International Conference on Calcium Aluminate Cements (CAC), IOM Communications, Edinburgh, Scotland, 2001, pp. 169-180.

[21] H. Fryda, K.L. Scrivener, G. Chanvillard, C. Feron, Relevance of Laboratory Tests to Field Applications of Calcium Aluminate Cement Concretes, in: International Conference on Calcium Aluminate Cements (CAC), IOM Communications, Heriot-Watt University, Edinburgh, Scotland, UK, 2001, pp. 215-247.

[22] H. Fryda, E. Charpentier, J.M. Bertino, Accelerated test for conversion of calcium aluminate cement concrete, in: C.H. Fentiman, R.J. Mangabhai, K.L. Scrivener (Eds.) Calcium Aluminate Cements: The Centenary Conference, IHS BRE Press, Avignon, FR, 2008.

[23] S. Rashid, P. Barnes, J. Bensted, X. Turrillas, Conversion of calcium aluminate cement hydrates re-examined with synchrotron energy-dispersive diffraction, Journal of materials science letters, 13 (1994) 1232-1234.

[24] K.L. Scrivener, Historical and present day applications of calcium aluminate cements, in: R.J. Mangabhai, F.P. Glasser (Eds.) Proceedings of the International Conference on Calcium Aluminate Cements (CAC), IOM Communications, Heriot-Watt University, Edinburgh, Scotland, UK, 2001, pp. 3-23.

[25] A. Negro, A. Bachiorrini, M. Murat, Interaction, in aqueous medium, between calcium carbonate and monocalcium aluminate at 5°C, 20°C, and 40°C, Bulletin de minéralogie, 105 (1982) 284-290.

[26] H.H.M. Darweesh, Limestone as an accelerator and filler in limestone-substituted alumina cement, Ceramics international, 30 (2004) 145-150.

[27] A. Bachiorrini, L. Cussino, Alumina cement hydration in pure water and in sulfate solution in the presence of siliceous or calcareous aggregate, in: 8th International Congress on the Cement of Chemistry, Rio de Janeiro, Brazil, 1986, pp. 383-388.

[28] F. Trivino, Aluminous cement: How to avoid degrading of mechanical resistance, in: 8th International Congress on the Chemistry of Cement, Rio de Janeiro, Brazil, 1986, pp. 417-422.

[29] W.G. Piasta, The Effect of Limestone Fillers on Sulphate Resistance of High Alumina Cement Compositers, in: R.J. Mangabhai (Ed.) Calcium Aluminate Cements, E. & F.N. Spon, London, UK, 1990, pp. 241-255.

[30] C.M. George, Aluminous cements, in: 7th International Congress on the Chemistry of Cement, Paris, France, 1980.

[31] C.M. George, Manufacture and performance of aluminous cement, in: R.J. Mangabhai (Ed.) Calcium Aluminate Cements, E. & F.N. Spon, London, UK, 1990, pp. 181-207.

[32] H.G. Midgley, High alumina cement in construction - a future based on experience, in: R.J. Mangabhai (Ed.) Calcium Aluminate Cements, E. & F.N. Spon, London, UK, 1990, pp. 1-13.

[33] F. Indelicato, On the correlation between porosity and strength in high-alumina cement mortars, Materials and Structures, 23 (1990) 289-295.

[34] A.P. Luz, V.C. Pandolfelli, $CaCO_3$ addition effect on the hydration and mechanical strength evolution of calcium aluminate cement for endodontic applications, Ceramics International, 38 (2012) 1417-1425.

[35] ASTM C 127 2015, Standard test method for relative density (specific gravity) and absorption capacity of coarse aggregate, in: A. International (Ed.), ASTM International, West Conshohocken, PA, 2015.

[36] ASTM C 128 2015, Standard test method for relative density (specific gravity) and absorption of fine aggregate, in: A. International (Ed.), ASTM International, West Conshohocken, PA, 2015.

[37] ASTM Standard C 136, 2006, Standard test method for sieve analysis of fine and coarse aggregates, in: A. International (Ed.), West Conshohocken, PA, 2014.

[38] CAN/CSA-A23.2-2a-14, Sieve analysis of fine and coarse aggregate, in: C.S. Association (Ed.), Canadian Standards Association, Toronto, Canada, 2014.

[39] M. Bittelli, G.S. Campbell, M. Flury, Characterization of Particle-Size Distribution in Soils with a Fragmentation Model, Soil Sci Soc Am J, 63 (1999) 782-788.

[40] S.H. Kosmatka, M.L. Wilson, Design and control of concrete mixtures, 14 ed., Portland Cement Association, Skokie, Illinois, 2011.

[41] ASTM Standard C 125 2014, Standard terminology relating to concrete and concrete aggregates, in: A. International (Ed.), ASTM International, West Conshohocken, PA, 2014.

[42] Concrete Society Technical Report, Calcium Aluminate Cements in Construction: A Reassessment, in, Concrete Society, 1997, pp. 63.

[43] European Committee for Standardization, Calcium aluminate cement - Composition, specifications, and conformity criteria, in: EN 14647, European Committee for Standardization, Brussels, 2005.

[44] ASTM C 305 2014, Standard practice for mechanical mixing of hydraulic cement pastes and mortars of plastic consistency, in: ASTM International (Ed.), ASTM International, West Conshocken, PA, 2015.

[45] ASTM C 192 2014, Standard practice for making and curing concrete test specimens in the laboratory, in: A. International (Ed.), ASTM International, West Conshohocken, PA, 2015.

[46] ASTM C39 2012a, Standad test method for compressive strength of cylindrical concrete specimens, in: A. International (Ed.), ASTM International, West Conshohocken, PA, 2015.

[47] ASTM C109-11b, ASTM C109-11b: Standard test method for compressive strength of hydraulic cement mortars (using 2 in. or [50mm] cube specimens), in: ASTM International (Ed.) ASTM C109-11b, ASTM International, West Conshocken, Pennsylvania, 2011, pp. 10.

[48] J. Zhang, G.W. Scherer, Comparison of methods for arresting hydration of cement, Cement and Concrete Research, 41 (2011) 1024-1036.

[49] C. Gosselin, Microstructural development of calcium aluminate cement based systems with and without supplementary cementitious materials, in: Labratoire des Materiaux de Construction, Ecole Polytechnique Federale de Lausanne 2009, pp. 219.

[50] J. Bizzozero, Hydration and dimensional stability of calcium aluminate cement based systems, in: Materials Science and Engineering, Ecole Polytechnique Federal de Lausanne, Lausanne, Switzerland, 2014.

[51] C. Gosselin, K.L. Scrivener, Microstructure development of calcium alumiante cements accelerated by lithuium sulphate, in: C.H. Fentiman, R.J. Mangabhai, K.L. Scrivener (Eds.) Centenary Conference on Calcium Aluminate Cements, IHS BRE Press, Avignon, 2008, pp. 109-122.

[52] M.T. Gaztanaga, S. Goni, A. Guerrero, Accelerated carbonation of calcium aluminate cement pastes, in: R.J. Mangabhai, F.P. Glasser (Eds.) International Conference on Calcium Aluminate Cements, IOM Communications, Edinburgh, UK, 2001.

[53] A. Hidalgo, S. Petit, J.L. García, C. Alonso, C. Andrade, Microstructure of the system calcium aluminate cement-silica fume: application in waste immobilization, in: Z.G.J.C. Ruren Xu, Y. Wenfu (Eds.) Studies in Surface Science and Catalysis, Elsevier, 2007, pp. 1617-1628.

[54] C. Gosselin, E. Gallucci, K. Scrivener, Influence of self heating and Li_2SO_4 addition on the microstructural development of calcium aluminate cement, Cement and Concrete Research, 40 (2010) 1555-1570.

[55] R.A. Cook, K.C. Hover, Mercury porosimetry of hardened cement pastes, Cement and Concrete Research, 29 (1999) 933-943.

[56] S. Diamond, Mercury porosimetry: An inappropriate method for the measurement of pore size distributions in cement-based materials, Cement and Concrete Research, 30 (2000) 1517-1525.

[57] S. Chatterji, A discussion of the paper "Mercury porosimetry—an inappropriate method for the measurement of pore size distributions in cement-based materials" by S. Diamond, Cement and Concrete Research, 31 (2001) 1657-1658.

[58] S. Wild, A discussion of the paper "Mercury porosimetry—an inappropriate method for the measurement of pore size distributions in cement-based materials" by S. Diamond, Cement and Concrete Research, 31 (2001) 1653-1654.

[59] M.P. Adams, J.H. Ideker, Chapter 2: Development of a test method for determining the converted strength of calcium aluminate cement concrete, in: Factors influencing conversion and converted strength in calcium aluminate cement concrete, Oregon State University, Corvallis, OR, 2015.

[60] M.P. Adams, J.H. Ideker, Pore solution chemistry of calcium aluminate cement concrete systems undergoing accelerated conversion, in: 14th International Conference on Cement Chemistry, Beijing, 2015 (Under Review).

[61] C.H. Fentiman, Hydration of carbo-aluminous cement at different temperatures, Cement and concrete Research, 15 (1985) 622-630.

[62] H. Midgley, Measurement of high-alumina cement-calcium carbonate reactions using DTA, Clay Minerals, 19 (1984) 857-864.

[63] H.-J. Kuzel, H. Baier, Hydration of calcium aluminate cements in the presence of calcium carbonate, European Journal of Mineralogy, 8 (1996) 129-141.

[64] W.A. Cordon, H.A. Gillespie, Variables in concrete aggregates and portland cement paste which influence the strength of concrete, Journal Proceedings of the American Concrete Institute, 60 (1963) 1029-1052.

[65] A.M. Neville, Aggregate Bond and Modulus of Elasticity of Concrete, ACI Materials Journal, 94 (1994) 71-75.

[66] P.K. Mehta, P.J.M. Monteiro, Concrete: microstructure, properties, and materials, 3 ed., McGraw-Hill, New York, 2006.

[67] P.C. Aitcin, P.K. Mehta, Effect of Coarse Aggregate Characteristics on Mechanical Properties of High-Strength Concrete, Materials Journal, 87.

[68] A. Bentivegna, Multi-scale characterization, implementation, and monitoring of calcium aluminate cement based systems, in: Civil Engineering, University of Texas at Austin, Austin, Texas, 2012.

[69] M.T. Gaztanaga, S. Goni, J.L. Sagrera, Reactivity of high-alumina cement in water: pore solution and solid phase characterization, Solid State Ionic, 63 (1993) 797-802.

[70] S.A. Rodger, D.D. Double, The chemistry of hydration of high alumina cement in the presence of accelerating and retarding admixtures, cement and Concrete Research, 14 (1984) 73-82.

[71] P. Barret, D. Bertrandie, Hydration of Aluminate Cements, in: M.W. Grutzeck, S.L. Sarkar (Eds.) Advances in Cement and Concrete, American Society of Civil Engineers, University of New Hampshire, Durham, NH, 1994, pp. 132-174.

[72] F. Winnefeld, B. Lothenbach, Hydration of calcium sulfoaluminate cements — Experimental findings and thermodynamic modelling, Cement and Concrete Research, 40 (2010) 1239-1247.

[73] H.F.W. Taylor, Calcium aluminate, expansive and other cements, in: Cement Chemistry, Thomas Telford, London, 1997, pp. 295-322.

[74] R.C. Hibbeler, Mechanics of Materials, Fifth ed., Prentice Hall Pearson Education, Inc., Upper Saddle River, NJ, USA, 2003.

Manuscript 4

Volume Stability of Calcium Aluminate Cement and Calcium Sulfoaluminate Cement Systems

Matthew P. Adams and Jason H. Ideker

This paper was published in a different format in: "Calcium Aluminates: Proceedings of the International Conference," C. Fentiman, R. Mangabhai, and K. Scrivener, Editors. 2014, IHS BRE Press: Avignon, FR.

6 Manuscript 4

Volume Stability of Calcium Aluminate Cement and Calcium Sulfoaluminate Cement Systems

Matthew P. Adams[1] and Jason H. Ideker[2]

Abstract: There is renewed interest in North America for use of calcium aluminate cement in infrastructure repair due to its ability to gain strength rapidly even at low temperatures, the ability to customize fresh workability, and durability in certain adverse environments. Calcium sulfoaluminate cement has also gained popularity for infrastructure repair due its ability to set rapidly and quickly gain strength. This paper examines the volume stability of both calcium aluminate cement and calcium sulfoaluminate cement systems. Chemical shrinkage, autogenous deformation, and drying shrinkage and mass loss are examined for both systems. Results of these tests are compared with ordinary portland cement systems. It was found that systems based on calcium aluminate cement experienced the highest levels of chemical shrinkage, autogenous shrinkage, and drying shrinkage compared to the calcium sulfoaluminate and ordinary portland cement systems. Additionally, it was found that the rapid setting nature of the calcium aluminate cement and calcium sulfoaluminate cement systems cause the pore structure to develop quickly, thus increasing the rate of early-age chemical shrinkage observed compared to ordinary portland cement systems.

Keywords: calcium aluminate cement, calcium sulfoaluminate cement, chemical shrinkage, autogenous deformation, drying shrinkage

[1] Corresponding author. Ph.D. Candidate, School of Civil and Construction Engineering, Oregon State University. matthewpadams@gmail.com
[2] Associate professor, School of Civil and Construction Engineering, Oregon State University

6.1 Introduction

Calcium aluminate cement (CAC) concrete has been used in the construction industry for over 100 years [1]. Calcium sulfoaluminate (CSA) cement, alternatively, was developed in the 1960s, and gained wide acceptance particularly in China [2]. Only recently however, has there been an increased interest in use of these non-calcium silicate cements in cast-in-place rapid repair settings, particularly in North America. However, despite the increased usage of these materials, the long-term durability of concrete containing these alternative cements has not been as widely investigated as for ordinary portland cement (OPC) systems. One area in particular, volume stability, is of particular concern. The volume stability of these systems is important to understand because changes in volume can affect both early-age and long-term durability properties such as transport properties as well as the propensity for cracking. This paper examines the volume stability of ordinary portland cement (OPC), CAC, and CSA systems through the use of chemical shrinkage, autogenous deformation, and drying shrinkage studies. Prior to a discussion of the testing program and presentation and discussion of results, a short review of the hydration of these materials is presented.

While the work presented in this paper did not examine the effect of conversion on volume stability, the process of hydration in CAC is still important to review. The main anhydrous phase in CAC, monocalcium aluminate (CA), forms four main phases during the hydration process: CAH10, C2AH8, C3AH6, and AH3. The first two hydrates, CAH10, C2AH8, are both metastable and will convert into the stable hydrate C3AH6. This reaction is known as conversion, and is accompanied by the formation of AH3 gel, and the release of water [3,4]. This process is thermodynamically inevitable, and the rate at which it occurs is a function of the time and temperature history of the material during hydration. Increasing the curing temperature and exposure to moisture will result in faster conversion from the metastable hydrates to the stable hydrates [5]. The density of the metastable hydrates is lower than that of the stable hydrates [6]. The increase in density as the hydrates undergo conversion causes porosity to form in the hydrated cement paste. Initial set time for CAC paste is generally similar to that of OPC, but the time between initial set and final set is rapid. Final set for CAC paste at 20 °C occurs around four hours. Setting time of CAC can vary widely with temperature, however, due to the formation of different hydrates as discussed above [3, 4].

CSA cement formulations can vary widely depending on the manufacture and intended use of the cement. The main compounds found in CSA cement are similar, however. The main compound found

in CSA cement is C4A3$. CSA cements also contain varying levels of C2S and C$. Hydration of CSA cement will form ettringite with smaller amounts of C2A$H12, AH3, and C6A$3H32, and C2ASH8 as the main hydration products. The final amount of ettringite is dependent on the amount of calcium sulfate [2, 7, 8]. The CSA cement used in this study contained 39.5% C2S and 26.6% C4A3$, by weight. Variations in the curing temperature of CSA systems will influence the rate of hardening, however, unlike CAC, it will not fundamentally change the hydrates that are formed. Some CSA formulations are expansive and used as shrinkage compensating formulations [9], however the CSA cement examined in this paper was not formulated to have expansive properties. The setting time of CSA cements can vary between thirty minutes and four hours, depending on their composition [2]. This study examined 100% CAC, 100% CSA, and 100% OPC systems. Blends of these cements will produce different hydrates, and therefore the results presented are only valid for systems presented here.

6.2 Experimental Methods

6.2.1 Chemical Shrinkage

Chemical shrinkage is a measurement of the relative volume reduction observed during cement hydration and does not result in macroscopic volume change after setting, but instead relates to the amount of porosity that develops in the system during hydration [10]. Chemical shrinkage measurements were performed according to ASTM C1608 [11] with some modifications. The mixtures used for the chemical shrinkage testing of cement paste were all made with a w/c of 0.35. Six hundred (600) grams of OPC, CAC or CSA cement were used for the mixtures. An oxide analysis of the cements used as a part of this study is presented in Table 6-1.

Table 6-1: Cement Oxide Analysis

Oxide (% wt)	SiO_2	Al_2O_3	Fe_2O_3	CaO	MgO	Na_2O	K_2O	SO_3	TiO_2	Mn_2O_3	P_2O_5	SrO	BaO	ZnO	LOI
OPC	20.46	5.00	3.44	63.29	0.87	0.27	0.34	3.13	0.23	0.10	0.06	0.17	0.09	-	2.50
CSA	11.82	13.63	1.11	52.21	2.18	0.09	0.90	14.83	0.58	0.03	0.08	0.19	-	0.03	2.04
CAC	5.93	39.15	14.23	35.34	0.70	0.08	0.19	0.16	1.81	1.75	0.48	0.17	0.03	0.01	-

No admixtures were used in the paste mixtures. The paste sample was mixed in accordance with ASTM C305 [12]. The cement powder was sieved through a sieve with opening size of 0.8 mm. It was then mixed with deionized and deaerated water at room temperature. The cement paste (~3 g per vial)

was then placed into 25 mL hard plastic vials. The vial was then filled with deionized and deaerated water. The vial was closed using a rubber stopper that was pierced with a 1mL glass pipette. Care was taken during this process and during the placing of the cement paste to ensure that no air bubbles were entrapped in the system. The pipette was then filled with water, and a small amount of oil with coloured dye was placed into the pipette to prevent water loss to the air. The vials and pipettes were then placed into a water bath to maintain a constant temperature of 20 ± 0.5 °C during the testing period. The pipette was then monitored over the test period to measure the amount of water sorbed into the system and the amount of chemical shrinkage was determined. Monitoring was automated through the use of a webcam and image analysis program as described by Fu et al [13]. Monitoring began 30 ± 5 minutes after the cement contact with water in the mixer.

6.2.2 Autogenous Deformation

Autogenous deformation is a measurement of the macroscopic volume change that occurs in a closed system due to hydration. Shrinkage may occur due to self-desiccation that causes water filled pores to collapse as the water is drawn out and consumed in hydration products [10]. Autogenous deformation was measured through the use of a small scale free deformation frame as described by Ideker et al. [14]. The free deformation frame measured the autogenous deformation of a 50.8 x 50.8 x 175 mm mortar bar that had an effective gage length of 135 mm. A mortar mixture was cast into the frame, and then sealed to prevent moisture loss to the outside environment. The mortar mixtures were made with a w/c of 0.35, a cement content of 2000g and a sand content of 3500g. The sand was siliceous river sand. Mixing was performed according to ASTM C305 [12]. Setting time samples were matched cured at 20 ± 3°C. Invar steel rods were embedded into the mortar bar with aluminium plates set at the gage length state above. The other ends of the bars were attached to linear control potentiometers at either end of the frame. Initially the mortar was prevented from slumping by two moveable steel plates at either end of the specimen. These plates were released after final set, as determined by ASTM C403 [15] to allow free movement of the specimen for the remainder of the testing period.

Temperature of the specimen in the free shrinkage frame was regulated through the use of a cooling/heating water circulator. The circulator pumped water through the formwork of the free deformation frame to maintain a temperature of 20°C in the sample. Temperature was monitored through the use of a thermocouple embedded into the specimen when it was cast.

6.2.3 Drying Shrinkage

Drying shrinkage is caused when water in capillary pores is lost to the environment. This will occur when concrete is exposed to an environment that has less than 100% relative humidity and will continue to occur until the relative humidity inside the concrete equilibrates with external humidity conditions. As the water leaves these small pores, it creates pressures which may cause the pores to collapse [10]. This can cause macroscopic volume change referred to as drying shrinkage. Free drying shrinkage testing was performed on concrete mixtures with a 0.35 w/c using ordinary portland cement, a standard grade calcium aluminum cement, or calcium sulfoaluminate cement. The mixture designs and curing durations for the drying shrinkage mixtures can be seen in Table 6-2.

Table 6-2: Mixture designs and fresh properties for drying shrinkage concrete prisms

Cement Type	w/cm	Cement Content (kg/m^3)	Fine Aggregate Content (kg/m^3)	Coarse Aggregate Content (kg/m^3)	Slump (mm)	Air Content (%)	Fresh Unit Weight (kg/m^3)	Curing Duration
Portland Cement	0.35	440	750	920	83	2.0	2388	24 Hr.
Calcium Sulfoalumiate Cement	0.35	440	750	920	38	3.0	2355	10 and 24 Hr.
Calcium Aluminate Cement	0.35	440	750	920	25	1.8	2289	10 and 24 Hr.

The fine aggregate used in this study was siliceous river sand, and the coarse aggregate was siliceous river gravel. The fine aggregate was comprised of particle sizes that ranged from 0.08 mm to 4.75 mm, and had a fineness modulus of 2.61.

Free drying shrinkage monitoring of specimens was implemented according to ASTM C157 [16]. Measurements were taken on hardened concrete prisms 75mm x 75 mm x 285mm. Specimens were cast in hard plastic moulds (3 prisms for each mixture), and then allowed to cure covered under wet burlap in ambient laboratory conditions (23 ± 4°C) for 10 hours or 24 hours according to the mixtures listed above. Specimens were then removed from their moulds and placed into an environmental chamber set to 23 ± 2°C and 50 ± 4% relative humidity. During drying, the length change and mass change were measured.

6.3 Results

6.3.1 Chemical Shrinkage

The results from the chemical shrinkage testing at 20°C of the OPC, CAC, and CSA cements can be seen in Figure 6-1.

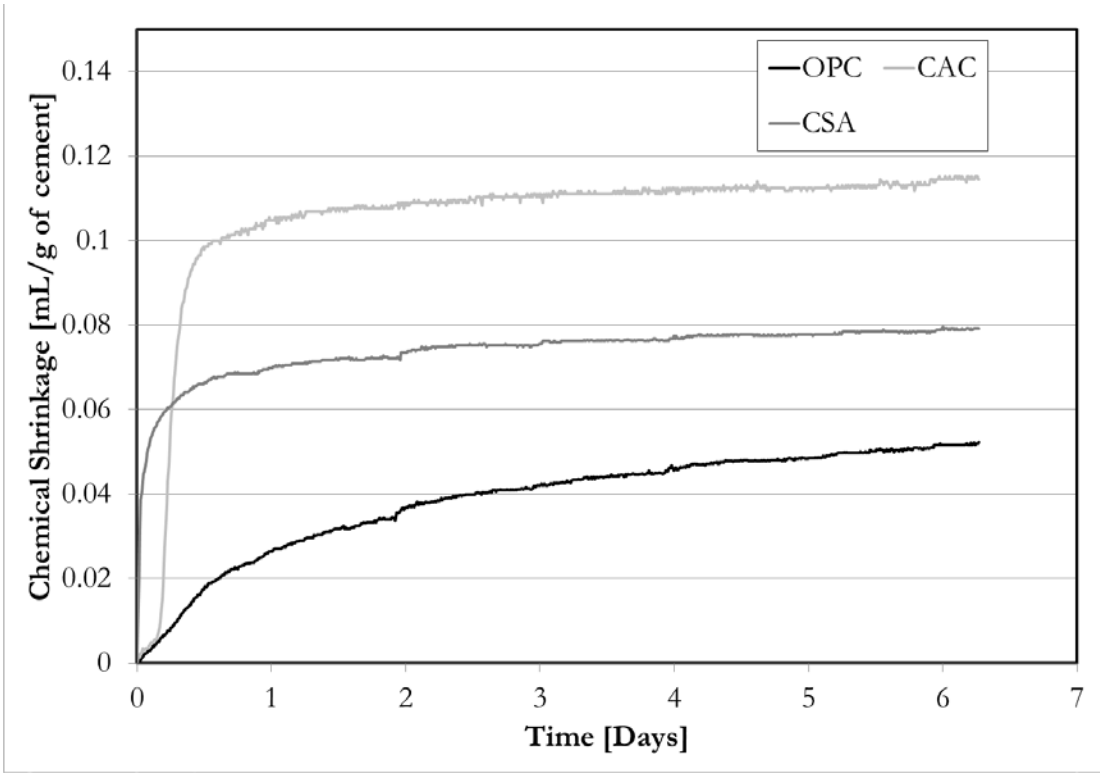

Figure 6-1: Chemical shrinkage of OPC, CAC, and CSA cement pastes

These results are the averages of all samples tested (three samples each) for each cement type. These results indicate that the CAC samples had the highest chemical shrinkage overall, and the OPC samples had the lowest. Both the CAC and CSA samples show rapid increases in chemical shrinkage at early ages (less than 12 hours) and then level off with only a relatively small amount of continued shrinkage over time. The OPC sample showed markedly different behaviour from the CSA and CAC samples. The OPC samples had a much slower initial chemical shrinkage development. Similar to the CAC and CSA samples, the rate of increase in chemical shrinkage diminished over time, however by 6 days, it had not completely stopped. These results do indicate, however, that the majority of chemical

shrinkage occurs prior to 12 hours in the rapidly hardening cement systems, CAC and CSA, whereas the chemical shrinkage increase is much slower for OPC and thus occurs over a longer time period.

6.3.2 Autogenous Deformation

Autogenous deformation was measured from the time of final set (see Figure 6-5 below) on mortar bars using the frame described above. Figures 6-2, 6-3, and 6-4 present the autogenous deformation of the CAC mortar bar and CSA mortar bar and OPC mortar bar samples over time at 20°C, respectively.

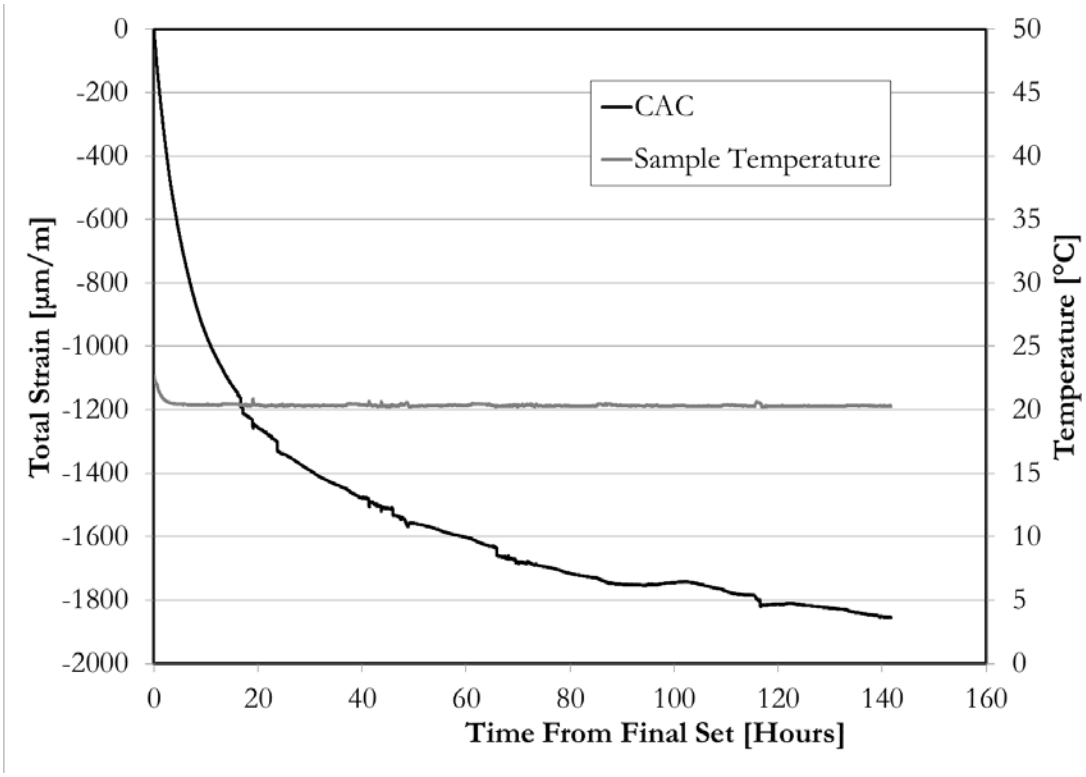

Figure 6-2: Autogenous deformation and temperature of CAC mortar sample

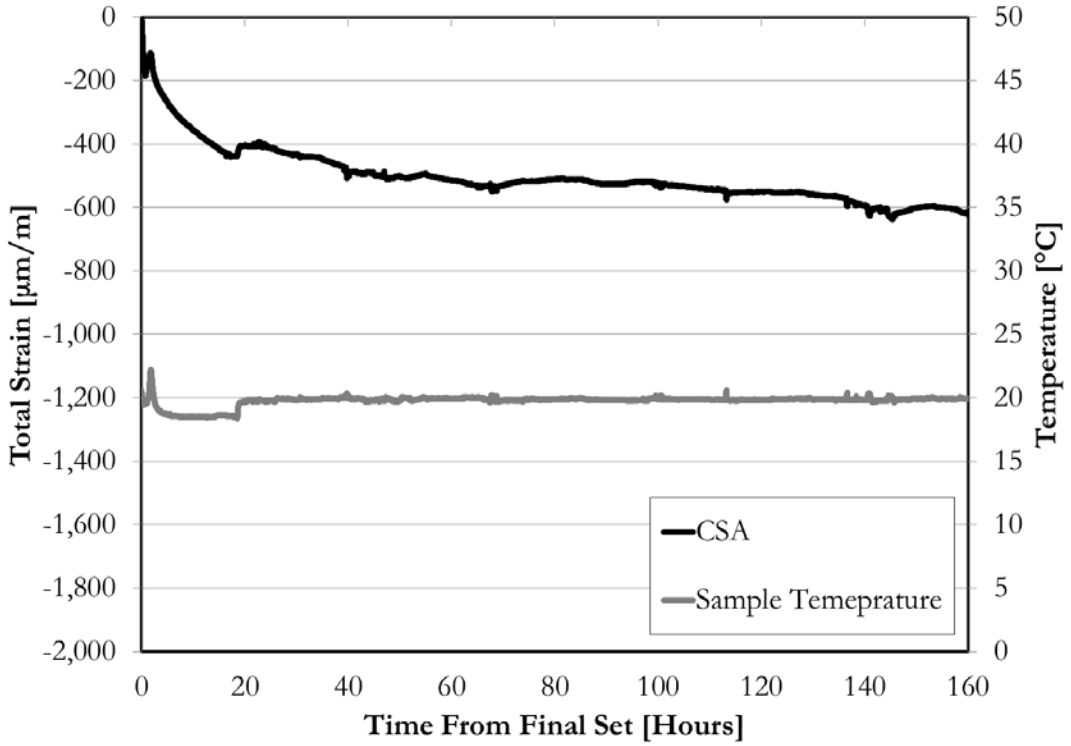

Figure 6-3: Autogenous deformation and temperature of CSA mortar sample

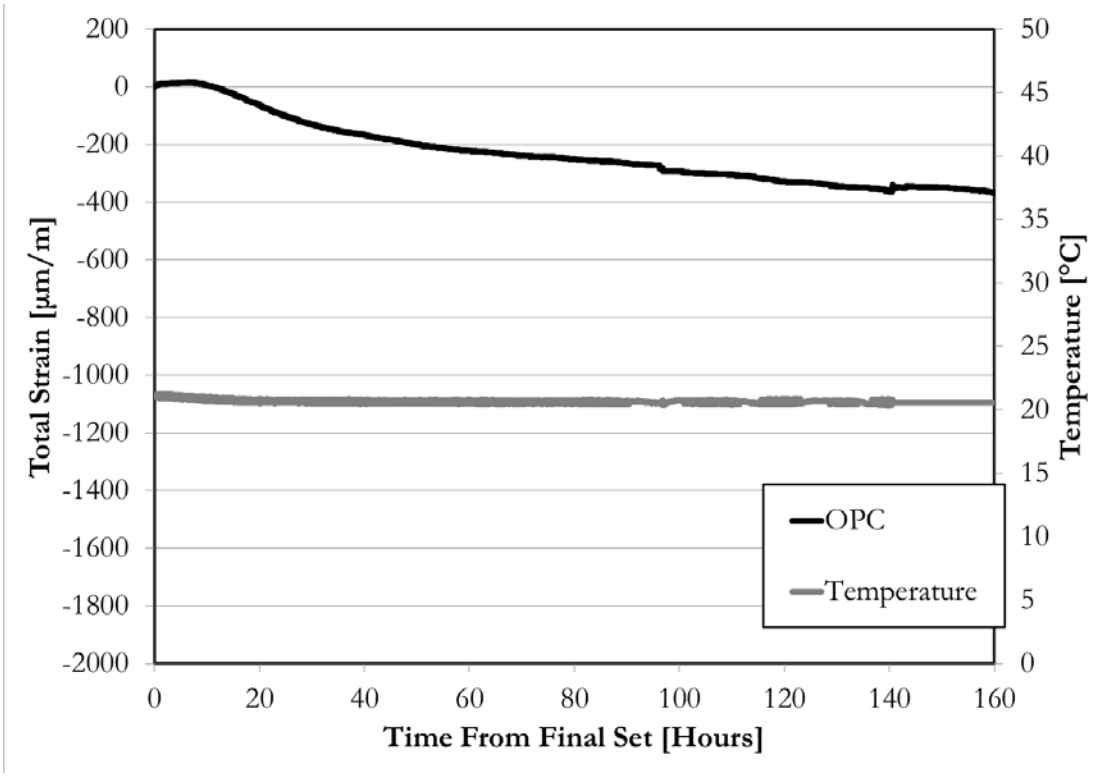

Figure 6-4: Autogenous deformation and temperature of OPC mortar sample

Shrinkage was the predominant autogenous deformation behaviour for all three systems. The results presented here indicate that the OPC mortar samples underwent the least amount of autogenous deformation. The CAC sample, at 20°C, underwent rapid autogenous shrinkage for the first 20 hours. After 20 hours, the autogenous shrinkage rate of CAC mortar samples decreased however was still higher than that of the CSA samples. The CSA sample experienced rapid shrinkage in the initial 24 hours, after which continued shrinkage occurred at a slower rate. The OPC sample experienced the least amount of autogenous shrinkage of all three sets, and had a much lower rate of autogenous shrinkage at all ages. During the initial 12 hours, the OPC system experienced expansion due to a slightly elevated temperature in the free deformation frame. Longer term testing is required to determine if the shrinkage remained constant beyond 160 hours after final set. Overall, the CAC sample exhibited shrinkage due to autogenous deformation three times larger than that of the CSA mortar sample and four and a half times larger than the OPC mortar sample.

Autogenous deformation measurements began from the time of final set. Figure 6-5 presents the setting time of the CAC and CSA mortars at 20°C. The CSA mortar reached final set before one hour

after mixing. The CAC had a longer final set time, setting at 3.6 hours after mixing. The CAC mortar reached initial set earlier than the OPC mortar, but final set was reached a half an hour after the OPC sample. While these set times were tested on mortars, they confirm the chemical shrinkage rates seen above for the CAC, CSA, and OPC cement pastes.

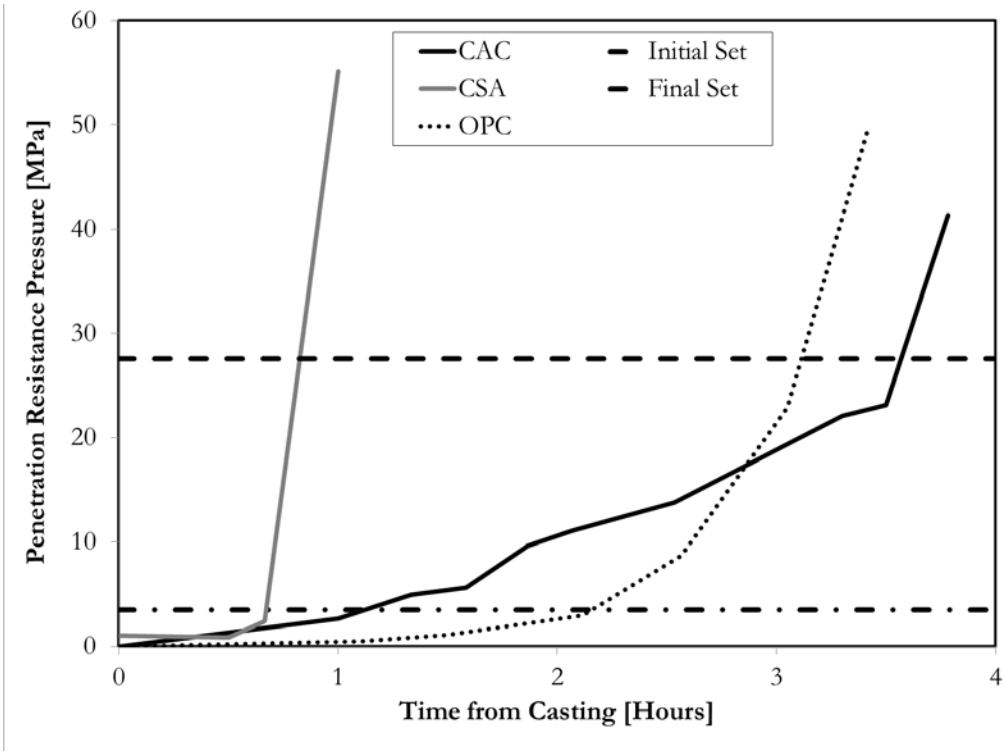

Figure 6-5: Setting time of CAC, CSA, and OPC mortar samples at 20°C

6.3.3 Drying Shrinkage and Mass Loss

Figure 6-6 presents the length change due to drying of the OPC, CAC, and CSA prisms cast for this study. These results present average data for sets of three prisms for each mixture. As these results indicate the specimens cast with CAC cement experienced the highest levels of drying shrinkage, and the specimens created with CSA cement experienced the lowest levels of drying shrinkage at 98 days after exposure to drying conditions. The duration of curing (10 hr. or 24 hr. cure) did not affect the length change for the CSA cement. The CAC concrete appears to have experienced higher levels of drying shrinkage when cured for 24 hours. However, the standard deviation between the three prisms for the CAC 24 hr cure was quite large in some cases (0.003% to 0.0313%) and the difference between

the two curing durations may not be significant. The C157 test method suggests that standard deviation among specimens of the same mixture should not exceed 0.0084% [16]. This value was developed for use with OPC, however, and may not be applicable for use with CAC.

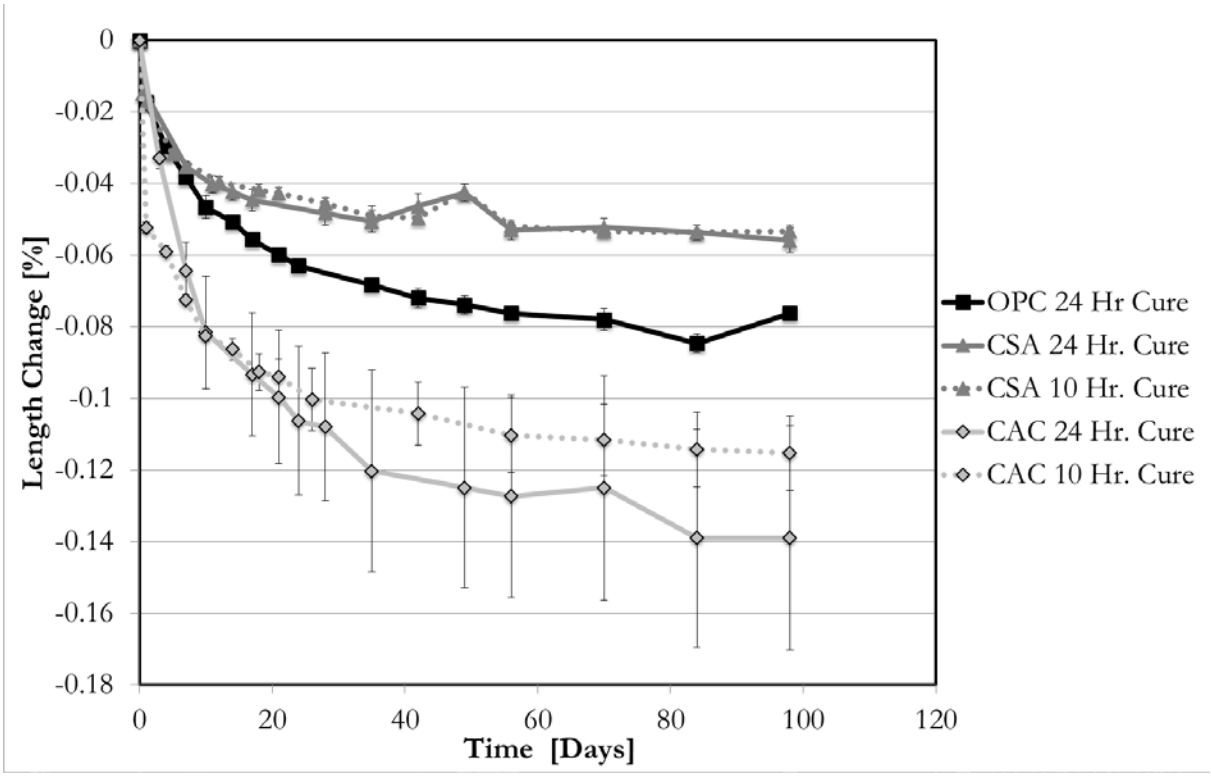

Figure 6-6: Length change of concrete prisms submitted to drying conditions

Mass loss due to drying indicates the amount of water lost from the system after the specimens are placed into the drying chamber. Figure 6-7 presents the mass loss over time due to drying of the OPC, CAC, and CSA prisms cast for this study. This graph indicates that the CAC specimens experienced the lowest amount of mass loss over time due to drying. The specimens made with OPC cement experienced the highest amount of mass loss due to drying. The different curing times to which the CAC and CSA concrete prisms were subjected did not affect the amount of mass loss observed.

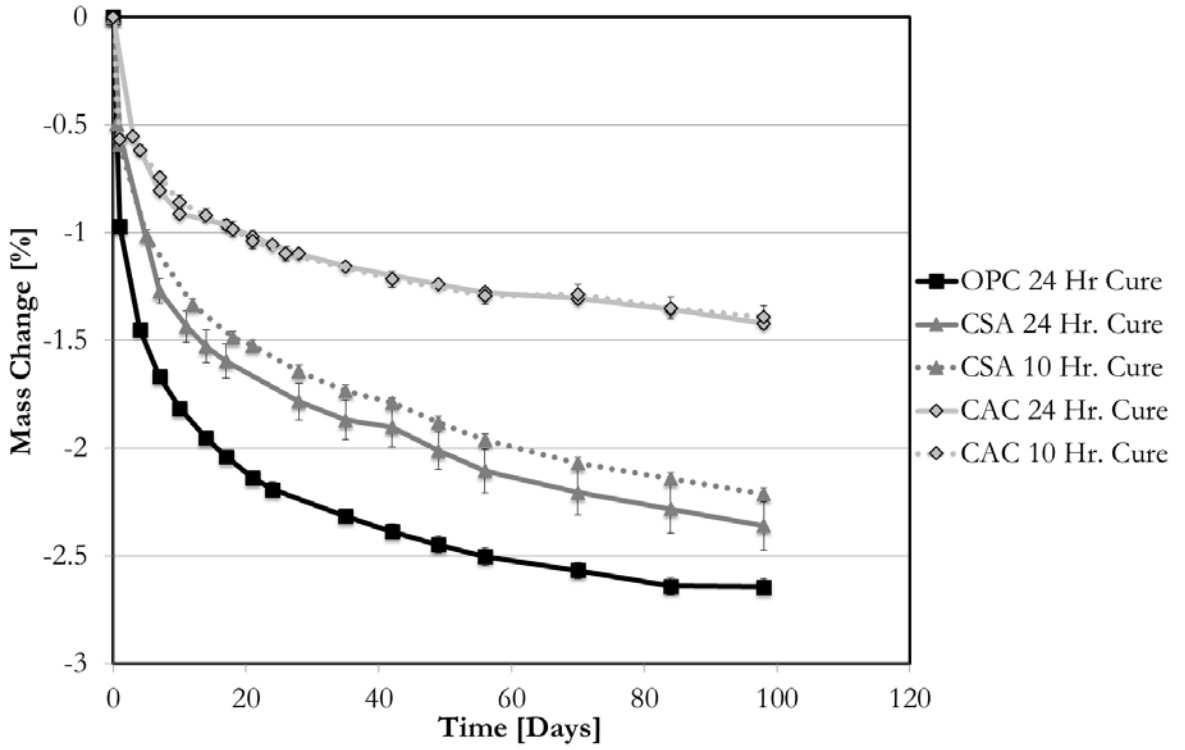

Figure 6-7: Mass loss of concrete prisms submitted to drying conditions

6.4 Discussion

The rapid increase in chemical shrinkage at early ages seen in both the CAC and CSA samples is related to the rapid hydration of these cements. If the curves for the CSA and CAC are examined, differences in the early age hydration can be observed. The CSA samples show rapid hydration from the beginning, however, the rapid hydration of the CAC sample does not start until 3.6 hours after casting. This indicates that the rapid hydration of CAC is delayed compared to that CSA cement samples. This period of rapid chemical shrinkage aligns closely with typical set times for CAC cast at 20°C. Previous work has shown that the setting time for pure CAC pastes at 20°C is around 4 hours [3]. Setting time for the CSA cement paste can be as low as 30 minutes depending on the cement composition [2], which can be observed in Figure 6-1 with the early increase in chemical shrinkage of the CSA paste. Though performed on mortars, the set times presented in Figure 6-5 align closely with the chemical shrinkage results presented in Figure 6-1. Hence the sudden increase in chemical shrinkage in the CAC and CSA systems aligned closely with the final setting time of the mortars. However, no large increase in chemical shrinkage is observed for the OPC paste, indicating that formation of large amounts of porosity at set time is a consequence of the rapid setting nature of the CAC and CSA cement systems.

The porosity for these systems is developed quickly as the hydration occurs rapidly causing the microstructure to stabilize during the early ages of the cement hydration. In the OPC system, however, the microstructure continues to evolve over time with the slower hydration process that occurs. Thus, the chemical shrinkage for OPC systems will continue to increase over a longer period of time.

The shrinkage dominated autogenous deformation of the mortar bars presented indicates that both (CAC & CSA) systems lost water to self-desiccation during hydration. As water is drawn out of capillary pores to aid in hydration, the pores will collapse due to local pressures, and cause autogenous shrinkage. The difference in autogenous deformation between the CAC and CSA mortar bars may be related to an increased water demand of CAC cement hydration at 20°C. The metastable hydrates that are produced from CAC hydration at 20°C contain large amounts of water [3]. The water demand of these metastable hydrates may cause a significant amount of autogenous shrinkage, particularly in low w/c systems. Additionally, the microstructure of unconverted CAC systems is quite dense, which results in a finer pore structure, which can increase the propensity for autogenous shrinkage in these systems [14]. Research has confirmed the fine pore structure of unconverted CAC [17]. A finer pore system may cause more shrinkage when water is removed from the pores. This is because higher levels of surface tension on the water as it is drawn out to aid in hydration (or lost to the environment) will induce larger tensile pressures, causing the pores to collapse more readily. CSA systems have also been shown to have similarly refined pore structures, however, the pore structures in CSA cement systems do not have such high levels of interconnectivity as seen by the bimodal distribution of pore sizes observed by Bernardo et al. [8]. The closure of an interconnected pore system occurs at early ages (less than 12 hours). This indicates that the lower autogenous shrinkage observed in the CSA system may not be due to a coarser pore system, but instead due to a lack of access to the water contained in the refined pore system. The drying shrinkage and mass loss curves contradict this conclusion that there is a lack of access to the water in the pores, however.

As can be seen from Figures 6-6 and 6-7, increased mass loss does not necessarily indicate an increased amount of drying shrinkage. Here the CSA prisms had the lowest drying shrinkage, but the higher mass loss than the CAC prisms; whereas the CAC prisms had the lowest mass loss, but the highest drying shrinkage. For the samples created with OPC, the drying shrinkage amounts were in between the CAC and CSA prisms but produced the highest mass loss. These drying shrinkage and mass loss results indicate that the concrete prisms made with CSA and OPC had a pore structure that was quite

coarse and interconnected, allowing water to escape to the environment easily without causing internal pressures that collapsed the pores. Further testing is required to truly understand the relationship between mass loss, drying shrinkage, and porosity in these systems, however.

It is important to understand that the drying shrinkage test does not necessarily account for autogenous shrinkage, much of which may occur earlier than the time periods examined as a part of this study as observed in the autogenous deformation results presented earlier. Additionally, autogenous shrinkage may continue to occur throughout the period of drying shrinkage that is examined, so the macroscopic volume change noted here may not be due entirely to drying shrinkage [18].

It should be noted that the CAC specimens did not fully convert during the time period in which they were tested, so the impact of conversion on drying shrinkage cannot be ascertained. Previous work has shown, however, that no change in macroscopic dimensions is observed during conversion [3]. Finally, it is interesting to note here that there were no significant differences between the prisms (CAC or CSA cement based) that were cured for 10 hours or the prisms that were cured for 24 hours before being exposed to drying conditions. These results are quite important for the rapid repair of concrete because, for pavements, it is necessary that the roadway be shut down for a little time as possible. These results indicate that shorter curing durations (and thus shorter road closures) will not be detrimental to the drying shrinkage performance of concrete made with these rapid hardening binders.

6.5 Future Work

These results indicate that there are still some questions to be answered concerning the volume stability of these alternative cement systems. Primarily, it is important to understand the causes in the differences seen in the levels of autogenous and drying shrinkage between the CAC, CSA, and OPC systems. It is unclear if this is due to water demand of the hydrating system, interconnectivity of pore structure, or size of pore structure. Further work is required to understand the effect of these three variables on the volume stability of these systems.

Secondly, it is important to understand how these systems behave at different temperatures, particularly CAC, which develops different hydration products depending on the temperature at which

it is cured and maintained. Ideker et al. showed that when cured isothermally above 30°C, CAC systems exhibit autogenous expansion [14]. This paper examined volume stability only at temperatures of 20°C (chemical shrinkage and autogenous deformation) and 23°C (drying shrinkage). It is important to understand whether expansions may also occur in CSA systems cured isothermally at different temperatures; as well as the reasons for which expansion is observed above 30°C, but shrinkage is observed below in CAC systems.

6.6 Conclusion

This work examined the volume stability of CAC, CSA and OPC systems through the use of chemical shrinkage, autogenous deformation, and drying shrinkage testing. Several conclusions can be drawn from the results presented here:

- Both the CAC and CSA cement pastes experienced higher levels of chemical shrinkage compared to the OPC paste. Additionally, the chemical shrinkage in the CSA and CAC systems experienced sharp increases at early ages, which is related to the rapid setting nature of these cements.
- The CAC system cured isothermally at 20°C experienced significantly higher levels of autogenous shrinkage than those observed in the CSA mortar bars. This may be due to the higher water demand of the CAC hydrates during hydration.
- The CAC system also experienced the highest levels of drying shrinkage compared to the CSA and OPC systems. This may be due to a more refined pore structure, susceptible to shrinkage upon water loss, compared to that of the CSA system.

6.7 Works Cited

[1] Scrivener K L. *100 years of calcium aluminate cements*, in Calcium Aluminate cements: Proceedings of the Centenary Conference, Avignon, 2008. Fentiman CH, Mangabhai RJ, and Scrivener KL (Eds). Bracknell: IHS BRE Press, 2008, pp. 3-6.

[2] Juenger M C G., et al., *Advances in alternative cementitious binders.* Cement and Concrete Research, 2011. 41(12): p. 1232-1243.

[3] Scrivener K L and Capmas A. *Calcium Aluminate Cements*, in *Lea's Chemistry of Cement and Concrete*, Hewlett PC (Ed). 1998, Elsevier - Butterworth-Heinemann: Oxford, UK. p. 713-782.

[4] Bushnell-Watson S M and Sharp J H. *On the cause of the anomalous setting bahaviour with respect to temperature of calcium aluminate cement.* Cement and Concrete Research, 1990. 20: pp. 677-686.

[5] Muller A. *Conversion & résistance en compression des ciments cT a lu m in a tes de calcium*, in Departement Genie Civil2010, Universite Laval: Quebec City.

[6] Fryda H, Charpentier E and J M Bertino. *Accelerated test for conversion of calcium aluminate cement concrete*, in Calcium Aluminate Cements: : Proceedings of the Centenary Conference, Avignon, 2008. Fentiman CH, Mangabhai RJ, and Scrivener KL (Eds). Bracknell: IHS BRE Press, 2008. pp. 159-169.

[7] Odler I. *Hydration, setting and hardening of portland cement*, in *Lea's Chemistry of Cement and Concrete*, Hewlett PC (Ed). 1998, Elsevier: Oxford, UK.

[8] Bernardo G, Telesca A and Valenti G L. *A porosimetric study of calcium sulfoaluminate cement pastes cured at early ages.* Cement and Concrete Research, 2006. 36: pp. 1042-1047.

[9] Chen I A, Hargis C W and Juenger M C G. *Understanding expansion in calcium sulfoalumiate-belite cements.* Cement and Concrete Research, 2012. 42(1): pp. 51-60.

[10] Mehta P K and Monteiro P J M. *Concrete: microstructure, properties, and materials*. 3rd edition. 2006, New York: McGraw-Hill.

[11] ASTM Standard C1608 2012. *Standard test method for chemical shrinkage of hydraulic cement paste*, ASTM International, Editor 2013: West Conshohocken, PA.

[12] ASTM Standard C305 2013. *Standard practice for mechanical mixing of hydraulic cement pastes and mortars of plastic consistency*, ASTM International, Editor 2006, ASTM International: West Conshocken, PA.

[13] Fu T, Deboodt T and Ideker J.H. *Simple procedure for determining long-term chemical shrinkage for cementitious systems using improved standard chemical shrinkage test.* Journal of Materials in Civil Engineering, 2012. 24(8): pp. 989 - 995.

[14] Ideker J H, Folliard K J and Thomas M D A. *Early-age properties of calcium aluminate cement concrete with rigid cracking and free shrinkage frames: isothermal testing.* in Calcium Aluminate Cements: : Proceedings

of the Centenary Conference, Avignon, 2008. Fentiman CH, Mangabhai RJ, and Scrivener KL (Eds). Bracknell: IHS BRE Press, 2008. Pp. 141-157.

[15] ASTM Standard C403 2008. *Standard test method for time of detting of concrete mixtures by penetration resistance*, ASTM International, Editor 2013: West Conshocken, PA.

[16] ASTM Standard C157 2008. *Standard test method for length change of hardened hydraulic-cment mortar and concrete*, A. International, Editor 2013: West Conshohocken, PA.

[17] Gosselin C. *Microstructural development of calcium aluminate cement based systems with and without supplementary cementitious materials*, in Faculte Sciences and Techniques de l'Ingenieur2008, Ecole Polytechnique Federale de Lausanne: Lausanne, Switzerland.

[18] Ideker J H. *Early-age behavior of Calcium Aluminate Cement Systems*, in Civil Engineering 2008, The University of Texas at Austin: Austin, TX.

6 Conclusion

CACs are versatile specialty cements that can be used in a wide array of applications. Despite the existence of this material for over 100 years, it is still not well understood within the general construction community. CACs, however, may be particularly useful for rapid repair due to their ability to quickly gain strength even at low temperatures. The work presented in this dissertation provided new data on the impact of curing procedures on conversion in CAC, showed information on changes in the pore solution of CAC systems during conversion, showed the impact of low dosages of finely ground limestone on converted CAC concrete strength, pushed forward the development of a test method to quickly determine minimum converted strength in CAC concrete while still being convenient for use in the field, and addressed existing gaps in literature concerning the impact of aggregate mineralogy on CAC concrete strength, hydration and conversion. Key findings from this work are summarized below:

6.1 Key Findings

The key findings from this work are listed below:

- The test method presented in Manuscript 1 shows promise for use in the field to determine the minimum converted compressive strength of CAC concrete.
    - This test method allows for samples to be cured at ambient temperatures in the field, and transported to the laboratory after hardening, where they are then placed into a 50°C water bath.
    - Any standardized test method based off of the procedure outlined in Manuscript 1 must be written with care to address changes in time to minimum converted strength based on ambient construction site temperatures, internal concrete temperatures, and the time at which the samples are placed in the water bath.
- Leaching from the concrete was not a concern when CAC concrete was placed into elevated temperature water baths.
- The initial ambient curing temperature at which CAC concrete was cured affected the time to minimum converted strength as observed using the test method presented in Manuscript 1.
    - Samples cured at ambient laboratory temperature (23°C) during the initial 24 hour curing period converted within 2 days after being placed in the 50°C water bath.
    - Samples cured at 38°C during the initial 24 hour curing period converted prior to the initial compressive strength testing performed at 24 hours after casting.
    - Samples cured at 5°C during the initial 24 hour curing period converted within 6 days after being placed in the 50°C water bath.

- Inherent variation in the compressive strength results between multiple laboratories for the same concrete mixtures was found to be higher in CAC concrete mixtures compared to what is currently stated in ASTM test methods for ordinary portland cement (OPC) concrete mixtures.
- Replacing CAC cement with up to 5% finely ground limestone (FGLS) increased the converted strength in CAC concrete without compromising early strength gain.
- Aggregate source had a significant impact unconverted and converted CAC concrete strength.
    - No correlation was found between aggregate properties (grading, G_s, absorption capacity, fineness modulus, and median aggregate size (D50)) and the converted strength of CAC concrete.
- Aggregate source impacted the time to conversion observed using the test method described in Manuscript 1, delaying time to minimum converted strength up to 27 days after submersion in the 50°C water bath compared to 2 days after submersion experienced for the majority of aggregate systems.
- CAC concrete systems containing carbonate limestone aggregates (CRC aggregate) had significantly different pore solution chemistry compared to CAC concrete systems containing siliceous river gravels (KRC aggregates).
    - In systems submitted to the same curing procedure described in Manuscript 1, sodium, potassium, and aluminum concentrations in pore solution peaked at 24 hours, and then reduced significantly after conversion in the limestone systems. The sodium, potassium, and aluminum concentrations in the siliceous aggregate system's pore solution remained low at all ages, experiencing no significant drop in concentration after conversion. Paste systems behaved similarly to the limestone system for sodium potassium and aluminum concentrations, however with comparatively lower overall concentrations of all three elements.
    - Overall concentrations of calcium were found to be comparatively low in all three systems, and silicon concentrations were below detection limits.
    - The use of siliceous aggregate in CAC concrete significantly lowered the pH in the pore solution of the concrete.
- Poor interfacial transition zones were observed in SEM images after conversion around aluminum bearing siliceous aggregates (KRC aggregate).
- Significantly lower levels of porosity were observed through both SEM image analysis and mercury intrusion porosimetry in the carbonate limestone aggregate (CRC aggregate) system compared to the siliceous river gravel system (KRC aggregate).
- Theories were proposed that, when taken in consort, may explain the differences between carbonate limestone CAC systems and siliceous river gravel CAC systems. These theories are:

    - The relatively low pH in the siliceous system reduced the degree of hydration and resulted in higher porosity after conversion compared to the limestone system due to the lack of material available to precipitate out of solution,
    - Aluminum bearing aggregates in the siliceous system develop poor interfacial transition zones reducing overall concrete strength in that system, and
    - The surface roughness of the limestone aggregates may provide additional site for nucleation of CAC hydrates creating increased bond strength between limestone aggregates and the cement paste matrix.
- CAC and CSA paste systems experienced significantly higher levels of chemical shrinkage compared to OPC pastes.
    - The majority of chemical shrinkage observed in CAC and CSA pastes was developed within the first 24 hours due to the rapid hydration experienced in these systems.
- When cured isothermally at 20°C, CAC mortar experienced significantly higher levels of autogenous shrinkage compared to the autogenous shrinkage observed in the CSA and OPC systems.
- CAC concrete experienced the highest amount of shrinkage due to drying compared to OPC concrete and CSA concrete systems despite having the least amount (by mass) of water lost to the environment. This was due to the more refined pore structure present in CAC cement paste which is more susceptible to shrinkage upon water loss.
- The length of moist curing (10 hours and 24 hours) was found to have little effect on the overall drying shrinkage observed in CAC and CSA.

6.2 Future Work

The following is a listed of recommendations for additional work to build on what was learned through the work presented in this dissertation:

- Further robustness testing is necessary to fully understand the impact of certain variables on the test method described in Manuscript 1, these include:
    - Study of additional aggregate sources to determine if the volatility in time to converted strength is related to only carbonate limestone aggregates, or could occur in other systems as well, and
    - A further study of additional carbonate limestone aggregates to determine what the time to converted strength is in those systems.
- A larger inter-laboratory variability study of the test method presented in Manuscript 1 including at least 6 different laboratories. Additionally, a study to determine within-laboratory variability. This study should also determine if within-laboratory variation differs between aggregate sources,

as well. These results will be necessary for the acceptance of a standardized test method for use the rapid determination of converted CAC concrete strength.

- A long-term examination of low-dosage FGLS CAC systems to determine the stability of strength in those systems. This work should be combined with analysis through SEM imaging, XRD, and MIP to determine the mechanism of strength enhancement post-conversion, and hydrated phases present in low dose FGLS CAC systems.
- An investigation to determine the reason for differences in pH between the carbonate limestone aggregate CAC concrete and siliceous river gravel CAC concrete system and an examination of the hydrate phases formed and degree of hydration in the carbonate limestone aggregate CAC concrete and siliceous river gravel CAC concrete systems to determine if there are significant differences in hydration between the two systems.
- A comprehensive study of a broad range of aggregates, including mineralogical investigations of each aggregate type, to determine the correlation between aggregate mineralogy, converted CAC strength, and systems chemistry. This work will allow better predictions of CAC concrete performance based on aggregate type.
- A further examination of the pore structure in CAC, CSA, and OPC systems is suggested to better understand how the microstructures impact shrinkage in each of these systems.

8 References

This section provides a compiled list of all references cited throughout the dissertation, in alphabetical order.

Beam failure— conversion of high alumina cement, Building Research and Practice, 2 (1974) 235-240.

A.C. 209, Report on Factors Affecting Shrinkage and Creep of Hardened Concrete (ACI 209.1R-05), in, American Concrete Institute, Farmington Hills, Michigan, 2005.

A. Abbas, G. Fathifazl, O. Isgor, A. Razaqpur, B. Fournier, S. Foo, Environmental benefits of green concrete, in: EIC Climate Change Technology, 2006 IEEE, IEEE, 2006, pp. 1-8.

A. Abbas, G. Fathifazl, O.B. Isgor, A. Razaqpur, B. Fournier, S. Foo, Proposed method for determining the residual mortar content of recycled concrete aggregates, Journal of ASTM International, 5 (2008) 12.

M.P. Adams, J.H. Ideker, Volume stability of calcium aluminate cement and calcium sulfoaluminate cement systems, in: C. Fentiman, R. Mangabhai, K. Scrivener (Eds.) International Conference on Calcium Aluminate Cements, IHS, Avignon, FR, 2014.

M.P. Adams, J.H. Ideker, Chapter 2: Development of a test method for determining the converted strength of calcium aluminate cement concrete, in: Factors influencing conversion and converted strength in calcium aluminate cement concrete, Oregon State University, Corvallis, OR, 2015.

M.P. Adams, J.H. Ideker, Pore solution chemistry of calcium aluminate cement concrete systems undergoing accelerated conversion, in: 14th International Conference on Cement Chemistry, Beijing, 2015 (Under Review).

P.C. Aitcin, P.K. Mehta, Effect of Coarse Aggregate Characteristics on Mechanical Properties of High-Strength Concrete, Materials Journal, 87.

M.G. Alexander, C.W. Fourie, Acid resistance of calcium alumiante cement in concrete sewer pipe mixtures, in: R.J. Mangabhai, F.P. Glasser (Eds.) International Conference on Calcium Aluminate Cements, IOM Communications, Edinburgh, UK, 2001, pp. 633-645.

American Concrete Institute, Removal and reuse of hardened concrete, in: American Concrete Institute (Ed.), American Concrete Institute, Farmington Hills, MI, 2001.

American Society of Civil Engineers, Report card for America's infrastructure, in, American Society of Civil Engineers, 2013.

V. Antonovič, J. Keriene, R. Boris, M. Aleknevičius, The effect of temperature on the formation of the hydrated calcium aluminate cement structure, Procedia Engineering, 57 (2013) 99-106.

ASTM C31, Standard practice for making and curing concrete test specimens in the field, in: A. International (Ed.), ASTM International, West Conshohocken, PA, 2012.

ASTM C39 2012a, Standad test method for compressive strength of cylindrical concrete specimens, in: A. International (Ed.), ASTM International, West Conshohocken, PA, 2015.

ASTM C39, Standad test method for compressive strength of Cylindrical Concrete Specimens, in: A. International (Ed.), ASTM International, West Conshohocken, PA, 2012a.

ASTM C143 2012, Standard test method for slump of hydraulic-cement concrete, in: A. International (Ed.), ASTM International, West Conshohocken, PA, 2015.

ASTM C143, Standard test method for slump of hydraulic-cement concrete, in: A. International (Ed.), ASTM International, West Conshohocken, PA, 2012.

ASTM C150, Standard Specification for Portland Cement, in: ASTM International (Ed.), West Conshocken, Pennsylvania, 2011.

ASTM C157, Standard test method for length change of hardened hydraulic-cment mortar and concrete, in: A. International (Ed.), ASTM International, West Conshohocken, PA, 2008.

ASTM C231, Standard test method for air content of freshly mixed concrete by the pressure method, in: A. International (Ed.), ASTM International, West Conshohocken, PA, 2010.

ASTM C469, Standard test method for static modulus of elasticity and Poisson's ratio of concrete in compression, in: A. International (Ed.), ASTM International, West Conshohocken, PA, 2010.

ASTM C494, Standard specification for chemical admixtures for concrete, in: A. International (Ed.), ASTM International, West Conshohocken, PA, 2013.

ASTM C496, Standard test method for splitting tensile strength of cylindrical concrete specimens, in: A. International (Ed.), ASTM International, West Conshohocken, PA, 2011.

ASTM C1017, Standard specification for chemical admixtures for use in producing flowing concrete, in: A. International (Ed.), ASTM International, West Conshohocken, PA, 2013.

ASTM C1581, Standard test method for determining age at cracking and induced tensile stress characteristics of mortar and concrete under restrained shrinkage, in: A. International (Ed.), ASTM International, West Conshohocken, PA, 2009.

ASTM C 109 2013, Standard test method for compressive strength of hydraulic cement mortars (using 2-in. or [50-mm] cube specimens, in: A. International (Ed.), ASTM International, West Conshohocken, PA, 2015.

ASTM C 127 2015, Standard test method for relative density (specific gravity) and absorption capacity of coarse aggregate, in: A. International (Ed.), ASTM International, West Conshohocken, PA, 2015.

ASTM C 128 2015, Standard test method for relative density (specific gravity) and absorption of fine aggregate, in: A. International (Ed.), ASTM International, West Conshohocken, PA, 2015.

ASTM C 136 2014, Standard test method for sieve analysis of fine and coarse aggregates, in: A. International (Ed.), ASTM International, West Conshohocken, PA, 2015.

ASTM C 138 2014, Standard test method for density (unit weight), yield, and air content (gravimetric) of concrete, in: A. International (Ed.), ASTM International, West Conshohocken, PA, 2015.

ASTM C 157 2008 (2014e1), Standard test method for length change of hardened hydraulic-cment mortar and concrete, in: A. International (Ed.), ASTM International, West Conshohocken, PA, 2015.

ASTM C 192 2014, Standard practice for making and curing concrete test specimens in the laboratory, in: A. International (Ed.), ASTM International, West Conshohocken, PA, 2015.

ASTM C 305 2014, Standard practice for mechanical mixing of hydraulic cement pastes and mortars of plastic consistency, in: ASTM International (Ed.), ASTM International, West Conshocken, PA, 2015.

ASTM C 403 2008, Standard test method for time of setting of concrete mixtures by penetration resistance, in: ASTM International (Ed.), ASTM International, West Conshocken, Pennsylvania, 2015.

ASTM C 469 2014, Standard test method for static modulus of elasticity and poisson's ratio of concrete in compression, in: A. International (Ed.), ASTM International, West Conshohocken, PA, 2015.

ASTM C 496 - 2011, Standard test method for splitting tensile strength of cylindrical concrete specimens, in: A. International (Ed.), ASTM International, West Conshohocken, PA, 2015.

ASTM International, Form and style for ASTM Standards, ASTM International, West Conshohocken, PA, 2015.

ASTM Standard C31, Standard practice for making and curing concrete test specimens in the field, in: ASTM International (Ed.), ASTM International, West Conshohocken, PA, 2012.

ASTM Standard C1608 2012, Standard test method for chemical shrinkage of hydraulic cement paste, in: ASTM International (Ed.), West Conshohocken, PA, 2013.

ASTM Standard C 125 2014, Standard terminology relating to concrete and concrete aggregates, in: A. International (Ed.), ASTM International, West Conshohocken, PA, 2014.

ASTM Standard C 136, 2006, Standard test method for sieve analysis of fine and coarse aggregates, in: A. International (Ed.), West Conshohocken, PA, 2014.

ASTM Standard E691 2014, Standard Practice for Conducting an Interlaboratory Study to Determine the Precision of a Test Method, in: A. International (Ed.), West Conshohocken, PA, 2015.

ASTM C109-11b, ASTM C109-11b: Standard test method for compressive strength of hydraulic cement mortars (using 2 in. or [50mm] cube specimens), in: ASTM International (Ed.) ASTM C109-11b, ASTM International, West Conshocken, Pennsylvania, 2011, pp. 10.

J.M. Auvray, H. Fryda, C. Zetterstrom, C. Wohrmeye, C. Parr, Hydration and properties of calcium magnesium aluminate cement, in: C. Fentiman, R. Mangabhai, K. Scrivener (Eds.) International Conference on Calcium Aluminate Cements, IHS BRE Press, Avignon, FR, 2014, pp. 130-139.

A. Bachiorrini, L. Cussino, Alumina cement hydration in pure water and in sulfate solution in the presence of siliceous or calcareous aggregate, in: 8th International Congress on the Cement of Chemistry, Rio de Janeiro, Brazil, 1986, pp. 383-388.

A. Bachiorrini, L. Montanaro, A. Delmastro, Microstructural disorder and calcium carbonate reactivity with monocalcium aluminate during hydration, Materials chemistry and physics, 14 (1986) 41-46.

P. Barret, D. Bertrandie, Minimum instability curve in metastable solution of CA, in: 7th International Conference on Cement Chemistry, Paris, 1980.

P. Barret, D. Bertrandie, Hydration of Aluminate Cements, in: M.W. Grutzeck, S.L. Sarkar (Eds.) Advances in Cement and Concrete, American Society of Civil Engineers, University of New Hampshire, Durham, NH, 1994, pp. 132-174.

J.P. Bayoux, J.P. Letourneux, S. Marcdargent, M. Vershaeve, Acidic corrosion of high alumina cement, in: R.J. Mangabhai (Ed.) International Symposium on Calcium Aluminate Cements, E. & F. N. Spon, London, UK, 2014, pp. 230-240.

A. Bentivegna, Multi-scale characterization, implementation, and monitoring of calcium aluminate cement based systems, in: Civil Engineering, University of Texas at Austin, Austin, Texas, 2012.

G. Bernardo, A. Telesca, G.L. Valenti, A porosimetric study of calcium sulfoaluminate cement pastes cured at early ages, Cement and Concrete Research, 36 (2006) 1042-1047.

M. Bittelli, G.S. Campbell, M. Flury, Characterization of Particle-Size Distribution in Soils with a Fragmentation Model, Soil Sci Soc Am J, 63 (1999) 782-788.

J. Bizzozero, Hydration and dimensional stability of calcium aluminate cement based systems, in: Materials Science and Engineering, Ecole Polytechnique Federal de Lausanne, Lausanne, Switzerland, 2014.

P. Boch, S. Masse, N. Lequeux, CAC in refractory applications: from LCCs to ZCCs, in: R.J. Mangabhai, F.P. Glasser (Eds.) International Conference on Calcium Aluminate Cements, IOM Communications, Edinburgh, UK, 2001.

A.D. Buck, Recycled concrete as a source of aggregate, ACI Journal, 74 (1977) 212-219.

A. Buhr, D. Schmidtmeier, G. Wams, S. Kuiper, S. Klaus, Testing of calcium aluminate cement bonded castables and influence of curing conditions on the strength development, in: C. Fentiman, R. Mangabhai, K. Scrivener (Eds.) International Conference on Calcium Aluminate Cements, IHS BRE Press, Avignon, FR, 2014, pp. 437-449.

J.W. Bullard, H.M. Jennings, R.A. Livingston, A. Nonat, G.W. Scherer, J.S. Schweitzer, K.L. Scrivener, J.J. Thomas, Mechanisms of Cement Hydration, Cement and Concrete Research, 41 (2011) 1208-1223.

J.L. Burati, R.M. Weed, C.S. Hughes, H.S. Hill, Optimal procedures for quality assurance specifications, in, Federal Highway Administration, McLean, VA, 2003.

S.M. Bushnell-Watson, On the Cause of the Anomalous Setting Behaviour With Respect to Temperature of Calcum Aluminate Cements, Cement and Concrete Research, 20 (1990) 677-686.

S.M. Bushnell-Watson, J. Sharp, The effect of temperature upon the setting behavior of refractory calcium aluminate cements, Cement and Concrete Research, 16 (1986) 875-884.

S.M. Bushnell-Watson, J.H. Sharp, Further studies of the effect of temperature upon the setting behavior of refractory calcium aluminate cements, cement and Concrete Research, 20 (1990) 623-635.

S.M. Bushnell-Watson, J.H. Sharp, On the cause of the anomalous setting bahavior with respect to temperature of calcium aluminate cement, Cement and Concrete Research, 20 (1990).

S.M. Bushnell-Watson, J.H. Sharp, The application of thermal analysis to the hydration of conversion reactions of calcium aluminate cements, Materiales De Construccion, 42 (1992) 13-32.

CAN/CSA-A23.2-2a-14, Sieve analysis of fine and coarse aggregate, in: C.S. Association (Ed.), Canadian Standards Association, Toronto, Canada, 2014.

A. Capmas, D. Ménétrier-Sorrentino, D. Damidot, Effect of temperature on setting time of calcium aluminate cements, in: R.J. Mangbhai (Ed.) International Symposium on Calcium Aluminate Cements, E & F N Spon, London, 1990, pp. 65-80.

E.T. Carlson, H.A. Berman, Some observations on the calcium aluminate carbonate hydrates, Journal of Research of the National Bureau of Standards, 64 (1960) 333-341.

J.O. Castano-Tabares, A. Domingo-Cabo, C. Lazaro, F. Lopez-Gayarre, P. Serna, M.A. Serrano-Lopez, Creep and shrinkage of recycled aggregate concrete, in: Constr Build Mater, 2009, pp. 2545+.

I.N. Chakraborty, S. Narayanan, D. Venkateswaran, S.K. Biswas, A.K. Chatterjee, Effect of morphology on the hydration characteristics of high alumina cements, in: R.J. Mangabhai (Ed.) International Symposium on Calcium Alumiante Cements, E. & F. N. Spon, London, 1990, pp. 17-26.

S. Chatterji, A discussion of the paper "Mercury porosimetry—an inappropriate method for the measurement of pore size distributions in cement-based materials" by S. Diamond, Cement and Concrete Research, 31 (2001) 1657-1658.

I.A. Chen, C.W. Hargis, M.C.G. Juenger, Understanding expansion in calcium sulfoalumiate-belite cements, Cement and Concrete Research, 42 (2012) 51-60.

T. Chotard, J. Barthelemy, A. Smith, N. Gimet-Breart, M. Huger, D. Fargeot, C. Gault, Acoustic emission monitoring of calcium aluminate cement setting at the early age, Journal of materials science letters, 20 (2001) 667-669.

T. Chotard, N. Gimet-Breart, A. Smith, D. Fargeot, J.P. Bonnet, C. Gault, Application of ultrasonic testing to describe the hydration of calcium aluminate cement at the early age, Cement and Concrete Research, 31 (2001) 405-412.

Concrete Society Technical Report, Calcium Aluminate Cements in Construction: A Reassessment, in, Concrete Society, 1997, pp. 63.

R.A. Cook, K.C. Hover, Mercury porosimetry of hardened cement pastes, Cement and Concrete Research, 29 (1999) 933-943.

W.A. Cordon, H.A. Gillespie, Variables in concrete aggregates and portland cement paste which influence the strength of concrete, Journal Proceedings of the American Concrete Institute, 60 (1963) 1029-1052.

V. Corinaldesi, G. Moriconi, Evaluation of recycled aggregate concrete cracking through ring test, Applied Mechanics and Materials, 174-177 (2012) 1475-1480.

N.J. Crammond, Long-term performance of high alumina cement concrete in sulphate-bearing environments, in: R.J. Mangabhai (Ed.) International Symposium on Calcium Aluminate Cements, Spon Press, London, UK, 1990, pp. 208-221.

L. Cussino, A. Negro, Hydration du ciment alumineux en présence d'agrégat siliceux et calcaire, in: 7th International Congress on the Chemistry of Cement, Paris, 1980.

H.H.M. Darweesh, Limestone as an accelerator and filler in limestone-substituted alumina cement, Ceramics international, 30 (2004) 145-150.

D. Darwin, J. Browning, W. Lindquist, H. McLeod, J. Yuan, M. Toledo, D. Reynolds, Low-cracking, high-performance concrete bridge decks, Transportation Research Record: Journal of the Transportation Research Board, 2202 (2010) 61-69.

M.B. de Oliveira, E. Vazquez, The influence of retained moisture in aggregates from recycling on the properties of new hardened concrete, Waste Management, 16 (1996) 113-117.

P. de Vries, Concrete recycled: Crushed concrete as aggregate, Concrete, 27 (1993) 9-13.

S. Diamond, Mercury porosimetry: An inappropriate method for the measurement of pore size distributions in cement-based materials, Cement and Concrete Research, 30 (2000) 1517-1525.

A. Dunster, I. Holton, A laboratory study of ther esistance of CAC concretes to chemical attack by sulphate and alkali carbonate solutions. , in: R.J. Mangabhai, F.P. Glasser (Eds.) International Conference on Calcium Aluminate Cements, IOM Communications, Edinburgh, UK, 2001, pp. 333-348.

M. Eglinton, Resistance of concrete to destructive agencies, in: P.C. Hewlett (Ed.) Lea's Chemistry of Cement and Concrete, Elsevier, Oxford, UK, 1998.

European Committee for Standardization, Calcium aluminate cement - Composition, specifications, and conformity criteria, in: EN 14647, European Committee for Standardization, Brussels, 2005.

G. Fathifazl, A. Abbas, A. Razaqpur, O. Isgor, B. Fournier, S. Foo, New mix design method for recycled aggregate concrete, ASCE Materials Journal, 21 (2009) 601-611.

G. Fathifazl, A. Razaqpur, O.B. Isgor, A. Abbas, B. Fournier, S. Foo, Flexural performance of steel-reinforced recycled concrete beams, ACI Structural Journal, 106 (2009).

G. Fathifazl, A. Razaqpur, O.B. Isgor, A. Abbas, B. Fournier, S. Foo, Shear strength of reinforced recycled concrete beams with stirrups, Mag Concr Res, 62 (2010) 685-699.

G. Fathifazl, A.G. Razaqpur, O.B. Isgor, A. Abbas, B. Fournier, S. Foo, Bond performance of deformed steel bars in concrete produced with coarse recycled concrete aggregate, Canadian Journal of Civil Engineering, 39 (2012) 128-139.

C.H. Fentiman, Hydration of carbo-aluminous cement at different temperatures, Cement and concrete Research, 15 (1985) 622-630.

K. Folliard, C. Smith, G. Sellers, M. Brown, J.E. Breen, Evaluation of Alternative Materials to Control Drying-Shrinkage Cracking in Concrete Bridge Decks, in, Report No. FHWA/TX-04/0-4098-4, , 2003.

K.J. Folliard, M.D.A. Thomas, B. Fournier, K.E. Kurtis, J.H. Ideker, Interim recommendations for the use of lithium to mitigate or prevent alkali-silica reaction (ASR), in: U. S. Department of Transportation: Federal Highway Association (Ed.), U.S. DoT, McLean, Virginia, USA, 2006.

J. Foster, V. Cervantes, Personal Communication about Source of Airfield Pavement RCA, in: J.H. Ideker (Ed.), 2013.

S. Froundistou-Yannis, Waste concrete as aggregate for new concrete, ACI Journal, 74 (1977) 373-376.

H. Fryda, C. Alt, Conversations with a CAC cement manufacturer, in: M.P. Adams (Ed.), 2013.

H. Fryda, E. Charpentier, J.M. Bertino, Accelerated test for conversion of calcium aluminate cement concrete, in: C.H. Fentiman, R.J. Mangabhai, K.L. Scrivener (Eds.) Calcium Aluminate Cements: The Centenary Conference, IHS BRE Press, Avignon, FR, 2008.

H. Fryda, K.L. Scrivener, G. Chanvillard, C. Feron, Relevance of Laboratory Tests to Field Applications of Calcium Aluminate Cement Concretes, in: International Conference on Calcium Aluminate Cements (CAC), IOM Communications, Heriot-Watt University, Edinburgh, Scotland, UK, 2001, pp. 215-247.

T. Fu, Autogenous deformation and chemical shrinkage of high performance cementitious systems, in: School of Civil and Construction Engineering, Oregon State University, Corvallis, OR, 2011.

T. Fu, Shrinkage study of high performance concrete for bridge decks, in: School of Civil and Construction Engineering, Oregon State University, Corvallis, OR, 2013.

T. Fu, T. Deboodt, J.H. Ideker, Simple procedure for determining long-term chemical shrinkage for cementitious systems using improved standard chemical shrinkage test, J Mater Civ Eng, 24 (2012) 989 - 995.

M.T. Gaztanaga, S. Goni, A. Guerrero, Accelerated carbonation of calcium aluminate cement pastes, in: R.J. Mangabhai, F.P. Glasser (Eds.) International Conference on Calcium Aluminate Cements, IOM Communications, Edinburgh, UK, 2001.

M.T. Gaztanaga, S. Goni, J.L. Sagrera, Reactivity of high-alumina cement in water: pore solution and solid phase characterization, Solid State Ionic, 63 (1993) 797-802.

C.M. George, Aluminous cements, in: 7th International Congress on the Chemistry of Cement, Paris, France, 1980.

C.M. George, Manufacture and performance of aluminous cement, in: R.J. Mangabhai (Ed.) Calcium Aluminate Cements, E. & F.N. Spon, London, UK, 1990, pp. 181-207.

C.M. George, Manufacture and performance of aluminous cement: a new perspective, in: R.J. Mangabhai (Ed.) International Symposium on Calcium Aluminate Cements, E&FN Spon, London, UK, 1990, pp. 181-207.

W. Gessner, S. Moehmel, T.A. Bier, Effects of the aluminat quality on hydration and thermal bahviour of calcium aluminate/alumina mixes, in: R.J. Mangabhai, F.P. Glasser (Eds.) International Conference on Calcium Aluminate Cements (CAC), IOM Communications Ltd., Edinburgh, Scotland, 2001, pp. 291-301.

W. Gessner, S. Mohmel, J. Kieser, M. Hawecker, Investigations of the composition of phases formed in low cement castables during hydration and after thermal treatment, in: R.J. Mangabhai (Ed.) International Symposium on Calcium Aluminate Cements, E & F. N. Spon, London, UK, 1990, pp. 52-64.

F. Goetz-Neunhoeffer, S.R. Klaus, J. Neubauer, Kinetics of CA and CA_2 dissolution by QXRD and corresponding enthalpies of reactions, in: C. Fentiman, R. Mangabhai, K. Scrivener (Eds.) International Conference on Calcium Aluminate Cements, IHS BRE, Avignon, FR, 2014, pp. 54-64.

J.M.F. Gomez-Soberon, Creep of concrete with substitution of normal aggregate by recycled concrete aggregate, ACI Special Publication, 209 (2002) 461-474.

J.M.V. Gomez-Soberon, Relationship between gas adsorption and the shrinkage and creep of recycled aggregate concrete, Cement Concrete Aggr, 25 (2003) 42-48.

C. Gosselin, Microstructural development of calcium aluminate cement based systems with and without supplementary cementitious materials, in: Faculte Sciences and Techniques de l'Ingenieur, Ecole Polytechnique Federale de Lausanne, Lausanne, Switzerland, 2008.

C. Gosselin, Microstructural development of calcium aluminate cement based systems with and without supplementary cementitious materials, in: Faculte sciences et techniques de l'ingenieur, Ecole Polytechniqe Federale de Lausanne, Lausanne, CH, 2009.

C. Gosselin, E. Gallucci, K. Scrivener, Influence of self heating and Li_2SO_4 addition on the microstructural development of calcium aluminate cement, Cement and Concrete Research, 40 (2010) 1555-1570.

C. Gosselin, K.L. Scrivener, Microstructure development of calcium alumiante cements accelerated by lithuium sulphate, in: C.H. Fentiman, R.J. Mangabhai, K.L. Scrivener (Eds.) Centenary Conference on Calcium Aluminate Cements, IHS BRE Press, Avignon, 2008, pp. 109-122.

A. Goyns, Calcium aluminate cement linings for cost-effective sewers, in: R.J. Mangabhai, F.P. Glasser (Eds.) International Conference on Calcium Aluminate Cements, IOM Communications, Edinburgh, UK, 2001, pp. 617-631.

A.M. Goyns, M.G. Alexander, Performance of various concretes in the Virginia experimental sewer over 20 years, in: C. Fentiman, R. Mangabhai, K. Scrivener (Eds.) International Conference on Calcium Aluminate Cements, IHS BRE Press, Avignon, FR, 2014, pp. 573-584.

T. Hansen, Recycled aggregates and recycled aggregate concrete second state-of-the-art report developments 1945–1985, Materials and Structures, 19 (1986) 201-246.

T.C. Hansen, Recycling of demolished concrete and masonry, in: Report of Technical Committee 37-DRC Demolition and Reuse of Concrete, Part 1, E&FN Spon, London, 1992, pp. 160.

R. Harebron, A general description of flow-applied floor screeds - An important application for complex formulations based on CAC, in: R.J. Mangabhai, F.P. Glasser (Eds.) International Conference on Calcium Aluminate Cements, IOM Communications, Edinburgh, Scotland, 2001, pp. 597-604.

J. Herisson, M. Gueguen-Minerbe, T. Chaussadent, E.D.v. Hullesbusch, Development of a reproducible, representative and accelerated biogenic corrosion test to deliver durable structures in sewer networks, in: C. Fentiman, R. Mangabhai, K. Scrivener (Eds.) International Conference on Calcium Aluminate Cements, IHS BRE Press, Avignon, FR, 2014, pp. 645-658.

J. Herisson, E.D.v. Hullebusch, M. Gueguen-Minerbe, T. Chaussadent, Biogenic corrosion mechanism: study of parameters explaining calcium alumiante cement durability, in: C. Fentiman, R. Mangabhai, K. Scrivener (Eds.) International Conference on Calcium Aluminate Cements, IHS BRE Press, Avignon, FR, 2014, pp. 621-659.

R.C. Hibbeler, Mechanics of Materials, Fifth ed., Prentice Hall Pearson Education, Inc., Upper Saddle River, NJ, USA, 2003.

A. Hidalgo, S. Petit, J.L. García, C. Alonso, C. Andrade, Microstructure of the system calcium aluminate cement-silica fume: application in waste immobilization, in: Z.G.J.C. Ruren Xu, Y. Wenfu (Eds.) Studies in Surface Science and Catalysis, Elsevier, 2007, pp. 1617-1628.

T.T.C. Hsu, Mathematical analysis of shrinakge stresses in a model of hardened concrete, Journal Proceedings of the American Concrete Institute, 60 (1963) 371-390.

T.T.C. Hsu, F.O. Slate, Tensile Bond Strength Between Aggregate and Cement Paste or Mortar, Journal Proceedings of the American Concrete Institute, 60 (1963) 465-486.

T.T.C. Hsu, F.O. Slate, G.M. Sturman, G. Winter, Microcracking of plain concrete and the shape of the stress-strain curve, Journal Proceedings of the American Concrete Institute, 60 (1963) 209-224.

J.H. Ideker, Early-age behavior of Calcium Aluminate Cement Systems, in: Civil Engineering, The University of Texas at Austin, Austin, TX, 2008.

J.H. Ideker, K.J. Folliard, M.D.A. Thomas, Early-age properties of calcium aluminate cement concrete with rigid cracking and free shrinkage frames: isothermal testing, in: C. Fentiman, R. Mangabhai, K. Scrivener (Eds.) Calcium Aluminate Cements: The Centenary Conference, IHS BRE Press, Avignon, FR, 2008.

J.H. Ideker, T. Fu, T. Deboodt, Development of shrinkage limits and testing protocols for ODOT high performance concrete - Final report, in, Oregon Department of Transportation, Salem, OR, 2013.

J.H. Ideker, J.E. Tanner, M.P. Adams, A. Jones, Durability asessment of recycled concrete aggregates for use in new concrete - Phase II Report, in, Oregon Transportation and Education Consortium, Portland, OR, 2014, pp. 98.

F. Indelicato, On the correlation between porosity and strength in high-alumina cement mortars, Materials and Structures, 23 (1990) 289-295.

J. H. Sharp, S.M. Bushnell-Watson, D. R. Payne, P.A. Ward, The effect of admixtures on the hydration of refractory calcium aluminate cements, in: R.J. Mangabhai (Ed.) International Symposium on Calcium Aluminate Cements, E. & F. N. Spon, London, UK, 1990, pp. 127-141.

O. Jensen, P.F. Hansen, Autogenous deformation and change of relative humidity in silica fume modified cement paste, ACI materials Journal, 28 (1996) 539-543.

H. Jeong, Processing and properties of recycled aggregate concrete, in: Civil Engineering, University of Illinois at Urbana-Champagne, Urbana, Illinois, 2011.

M.C.G. Juenger, F. Winnefeld, J.L. Provis, J.H. Ideker, Advances in alternative cementitious binders, Cement and Concrete Research, 41 (2011) 1232-1243.

P. Juilland, E. Gallucci, R. Flatt, K. Scrivener, Dissolution theory applied to the induction period in alite hydration, Cement and Concrete Research, 40 (2010) 831-844.

H. Justnes, Rapid repair of airfield runway in cold weather using CAC mortar, in: C. Fentiman, R. Mangabhai, K. Scrivener (Eds.) Calcium Aluminate Cements: The Centenary Conference, IHS BRE Press, Avignon, FR, 2008.

J. Kasper, O. Krause, Mixing optimization of an alumina based LC-castable by applying ariable power inputs, in: C. Fentiman, R. Mangabhai, K. Scrivener (Eds.) International Conference on Calcium Aluminate Cements, IHS BRE Press, Avignon, FR, 2014, pp. 450-456.

S. Kennedy, R. Detwiler, J. Bickley, M. Thomas, Results of an interlaboratory test program: compressive strength of concrete, Cement, Concrete, and Aggregates, 17 (1995) 3-10.

J.M. Khatib, Properties of concrete incorporating fine recycled aggregate, Cement and Concrete Research, 35 (2005) 763-769.

G.F. Kheder, S.A. Al-Windaw, Variation in mechanical properties of natural and recycled aggregate concrete as related to the strength of their binding mortar, Materials and Structures, 38 (2005) 701-709.

M. Kikuchi, T. Miura, Y. Dosho, M. Narikawa, Application of recycled aggregate concrete for structural concrete. Part 1- experimental study on the quality of recycled aggregate and recycled aggregate concrete, in: R.K. Dhir, N.A. Henderson, M.C. Limbachiya (Eds.) Sustainable construction: use of recycled concrete aggregate, Thomas Telford, London, UK, 1998, pp. 55-68.

T. Kikuchi, E. Horiuchi, An experimental study on recycling concrete by using high quality recycled coarse aggregates, Mem Fac Eng, Osaka City University, 44 (2003) 37-33.

O. Kirca, I. Yaman, M. Tokyay, Strength Development of Calcium Aluminate Cement Blends at Different Temperatures, in: C. Fentiman, R.J. Mangabhai, K.L. Scrivener (Eds.) Calcium Aluminate Cements Proceedings of the Centenary Conference, IHS BRE Press, Palais des Papes, Avignon, France, 2008, pp. 487-499.

S. Klaus, J. Neubauer, F. Goetz-Neunhoeffer, Hydration kinetics of CA_2 and CA—Investigations performed on a synthetic calcium aluminate cement, Cement and Concrete Research, 43 (2013) 62-69.

S.R. Klaus, J. Neubauer, F. Goetz-Neunhoeffer, How to increase the hydration degree of CA - the influence of CA particle fineness, Cement and Concrete Research, 67 (2015) 11-20.

S.R. Klaus, J. Neubauer, F. Goetz-Neunhoeffer, B. A, D. Schmidtmeier, Application of heat flow calculation to synthetic calcium aluminate cement mixes, in: C. Fentiman, R. Mangabhai, K. Scrivener (Eds.) International Conference on Calcium Aluminate Cements, IHS BRE, Avignon, FR, 2014, pp. 65-74.

S.H. Kosmatka, M.L. Wilson, Design and control of concrete mixtures, 14 ed., Portland Cement Association, Skokie, Illinois, 2011.

S.-C. Kou, C.-S. Poon, M. Etxeberria, Influence of recycled aggregates on long term mechanical properties and pore size distribution of concrete, Cement and Concrete Composites, 33 (2011) 286-291.

H.-J. Kuzel, H. Baier, Hydration of calcium aluminate cements in the presence of calcium carbonate, European Journal of Mineralogy, 8 (1996) 129-141.

V. Lamour, P. Monteiro, K. Scrivener, H. Fryda, Mechanical properties of calcium aluminate cement concretes, in: International conference on calcium aluminate cements, 2001, pp. 199-213.

V.H.R. Lamour, P.J.M. Monteiro, K.L. Scrivener, H. Fryda, Microscopic studies of the early hydration of calcium aluminate cements, in: R.J. Mangabhai, F.P. Glasser (Eds.) International Conference on Calcium Aluminate Cements (CAC), IOM Communications, Edinburgh, Scotland, 2001, pp. 169-180.

M.P. Lavigne, J.N. Foussard, A. Cockx, E. Paul, A. Bertron, G. Escadeillas, A new method for evaluation of cement-based material resistance against biogenic attacks in sewer-like environments:

comparison between CAC and BFSC linings, in: C. Fentiman, R. Mangabhai, K. Scrivener (Eds.) International Conference on Calcium Aluminate Cements, IHS BRE Press, Avignon, FR, 2014, pp. 621-633.

M.C. Limbachiya, T. Leelawat, R.K. Dhir, Use of recycled concrete aggregate in high-strength concrete, Materials and Structures, 33 (2000) 574-580.

B. Lothenbach, T. Matschei, G. Moschner, F.P. Glasser, Thermodynamic modelling of the effect of temperature on the hydration and porosity of Portland cement, Cement and Concrete Research, 38 (2008) 1-18.

P. Lura, Autogenous deformation and internal curing of concrete, in: DUP Science, Delft University, Delft, NL, 2003.

P. Lura, K.v. Breugel, I. Maruyama, Effect of curing temperature and type of cement on early-age shrinkage of high-performance concrete, Cement and Concrete Research, 2001 (2001) 1967-1872.

A.P. Luz, V.C. Pandolfelli, $CaCO_3$ addition effect on the hydration and mechanical strength evolution of calcium aluminate cement for endodontic applications, Ceramics International, 38 (2012) 1417-1425.

D. Madej, J. Szczerba, W. Kagan, Investigations on the hydratable compounds in the CaO-Al_2O_3-ZrO_2 system, in: C. Fentiman, R. Mangabhai, K. Scrivener (Eds.) International Conference on Calcium Aluminate Cements, IHS BRE Press, Avignon, FR, 2014, pp. 140-149.

S. Mandal, S. Chakraborty, A. Gupta, Some studies on durability of recycled aggregate concrete, The Indian Concrete Journal, 76 (2002) 385-388.

M.S. Maruyama, T. Sogabe, R. Sato, K. Kawai, Flexural properties of reinforced recycled concrete beams, in: Conference on the Use of Recycled Materials in Building and Structures, RILEM Publications SARL, Bagneux, France, 2004, pp. 610-618.

T. Matschei, Thermodynamics of Cement Hydration, in: Department of Chemistry, University of Aberdeen, 2007, pp. 222.

T. Matschei, B. Lothenbach, F.P. Glasser, The role of calcium carbonate in cement hydration, Cement and Concrete Research, 37 (2007) 551-558.

T. Matschei, B. Lothenbach, F.P. Glasser, Thermodynamic properties of Portland cement hydrates in the system CaO-Al_2O_3-SiO_2-$CaSO_4$-$CaCO_3$-H_2O, Cement and Concrete Research, 37 (2007) 1379-1410.

T. Matusinović, J. Šipušić, N. Vrbos, Porosity–strength relation in calcium aluminate cement pastes, Cement and concrete research, 33 (2003) 1801-1806.

P.K. Mehta, Reducing the environmental impact of concrete, in: Concrete International, American Concrete Institute, ACI, 2001, pp. 61-66.

P.K. Mehta, P.J.M. Monteiro, Concrete: microstructure, properties, and materials, 3 ed., McGraw-Hill, New York, 2006.

P.K. Mehta, P.J.M. Monteiro, Dimensional stability, in: Concrete: Microstructure, properties, and materials, McGraw Hill, New York, 2006, pp. 85-120.

H. Midgley, Measurement of high-alumina cement-calcium carbonate reactions using DTA, Clay Minerals, 19 (1984) 857-864.

H.G. Midgley, High alumina cement in construction - A future based on experience, in: R.J. Mangabhai (Ed.) International Symposium on Calcium Aluminate Cements, E & F. N. Spon, London, 1990, pp. 1-13.

H.G. Midgley, A. Midgley, The conversion of high alumina cement, Mag Concr Res, 27 (1975) 59-77.

S. Mindess, J.F. Young, D. Darwin, Concrete, 2 ed., Pearson Education, Inc., Upper Saddle River, NJ, 2003.

N. Motsieloa, M.G. Alexander, H. Beushausen, Acid resistance of calcium alumiante cement concrete blended with supplementary cementitious materials for application in sewer pipes, in: C. Fentiman, R. Mangabhai, K. Scrivener (Eds.) International Conference on Calcium Aluminate Cements, IHS BRE Press, Avignon, FR, 2014, pp. 608-320.

A. Muller, Conversion & résistance en compression des ciments aluminates de calcium, in: Department Genie Civil, Universite Laval, Quebec City, 2010.

A. Muller, Conversion & résistance en compression des ciments cT a lu m in a tes de calcium, in: DEPARTEMENT GENIE CIVIL, UNIVERSITE LAVAL, Quebec City, 2010.

A. Negro, A. Bachiorrini, M. Murat, Interaction, in aqueous medium, between calcium carbonate and monocalcium aluminate at 5°C, 20°C, and 40°C, Bulletin de minéralogie, 105 (1982) 284-290.

A.M. Neville, Aggregate Bond and Modulus of Elasticity of Concrete, ACI Materials Journal, 94 (1994) 71-75.

S. Nishibayashi, K. Yamura, Mechanical properties and durability of concrete from recycled coarse aggregate prepared by crushing concrete, in: Proceedings of the second international symposium (RILEM) on Demolition and Reuse of Concrete and Masonry, Tokyo, Japan, 1988, pp. 643-651.

I. Odler, Calcium aluminate cement, in: Special Inorganic Cements, E & FN Spon, London, 2000, pp. 173-204.

A.K. Padmini, K. Ramamurthy, M.S. Mathews, Influence of parent concrete on the properties of recycled aggregate concrete, Constr Build Mater, 23 (2009) 829-836.

C. Parr, D. Verat, C. Wohrmeyer, J.P. Letourneux, High purity calcium aluminate binders for demanding high temperature applications, in: C. Fentiman, R. Mangabhai, K. Scrivener (Eds.) Centenary Conference on Calcium Alumiante Cements, IHS BRE Press, Avignon, FR, 2008.

W.G. Piasta, The Effect of Limestone Fillers on Sulphate Resistance of High Alumina Cement Compositers, in: R.J. Mangabhai (Ed.) Calcium Aluminate Cements, E. & F.N. Spon, London, UK, 1990, pp. 241-255.

P. Picariello, Fact vs. fiction: The truth about precision and bias, in: ASTM Standardization News, ASTM International, West Conshohocken< PA, 2000, pp. 16-19.

H. Pöllman, Calcium alumiante cements- Raw materials, differences, hydration and properties, in: M.A.T.M. Broekmans, H. Pöllmann (Eds.) Applied mineralogy of cement & concrete, The Mineralogical Society of Virginia, Chantilly, Virginia, USA, 2012, pp. 1-82.

T.C. Powers, Structure and physical properties of hardened portland cement paste, Journal of the American Ceramic Society, 41 (1958) 1-6.

P. Qiao, D. McLean, J. Zhuang, Mitigation strategies for early-age shrinkage cracking in bridge decks, in, Washington DOT, Olympia, WA, 2010.

A. Radlinska, B. Bucher, R. Henkensiefken, G. Sant, J. Weiss, Shrinkage mitigation strategies in cementitious systems: A closer look at differences in sealed and unsealed behavior, Transportation Research Record: Journal of the Transportation Research Board, 2070 (2008) 59-67.

S. Rashid, P. Barnes, J. Bensted, X. Turrillas, Conversion of calcium aluminate cement hydrates re-examined with synchrotron energy-dispersive diffraction, Journal of materials science letters, 13 (1994) 1232-1234.

S. Rashid, P. Barnes, X. Turrillas, The rapid conversion of calcium aluminate cement hydrates, as revealed by synchrotron energy-dispersive diffraction, Advances in Cement Research, 4 (1992) 61-67.

S. Rashid, X. Turrillas, Hydration kinetics of $CaAl_2O_4$ using synchrotron energy-dispersive diffraction, Thermochemica Acta, 302 (1997) 25-34.

R.S. Ravindrarajah, Effects of using recycled concrete as aggregate on the engineering properties of concrete, in: National Symposium on the Use of Recycled Materials in Engineering Construction: 1996, Barton, ACT: Institution of Engineers, Australia, Sydney, N.S.W., Australia, 1996, pp. 147-152.

A. Rettel, W. Gessner, D. Muller, G. Scheler, On the hydration of $CaAl_2O_4$ at various temperatures, Transactions and journal of the British Ceramic Society, 84 (1985) 25-28.

M. Roberts, The effect of utilising calcium aluminate cements in the development of self-smoothing cementitious floor, in: R.J. Mangabhai, F.P. Glasser (Eds.) International Conference on Calcium Aluminate Cements, IOM Communications, Edinburgh, Scotland, 2001, pp. 605-614.

T.D. Robson, High Alumina Cements and Concretes, John Wiley & Sons, Inc., New York, NY, 1962.

S.A. Rodger, D.D. Double, The chemistry of hydration of high alumina cement in the presence of accelerating and retarding admixtures, cement and Concrete Research, 14 (1984) 73-82.

K.K. Sagoe-Crentsil, T. Brown, A.H. Taylor, Performance of concrete made with commercially produced coarse recycled concrete aggregate, Cement and Concrete Research, 31 (2001) 707-712.

K.A. Sakata, T., Improvement of concrete with recycled aggregate, ACI Special Publication, 192 (2000) 1089-1108.

J. Sawkow, High alumina cements based on calcium aluminate clinker with different phase compositions and sintering degrees, in: R.J. Mangabhai (Ed.) International Symposium on Calcium Aluminate Cements, E & F. N. Spon, London, UK, 1990, pp. 27-38.

K.L. Scrivener, Historical and present day applications of calcium aluminate cements, in: R.J. Mangabhai, F.P. Glasser (Eds.) Proceedings of the International Conference on Calcium Aluminate Cements (CAC), IOM Communications, Heriot-Watt University, Edinburgh, Scotland, UK, 2001, pp. 3-23.

K.L. Scrivener, Calcium Aluminate Cements, in: J. Newman, B.S. Choo (Eds.) Advanced Concrete Technology, Butterworth-Heinemann, 2003, pp. 2-30.

K.L. Scrivener, 100 years of calcium aluminate cements, in: C.H. Fentiman, R.J. Mangabhai, K.L. Scrivener (Eds.) Calcium aluminate cements : Proceedings of the centenary conference, IHS BRE Press, Avignon, France, 2008, pp. 3-6.

K.L. Scrivener, J.-L. Cabiron, R. Letourneux, High-performance concretes from calcium aluminate cements, Cement and Concrete Research, 29 (1999) 1215-1223.

K.L. Scrivener, A. Capmas, Calcium Aluminate Cements, in: P.C. Hewitt (Ed.) Lea's Chemistry of Cement and Concrete, Elsevier - Butterworth-Heinemann, Oxford, UK, 1998, pp. 713-782.

K.L. Scrivener, A. Nonat, Hydration of cementitious materials, present and future, Cement and Concrete Research, 41 (2011) 651-665.

K.L. Scrivener, H.F.W. Taylor, Microstructural development in pastes of a calcium aluminate cement, in: R.J. Mangabhai (Ed.) International Symposium on Calcium Aluminate Cements, E. & F. N. Spon, London, 1990, pp. 41-51.

H.T. See, E.K. Attiogbe, M.A. Miltenberger, Potential for Restrained Shrinkage Cracking of Concrete and Mortar, Cement, Concrete and Aggregates, 26 (2004) 123-130.

F.O. Slate, S. Olseefski, X-Rays for study of internal structure and microcracking of concrete, Journal Proceedings of the American Concrete Institute, 60 (1963) 575-588.

F. Sorrentino, D. Damidot, Mineralogy of a 90 year old structure "Le Tunnel Des Valois", in: C.H. Fentiman, R.J. Mangabhai, K.L. Scrivener (Eds.) Calcium Aluminates: Proceedings of the International Conference, IHS BRE Press, Avignon, France, 2014, pp. 535-544.

C. Stancu, N. Angelescu, M. Muntean, The influence of mineralogical composition of high alumina cement on its physical-mechanical properties, in: C. Fentiman, R. Mangabhai, K. Scrivener (Eds.) International Conference on Calcium Aluminate Cements, IHS BRE Press, Avignon, FR, 2014, pp. 364-370.

T. Sugiyama, K. Tabara, M. Morioka, E. Sakai, The influence of water/poweder ratio on the resistance fo sulfuric acid on hardened calcium aluminate cement containing blast furnace slag, in: C. Fentiman, R. Mangabhai, K. Scrivener (Eds.) International Conference on Calcium Aluminate Cements, IHS BRE Press, Avignon, FR, 2014, pp. 600-607.

H.N. Tamura, J.; Ohashi, J.; Imamato, K., High quality recycled aggregate concrete (HiRAC) processed by decompression and rapid release, ACI Special Publication, 200 (2001) 491-502.

H.F.W. Taylor, Calcium aluminate, expansive and other cements, in: Cement Chemistry, Thomas Telford, London, 1997, pp. 295-322.

Texas Department of Transportation, TxDoT SS-4491 Class CAC Concrete, in, Texas Department of Transportation, Austin, TX, 2009.

B. Touzo, P.A. Andreani, Mineral composition of hydration of a $C_{12}A_7$ rich binder, in: C. Fentiman, R. Mangabhai, K. Scrivener (Eds.) Internation Conference on Calcium Aluminate Cements, IHS BRE, Avignon, FR, 2014, pp. 33-41.

F. Trivino, Aluminous cement: How to avoid degrading of mechanical resistance, in: 8th International Congress on the Chemistry of Cement, Rio de Janeiro, Brazil, 1986, pp. 417-422.

N. Ukrainczyk, T. Matusinović, Thermal properties of hydrating calcium aluminate cement pastes, Cement and Concrete Research, 40 (2010) 128-136.

M. Valix, A.W.H. Cheung, J. Sunarho, H. Bustamente, The impact of calcium aluminate cement and aggregates on conversion and on field performance in sewers, in: C. Fentiman, R. Mangabhai, K. Scrivener (Eds.) International Conference on Calcium Aluminate Cements, IHS BRE Press, Avignon, FR, 2014, pp. 585-599.

Various, Calcium Aluminate Cements: Proceedings of the International Symposium in London, England, E & F N Spon, London, 1990.

Various, Proceedings of the International Conference on Calcium Alumiante Cements in Edinburgh, Scotland, IOM Communications, 2001.

Various, Calcium aluminate cements: Proceedings of the centenary conference in Avignon, France, IHS BRE Press, London, England, 2008.

Various, Calcium Aluminates: Proceedings of the International Conference in Avignon France, IHS BRE Press, U. K. , 2014.

S. Wild, A discussion of the paper "Mercury porosimetry—an inappropriate method for the measurement of pore size distributions in cement-based materials" by S. Diamond, Cement and Concrete Research, 31 (2001) 1653-1654.

C.M. Williams, F. Garrott, Recycling/Reclaiming a savings spree: Chicago reuses to the max on famous shopping mile, in: Illinois Interchange, Illinois Department of Transportation, Springfield, IL, 2012.

F. Winnefeld, B. Lothenbach, Hydration of calcium sulfoaluminate cements — Experimental findings and thermodynamic modelling, Cement and Concrete Research, 40 (2010) 1239-1247.

J. Zhang, G.W. Scherer, Comparison of methods for arresting hydration of cement, Cement and Concrete Research, 41 (2011) 1024-1036.

Appendix A

Manuscript 5

Cracking Susceptibility of Concrete Made with Recycled Concrete Aggregates

Matthew P. Adams, Tengfei Fu, Adal Guerra Cabrera, Monica Morales, Jason H. Ideker, O. Burkan Isgor

This manuscript will be submitted to: Cement and Concrete Composites

A. Manuscript 5

Cracking Susceptibility of Concrete Made with Recycled Concrete Aggregates

Matthew P. Adams[1,2], Tengfei Fu[2], Adal Guerra Cabrera[2], Monica Morales[2], Jason H. Ideker[2], O. Burkan Isgor[2]

Abstract: This study tested the hypothesis that concrete produced with recycled concrete aggregate (RCA) has increased cracking resistance compared to concrete incorporating natural aggregates. Two sources of RCA were used: 1) a laboratory created RCA produced by crushing previously produced laboratory concrete; and 2) a field RCA obtained from a demolished airfield pavement. Mechanical properties, and shrinkage and cracking due to drying of concrete produced with RCA replacement were studied. Adequate compressive strength (39.3 to 43.4 MPa), splitting tensile strength (3.7 to 4.4 MPa), and modulus of elasticity (27.2 to 28.3 GPa) were obtained in mixtures including coarse RCA, even at 100% replacement levels. The use of RCA did not significantly increase the drying shrinkage of concrete. It was shown that the use of RCA significantly reduced the cracking risk of concrete from "high" to "moderate-high" when incorporated into a high cracking risk mixture.

Keywords: recycled concrete aggregate; aggregate; restrained cracking; drying shrinkage; sustainable construction; concrete.

[1] Corresponding Author: matthewpadams@gmail.com
[2] School of Civil and Construction Engineering, 101 Kearney Hall, Oregon State University, Corvallis, OR 97333

A.1 Introduction

Extraction of natural aggregates to produce concrete has considerable environmental consequences: it destroys the natural habitat of species and causes deforestation, top-soil erosion, and loss of water storage capacity of the ground [1]. Furthermore, mining, processing and transportation of natural aggregates contribute to greenhouse gas emissions [2]. There is a need to mitigate these environmental impacts by reducing the amount of natural aggregates used in concrete; the use of recycled concrete aggregates (RCA) obtained from demolished concrete as a replacement for natural aggregates is motivated partially by this demand. From an economic point of view, as usable natural aggregate supplies that are close to major construction activities diminish [2], there will be increasing demand for RCA to be used in new concrete because aggregates need not be hauled from remote locations but obtained locally.

Although concrete structures usually last for several decades, they are typically demolished at the end of their service lives. RCA is produced from demolished concrete structures and pavements. After demolition, the concrete is cleaned of contaminants such as steel, masonry, wood, and asphalt; and then sent to crushing facilities where it is reduced to the appropriate grading for engineering applications [3]. After the material is graded, it can be used as aggregate in new concrete, rip rap, road base or sub-base, and fills. RCA consists of two-phase particles that contain both the original natural aggregate and the residual mortar. The residual mortar is composed of both the original cement paste and the original fine natural aggregate [4-6].

The global concrete and masonry rubble production is estimated to be one billion tons per year [7]. However, only a small fraction of this waste is used in the construction of new structures despite the environmental and economic benefits of recycling [2]. This can be attributed to the lack of technical data, specifications, quality control, and quality assurance procedures for making and using concrete made with RCA. There is also a perception that RCA is inherently a lower quality material compared to natural aggregates. This perception mostly originated from early studies on RCA that have shown that concrete produced with RCA had smaller elastic modulus [8-13], and larger creep and shrinkage values [14-20] than similar concrete made with natural aggregates. However, more recent work has shown mechanical properties equaling or exceeding those of a similar natural aggregate concrete mixture can be obtained, through modifications to mixture design, while still maintaining sufficient workability in the fresh concrete [21-27].

Despite the increasing number of studies demonstrating the feasibility of using RCA in structural-grade concrete, in a recent survey of state Departments of Transportation [28], it was found that the use of RCA is still limited by a concern over the long-term durability of concrete made with the material. A paramount concern was the cracking susceptibility of concrete made with RCA, particularly as a result of drying shrinkage [28].

Drying shrinkage is the contraction of hardened concrete caused by the loss of capillary water to the surrounding environment [29]. Drying shrinkage will occur until the internal relative humidity of the cement paste reaches equilibrium with the atmospheric relative humidity. As water evaporates to the surrounding environment, vapor pressure decreases and tensile stress in the remaining water increases. This eventually results in a capillary tension large enough that can lead to shrinkage and residual tensile stresses throughout the entire paste matrix, which may lead to cracking. Many factors affect drying shrinkage of concrete. These factors include the type and fineness of cement, composition and fineness of supplementary cementing materials, type of aggregate, aggregate size, water to cement ratio (w/c), relative humidity, admixtures, duration of curing and the size of the concrete specimen [30].

Studies have shown that when using RCA as a replacement for coarse natural aggregate in concrete, an increase in drying shrinkage is typically observed [31-34]. However, more recently, it has been shown that higher levels of shrinkage did not necessarily correspond to higher stress levels nor higher cracking susceptibility in concrete containing recycled concrete aggregates [35, 36]. In these studies, the reduced cracking susceptibility of concrete produced with RCA has been ascribed to the lower modulus of elasticity of the concrete. The lower modulus of elasticity was attributed to the larger volume of mortar that existed in the RCA mixtures which contained the residual mortar from RCA and the new mortar in the concrete. However, this relationship has not been systematically investigated; the current study is motivated by the need to address this gap.

This investigation tested the hypothesis that unique properties of concrete produced with RCA due to the presence of residual mortar might provide increased cracking resistance during drying shrinkage. For this purpose, mechanical properties, drying shrinkage and cracking potential of concrete produced with different levels of RCA replacement were studied. The RCA used in this research came from different sources: one type was created in the laboratory by crushing previously produced concrete following Oregon DOT guidelines for typical concrete bridge decks; another type was field RCA

obtained from a demolished airfield pavement. The results were compared with those obtained from conventional concrete produced with two types of natural aggregates: rounded river gravel and crushed river gravel. The crushed natural aggregate mixture was also compared to the rounded aggregate mixture to investigate the effect of particle shape.

A.2 Materials and Methods

A.2.1 Materials

In this study four coarse aggregate types were used: rounded local natural gravel (Rounded), crushed natural river gravel (Crushed), and two recycled concrete aggregates (FLDRCA and LABRCA). Crushed natural aggregates were obtained by crushing the Rounded material that was larger than 19 mm. Siliceous river sand was used as the fine aggregate for all mixtures – no recycled fine aggregate was used in this study. Table A-1 presents aggregate names, aggregate source, absorption capacities, specific gravities, residual mortar contents (RMC), and a short description for each aggregate used.

Table A-1: Aggregate properties and descriptions

Aggregate Name	Aggregate Source	Absorption Capacity (%)	Specific Gravity	RMC (%)	Description
Rounded	Oregon natural river gravel	3.15	2.52	N/A	Rounded, siliceous river gravel.
Crushed	Oregon natural river gravel (crushed)	2.61	2.57	N/A	Crushed, angular siliceous river gravel.
FLDRCA	Demolished California airfield pavement	4.34	2.4	14.3	Recycled concrete aggregate that contains adhered mortar and rough, angular natural coarse aggregate. Source of original natural aggregate unknown.
LABRCA	Laboratory produced	5.71	2.24	19.2	Recycled concrete aggregate that contains adhered mortar and broken rounded gravel. Original natural aggregate is the control aggregate.
Fine Aggregate	Oregon natural river sand	3.08	2.41	N/A	Siliceous river sand.

The field-produced RCA, FLDRCA, was obtained from a demolished airfield pavement from Naval Base Ventura County, near Oxnard, California. The pavement was taken out of service due to deterioration from suspected, but unconfirmed, alkali-silica reaction. Information regarding the original concrete mixture design or concrete strength was unknown [37]. The possibility of ongoing alkali-silica reaction affecting results in this study was not a concern as conditions to which the concrete was exposed were below relative humidity thresholds that promote alkali-silica reaction [38]. The material was received from a crushing facility, free of contaminants in sizes ranging from below 100 μm to 25 mm. The material was separated into various sizes in the laboratory and then the large material was crushed down to 12.5 mm nominal maximum size aggregate and sorted into different sizes using 12.5 mm, 6.25 mm, 4.75 mm and 2.36 mm sieves.

The laboratory-produced RCA, LABRCA, was obtained from concrete with a w/cm of 0.37 and total cementitious materials content of 375 kg/m^3, containing 30% class F fly ash and 4% silica fume as mass replacement. The coarse and fine aggregate content were 1071 kg/m^3, and 659 kg/m^3, respectively. The coarse aggregate used in the original concrete mixture was the Rounded aggregate listed in Table A-1. The concrete was cast into large concrete discs 405 mm in diameter by 150 mm thick. The concrete discs were demolished between 90 and 180 days after casting. They were first demolished using a sledgehammer. Concrete pieces with a maximum cross section of 50 mm were then passed through a laboratory sized jaw crusher. The material was crushed to a 12.5 mm nominal maximum size aggregate and sorted into different sizes using 12.5 mm, 6.25 mm, 4.75 mm and 2.36 mm sieves.

The residual mortar content (RMC) of each source of RCA were obtained following the method developed by Abbas et al. [39]. The method comprises a combination of mechanical and chemical stresses that disintegrate the residual mortar and destroy the bond between the mortar and the original natural aggregates. The mechanical stresses are created through subjecting RCA to freeze-and-thaw action, while the chemical degradation is achieved through exposure of the RCA to a sodium sulfate solution. Figure A-1 illustrates the RMC values of individual aggregate sizes retained on 12.5 mm, 6.25 mm, 4.75 mm and 2.36 mm sieves and graded blend (following the gradation shown in Figure A-3) for both sources of RCA.

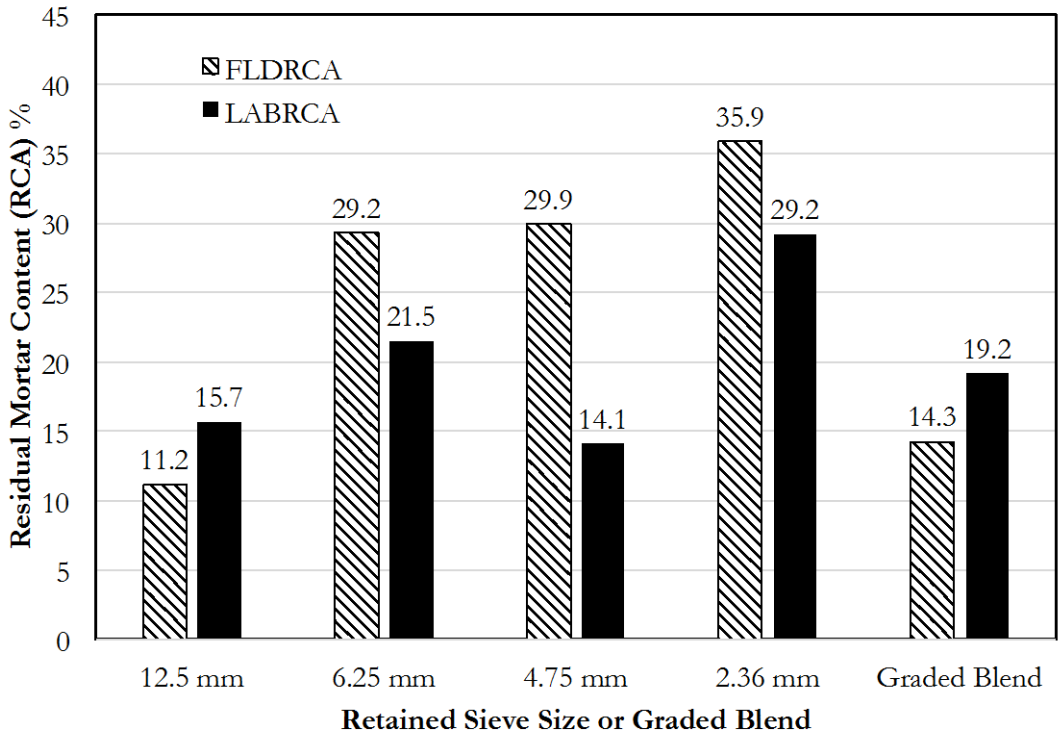

Figure A-1: Residual mortar content (RMC) values of FLDRCA and LABRCA

It can be seen that two RCA sources have moderate amounts of adhered mortar (less than 20% RMC) with relatively different RMC values for different sizes and the graded blend. Although FLDRCA shows higher RMC for smaller sizes (6.25 mm, 4.75 mm ad 2.36 mm), since the graded blend contained mostly aggregates retained on 12.5 mm sieve (about 65% by mass of aggregates are larger than 12.5 mm) and for this size LABRCA had higher RMC, the RMC of the graded blend for LABRCA was about 35% higher than the RMC of FLDRCA (19.2% for LABRCA vs. 14.3% for FLDRCA).

Each source of RCA (FLDRCA and LABRCA) and the Crushed aggregates were graded to match closely the as-received grading of the Rounded aggregate. The grading of these aggregates are shown in Figure A-2.

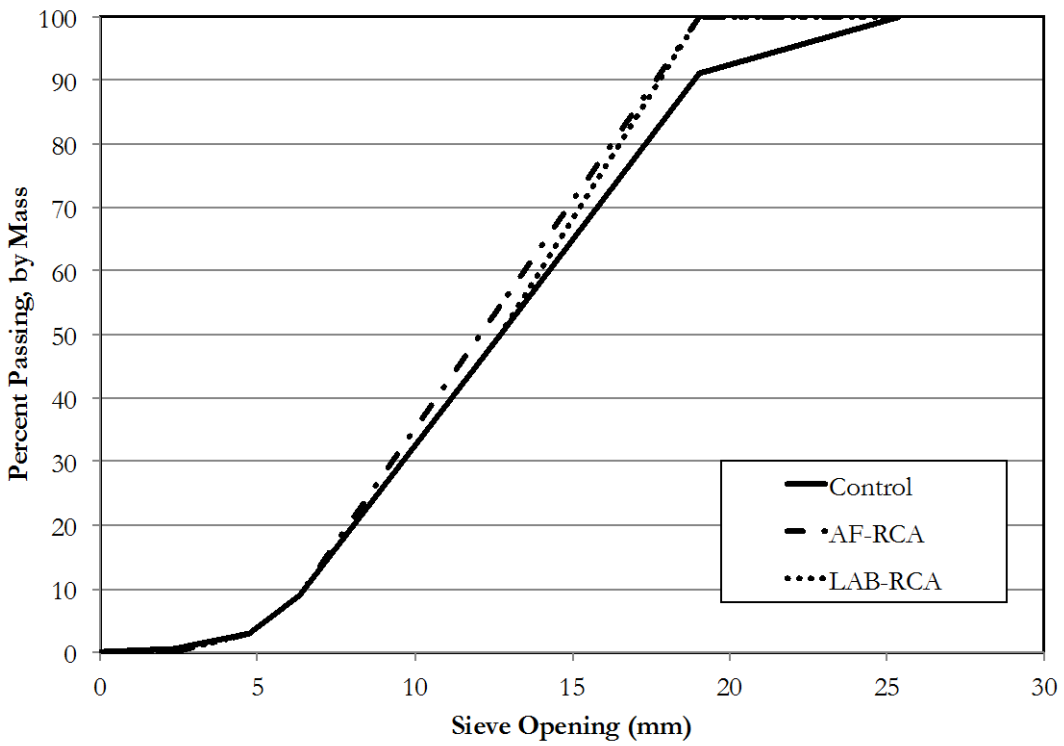

Figure A-2: Grading of coarse RCA and control aggregates

Some modifications were made due to limited RCA material resources. Both RCA mixtures were more gap-graded than the control mixture due to a lack of available larger sized (12.5 mm and greater) material that prevented a more closely matched curve.

The cement was a Type I/II portland cement conforming to ASTM C150 [40]. A polycarboxylate-based water reducer conforming to ASTM C494 Type F [41] and ASTM C 1017 Type I [42] was used to increase workability in all mixtures.

A.2.2 Experimental Methods

A.2.2.1 Mixture Design

Six different concrete mixtures were produced with design details presented in Table A-2.

Table A-2: Mixture design and fresh properties

Mixture Name	w/c	Cement Content (kg/m³)	Coarse Aggregate Type				Fine Aggregate (kg/m³)	Air Content (%)	Slump (mm)	Fresh Unit Weight (kg/m³)
			Rounded (kg/m³)	Crushed (kg/m3)	AFRCA (kg/m³)	LABRCA (kg/m³)				
Rounded	0.40	394	1092	0	0	0	682	1.5	76	2399
Crushed	0.40	375	0	1074	0	0	658	1.5	38	2468
FLDRCA 25%	0.40	394	819	0	273	0	682	1.5	95	2346
FLDRCA 100%	0.40	394	0	0	1092	0	682	1.5	76	2399
LABRCA 25%	0.40	394	800	0	0	267	635	1.5	57	2350
LABRCA 100%	0.40	394	0	0	0	1067	635	1.5	57	2350

Two of these mixtures were prepared using Rounded and Crushed natural aggregates. In addition, the Rounded aggregate was replaced with each RCA at 25% and 100% volume replacement levels. All concrete mixtures were prepared with a water to cement (w/c) ratio of 0.40. Fresh properties for each mixture are provided in Table A-2.

Aggregates were not washed prior to their use in the mixtures to try to mimic probable usage in the field. Prior to each mixture, the moisture content of the aggregate was measured, and the water content for the mixture was adjusted to ensure an effective w/c of 0.40. Air entraining admixtures were not used, and the measured air content of the mixtures match typical values for non-air entrained concrete. Air content testing was performed in accordance with ASTM C 231 [43]. Superplasticizer was used to maintain sufficient workability for the mixtures without altering the w/c. A dosage of 224 mL/100 kg of cement was used for the Rounded and Crushed mixtures, and 254 mL/100 kg of cement was used for the mixtures containing RCA. Slump testing was performed in accordance with ASTM C 143 [44] and acceptable slumps were achieved for all mixtures.

A.2.2.2 Mechanical Properties Testing

Sample cylinders were cast according to ASTM C31 [45] in plastic cylinder molds with a diameter of 100 mm and a height of 200mm. Cylinders were left to cure in the plastic molds for 24 hours after casting. The cylinders were then removed from their molds and moved to a moist room with a relative humidity of >95% at 23 ± 2°C. Compressive strength, splitting tensile strength, and modulus of elasticity testing were performed for each mixture at 28 days of age. Compressive strength testing was done in accordance with ASTM C39 [46]. Splitting tensile strength testing was done in accordance with ASTM C496 [47]. Modulus of elasticity testing was done in accordance with ASTM C469 [48].

A.2.2.3 Free Shrinkage and Mass Change

The ASTM C157 test was used to evaluate the free drying shrinkage [49]. The ASTM C157 test is the most commonly used method to determine the change in length of hardened concrete specimens prepared in the laboratory and subjected to drying. Length change was measured on hardened concrete prisms (75mm × 75mm × 285mm). The prisms were cast into molds, allowed to cure under wet burlap, and sealed with plastic sheeting. The prisms were then removed from the molds 24 hours after casting. The specimens (3 prisms for each mixture) were then stored in a moist room of 23 ± 2 °C and >95% relative humidity for the 14 days for curing. Upon the end of curing duration, the specimens were transferred to an environmental chamber with controlled condition of 23 ± 2 °C and 50 ± 4 % relative humidity. During drying, the length change of each prism was monitored by a comparator. The mass change was also recorded.

A.2.2.4 Restrained Shrinkage Ring Test

The ASTM C1581 test [50] (also known as the restrained ring test) has been frequently used to identify cracking potential of concrete and mortar mixtures. All restrained ring specimens were prepared according to ASTM C1581. A sample of freshly mixed concrete was placed and compacted in a circular molds around a steel ring. The specimens were immediately covered with wet burlap and sealed with plastic sheeting. The specimens were stored (under the burlap and plastic sheeting) in an environmental chamber with controlled conditions of 23 ± 2 °C and 50 ± 4 % relative humidity for 24 hours. The outer ring was then removed and the moist curing using the wet burlap and plastic sheeting was continued through 14 day after casting. At the end of the moist curing period, all burlap and plastic sheeting were removed. To ensure drying only occurred in the radial direction, a layer of silicone sealant was applied on the top surface of the concrete ring. As the concrete shrank, the compressive strain in the steel ring was recorded by four strain gauges attached 90° apart to the inner surface of the steel ring at mid-height. At the end of the test, a sharp change in the strain gauge reading toward zero strain indicated the stress is released due to cracking in the concrete ring. According to the strain gauge reading, an average stress rate (MPa/day) in the concrete ring specimen could be calculated per ASTM C1581. The time between exposure to drying and cracking is called time-to-cracking. Based on both the time-to-cracking and stress rate, a cracking potential classification (as shown in A-3) can be assigned to each mixture [50, 51].

Table A-3: Cracking potential index

Time-to-Cracking, t_{cr}, Days	Stress Rate at Cracking, S, MPa/Day	Potential for Cracking
$0 < t_{cr} \leq 7$	$S \geq 0.34$	High
$7 < t_{cr} \leq 14$	$0.17 < S < 0.34$	Moderate-High
$14 < t_{cr} \leq 28$	$0.10 < S < 0.17$	Moderate-Low
$t_{cr} > 28$	$S < 0.10$	Low

A.3 Results and Discussion

A.3.1 Mechanical Properties

Average 28-day compressive strength, splitting tensile strength, and modulus of elasticity for all mixtures are reported in Table A-4.

Table A-4: 28-Day compressive strength, splitting tensile strength, and modulus of elasticity

Mixture Name	28-Day Compressive Strength (Standard Deviation), MPa	28-Day Splitting Tensile Strength (Standard Deviation), MPa	28-Day Modulus of Elasticity (Standard Deviation), GPa
Rounded	39.1 (4.7)	3.8 (0.3)	28.8 (1.3)
Crushed	50.1 (2.7)	4.2 (0.4)	33.2 (2.2)
FLDRCA 25%	42.8 (1.9)	4.0 (0.2)	28.1 (0.1)
FLDRCA 100%	42.5 (1.2)	3.7 (0.4)	27.2 (0.4)
LABRCA 25%	43.4 (3.6)	4.2 (0.2)	28.3 (0.1)
LABRCA 100%	39.3 (3.4)	4.4 (0.7)	28.1 (0.8)

Standard deviations for all specimen sets tested are also presented. The Crushed mixture exhibited the highest compressive strength (50.1 MPa) and the Rounded mixture exhibited the lowest compressive strength (39.1 MPa). The mixtures containing RCA had 28-day compressive strengths ranging from 39.3 MPa to 43.4 MPa. These results indicate that the use of the crushed natural aggregates in the Crushed mixture had a significant impact on the strength of the material. The particle shape of the crushed coarse aggregates was more angular and surface texture rougher than the rounded coarse aggregates. This was due to the mechanical crushing procedures used during production. The increase in angularity resulted in an 11 MPa increase in 28-day compressive strength of the Crushed mixture over the Rounded mixture. This increase in compressive strength occurred despite the lower cement content that was used in the Crushed mixture compared to the Rounded mixture. Lower cement

contents typically result in lower strengths, however as indicated here, the use of a more angular and rough aggregate offset, and even increased the strength of the Crushed mixture compared to the Rounded mixture that contained higher cement content. Previous work by Corden and Gillespie has shown that substituting a crushed material with a higher angularity and surface roughness can increase the strength of the concrete compared to concrete made with smoother aggregates [52].

Both RCAs used in this study were also angular and rough, and subsequently these mixtures also had an increase in the average 28-day compressive strength compared to the Rounded mixture. However, when the standard deviation of these mixtures was examined there was not a significant difference between the 28-day compressive strengths seen in the mixtures containing RCA and the Rounded mixture. Historically, mixtures containing RCA exhibit lower mechanical properties [24, 26, 31, 32]. Quite often this was due to the need to increase the w/c to account for the loss of workability that is seen when using RCA. However, the reduction in strength can be avoided through proper mixture design modifications and the use of superplasticizers [25, 26]. For this study no significant changes were made to the mixture designs other than changing the aggregate type used between the Rounded mixture and the mixtures containing RCA. Superplasticizer was used to provide workability for all mixtures. The cement content and w/c was kept constant throughout. These results indicate that comparable strengths can be obtained in mixtures with simple substitutions of RCA for natural aggregates. This was true even for the mixtures that contained a 100% replacement of the coarse natural aggregates. Therefore, there was little impact on compressive strength caused by the inclusion of RCA.

The 28-day splitting tensile strength results, seen in Table A-4, show that the LABRCA 100% mixture produced the highest 28-day splitting tensile strength (4.4 MPa) of all mixtures tested, the FLDRCA 100% exhibited the lowest (3.7 MPa). As with the compressive strength results, no significant differences between the Rounded mixture and the mixtures containing RCA were observed. This observation indicates that with proper mixture design, the incorporation of RCA also has little effect on the splitting tensile strength of concrete. Additionally, the Crushed mixture also exhibited similar results. This indicates that the particle shape and surface texture of the aggregate may have less of an effect on splitting tensile strength of concrete compared to the effect it had on the compressive strength.

When the 28-day moduli of elasticity are examined for all mixtures, similar results as for the 28-day compressive strengths can be observed. The Crushed mixture exhibited the highest 28-day modulus of elasticity (33.2 GPa) and the FLDRCA 100% exhibited the lowest (27.2 GPa). The increase in modulus for the Crushed mixture compared to the other mixtures was significant. The increase in modulus can be attributed to the particle shape and surface texture of the crushed aggregate. This aggregate has a more angular shape and rougher surface texture which can help to increase the mechanical interlocking of the aggregate with the paste and increase the modulus of elasticity in the mixture [53]. A similar increase in surface roughness may be expected for the RCA coarse aggregate due to the residual mortar content that was adhered to the surface of some RCA particles, however the mixtures that contained RCA did not exhibit an increase in moduli of elasticity compared to the Rounded mixture. When the residual mortar content of the RCA is examined (Table A-1) it can be seen that it was less than 20% for both aggregates. Therefore, the difference in surface texture may not be significant enough to result in an increase in elastic modulus compared to the Rounded mixture.

The amount of residual mortar remaining in the RCA had no discernable effect on any of the mechanical properties examined as a part of this study. As shown in Table A-1, the RMC of the FLDRCA was 14.3%, and the RMC of the LABRCA was 19.2%. Mixtures containing either RCA exhibited similar compressive strengths, splitting tensile strengths, and moduli of elasticity compared to the Rounded mixture. Additionally, there were no significant differences observed at higher replacement levels (100%) compared to lower replacement levels (25%).

A.3.2 Free Shrinkage and Mass Loss

Length change of the prisms was monitored over a span of 98 days after they were placed into the drying chamber. Results of the length change of these prisms over time are presented in Figure A-3.

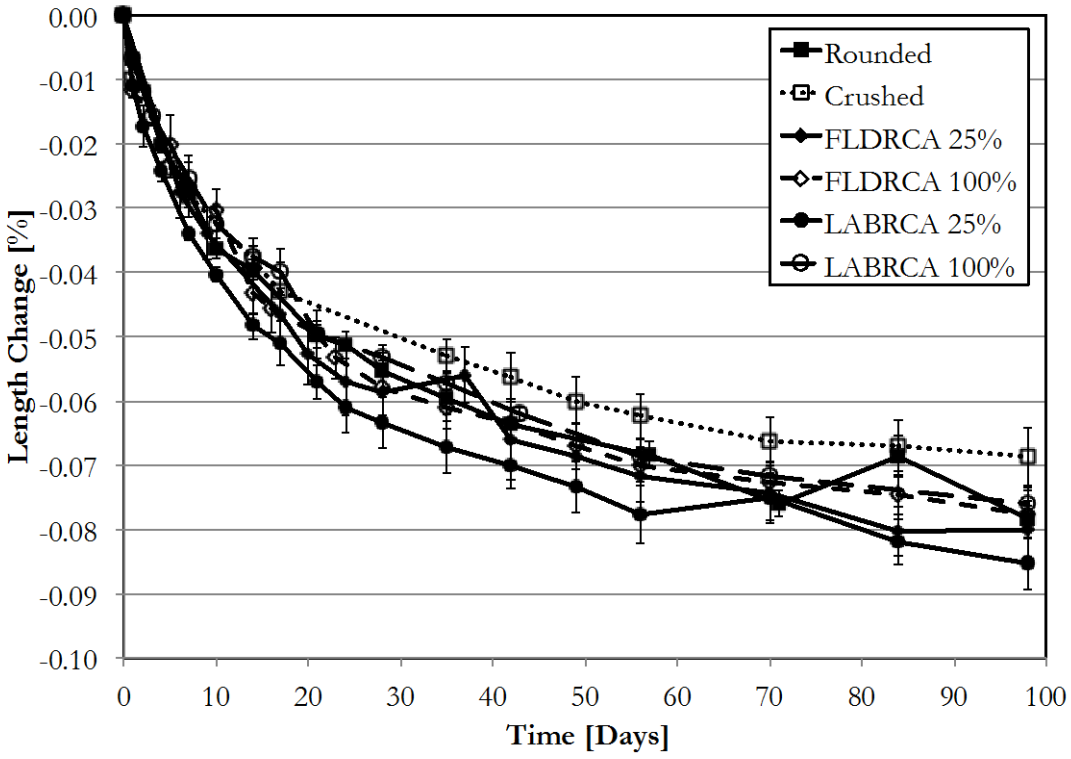

Figure A-3: Length change due to drying of concrete prisms

Initial length was recorded 14 days after casting, when they were removed from the moist room and placed in the drying chamber. The length measured at this time was taken as the zero point for length change measurements shown on the ordinate axis over the observation period. The time scale noted on the abscissa was also zeroed at the time of placement in the drying chamber.

Figure A-3 indicates that the length change at 98 days after exposure to the drying condition was statistically similar for all mixtures except for the Crushed mixture. The Crushed mixture exhibited the lowest amount of shrinkage (0.069%) and the LABRCA 25% mixture exhibited the highest amount of shrinkage (0.082%). The more angular particle shape of the aggregate and rougher surface texture may provide a better mechanical bond between the aggregates and the paste thus helping to reduce shrinkage [54, 55]. However, the reduction in shrinkage seen in the Crushed mixture may be due to the lower cement content of that particular mixture compared to the Rounded mixture and the mixtures containing RCA [56, 57]. Lower cement content in a mixture will result in lower relative amounts of paste. Paste content is a controlling factor in the amount of shrinkage in a system, because more paste content will result in more overall porosity that will be affected by drying. Therefore, a

lower paste content system will experience less shrinkage compared to a similar system with higher paste content. These results may also represent a combination of effects of the lower cement content and aggregate surface texture and shape.

The measurement of shrinkage of prisms exposed to drying conditions indicates that the inclusion of RCA in concrete mixtures did not cause a significant change in the amount of drying shrinkage that occurred by 98 days after they were exposed to drying. Additionally, the rate of length change was not significantly different between mixtures. Shrinkage is caused when water leaves the system (due to drying or self dessication) resulting in the collapse of the capillary pores in the cement paste system. As water leaves the system capillary tensions form on the walls of the pores; if the resulting stress exceeds the tensile capacity of the surrounding matrix the pore will collapse. The magnitude of capillary tension is inversely proportionate to the size of the capillary pore such that smaller pores result in higher capillary tensions [58]. Therefore, a concrete mixture with a finer pore structure will be more susceptible to shrinkage compared to that with a coarser pore structure. The shrinkage between the mixtures containing RCA and those the Rounded mixture were not significantly different, demonstrating that the inclusion of coarse RCA in the mixture does not have a significant impact on the microstructure of the surrounding mortar matrix in a way that impacts shrinkage susceptibility.

Figure A-4 presents the mass change measurements for the drying shrinkage prisms to 98 days after exposure to drying conditions.

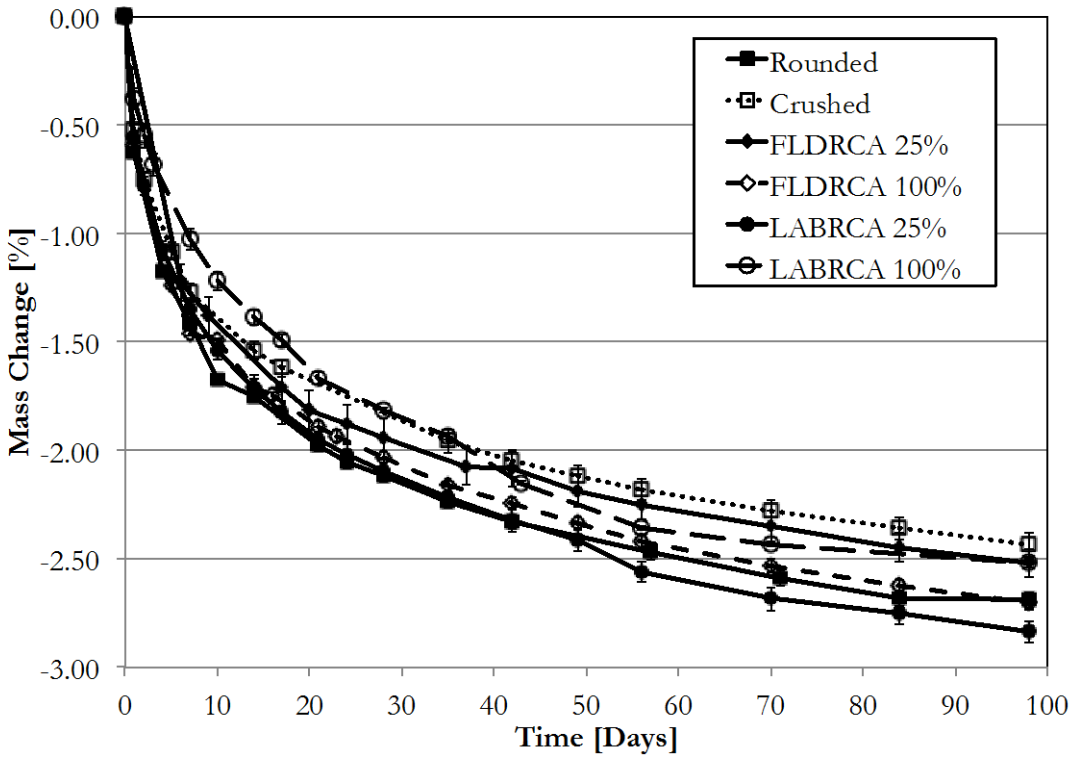

Figure A-4: Mass change due to drying of concrete prisms

The initial mass measurements were taken at 14 days after casting, when they were removed from the moist curing chamber (>95% relative humidity) and placed into the drying chamber. These results show that the Crushed mixture exhibited the lowest amount of mass loss (-2.18% mass change) and the LABRCA 25% experienced the highest amount of mass loss (-2.75% mass change). The mass loss measurement is a measure of the amount of moisture in the system that is lost to the environment during drying. Large differences in mass loss between systems may indicate differences in the microstructure that allow more or less water to leave the system (and thus impact shrinkage) over a period of time. There was more scatter observed in the mass loss results presented in Figure A-4 compared to the length change results presented in Figure A-3. No trends were observed between the amount of RCA included in a mixture and the mass loss of the system. These results indicate that aggregate type has little influence on the amount of mass loss in the systems. The Crushed mixture exhibited the smallest amount of mass loss compared to other mixtures, and again this may be due to the relatively lower paste content compared to other mixtures.

A.3.3 Restrained Shrinkage

Table A-5 presents a summary results from the restrained shrinkage ring test for all mixtures. Time to cracking and stress rate at time of cracking are presented for each ring, as well as an average for each mixture. Also presented is the cracking potential classification for each mixture according to the information presented in Table A-3.

Table A-5: Time to cracking, stress rate, and cracking potential classification for all mixtures

Mixture	Time-to-Cracking, Days				Stress Rate, MPa/Day				Cracking Potential Classification
	A	B	C	Average	A	B	C	Average	
Rounded	4.8	5.8	5.5	5.4	0.392	0.357	0.366	0.372	High
Crushed	6.3	7.0	10.3	7.9	0.343	0.348	0.239	0.310	Moderate High
FLDRCA 25%	7	8.2	8.4	7.9	0.271	0.248	0.268	0.263	Moderate High
FLDRCA 100%	9.2	10.6	12.5	10.8	0.224	0.212	0.185	0.207	Moderate High
LABRCA 25%	6.1	7.7	7.9	7.2	0.403	0.296	0.279	0.326	Moderate High
LABRCA 100%	7.1	7.5	7.9	7.5	0.180	0.297	0.279	0.252	Moderate High

Strain development versus time in individual rings over drying period for each mixture can be found in Figures A-5a to A-5f.

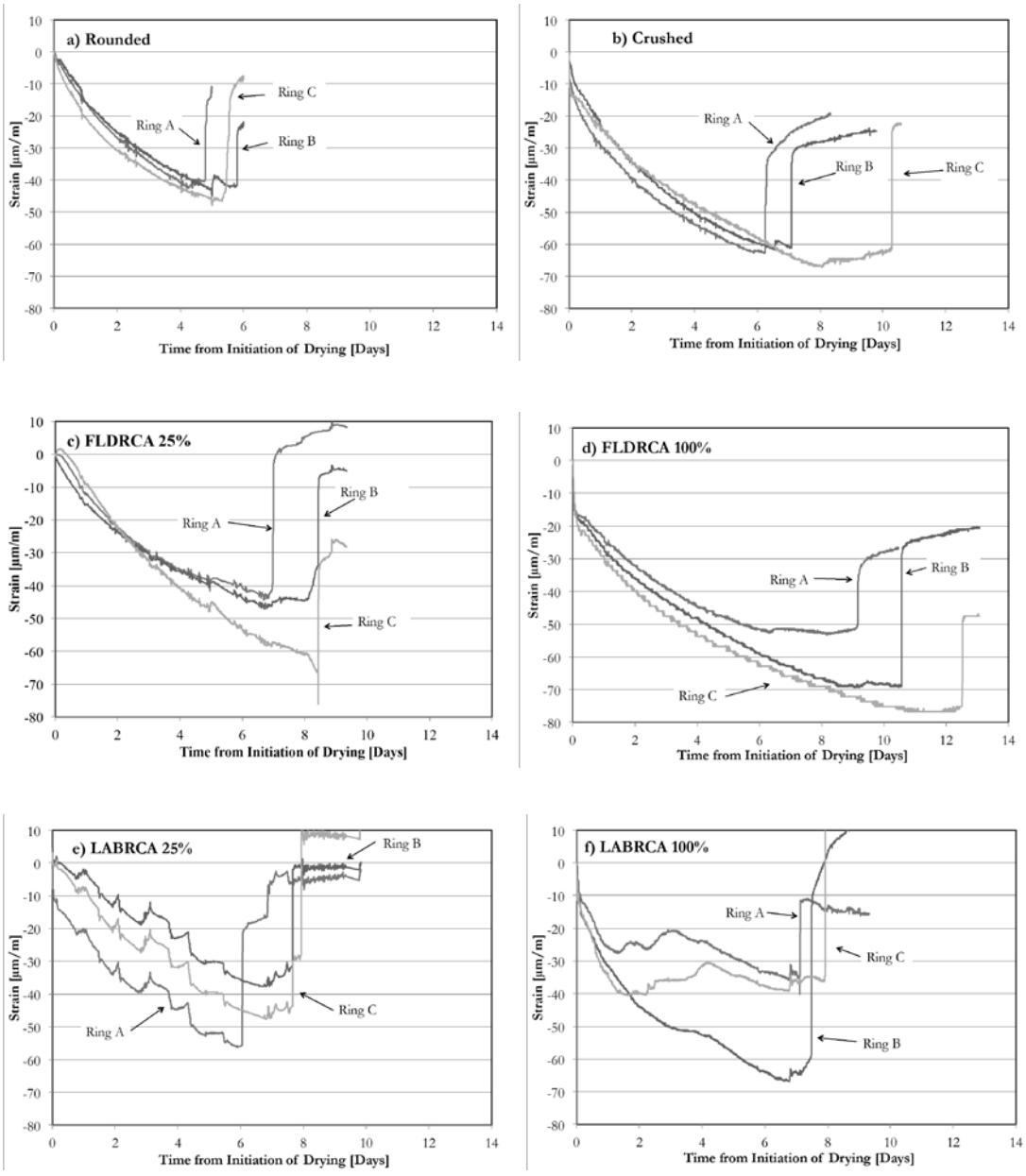

Figure A-5: Restrained shrinkage ring results for all mixtures

The average time to cracking for all mixtures was increased compared to the Rounded mixture. The FLDRCA 100% mixture did not crack until 10.8 days (average), which was twice the average amount of time in which the Rounded mixture cracked (5.4 days). All other mixtures cracked after 7 days. Stress rates at the time of cracking were also reduced for all mixtures compared to the Rounded mixture. The FLDRCA 100% had the lowest stress rate at time of cracking (0.207 MPa/Day). The Rounded mixture's cracking potential classification, based on the results of this test, was "high". The

Crushed mixture and all mixtures containing RCA had a reduced cracking potential, registering on the cracking potential classification scale as "moderate high". The use of RCA, as well as the change from a rounded aggregate to an angular aggregate, was able to reduce the cracking potential of the concrete mixture one classification level.

Upon examination of the individual ring results for the Crushed mixture, ring C was an outlier both in time to cracking and stress rate. This ring had a significantly longer time to cracking and significantly lower stress rate compared to ring A and B. Without this ring's data, the average time to cracking decreases significantly to 6.7 days, and the average stress rate becomes 0.346 MPa/Day, in the Crushed mixture. This indicated that the inclusion of the crushed aggregate provided a benefit in terms of time-to-cracking and a reduction of stress rate compared to the Rounded mixture. The benefit seen here may be attributed to the lower shrinkage due to drying seen in the Crushed mixture compared to the Rounded mixture. The lower shrinkage suggests that less tensile stress was developed in the concrete in the restrained shrinkage ring during testing, leading to a prolonged time-to-cracking for this mixture. Generally, a mixture with a low cracking risk potential will have a comparatively low shrinkage, low modulus of elasticity and high tensile strength. The low modulus of elasticity and high tensile strength will accommodate more stress buildup before cracking occurs [59, 60]. However, despite having higher modulus of elasticity, the Crushed mixture had a longer time-to-cracking compared to the Rounded mixture. Therefore, the particle shape, and amount of shrinkage may have more of an effect on cracking susceptibility than varying moduli of elasticity.

A benefit in time-to cracking and a lower stress rate was also observed in the mixtures that incorporated RCA compared to the Rounded mixture. Further, a longer time to cracking was observed in mixtures with a 100% RCA replacement level compared with a 25% replacement level. The RMC content may have an effect on micro-cracking and crack propagation in these systems. Micro-cracking can occur in the interfacial transition zone (ITZ) between natural aggregates and the bulk cement paste due to differential strains set up by the differences in moduli of elasticity between the natural aggregates and the cement paste matrix [61-64]. In systems that contain RCA, there are less of these areas of differential moduli of elasticity because there is less natural aggregate overall. Therefore, the use of RCA may increase the time-to-cracking during shrinkage because the areas where differential stresses caused by incompatible areas of moduli of elasticity may exist are reduced. Each RCA also contained varying levels of RMC. The FLDRCA contained 14.3% RMC, and the LABRCA contained

19.3% RMC (Table A-1 and Figure A-1). Despite the larger RMC of the LABRCA mixtures, FLDRCA mixtures cracked later and generally developed lower stress rates. Therefore, while both the LABRCA and FLDRCA were recycled concrete materials, it is difficult to compare the two systems to each other based solely on the RMC amount of the graded blends. As shown in Figure A-1, RMC values for smaller aggregate sizes for FLDRCA (specifically aggregate retained on 6.25 mm, 4.75 mm and 2.36 mm sieves) were considerably larger than the RMC values of the corresponding sizes of LABRCA. The differences in the time-to-cracking and stress rate observed between the FLDRCA 100% mixture and the LABRCA 100% mixture may be attributed partially to the difference in RMC distribution of different sizes within each blend.

Additionally, as can be observed from the differences between the Rounded and the Crushed mixtures, aggregate type can have a significant impact on the concrete performance. The original natural aggregates used in the RCAs were from different natural aggregate sources. Therefore, the type of natural aggregate used in the original concrete may have an effect on the performance of the concrete made with RCA produced from the natural aggregates.

The results from the Rounded mixture and the mixtures containing LABRCA did clearly indicate that there was a beneficial effect on cracking susceptibility when RCA is used. These mixtures contained the same natural aggregate, the Rounded aggregate. The LABRCA was produced using the Rounded aggregate as part of its original concrete mixture. This concrete was then crushed and used as a new aggregate in the LABRCA 25% and LABRCA 100% mixtures. The use of the RCA, even at a 25% replacement level, resulted in an increased time to cracking compared to the Rounded mixture and a decreased stress rate. The mixture containing 100% LABRCA did not have an increased time to cracking when compared to the mixture containing on 25%, but the stress rate on the LABRCA 100% was significantly lower than the stress rate for the LABRCA 25% mixture. This indicates that the inclusion of RCA, particularly the amount of RMC, can reduce the stress rate development in the mixtures during drying. This lead to longer time-to-cracking in both mixtures. This may be due to a lower amount of restraint in systems that contain RCA. Each recycled concrete aggregate is a two-phase particle that consists of both the RMC and the original natural aggregate. In mixtures that were made with the RCA there was less natural coarse aggregate compared to the Rounded mixture. The aggregate acts as a restraint point that can develop high stress concentrations providing crack initiation sites during shrinkage [62]. In the mixtures that contain RCA, there was less of this natural aggregate

to provide restraint in the system, and therefore the time-to-cracking is increased, even at similar amounts of drying shrinkage. Additionally, there may be an increased bond between the RCA and the surrounding mortar of the concrete, improving the mixtures ability to resist the stress concentrations that form at aggregate sites.

According to the cracking potential classification system, presented in Table A-3, the Rounded mixture was classified as a "high" risk for cracking. The mixtures containing crushed natural aggregate as well as all four RCA mixtures were classified as "moderate-high" cracking risk. While the use of RCA was not able to completely mitigate the cracking risk of the concrete mixture, the classification was reduced an entire level from "high" to "moderate-high". Combined with the shrinkage and mass loss data presented above, these results show that the use of RCA does not necessarily increase the potential for cracking in concrete. In fact, some beneficiation was observed when RCA was included in the mixtures presented here. When combined with other shrinkage mitigation techniques such as shrinkage reducing admixtures or internal curing, RCA may be able to be used to reduce the cracking susceptibility of high cracking risk mixtures into acceptable ranges.

A.4 Conclusions

This work examined the effect of using coarse recycled concrete aggregate as a replacement for natural aggregate on drying shrinkage and cracking susceptibility of concrete. It was shown that when RCA with moderate amounts of RMC is used (in this study the RMC for both sources were less than 20%), adequate compressive strength, splitting tensile strength, and modulus of elasticity can be obtained in mixtures including coarse RCA, at 25% and 100% replacement levels. Further, the use of RCA does not necessarily significantly increase the drying shrinkage of concrete when incorporated into the mixture. More importantly, it was demonstrated that the use of RCA can significantly reduce the cracking risk of concrete when incorporated into a high cracking risk mixture. While past results have shown that concrete that includes RCA is often substandard compared to natural aggregate concrete; these results indicate that the inclusion of RCA will not necessarily result in inferior quality concrete – on the contrary may improve concrete's cracking resistance. Further study is required, however, to understand how RCA affects the microstructure of concrete, as well as the interfacial transition zone around the aggregate. Additionally, further research on the impact of natural aggregate mineralogy, shape, and surface texture on concrete properties (particularly durability) is required to further advance our understanding of aggregate interactions in concrete.

A.5 Acknowledgements

The authors would like to thank the Oregon Transportation Research and Education Consortium and the National Institute for Transportation and Communities for generously funding the work presented here. We would also like to thank the NAVFAC Engineering and Expeditionary Warfare Center for providing RCA, the Knife River Corporation for providing the sources of natural aggregate, Lafarge North America for providing cement, and W. R. Grace Co. for providing admixtures. Additionally we would like to thank undergraduate research assistants Nick Briesach and Silas Shields who helped in the batching, mixing, casting, and measuring for this study.

A.6 Works Cited

[1] M.S. Winfield, A. Taylor, Replacing the Load: The Need for an Aggregates Conservation Strategy for Ontario, in, Pembina Institute for Appropriate Development, 2005.

[2] A. Abbas, G. Fathifazl, O. Isgor, A. Razaqpur, B. Fournier, S. Foo, Environmental benefits of green concrete, in: EIC Climate Change Technology, 2006 IEEE, IEEE, 2006, pp. 1-8.

[3] American Concrete Institute, Removal and reuse of hardened concrete, in: American Concrete Institute (Ed.), American Concrete Institute, Farmington Hills, MI, 2001.

[4] A.D. Buck, Recycled concrete as a source of aggregate, ACI Journal, 74 (1977) 212-219.

[5] S. Froundistou-Yannis, Waste concrete as aggregate for new concrete, ACI Journal, 74 (1977) 373-376.

[6] G. Fathifazl, A. Abbas, A. Razaqpur, O. Isgor, B. Fournier, S. Foo, New mix design method for recycled aggregate concrete, ASCE Materials Journal, 21 (2009) 601-611.

[7] P.K. Mehta, Reducing the environmental impact of concrete, in: Concrete International, American Concrete Institute, ACI, 2001, pp. 61-66.

[8] K.A. Sakata, T., Improvement of concrete with recycled aggregate, ACI Special Publication, 192 (2000) 1089-1108.

[9] G.F. Kheder, S.A. Al-Windaw, Variation in mechanical properties of natural and recycled aggregate concrete as related to the strength of their binding mortar, Materials and Structures, 38 (2005) 701-709.

[10] T.C. Hansen, Recycling of demolished concrete and masonry, in: Report of Technical Committee 37-DRC Demolition and Reuse of Concrete, Part 1, E&FN Spon, London, 1992, pp. 160.

[11] M.B. de Oliveira, E. Vazquez, The influence of retained moisture in aggregates from recycling on the properties of new hardened concrete, Waste Management, 16 (1996) 113-117.

[12] T. Kikuchi, E. Horiuchi, An experimental study on recycling concrete by using high quality recycled coarse aggregates, Mem Fac Eng, Osaka City University, 44 (2003) 37-33.

[13] M.S. Maruyama, T. Sogabe, R. Sato, K. Kawai, Flexural properties of reinforced recycled concrete beams, in: Conference on the Use of Recycled Materials in Building and Structures, RILEM Publications SARL, Bagneux, France, 2004, pp. 610-618.

[14] M.C. Limbachiya, T. Leelawat, R.K. Dhir, Use of recycled concrete aggregate in high-strength concrete, Materials and Structures, 33 (2000) 574-580.

[15] J.M.V. Gomez-Soberon, Relationship between gas adsorption and the shrinkage and creep of recycled aggregate concrete, Cement Concrete Aggr, 25 (2003) 42-48.

[16] H.N. Tamura, J.; Ohashi, J.; Imamato, K., High quality recycled aggregate concrete (HiRAC) processed by decompression and rapid release, ACI Special Publication, 200 (2001) 491-502.

[17] J.M.F. Gomez-Soberon, Creep of concrete with substitution of normal aggregate by recycled concrete aggregate, ACI Special Publication, 209 (2002) 461-474.

[18] T. Hansen, Recycled aggregates and recycled aggregate concrete second state-of-the-art report developments 1945–1985, Materials and Structures, 19 (1986) 201-246.

[19] P. de Vries, Concrete recycled: Crushed concrete as aggregate, Concrete, 27 (1993) 9-13.

[20] S. Nishibayashi, K. Yamura, Mechanical properties and durability of concrete from recycled coarse aggregate prepared by crushing concrete, in: Proceedings of the second international

symposium (RILEM) on Demolition and Reuse of Concrete and Masonry, Tokyo, Japan, 1988, pp. 643-651.

[21] G. Fathifazl, A. Razaqpur, O.B. Isgor, A. Abbas, B. Fournier, S. Foo, Flexural performance of steel-reinforced recycled concrete beams, ACI Structural Journal, 106 (2009).

[22] G. Fathifazl, A. Razaqpur, O.B. Isgor, A. Abbas, B. Fournier, S. Foo, Shear strength of reinforced recycled concrete beams with stirrups, Mag Concr Res, 62 (2010) 685-699.

[23] G. Fathifazl, A.G. Razaqpur, O.B. Isgor, A. Abbas, B. Fournier, S. Foo, Bond performance of deformed steel bars in concrete produced with coarse recycled concrete aggregate, Canadian Journal of Civil Engineering, 39 (2012) 128-139.

[24] S.-C. Kou, C.-S. Poon, M. Etxeberria, Influence of recycled aggregates on long term mechanical properties and pore size distribution of concrete, Cement and Concrete Composites, 33 (2011) 286-291.

[25] K.K. Sagoe-Crentsil, T. Brown, A.H. Taylor, Performance of concrete made with commercially produced coarse recycled concrete aggregate, Cement and Concrete Research, 31 (2001) 707-712.

[26] A.K. Padmini, K. Ramamurthy, M.S. Mathews, Influence of parent concrete on the properties of recycled aggregate concrete, Constr Build Mater, 23 (2009) 829-836.

[27] S. Mandal, S. Chakraborty, A. Gupta, Some studies on durability of recycled aggregate concrete, The Indian Concrete Journal, 76 (2002) 385-388.

[28] J.H. Ideker, J.E. Tanner, M.P. Adams, A. Jones, Durability asessment of recycled concrete aggregates for use in new concrete - Phase II Report, in, Oregon Transportation and Education Consortium, Portland, OR, 2014, pp. 98.

[29] P.K. Mehta, P.J.M. Monteiro, Concrete: Microstructure, Properties, and Materials, 3 ed., McGraw-Hill, New York, 2006.

[30] A.C. 209, Report on Factors Affecting Shrinkage and Creep of Hardened Concrete (ACI 209.1R-05), in, American Concrete Institute, Farmington Hills, Michigan, 2005.

[31] R.S. Ravindrarajah, Effects of using recycled concrete as aggregate on the engineering properties of concrete, in: National Symposium on the Use of Recycled Materials in Engineering Construction: 1996, Barton, ACT: Institution of Engineers, Australia, Sydney, N.S.W., Australia, 1996, pp. 147-152.

[32] M. Kikuchi, T. Miura, Y. Dosho, M. Narikawa, Application of recycled aggregate concrete for structural concrete. Part 1- experimental study on the quality of recycled aggregate and recycled aggregate concrete, in: R.K. Dhir, N.A. Henderson, M.C. Limbachiya (Eds.) Sustainable construction: use of recycled concrete aggregate, Thomas Telford, London, UK, 1998, pp. 55-68.

[33] J.M. Khatib, Properties of concrete incorporating fine recycled aggregate, Cement and Concrete Research, 35 (2005) 763-769.

[34] J.O. Castano-Tabares, A. Domingo-Cabo, C. Lazaro, F. Lopez-Gayarre, P. Serna, M.A. Serrano-Lopez, Creep and shrinkage of recycled aggregate concrete, in: Constr Build Mater, 2009, pp. 2545+.

[35] V. Corinaldesi, G. Moriconi, Evaluation of recycled aggregate concrete cracking through ring test, Applied Mechanics and Materials, 174-177 (2012) 1475-1480.

[36] H. Jeong, Processing and properties of recycled aggregate concrete, in: Civil Engineering, University of Illinois at Urbana-Champagne, Urbana, Illinois, 2011.

[37] J. Foster, V. Cervantes, Personal Communication about Source of Airfield Pavement RCA, in: J.H. Ideker (Ed.), 2013.

[38] K.J. Folliard, M.D.A. Thomas, B. Fournier, K.E. Kurtis, J.H. Ideker, Interim recommendations for the use of lithium to mitigate or prevent alkali-silica reaction (ASR), in: U. S. Department of Transportation: Federal Highway Association (Ed.), U.S. DoT, McLean, Virginia, USA, 2006.

[39] A. Abbas, G. Fathifazl, O.B. Isgor, A. Razaqpur, B. Fournier, S. Foo, Proposed method for determining the residual mortar content of recycled concrete aggregates, Journal of ASTM International, 5 (2008) 12.

[40] ASTM C150, Standard Specification for Portland Cement, in: ASTM International (Ed.), West Conshocken, Pennsylvania, 2011.

[41] ASTM C494, Standard specification for chemical admixtures for concrete, in: A. International (Ed.), ASTM International, West Conshohocken, PA, 2013.

[42] ASTM C1017, Standard specification for chemical admixtures for use in producing flowing concrete, in: A. International (Ed.), ASTM International, West Conshohocken, PA, 2013.

[43] ASTM C231, Standard test method for air content of freshly mixed concrete by the pressure method, in: A. International (Ed.), ASTM International, West Conshohocken, PA, 2010.

[44] ASTM C143, Standard test method for slump of hydraulic-cement concrete, in: A. International (Ed.), ASTM International, West Conshohocken, PA, 2012.

[45] ASTM C31, Standard practice for making and curing concrete test specimens in the field, in: A. International (Ed.), ASTM International, West Conshohocken, PA, 2012.

[46] ASTM C39, Standad test method for compressive strength of Cylindrical Concrete Specimens, in: A. International (Ed.), ASTM International, West Conshohocken, PA, 2012a.

[47] ASTM C496, Standard test method for splitting tensile strength of cylindrical concrete specimens, in: A. International (Ed.), ASTM International, West Conshohocken, PA, 2011.

[48] ASTM C469, Standard test method for static modulus of elasticity and Poisson's ratio of concrete in compression, in: A. International (Ed.), ASTM International, West Conshohocken, PA, 2010.

[49] ASTM C157, Standard test method for length change of hardened hydraulic-cment mortar and concrete, in: A. International (Ed.), ASTM International, West Conshohocken, PA, 2008.

[50] ASTM C1581, Standard test method for determining age at cracking and induced tensile stress characteristics of mortar and concrete under restrained shrinkage, in: A. International (Ed.), ASTM International, West Conshohocken, PA, 2009.

[51] H.T. See, E.K. Attiogbe, M.A. Miltenberger, Potential for Restrained Shrinkage Cracking of Concrete and Mortar, Cement, Concrete and Aggregates, 26 (2004) 123-130.

[52] W.A. Cordon, H.A. Gillespie, Variables in concrete aggregates and portland cement paste which influence the strength of concrete, Journal Proceedings of the American Concrete Institute, 60 (1963) 1029-1052.

[53] A.M. Neville, Aggregate Bond and Modulus of Elasticity of Concrete, ACI Materials Journal, 94 (1994) 71-75.

[54] T. Fu, Shrinkage study of high performance concrete for bridge decks, in: School of Civil and Construction Engineering, Oregon State University, Corvallis, OR, 2013.

[55] T.T.C. Hsu, F.O. Slate, Tensile Bond Strength Between Aggregate and Cement Paste or Mortar, Journal Proceedings of the American Concrete Institute, 60 (1963) 465-486.

[56] D. Darwin, J. Browning, W. Lindquist, H. McLeod, J. Yuan, M. Toledo, D. Reynolds, Low-cracking, high-performance concrete bridge decks, Transportation Research Record: Journal of the Transportation Research Board, 2202 (2010) 61-69.

[57] P. Qiao, D. McLean, J. Zhuang, Mitigation strategies for early-age shrinkage cracking in bridge decks, in, Washington DOT, Olympia, WA, 2010.

[58] A. Radlinska, B. Bucher, R. Henkensiefken, G. Sant, J. Weiss, Shrinkage mitigation strategies in cementitious systems: A closer look at differences in sealed and unsealed behavior, Transportation Research Record: Journal of the Transportation Research Board, 2070 (2008) 59-67.

[59] K. Folliard, C. Smith, G. Sellers, M. Brown, J.E. Breen, Evaluation of Alternative Materials to Control Drying-Shrinkage Cracking in Concrete Bridge Decks, in, Report No. FHWA/TX-04/0-4098-4, , 2003.

[60] J.H. Ideker, T. Fu, T. Deboodt, Development of shrinkage limits and testing protocols for ODOT high performance concrete - Final report, in, Oregon Department of Transportation, Salem, OR, 2013.

[61] P.K. Mehta, P.J.M. Monteiro, Dimensional stability, in: Concrete: Microstructure, properties, and materials, McGraw Hill, New York, 2006, pp. 85-120.

[62] T.T.C. Hsu, Mathematical analysis of shrinakge stresses in a model of hardened concrete, Journal Proceedings of the American Concrete Institute, 60 (1963) 371-390.

[63] T.T.C. Hsu, F.O. Slate, G.M. Sturman, G. Winter, Microcracking of plain concrete and the shape of the stress-strain curve, Journal Proceedings of the American Concrete Institute, 60 (1963) 209-224.

[64] F.O. Slate, S. Olseefski, X-Rays for study of internal structure and microcracking of concrete, Journal Proceedings of the American Concrete Institute, 60 (1963) 575-588.

Appendix B

B Appendix B

Additional Data

B.1 Manuscript 3 Additional Data

This section presents additional data for Chapter 5: Manuscript 3 as discussed within that chapter. The mixtures named are as described in Chapter 5: Manuscript 3.

B.1.1 Aggregate Property vs. Compressive Strength Results

This section presents figures that examine aggregate properties against compressive strength results for the KRC, CRC, BLG, and MM mixtures, as presented in Chapter 5: Manuscript 3. These results are discussed within Chapter 5: Manuscript 3. Figure B-1 shows the compressive strengths for Day 1, Day 3, and Day 28 for the KRC, CRC, BLG, and MM mixtures against fine aggregate D50 values.

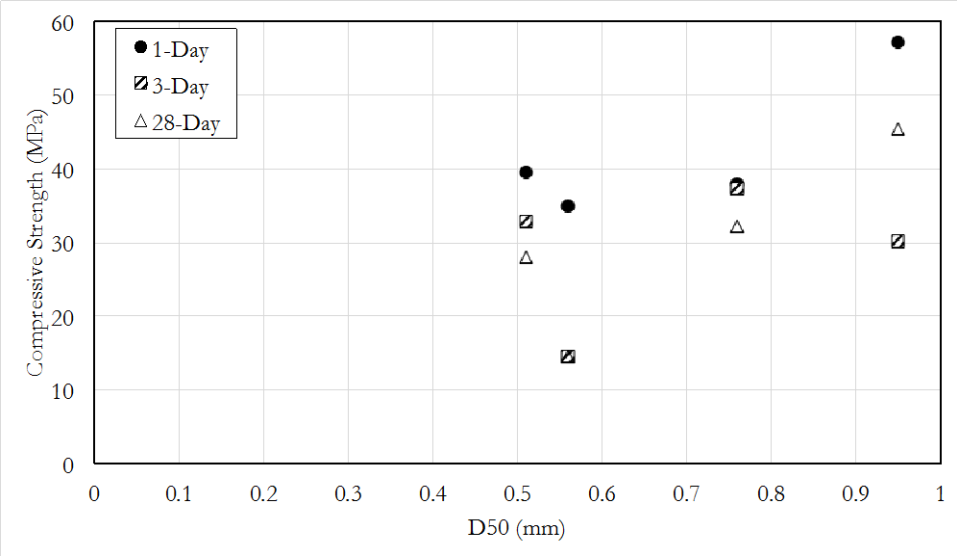

Figure B-1: 1, 3, and 28-day compressive strengths against fine aggregate D50 values

Figure B-2 shows the percent strength reduction due to conversion for the KRC, CRC, BLG, and MM mixtures against fine aggregate D50 values.

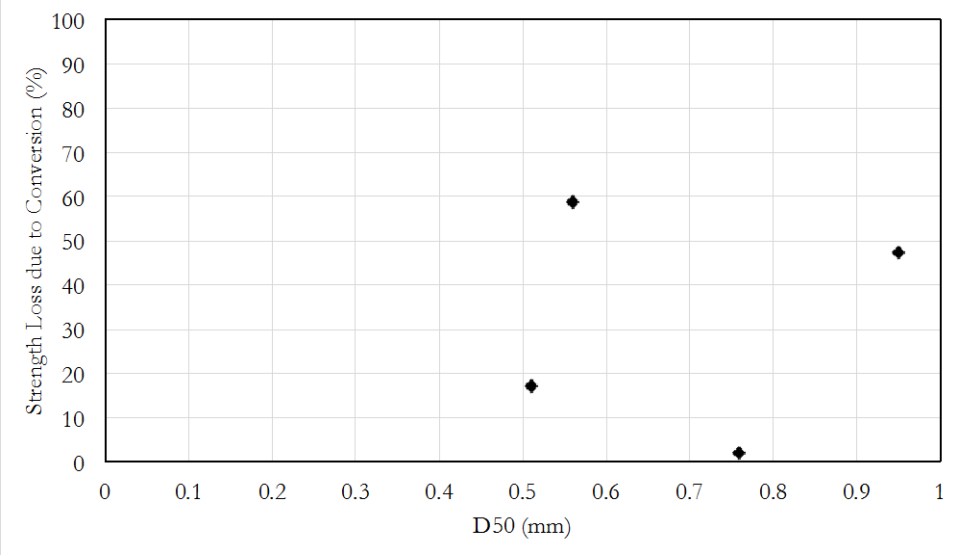

Figure B-2: Percent strength reduction due to conversion against coarse aggregate D50 values

Figure B-3 shows the compressive strengths for Day 1, Day 3, and Day 28 for the KRC, CRC, BLG, and MM mixtures against coarse aggregate D50 values.

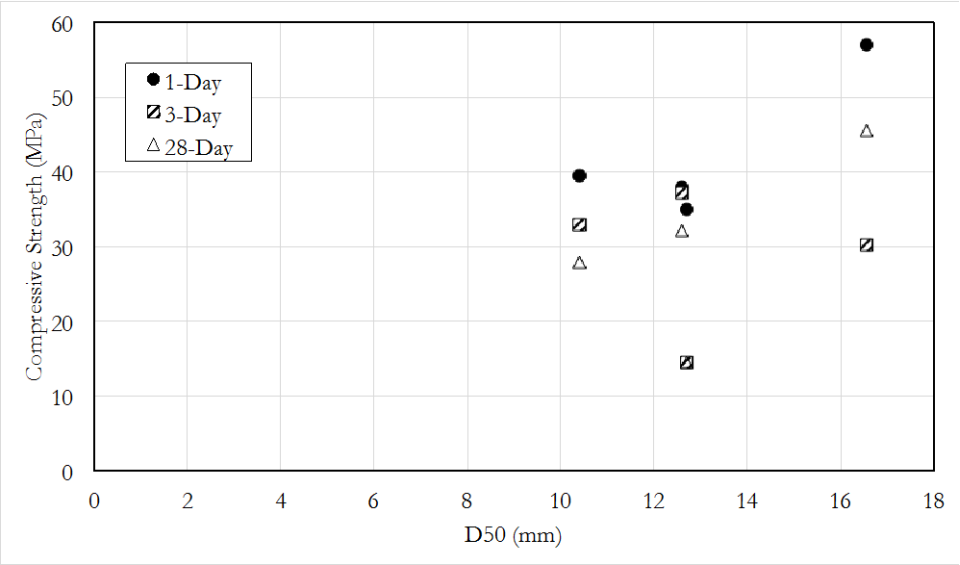

Figure B-3: 1, 3, and 28-day compressive strengths against coarse aggregate D50 values

Figure B-4 shows the percent strength reduction due to conversion for the KRC, CRC, BLG, and MM mixtures against coarse aggregate D50 values.

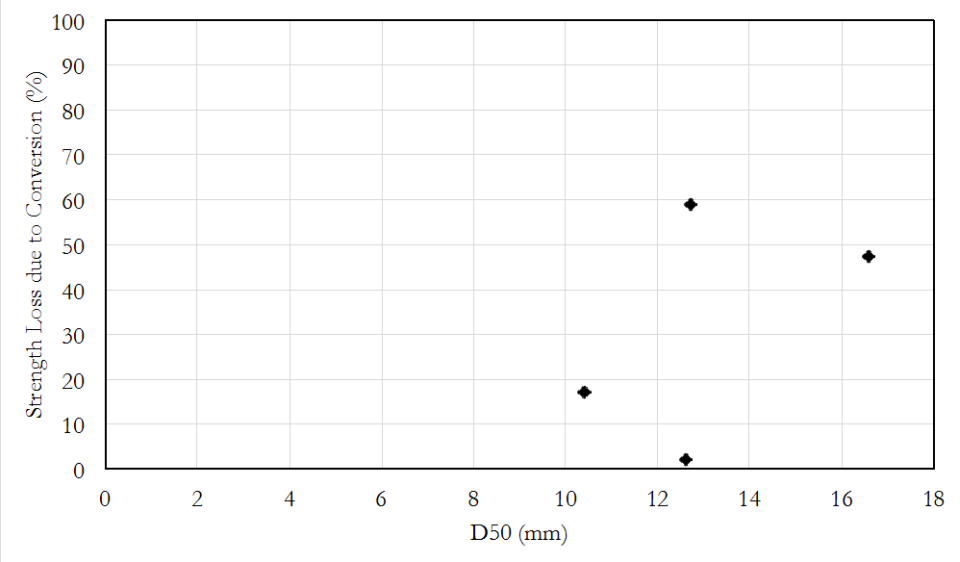

Figure B-4: Percent strength reduction due to conversion against coarse aggregate D50 values

Figure B-5 shows the compressive strengths for Day 1, Day 3, and Day 28 for the KRC, CRC, BLG, and MM mixtures against fine aggregate FM values.

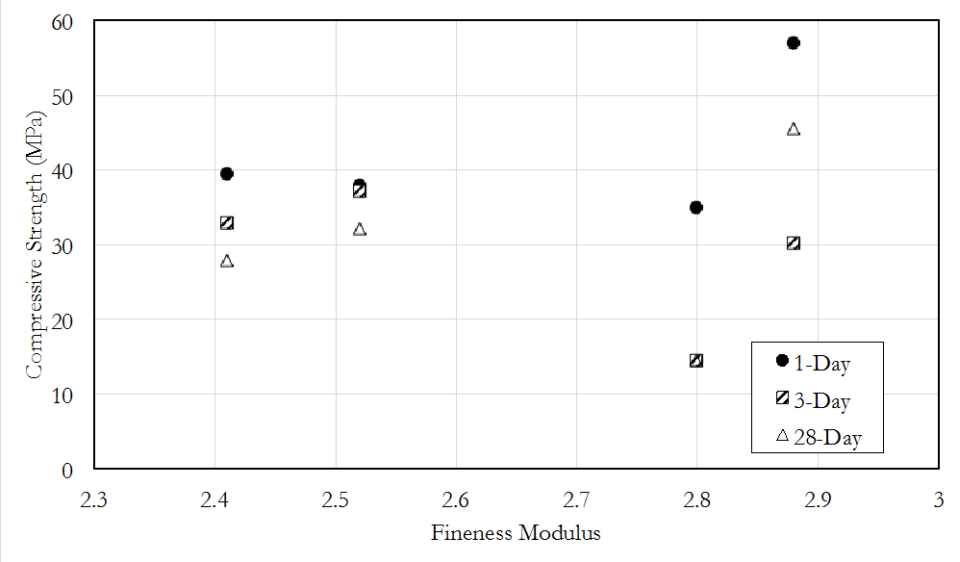

Figure B-5: 1, 3, and 28-day compressive strengths against fine aggregate FM values

Figure B-6 shows the percent strength reduction due to conversion for the KRC, CRC, BLG, and MM mixtures against fine aggregate FM values.

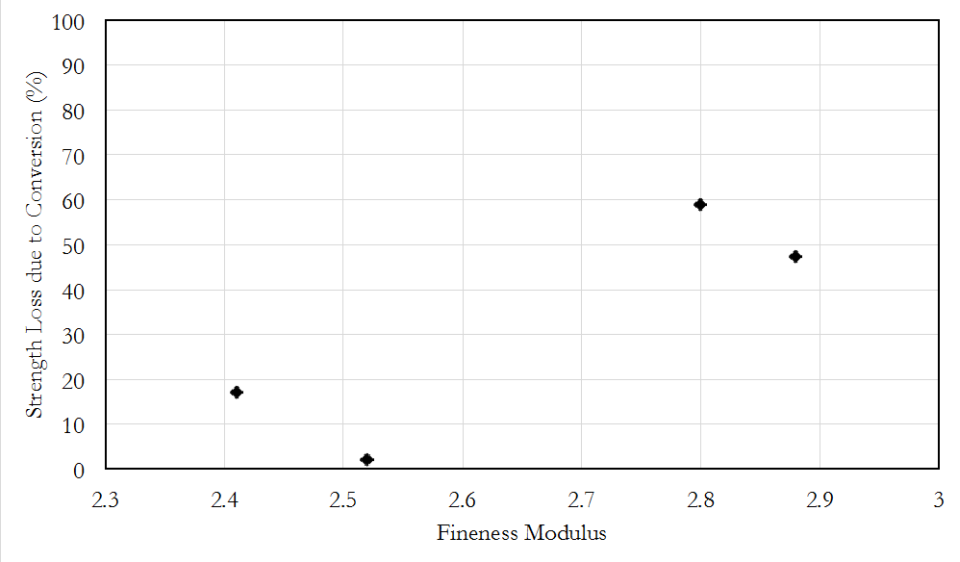

Figure B-6: Percent strength reduction due to conversion against fine aggregate FM values

Figure B-7 shows the compressive strengths for Day 1, Day 3, and Day 28 for the KRC, CRC, BLG, and MM mixtures against fine aggregate G_s values.

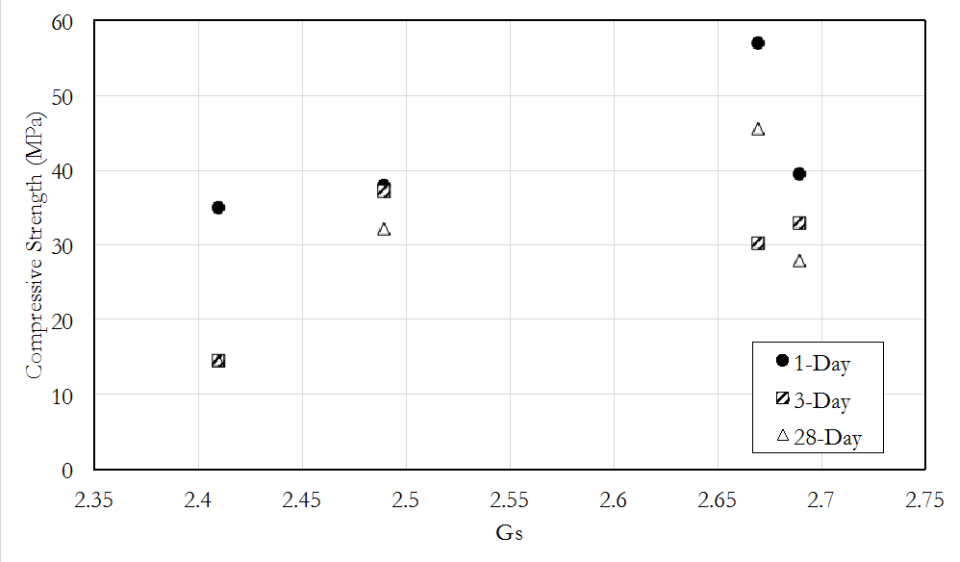

Figure B-7: 1, 3, and 28-day compressive strengths against fine aggregate G_s values

Figure B-8 shows the percent strength reduction due to conversion for the KRC, CRC, BLG, and MM mixtures against fine aggregate G_s values.

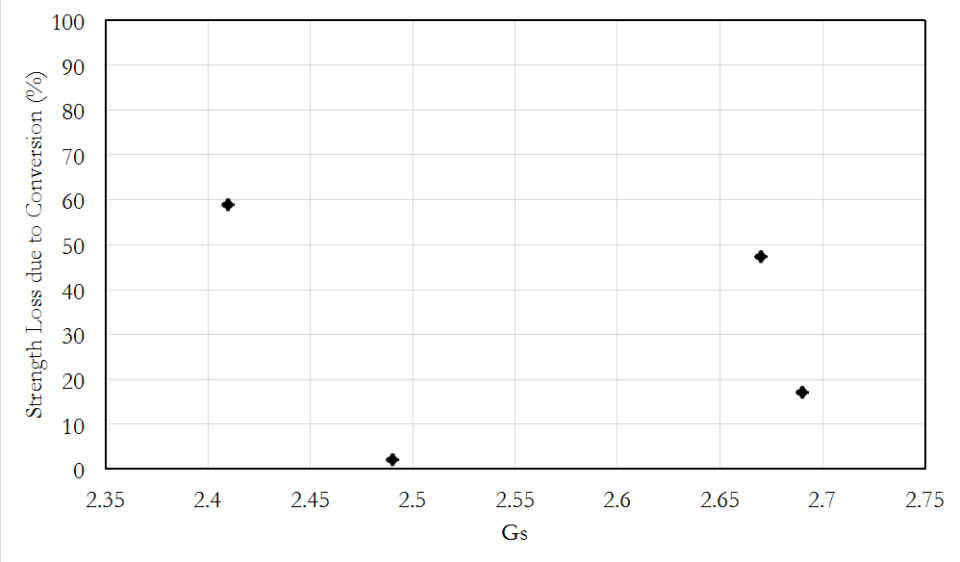

Figure B-8: Percent strength reduction due to conversion against fine aggregate G_s values

Figure B-9 shows the compressive strengths for Day 1, Day 3, and Day 28 for the KRC, CRC, BLG, and MM mixtures against coarse aggregate G_s values.

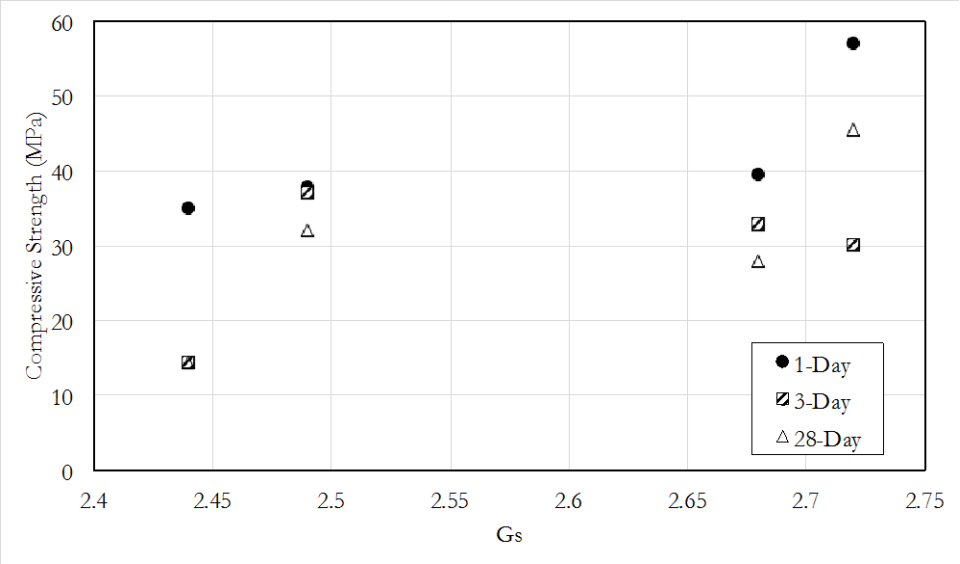

Figure B-9: 1, 3, and 28-day compressive strengths against coarse aggregate G_s values

Figure B-10 shows the percent strength reduction due to conversion for the KRC, CRC, BLG, and MM mixtures against coarse aggregate G_s values.

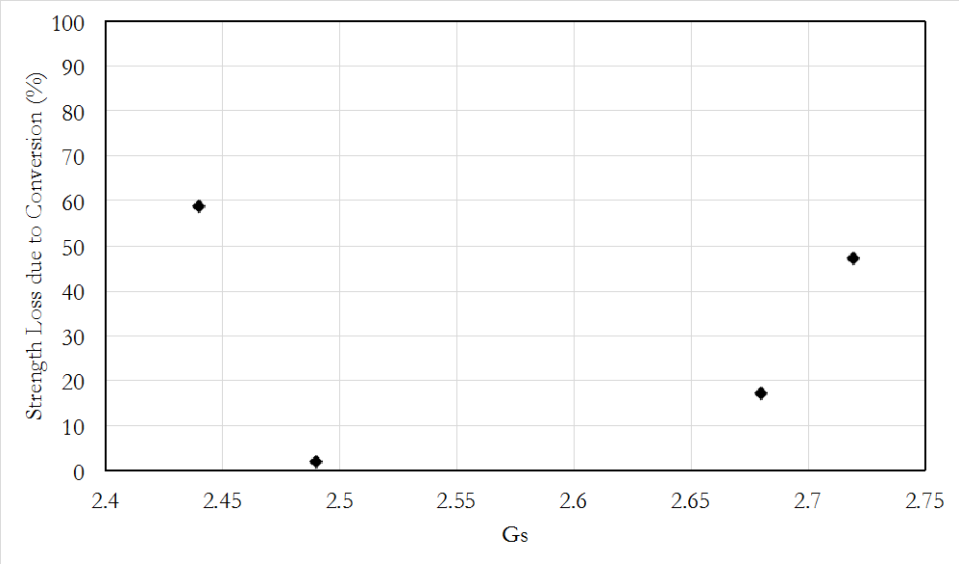

Figure B-10: Percent strength reduction due to conversion against coarse aggregate G_s values

Figure B-11 shows the compressive strengths for Day 1, Day 3, and Day 28 for the KRC, CRC, BLG, and MM mixtures against fine aggregate absorption capacity values.

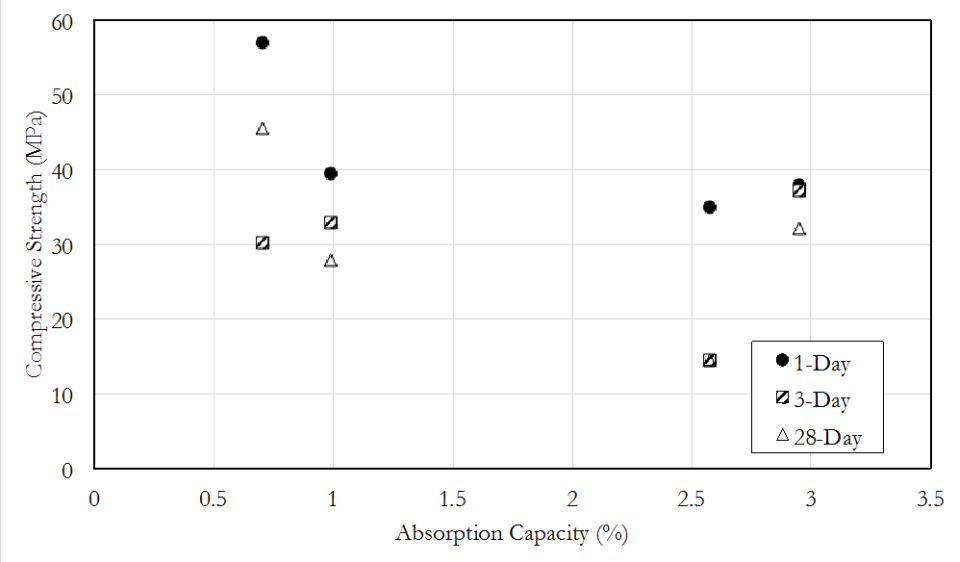

Figure B-11: 1, 3, and 28-day compressive strengths against fine aggregate absorption capacity values

Figure B-12 shows the percent strength reduction due to conversion for the KRC, CRC, BLG, and MM mixtures against fine aggregate absorption capacity values.

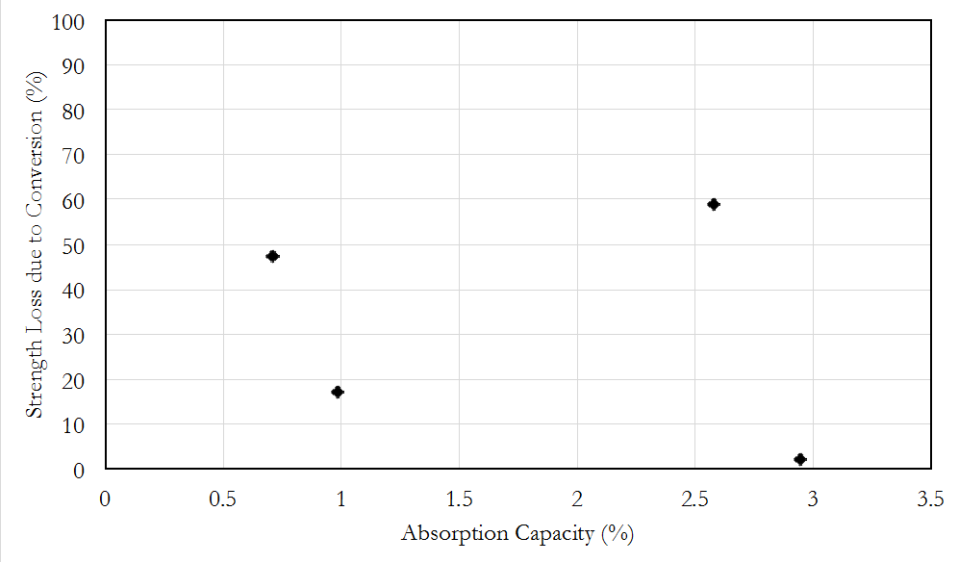

Figure B-12: Percent strength reduction due to conversion against fine aggregate absorption capacity values

Figure B-13 shows the compressive strengths for Day 1, Day 3, and Day 28 for the KRC, CRC, BLG, and MM mixtures against coarse aggregate absorption capacity values.

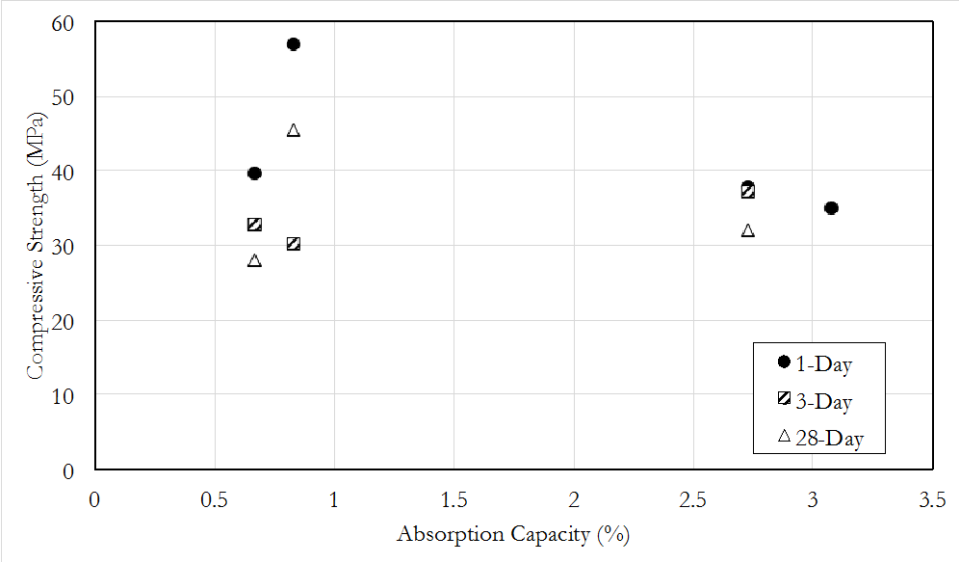

Figure B-13: 1, 3, and 28-day compressive strengths against coarse aggregate absorption capacity values

Figure B-14 shows the percent strength reduction due to conversion for the KRC, CRC, BLG, and MM mixtures against coarse aggregate absorption capacity values.

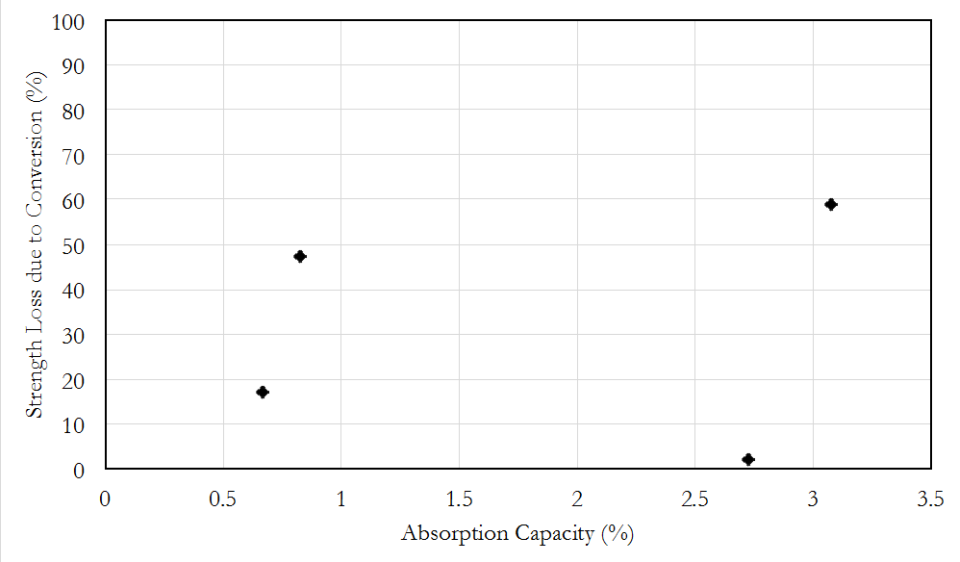

Figure B-14 Percent strength reduction due to conversion against coarse aggregate absorption capacity values

B.1.2 Additional KRC System SEM Images

B.1.2.1 Day 1

Figure B-15 A-F presents selected BSE-SEM images used for measuring porosity and examining microstructure of the KRC system at Day 1.

A) 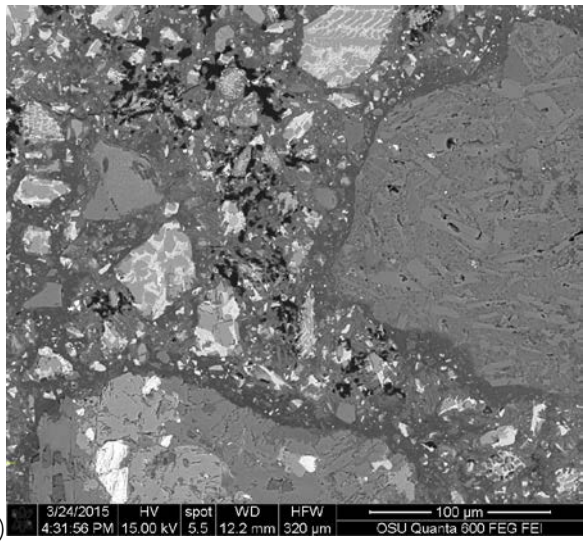

B) 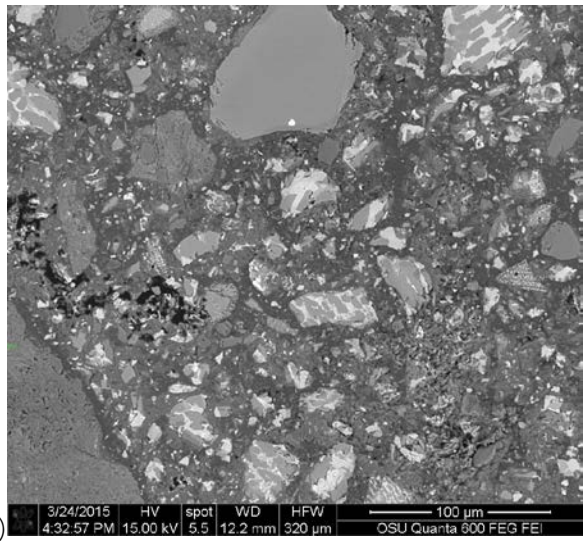

C) 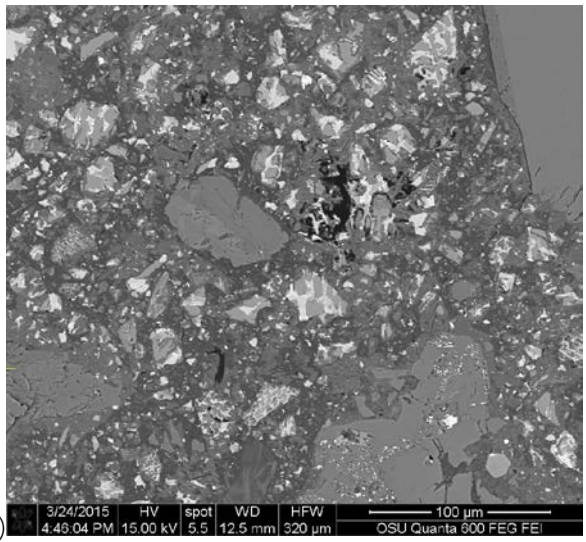
3/24/2015 4:48:04 PM
HV 15.00 kV
spot 5.5
WD 12.5 mm
HFW 320 µm
100 µm
OSU Quanta 600 FEG FEI

D) 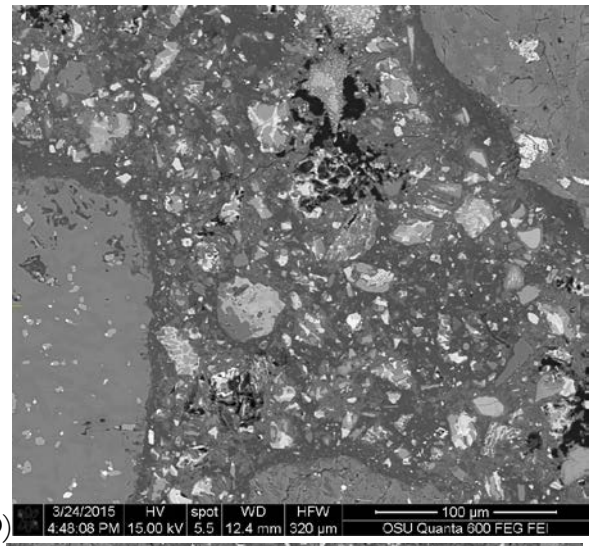
3/24/2015 4:48:08 PM
HV 15.00 kV
spot 5.5
WD 12.4 mm
HFW 320 µm
100 µm
OSU Quanta 600 FEG FEI

E) 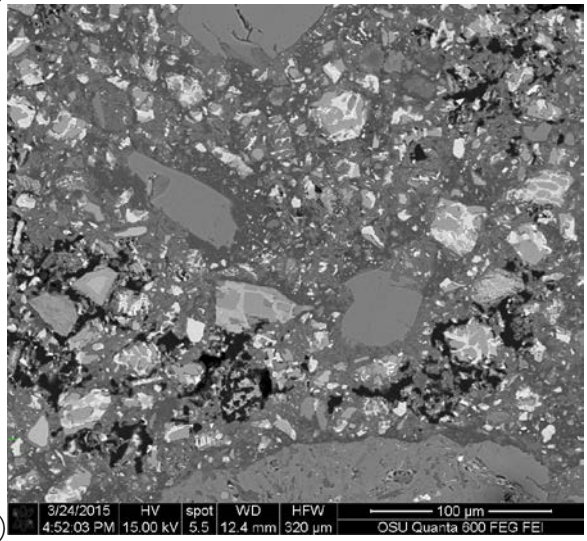
3/24/2015 4:52:03 PM
HV 15.00 kV
spot 5.5
WD 12.4 mm
HFW 320 µm
100 µm
OSU Quanta 600 FEG FEI

F) 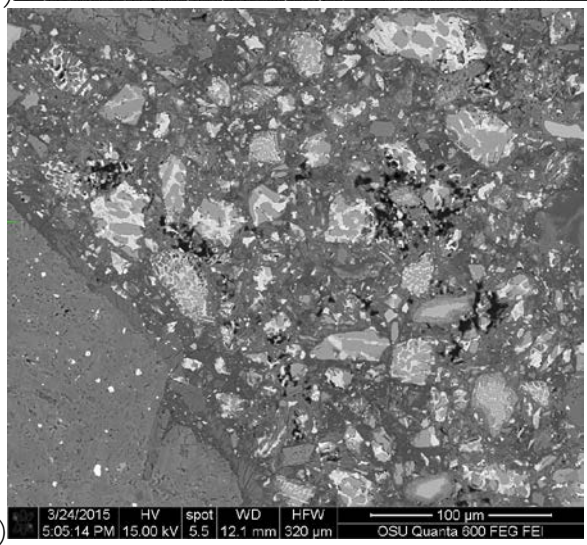
3/24/2015 5:05:14 PM
HV 15.00 kV
spot 5.5
WD 12.1 mm
HFW 320 µm
100 µm
OSU Quanta 600 FEG FEI

G) 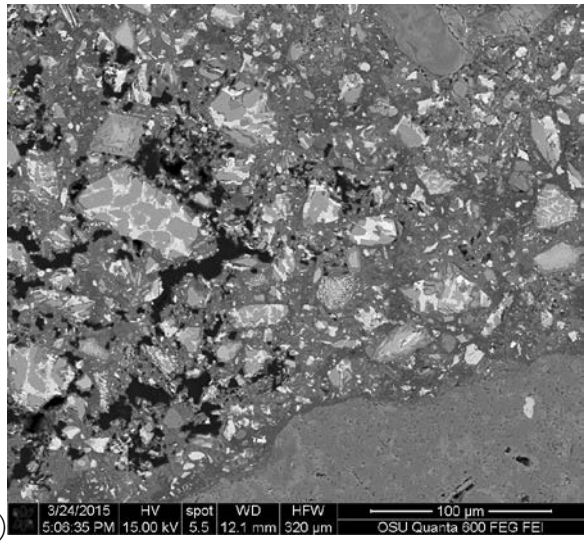
3/24/2015 5:08:35 PM
HV 15.00 kV
spot 5.5
WD 12.1 mm
HFW 320 µm
100 µm
OSU Quanta 600 FEG FEI

H) 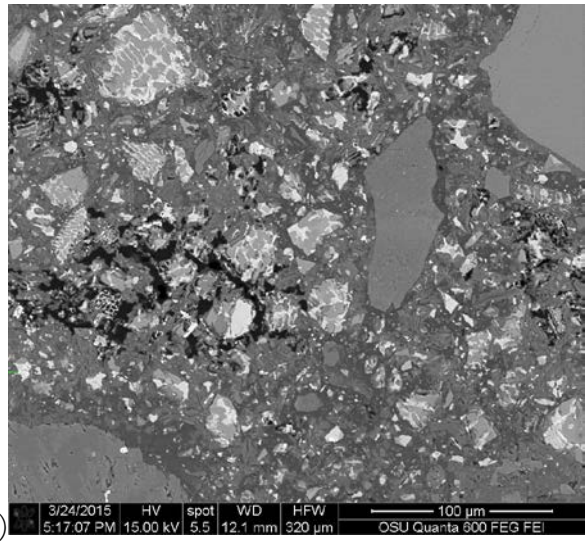
3/24/2015 5:17:07 PM
HV 15.00 kV
spot 5.5
WD 12.1 mm
HFW 320 µm
100 µm
OSU Quanta 600 FEG FEI

I) 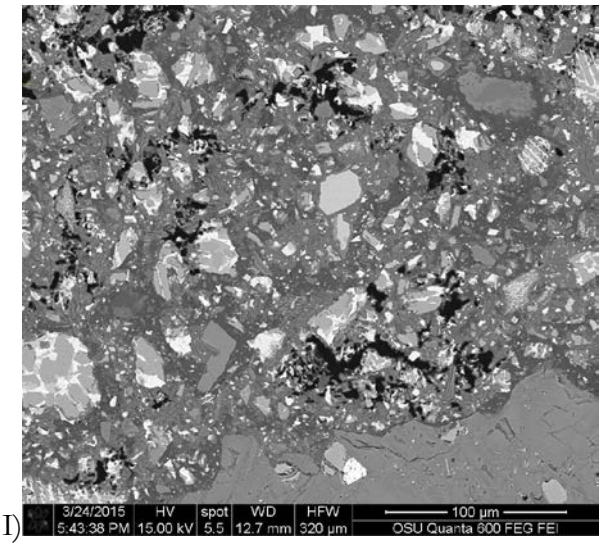

J) 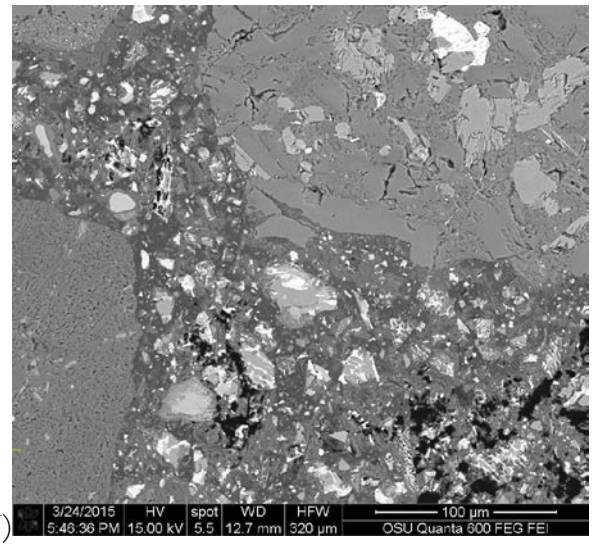

Figure B-15 A-J: BSE-SEM images of the KRC system at Day 1

B.1.2.2 Day 3

Figure B-16 A-F presents selected BSE-SEM images used for measuring porosity and examining microstructure of the KRC system at Day 3.

A) 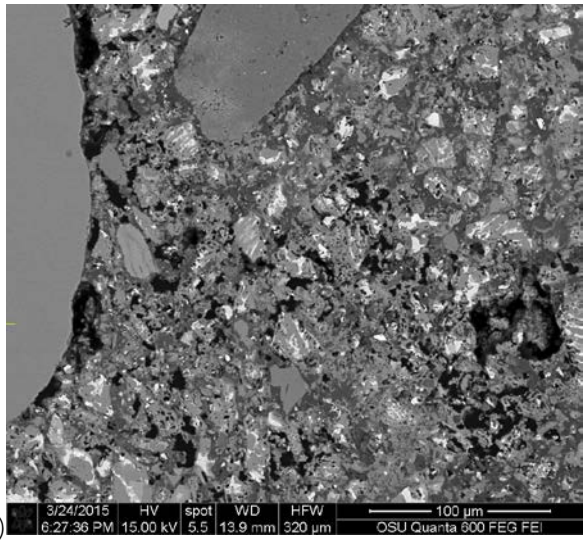

B) 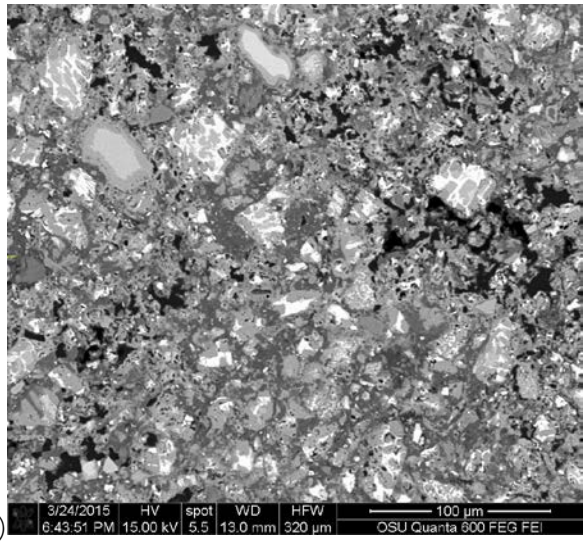

C) 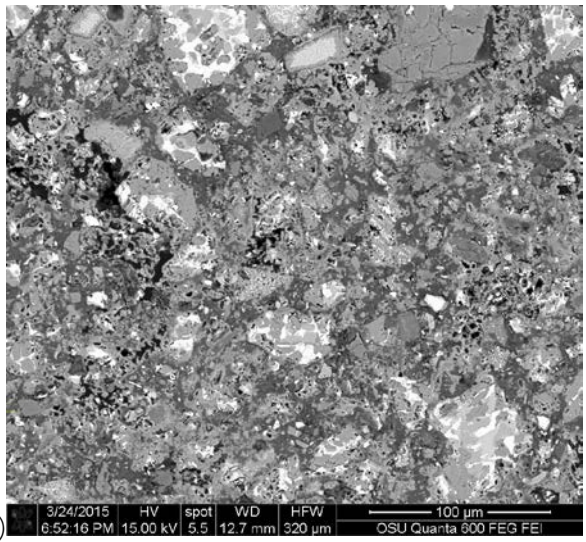
3/24/2015 6:52:16 PM
HV 15.00 kV
spot 5.5
WD 12.7 mm
HFW 320 µm
100 µm
OSU Quanta 600 FEG FEI

D) 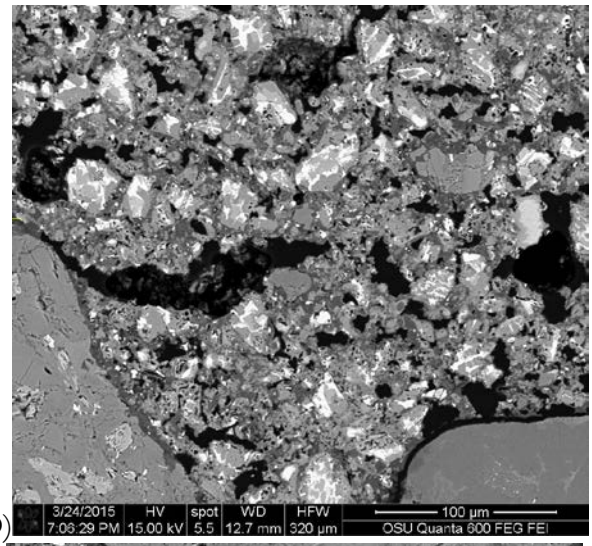
3/24/2015 7:03:29 PM
HV 15.00 kV
spot 5.5
WD 12.7 mm
HFW 320 µm
100 µm
OSU Quanta 600 FEG FEI

E) 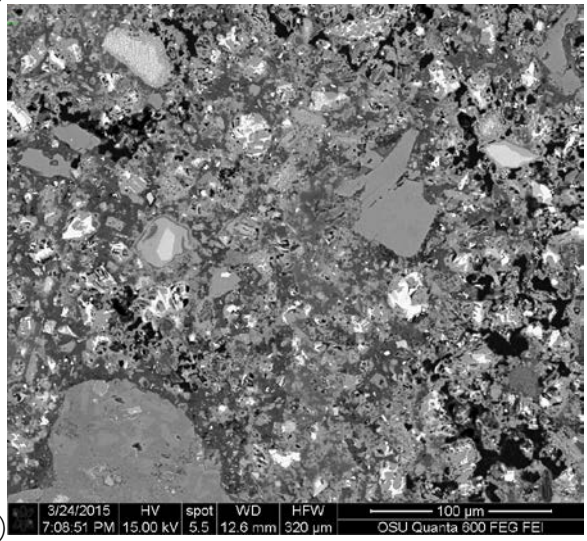
3/24/2015 7:08:51 PM
HV 15.00 kV
spot 5.5
WD 12.6 mm
HFW 320 µm
100 µm
OSU Quanta 600 FEG FEI

F) 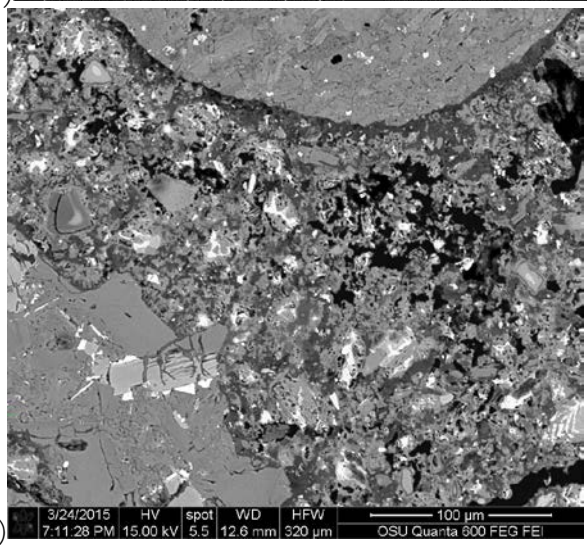
3/24/2015 7:11:28 PM
HV 15.00 kV
spot 5.5
WD 12.6 mm
HFW 320 µm
100 µm
OSU Quanta 600 FEG FEI

G) 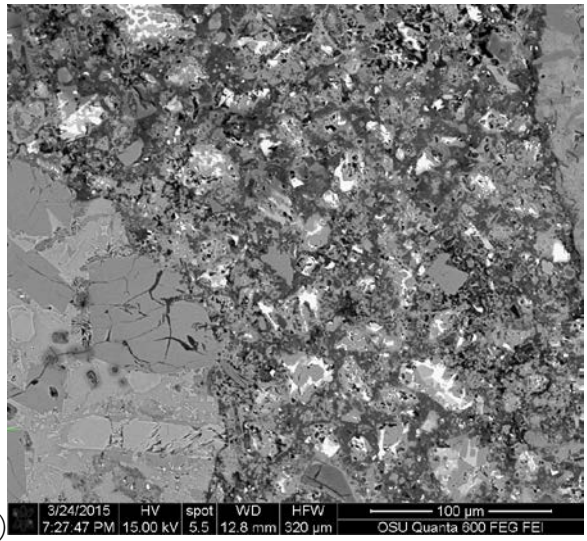
3/24/2015 7:27:47 PM
HV 15.00 kV
spot 5.5
WD 12.8 mm
HFW 320 µm
100 µm
OSU Quanta 600 FEG FEI

H) 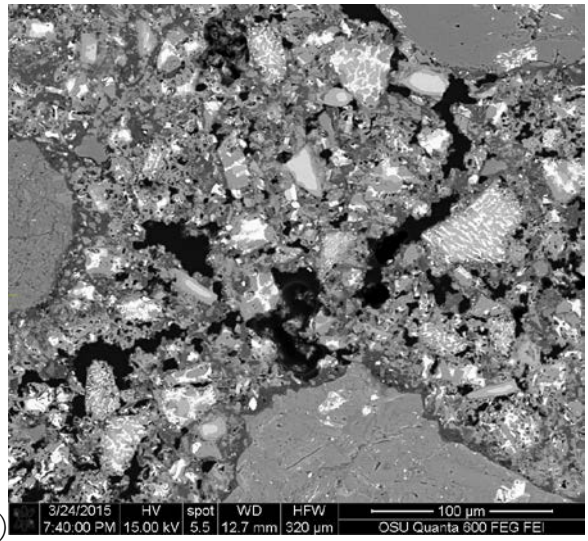
3/24/2015 7:40:00 PM
HV 15.00 kV
spot 5.5
WD 12.7 mm
HFW 320 µm
100 µm
OSU Quanta 600 FEG FEI

I) 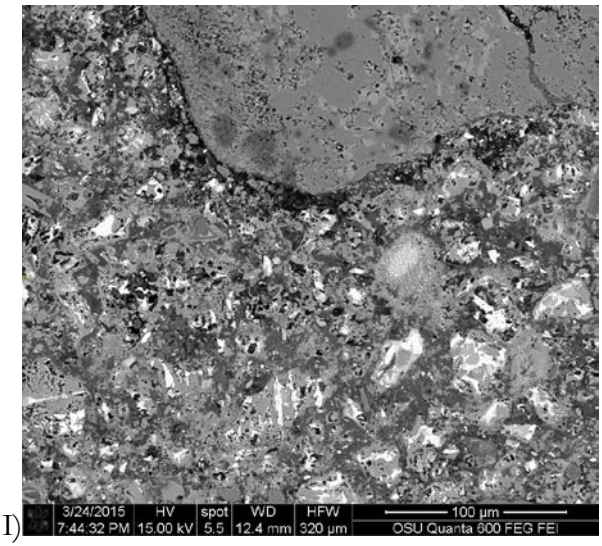

J) 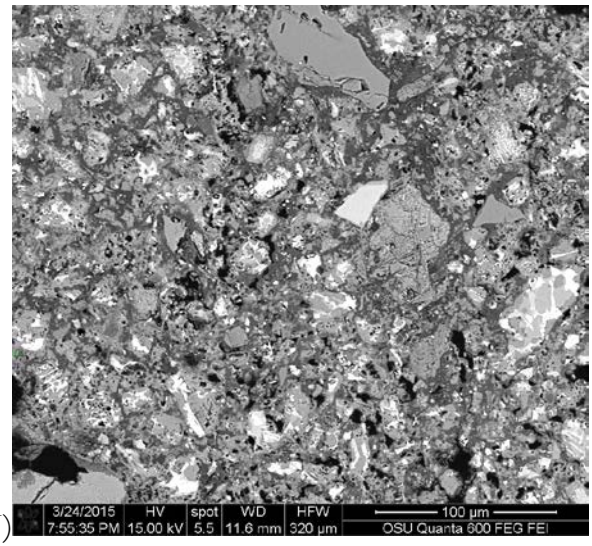

Figure B-16 A-J: BSE-SEM images of the KRC system at Day 3

B.1.2.3 Day 7

Figure B-17 A-F presents selected BSE-SEM images used for measuring porosity and examining microstructure of the KRC system at Day 7.

A) 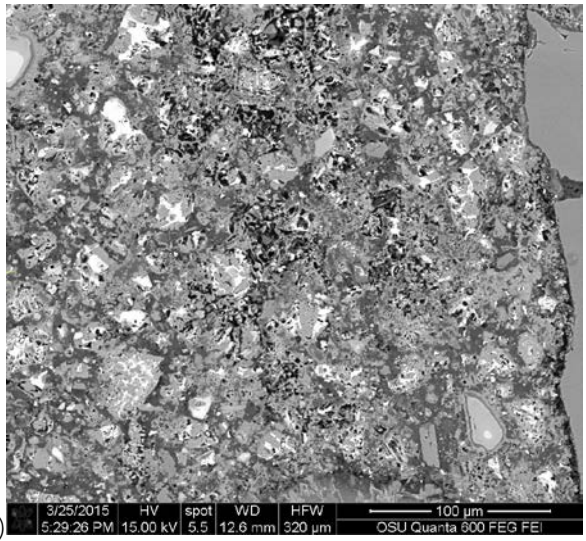

B) 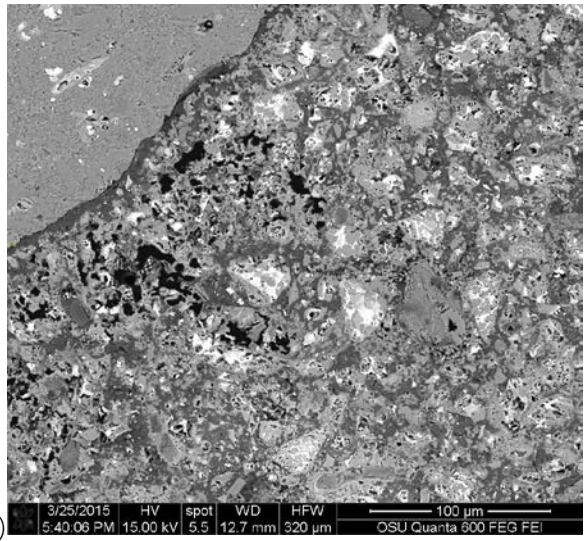

C) 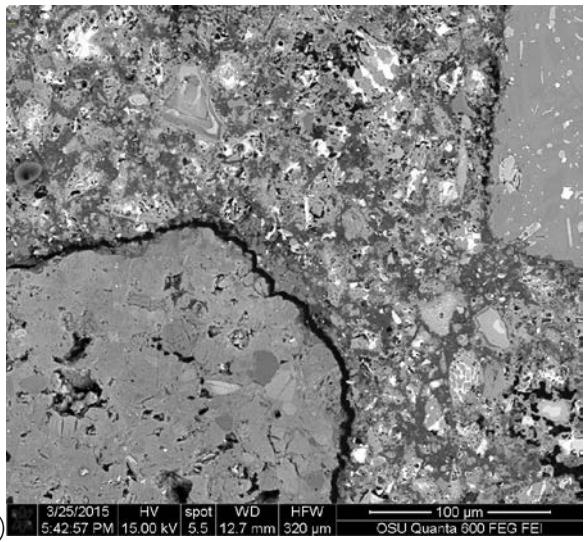
3/25/2015 5:42:57 PM
HV 15.00 kV
spot 5.5
WD 12.7 mm
HFW 320 µm
100 µm
OSU Quanta 600 FEG FEI

D) 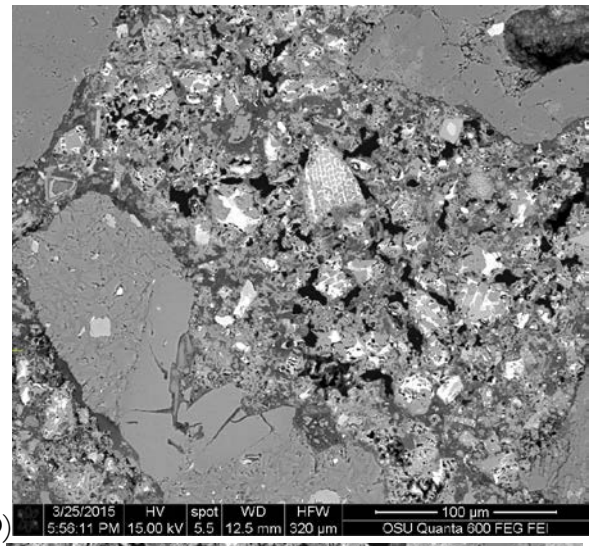
3/25/2015 5:58:11 PM
HV 15.00 kV
spot 5.5
WD 12.5 mm
HFW 320 µm
100 µm
OSU Quanta 600 FEG FEI

E) 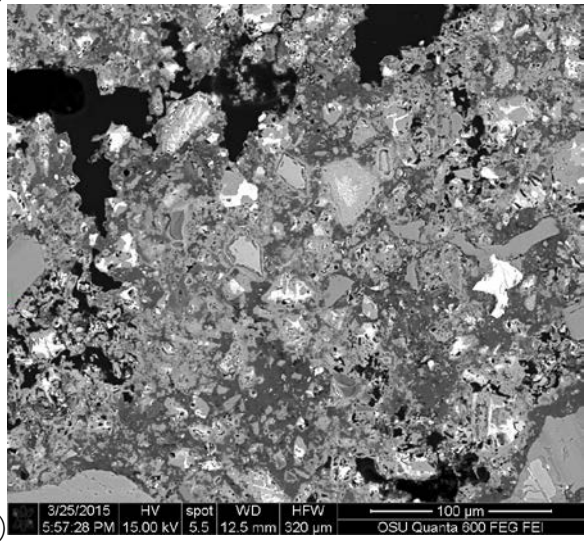
3/25/2015 5:57:28 PM
HV 15.00 kV
spot 5.5
WD 12.5 mm
HFW 320 µm
100 µm
OSU Quanta 600 FEG FEI

F) 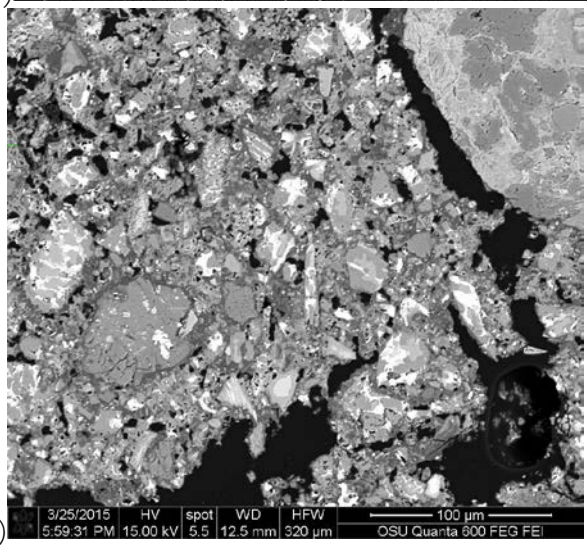
3/25/2015 5:59:31 PM
HV 15.00 kV
spot 5.5
WD 12.5 mm
HFW 320 µm
100 µm
OSU Quanta 600 FEG FEI

G) 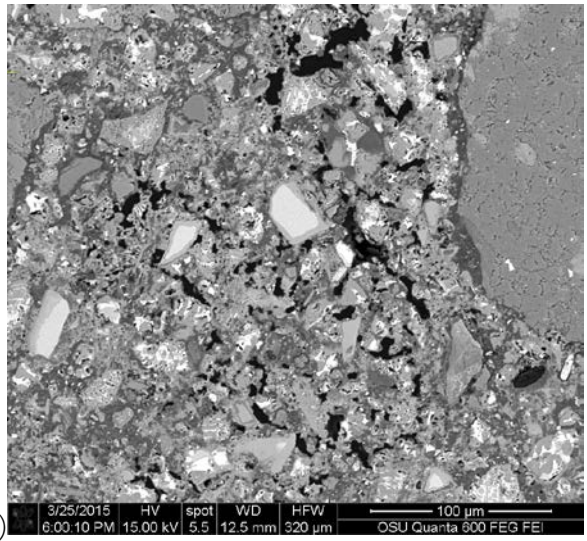
3/25/2015 6:00:10 PM
HV 15.00 kV
spot 5.5
WD 12.5 mm
HFW 320 µm
100 µm
OSU Quanta 600 FEG FEI

H) 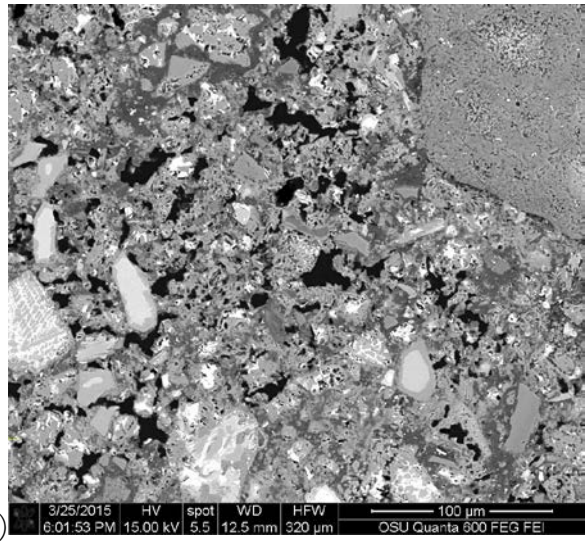
3/25/2015 6:01:53 PM
HV 15.00 kV
spot 5.5
WD 12.5 mm
HFW 320 µm
100 µm
OSU Quanta 600 FEG FEI

I) 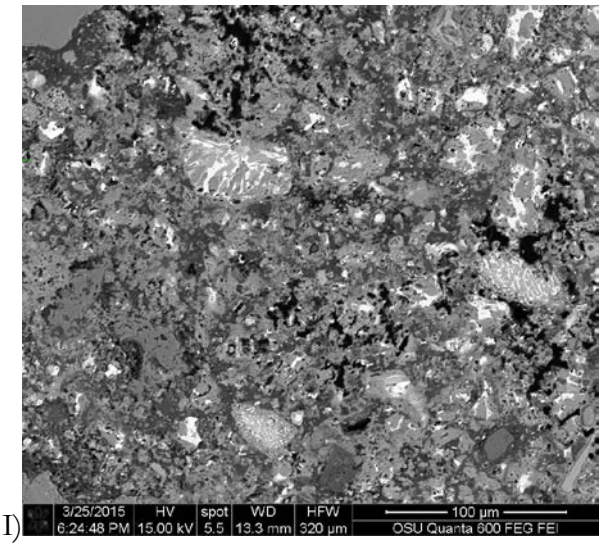

J) 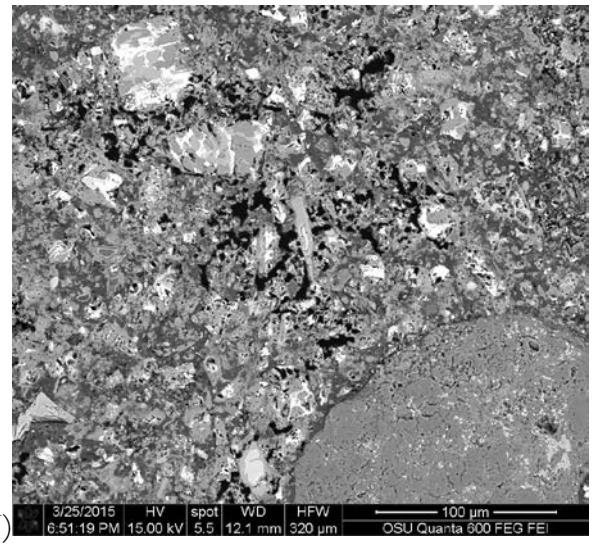

Figure B-17 A-J: BSE-SEM images of the KRC system at Day 7

B.1.2.4 Day 14

Figure B-18 A-F presents selected BSE-SEM images used for measuring porosity and examining microstructure of the KRC system at Day 14.

A) 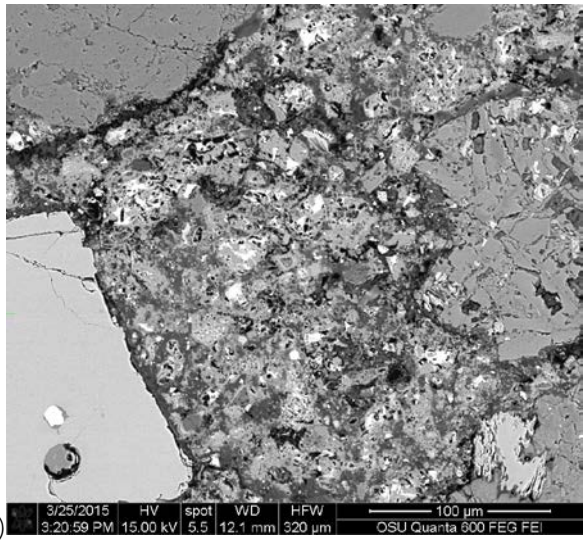

B) 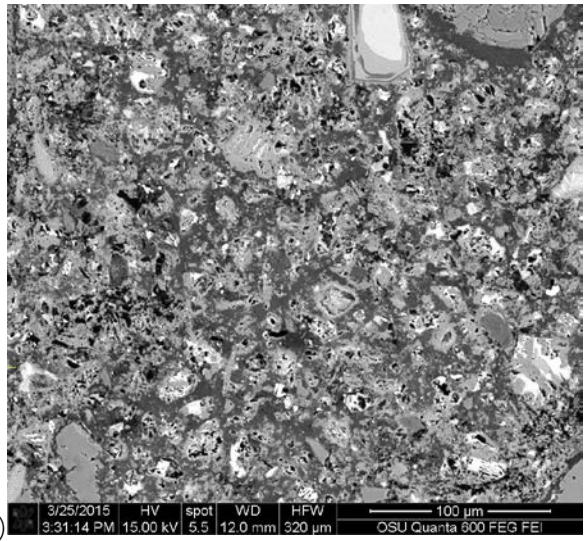

C) 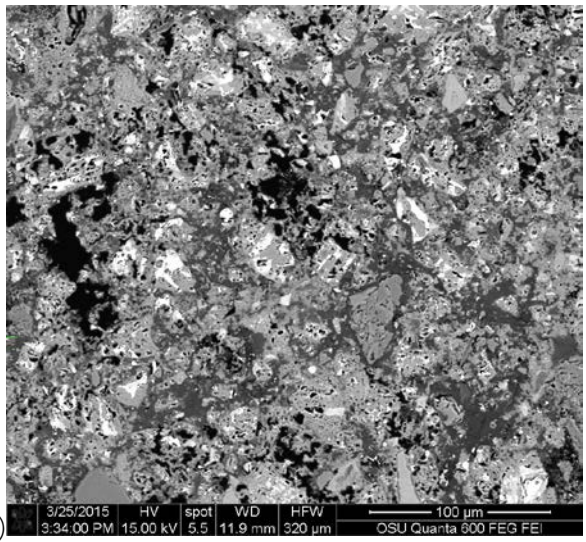
3/25/2015 3:34:00 PM
HV 15.00 kV
spot 5.5
WD 11.9 mm
HFW 320 µm
100 µm
OSU Quanta 600 FEG FEI

D) 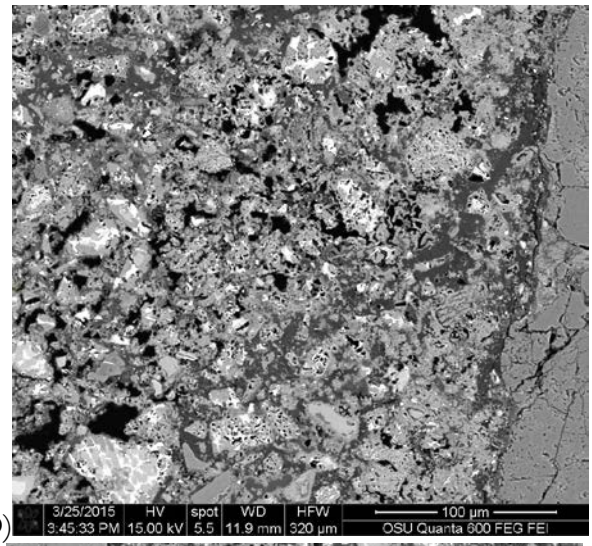
3/25/2015 3:45:33 PM
HV 15.00 kV
spot 5.5
WD 11.9 mm
HFW 320 µm
100 µm
OSU Quanta 600 FEG FEI

E) 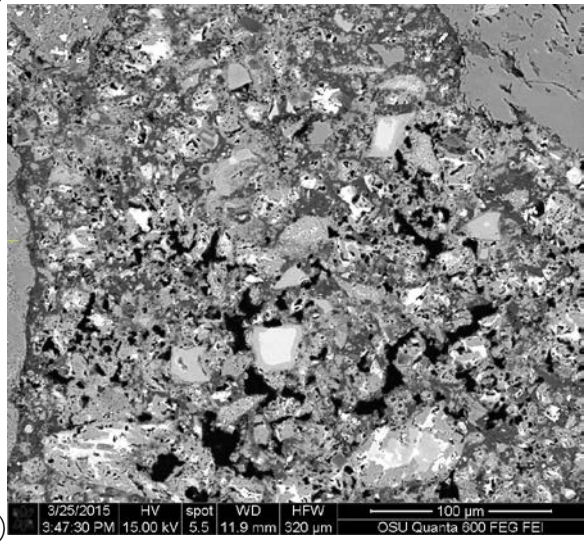
3/25/2015 3:47:30 PM
HV 15.00 kV
spot 5.5
WD 11.9 mm
HFW 320 µm
100 µm
OSU Quanta 600 FEG FEI

F) 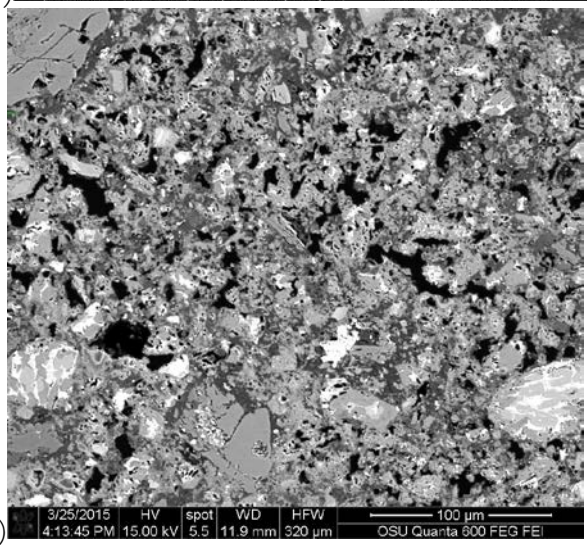
3/25/2015 4:13:45 PM
HV 15.00 kV
spot 5.5
WD 11.9 mm
HFW 320 µm
100 µm
OSU Quanta 600 FEG FEI

G) 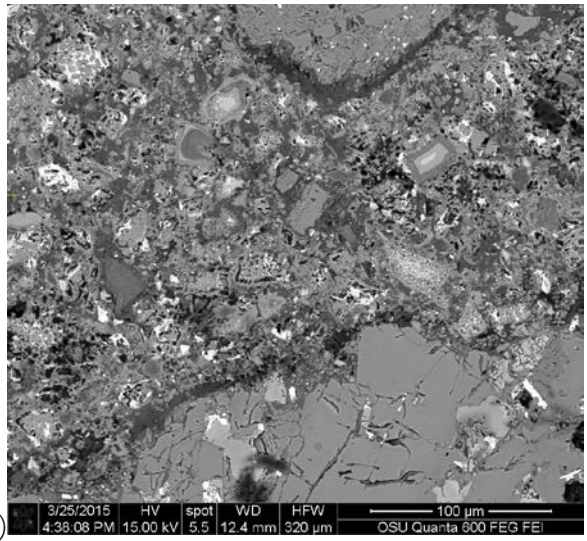
3/25/2015 4:38:08 PM
HV 15.00 kV
spot 5.5
WD 12.4 mm
HFW 320 µm
100 µm
OSU Quanta 600 FEG FEI

H) 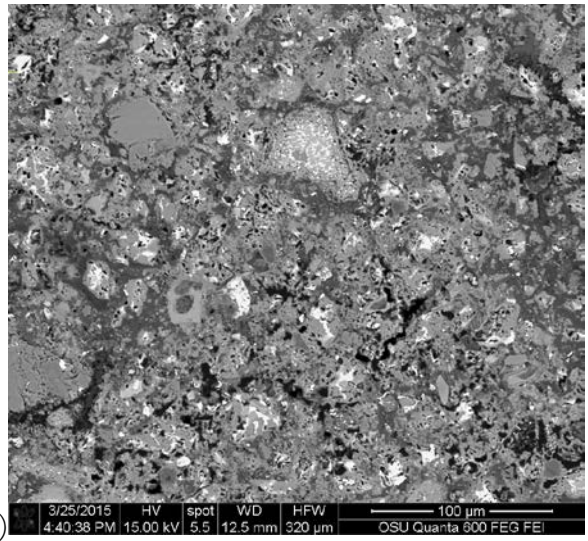
3/25/2015 4:40:38 PM
HV 15.00 kV
spot 5.5
WD 12.5 mm
HFW 320 µm
100 µm
OSU Quanta 600 FEG FEI

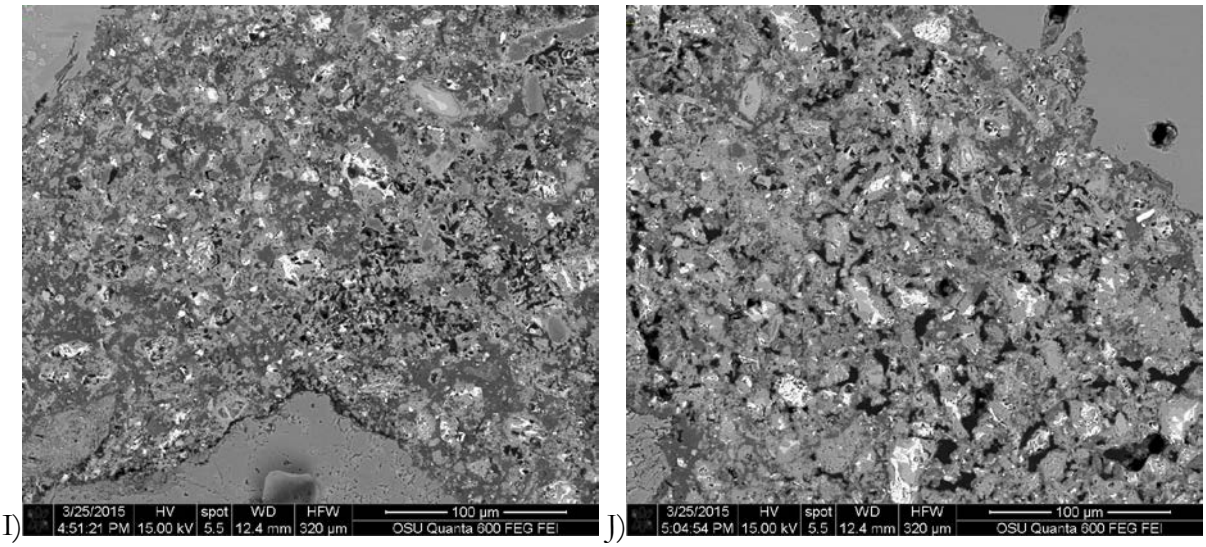

Figure B-18 A-J: BSE-SEM images of the KRC system at Day 14

B.1.3 Additional CRC System SEM Images

B.1.3.1 Day 1

Figure B-19 A-F presents selected BSE-SEM images used for measuring porosity and examining microstructure of the CRC system at Day 1.

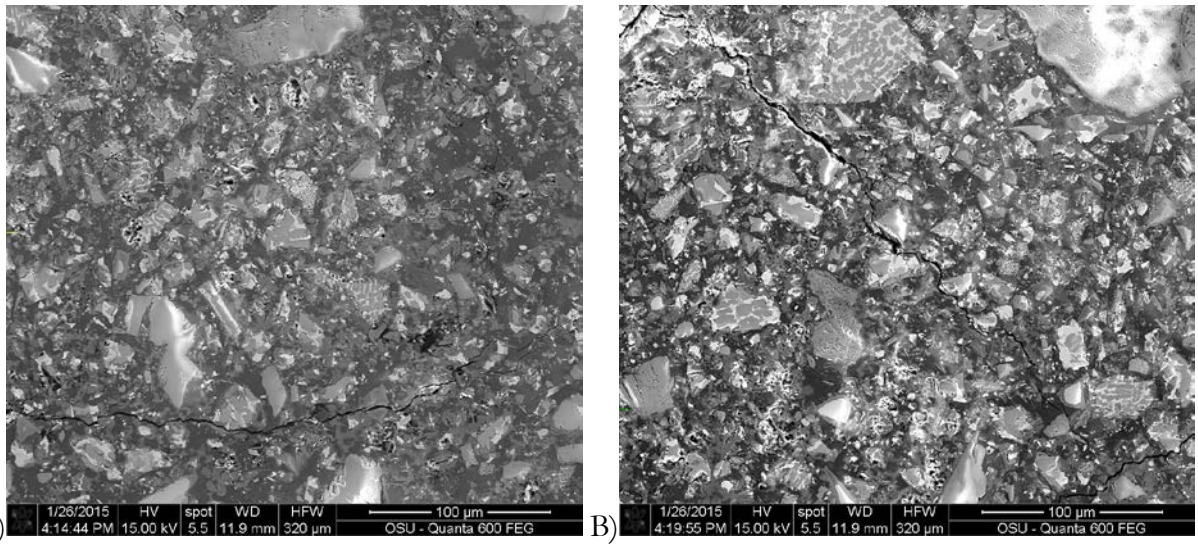

C) 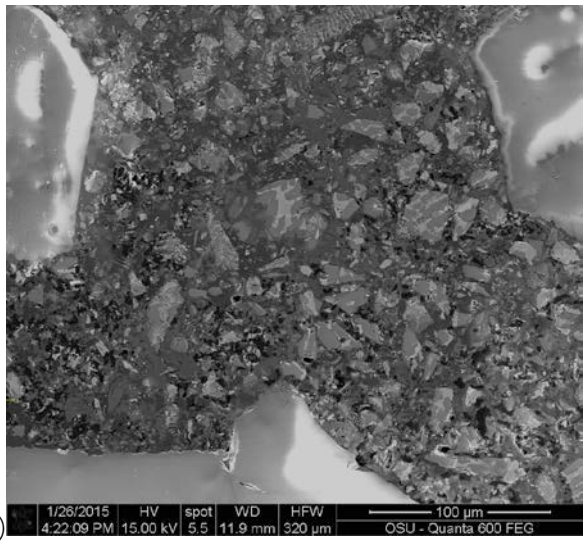
1/26/2015 4:22:09 PM
HV 15.00 kV
spot 5.5
WD 11.9 mm
HFW 320 µm
100 µm
OSU - Quanta 600 FEG

D) 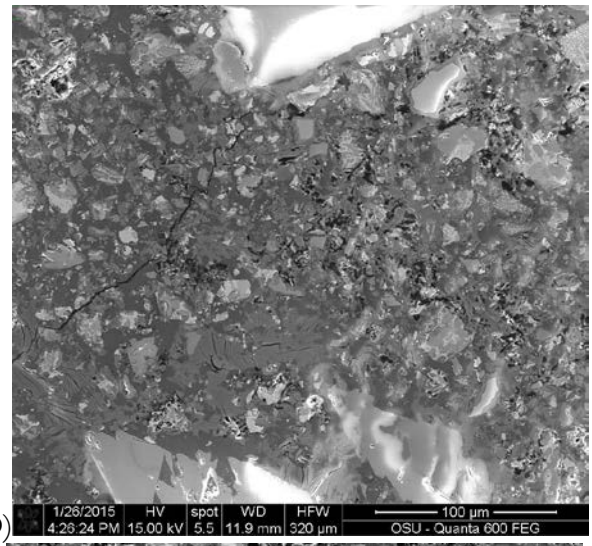
1/26/2015 4:26:24 PM
HV 15.00 kV
spot 5.5
WD 11.9 mm
HFW 320 µm
100 µm
OSU - Quanta 600 FEG

E) 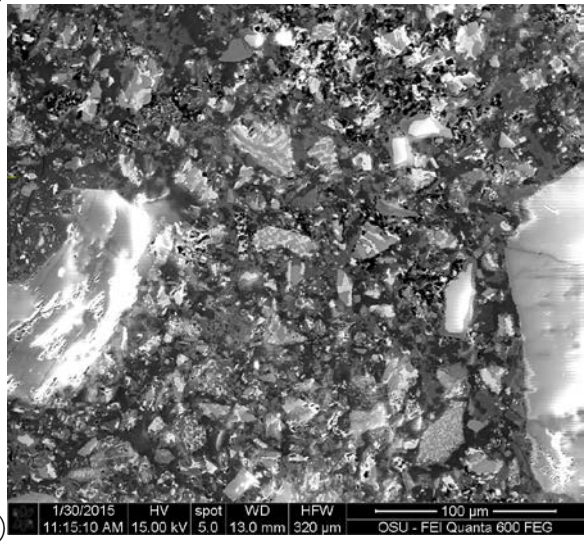
1/30/2015 11:15:10 AM
HV 15.00 kV
spot 5.0
WD 13.0 mm
HFW 320 µm
100 µm
OSU - FEI Quanta 600 FEG

F) 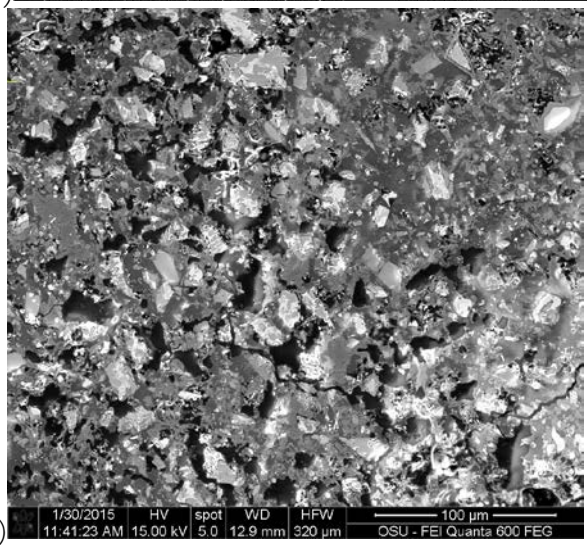
1/30/2015 11:41:23 AM
HV 15.00 kV
spot 5.0
WD 12.9 mm
HFW 320 µm
100 µm
OSU - FEI Quanta 600 FEG

G) 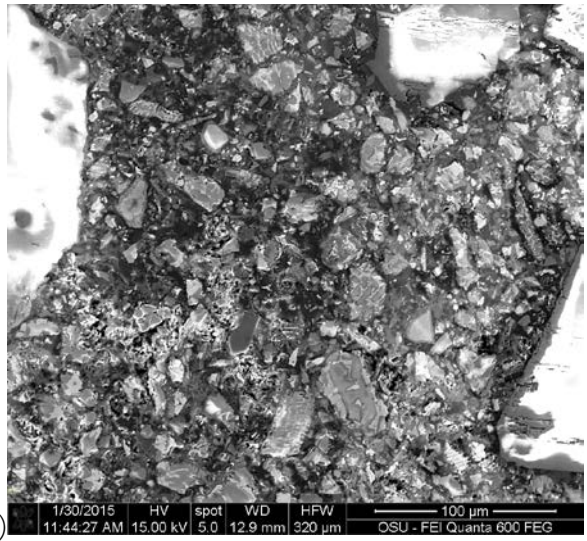
1/30/2015 11:44:27 AM
HV 15.00 kV
spot 5.0
WD 12.9 mm
HFW 320 µm
100 µm
OSU - FEI Quanta 600 FEG

H) 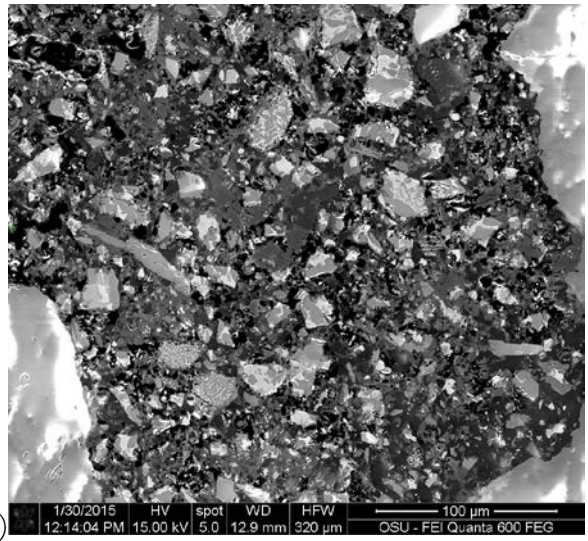
1/30/2015 12:14:04 PM
HV 15.00 kV
spot 5.0
WD 12.9 mm
HFW 320 µm
100 µm
OSU - FEI Quanta 600 FEG

I) 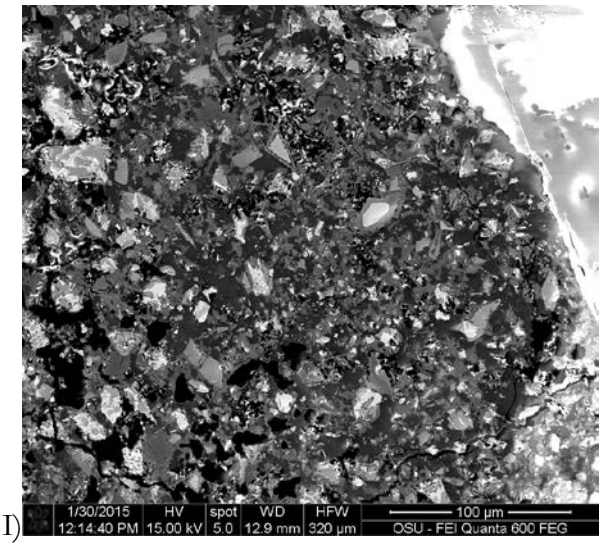

J) 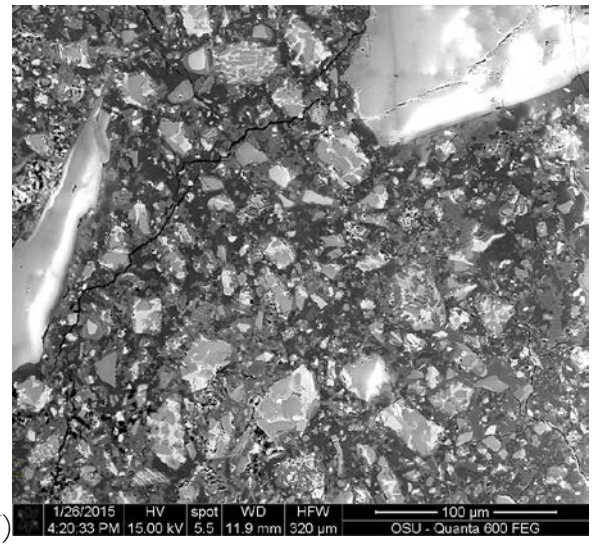

Figure B-19 A-J: BSE-SEM images of the CRC system at Day 1

B.1.3.2 Day 3

Figure B-20 A-F presents selected BSE-SEM images used for measuring porosity and examining microstructure of the CRC system at Day 3.

A) 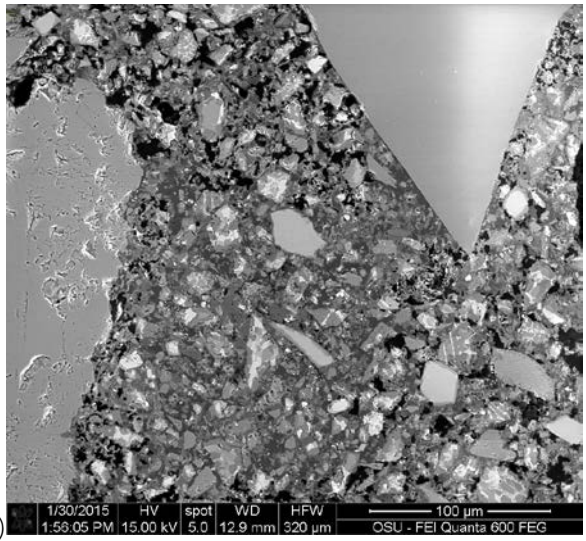

B) 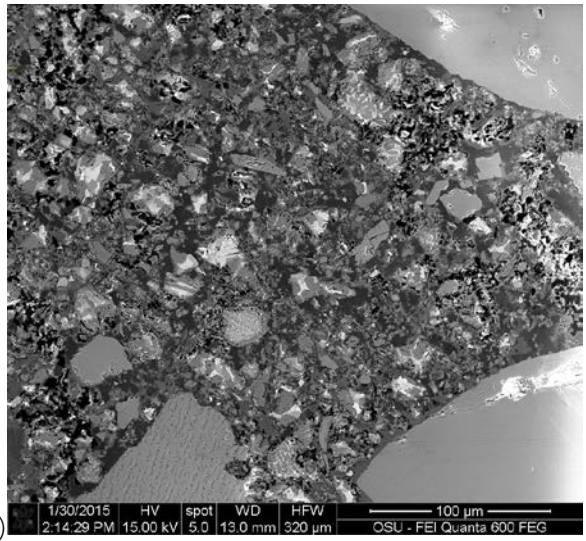

C) 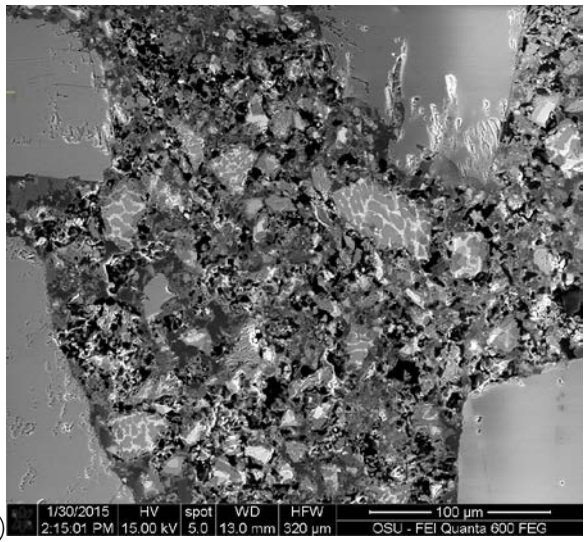
1/30/2015 HV spot WD HFW 100 µm
2:15:01 PM 15.00 kV 5.0 13.0 mm 320 µm OSU - FEI Quanta 600 FEG

D) 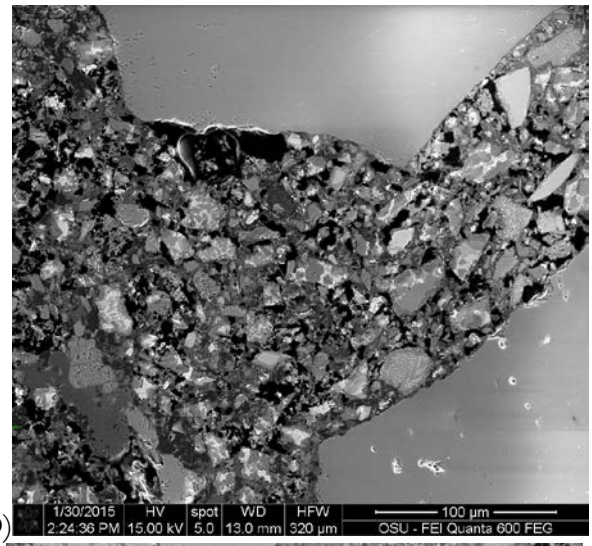
1/30/2015 HV spot WD HFW 100 µm
2:24:36 PM 15.00 kV 5.0 13.0 mm 320 µm OSU - FEI Quanta 600 FEG

E) 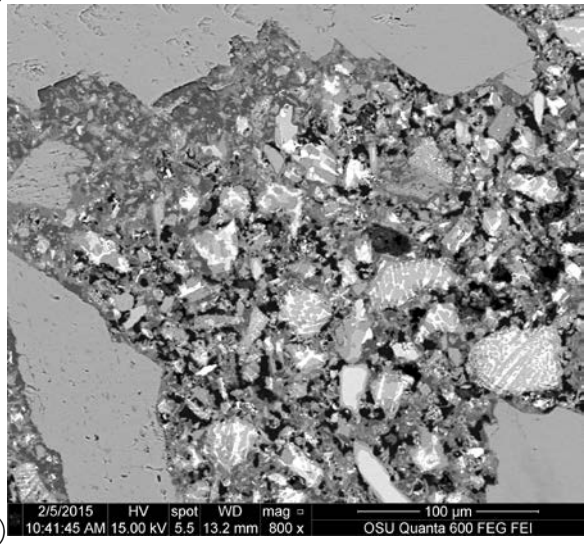
2/5/2015 HV spot WD mag 100 µm
10:41:45 AM 15.00 kV 5.5 13.2 mm 800 x OSU Quanta 600 FEG FEI

F) 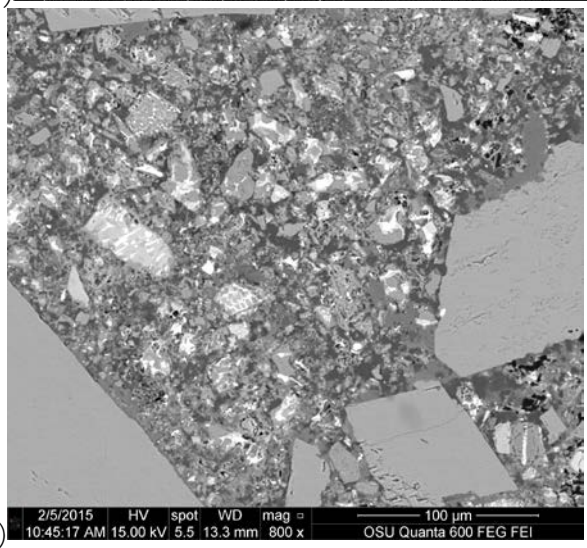
2/5/2015 HV spot WD mag 100 µm
10:45:17 AM 15.00 kV 5.5 13.3 mm 800 x OSU Quanta 600 FEG FEI

G) 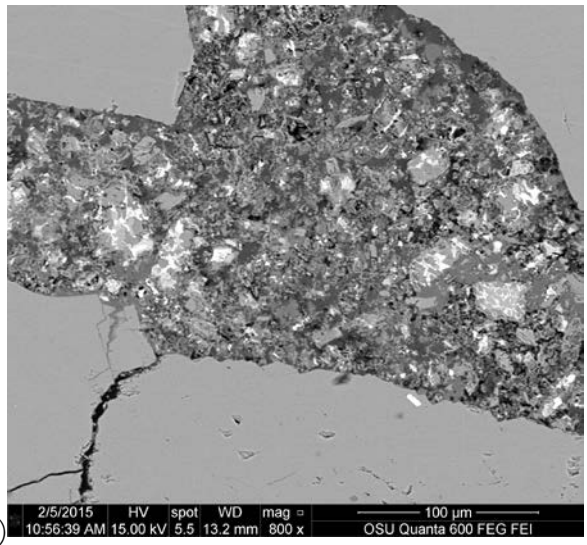
2/5/2015 HV spot WD mag 100 µm
10:56:39 AM 15.00 kV 5.5 13.2 mm 800 x OSU Quanta 600 FEG FEI

H) 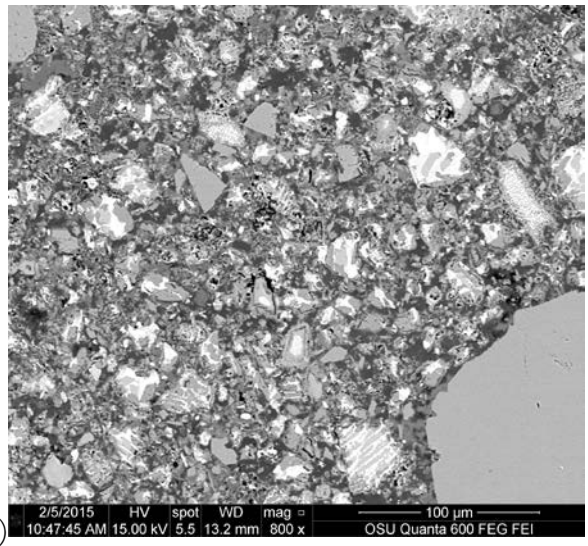
2/5/2015 HV spot WD mag 100 µm
10:47:45 AM 15.00 kV 5.5 13.2 mm 800 x OSU Quanta 600 FEG FEI

I) 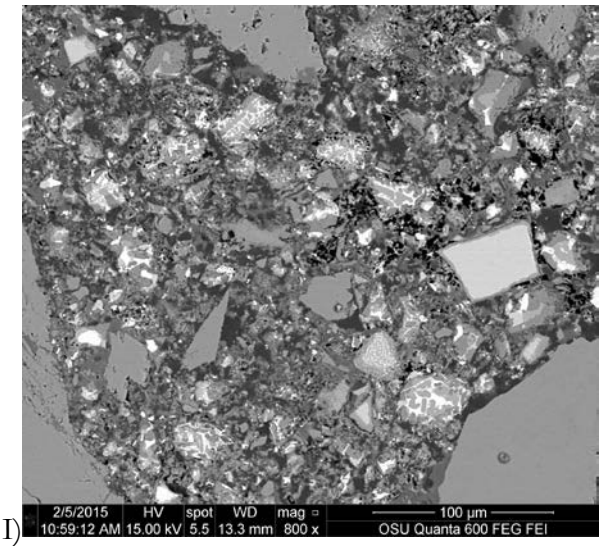

J) 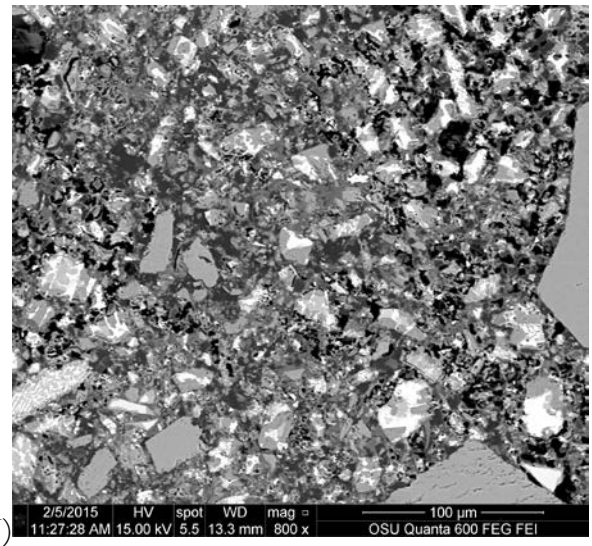

Figure B-20 A-J: BSE-SEM images of the CRC system at Day 3

B.1.3.3 Day 7

Figure B-21 A-F presents selected BSE-SEM images used for measuring porosity and examining microstructure of the CRC system at Day 7.

A) 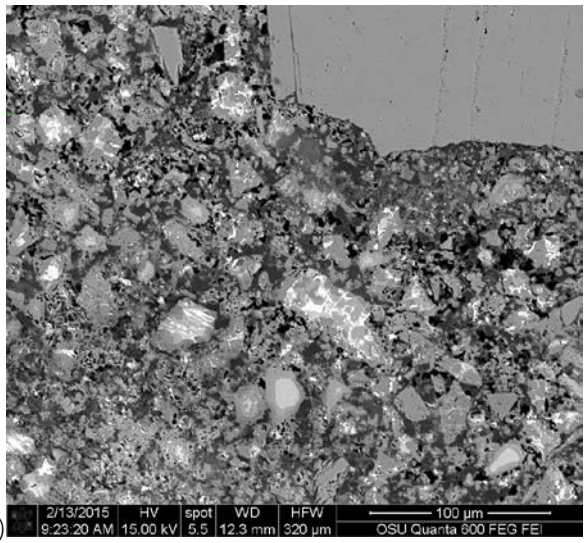

B) 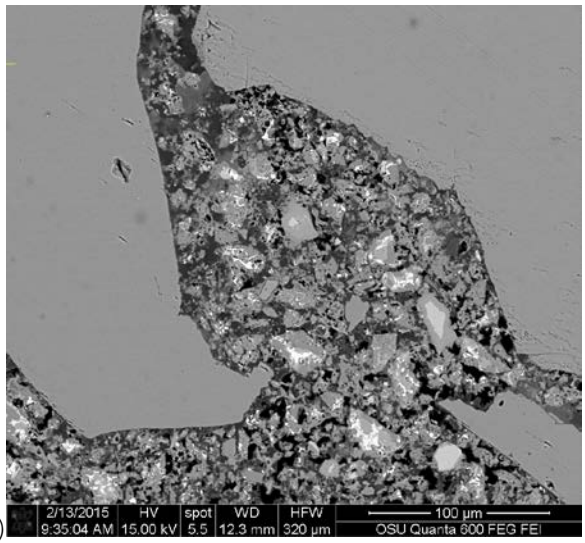

C) 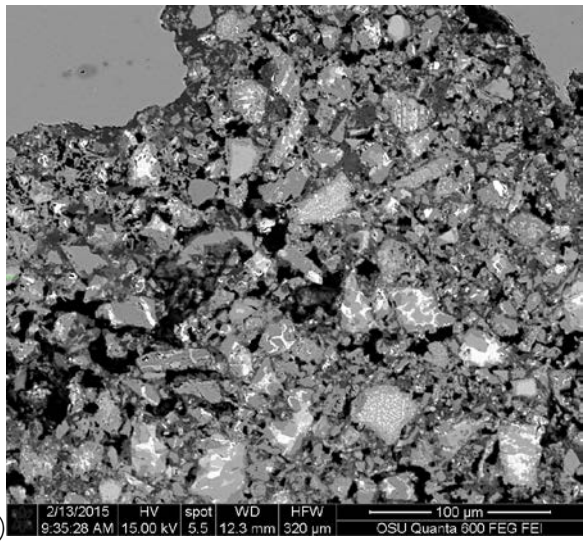
2/13/2015 9:35:28 AM
HV 15.00 kV
spot 5.5
WD 12.3 mm
HFW 320 µm
100 µm
OSU Quanta 600 FEG FEI

D) 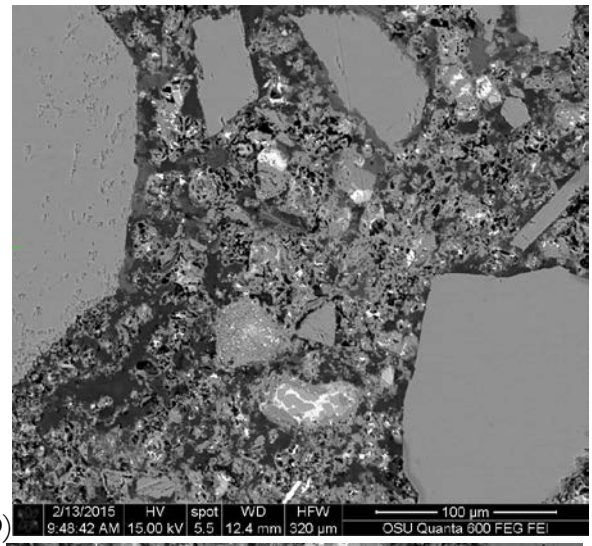
2/13/2015 9:48:42 AM
HV 15.00 kV
spot 5.5
WD 12.4 mm
HFW 320 µm
100 µm
OSU Quanta 600 FEG FEI

E) 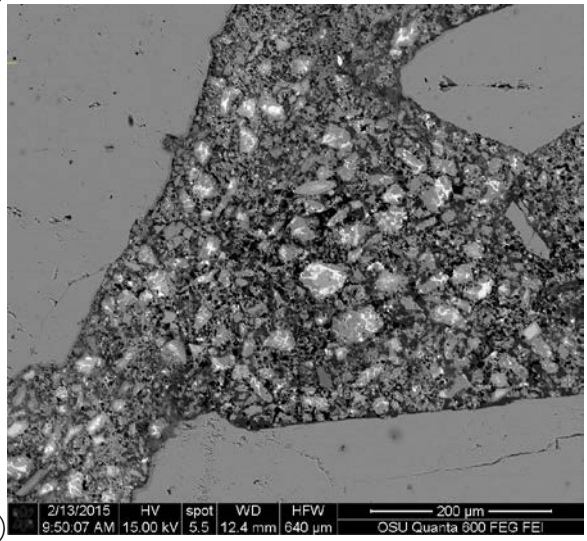
2/13/2015 9:50:07 AM
HV 15.00 kV
spot 5.5
WD 12.4 mm
HFW 640 µm
200 µm
OSU Quanta 600 FEG FEI

F) 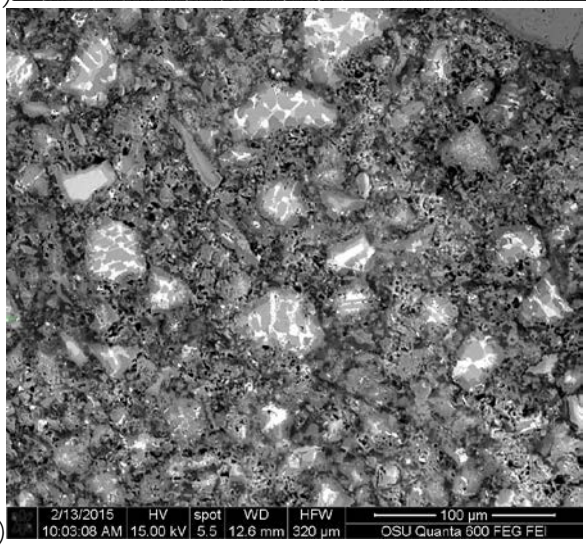
2/13/2015 10:03:08 AM
HV 15.00 kV
spot 5.5
WD 12.6 mm
HFW 320 µm
100 µm
OSU Quanta 600 FEG FEI

G) 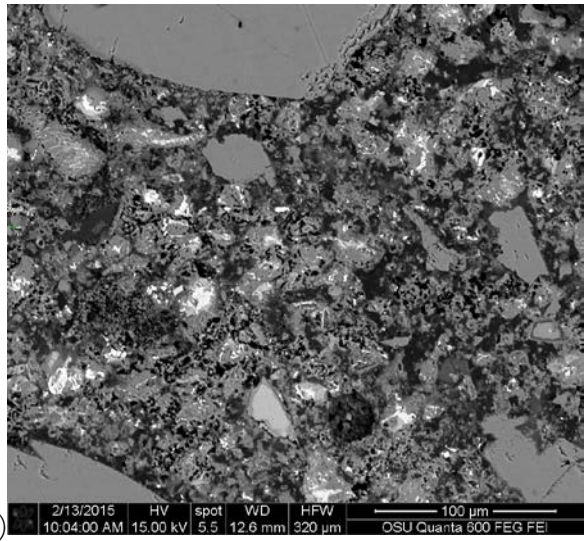
2/13/2015 10:04:00 AM
HV 15.00 kV
spot 5.5
WD 12.6 mm
HFW 320 µm
100 µm
OSU Quanta 600 FEG FEI

H) 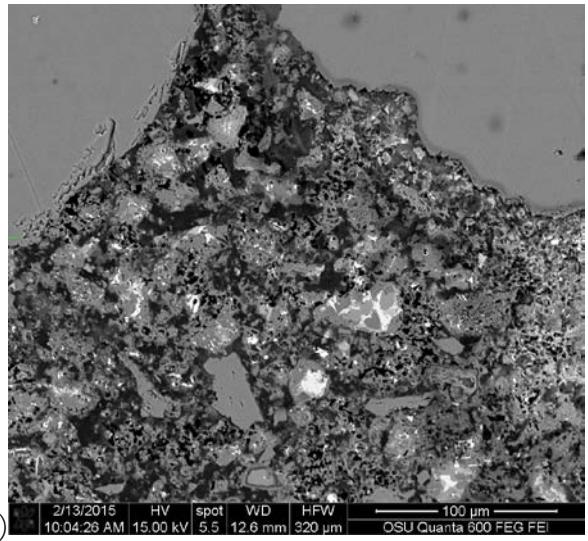
2/13/2015 10:04:26 AM
HV 15.00 kV
spot 5.5
WD 12.6 mm
HFW 320 µm
100 µm
OSU Quanta 600 FEG FEI

I) 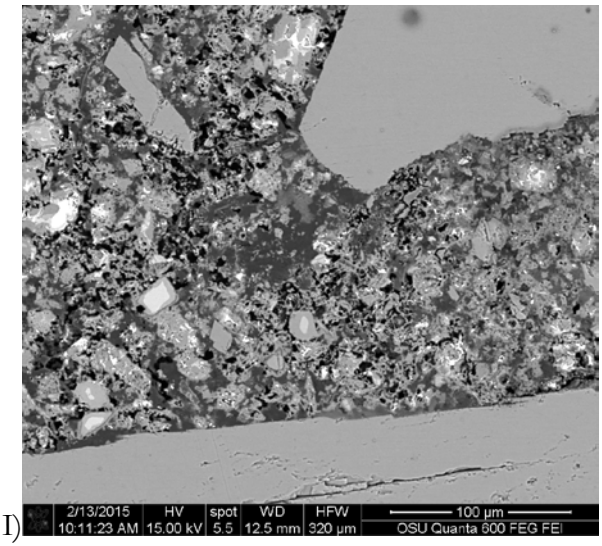

J) 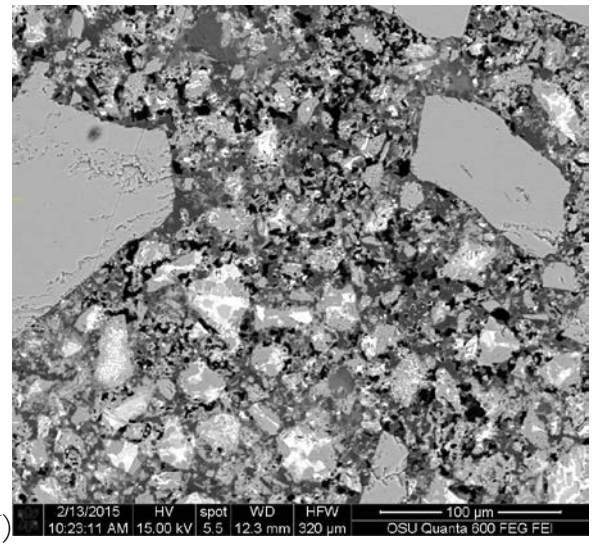

Figure B-21 A-J: BSE-SEM images of the CRC system at Day 7

B.1.3.4 Day 14

Figure B-22 A-F presents selected BSE-SEM images used for measuring porosity and examining microstructure of the CRC system at Day 14.

A) 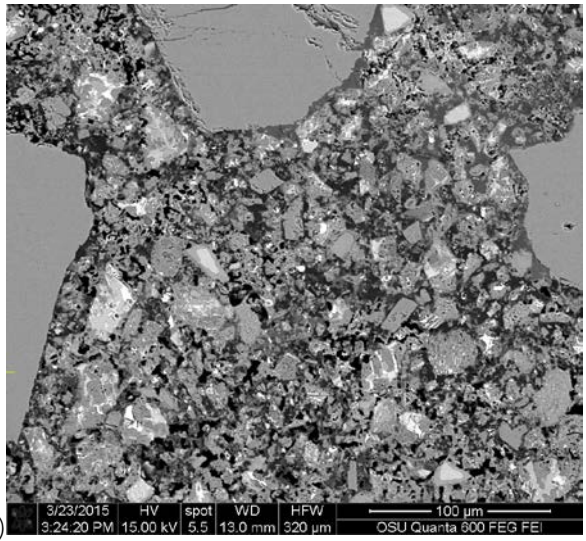

B) 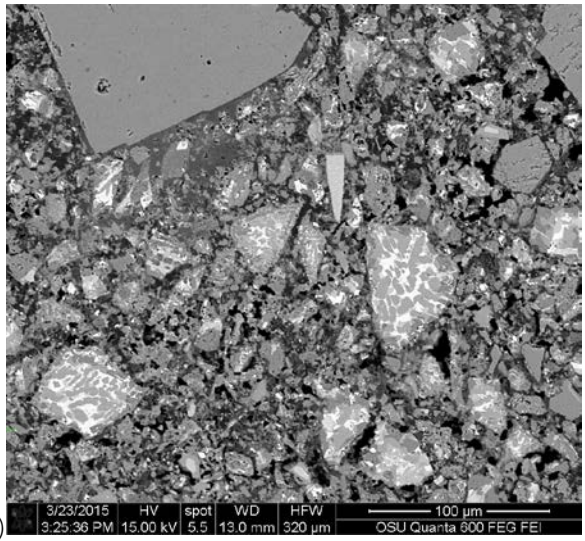

C) 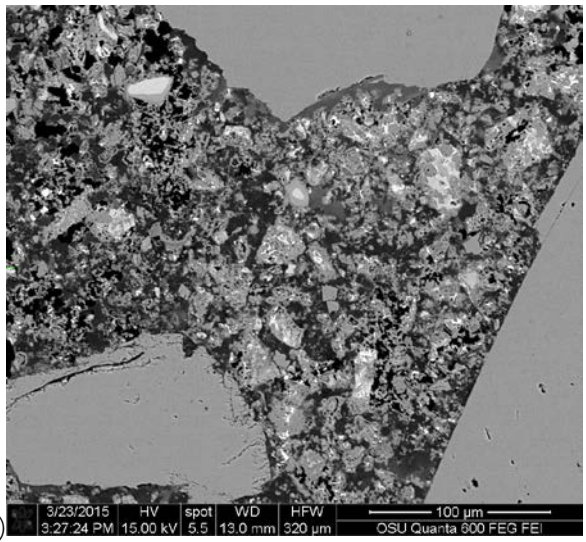
3/23/2015 3:27:24 PM
HV 15.00 kV
spot 5.5
WD 13.0 mm
HFW 320 µm
100 µm
OSU Quanta 600 FEG FEI

D) 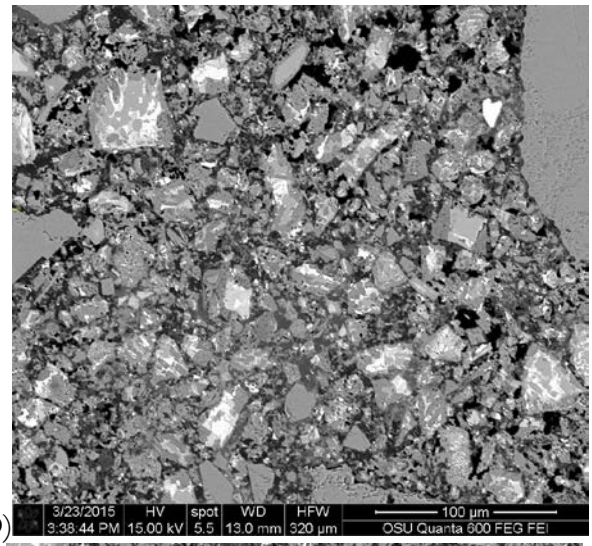
3/23/2015 3:38:44 PM
HV 15.00 kV
spot 5.5
WD 13.0 mm
HFW 320 µm
100 µm
OSU Quanta 600 FEG FEI

E) 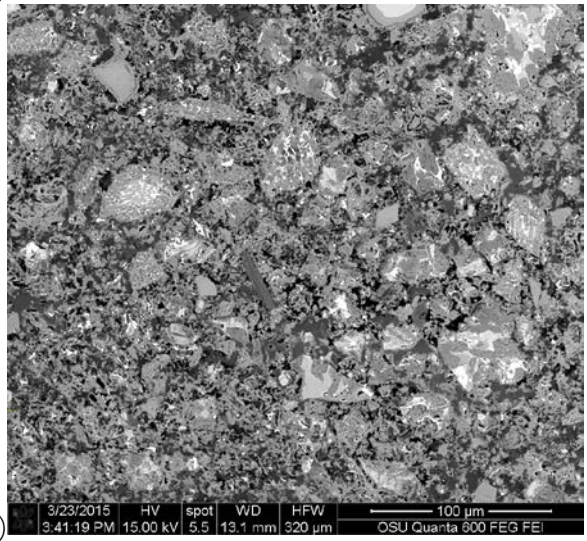
3/23/2015 3:41:19 PM
HV 15.00 kV
spot 5.5
WD 13.1 mm
HFW 320 µm
100 µm
OSU Quanta 600 FEG FEI

F) 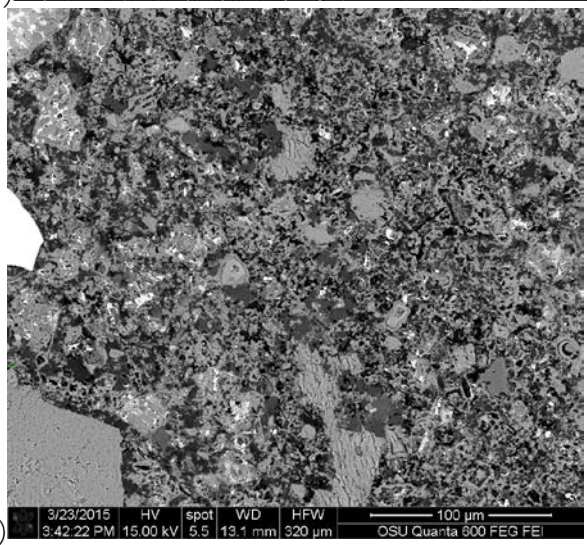
3/23/2015 3:42:22 PM
HV 15.00 kV
spot 5.5
WD 13.1 mm
HFW 320 µm
100 µm
OSU Quanta 600 FEG FEI

G) 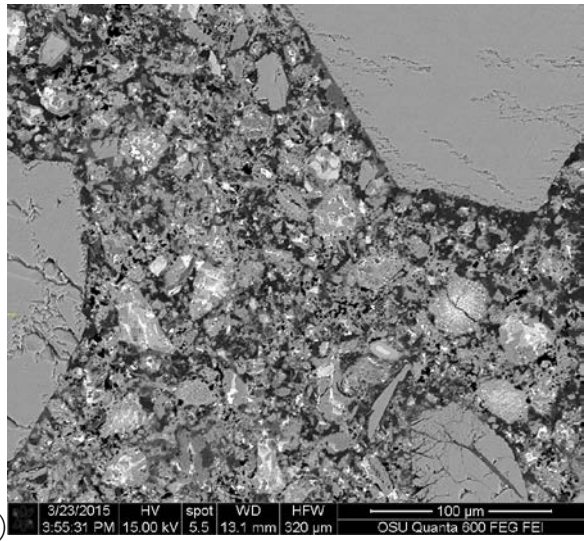
3/23/2015 3:55:31 PM
HV 15.00 kV
spot 5.5
WD 13.1 mm
HFW 320 µm
100 µm
OSU Quanta 600 FEG FEI

H) 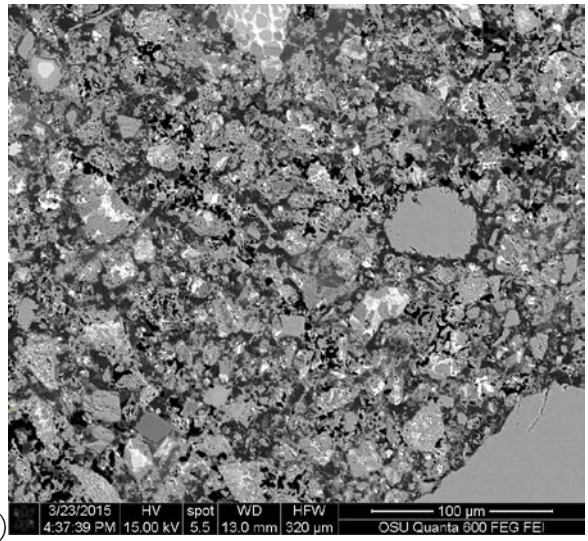
3/23/2015 4:37:39 PM
HV 15.00 kV
spot 5.5
WD 13.0 mm
HFW 320 µm
100 µm
OSU Quanta 600 FEG FEI

I) 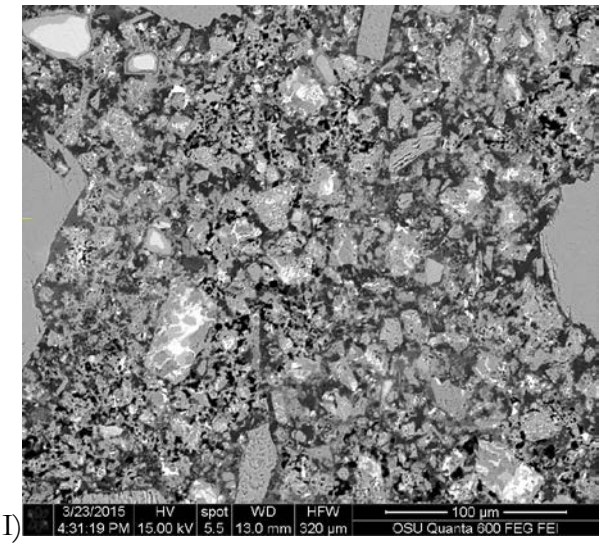

J) 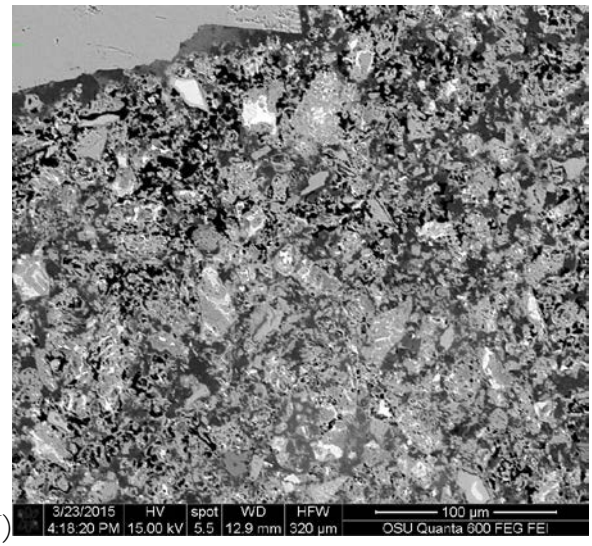

Figure B-22 A-J: BSE-SEM images of the CRC system at Day 14

B.1.4 Additional KRC System EDX Map

B.1.4.1 Day 1

Figure B-23 A and B presents selected BSE-SEM images with corresponding EDX maps used for examining microstructure of the KRC system at Day 1.

A)

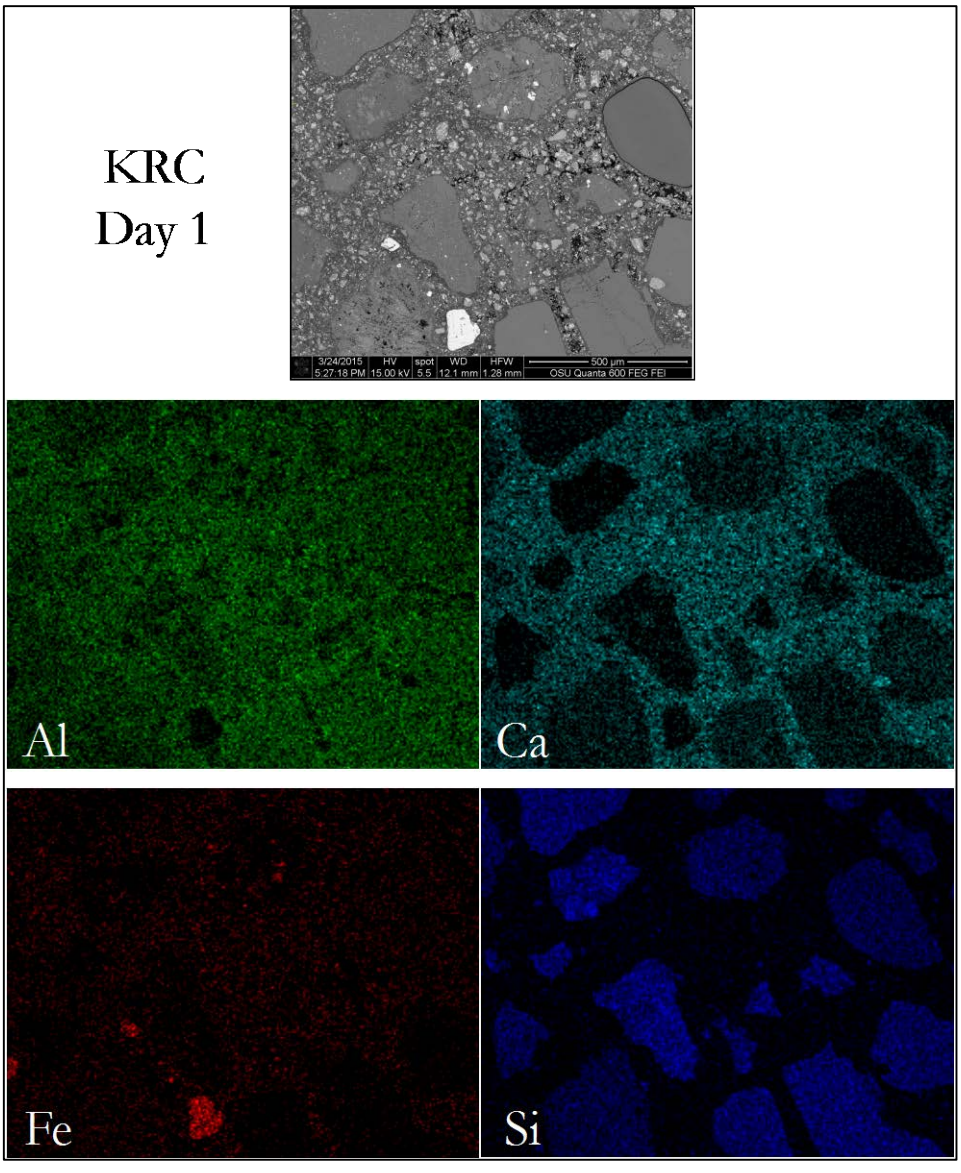

B)

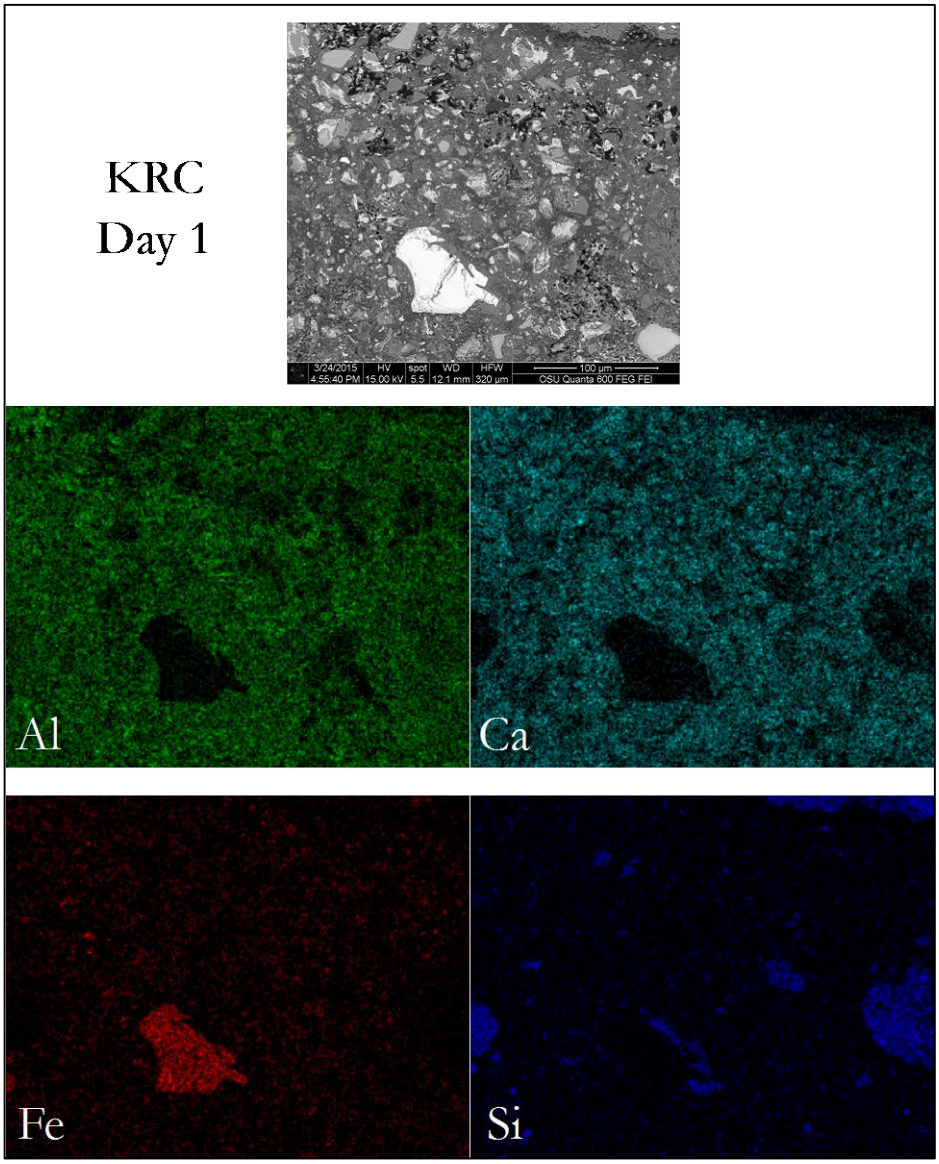

Figure B-23 A and B: Day 1 KRC EDX Map

B.1.4.2 Day 3

Figure B-24 A and B presents selected BSE-SEM images with corresponding EDX maps used for examining microstructure of the KRC system at Day 3.

A)

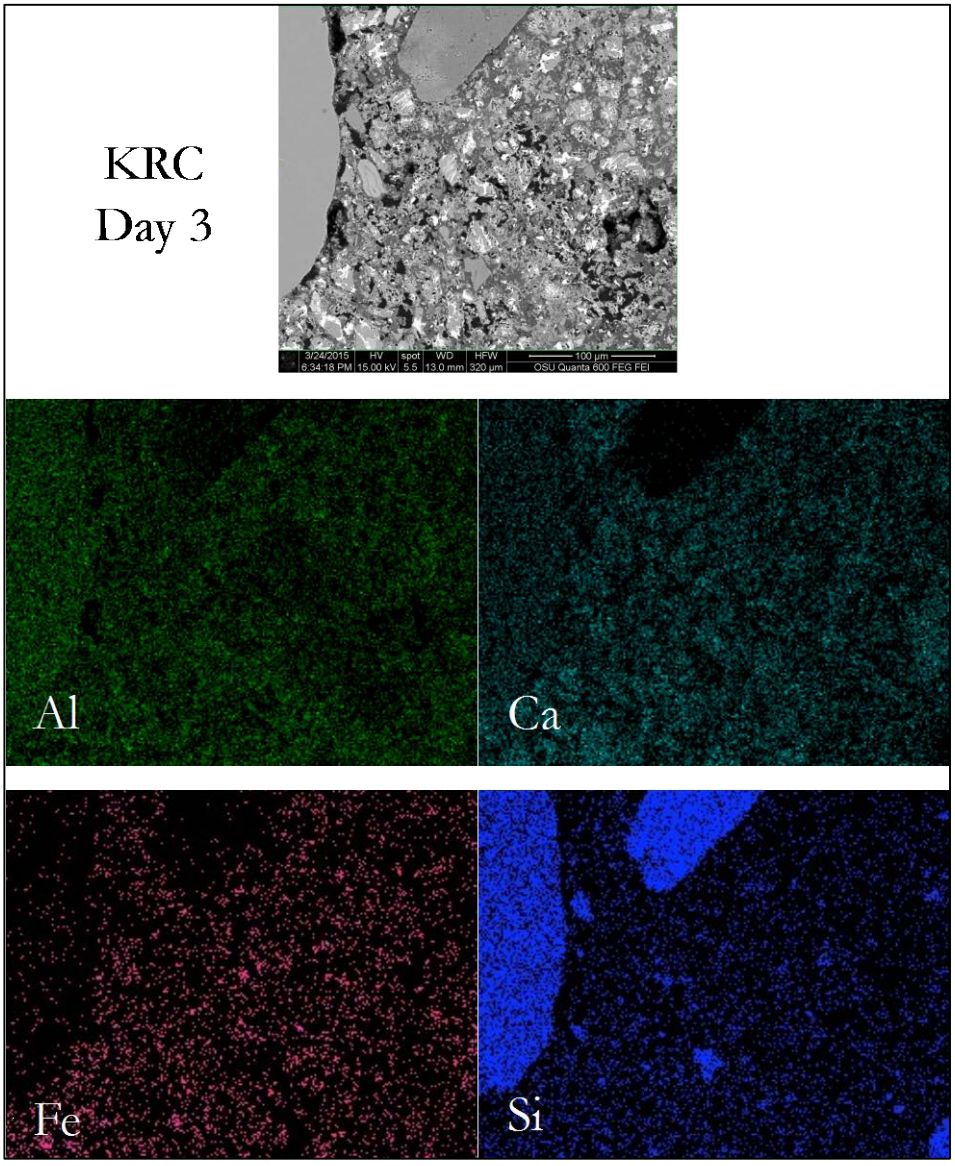

B)

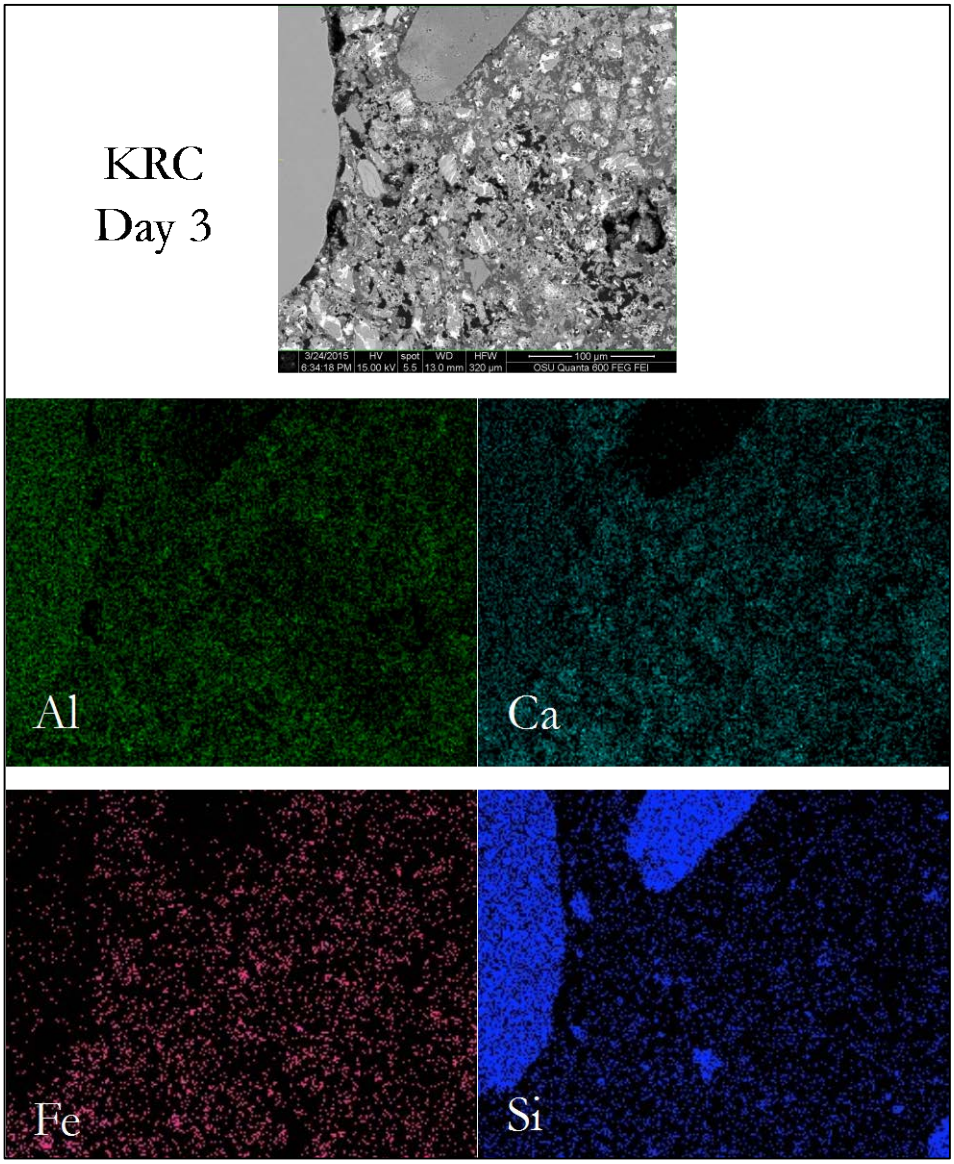

Figure B-24 A and B: Day 3 KRC EDX Map

B.1.4.3 Day 7

Figure B-25 A and B presents selected BSE-SEM images with corresponding EDX maps used for examining microstructure of the KRC system at Day 7.

A)

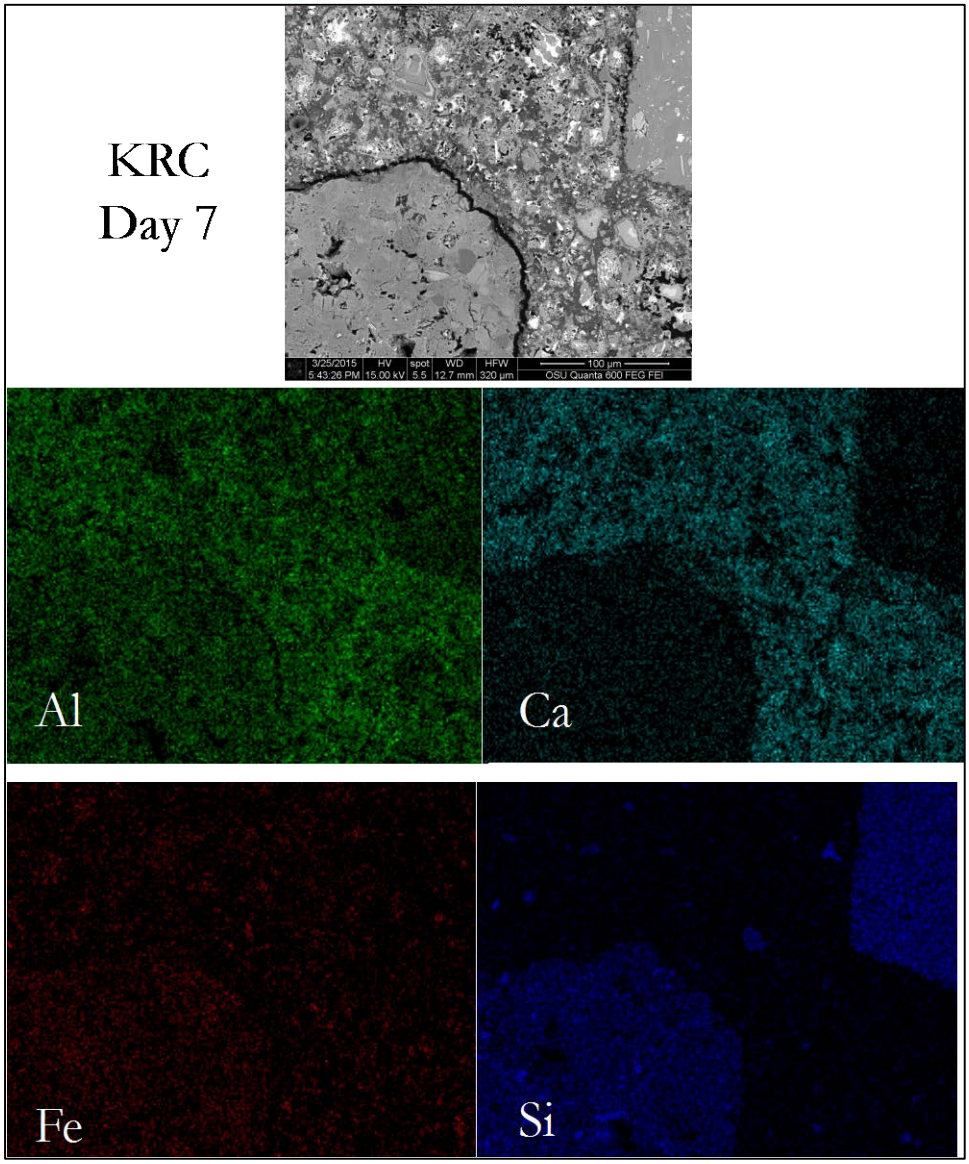

B)

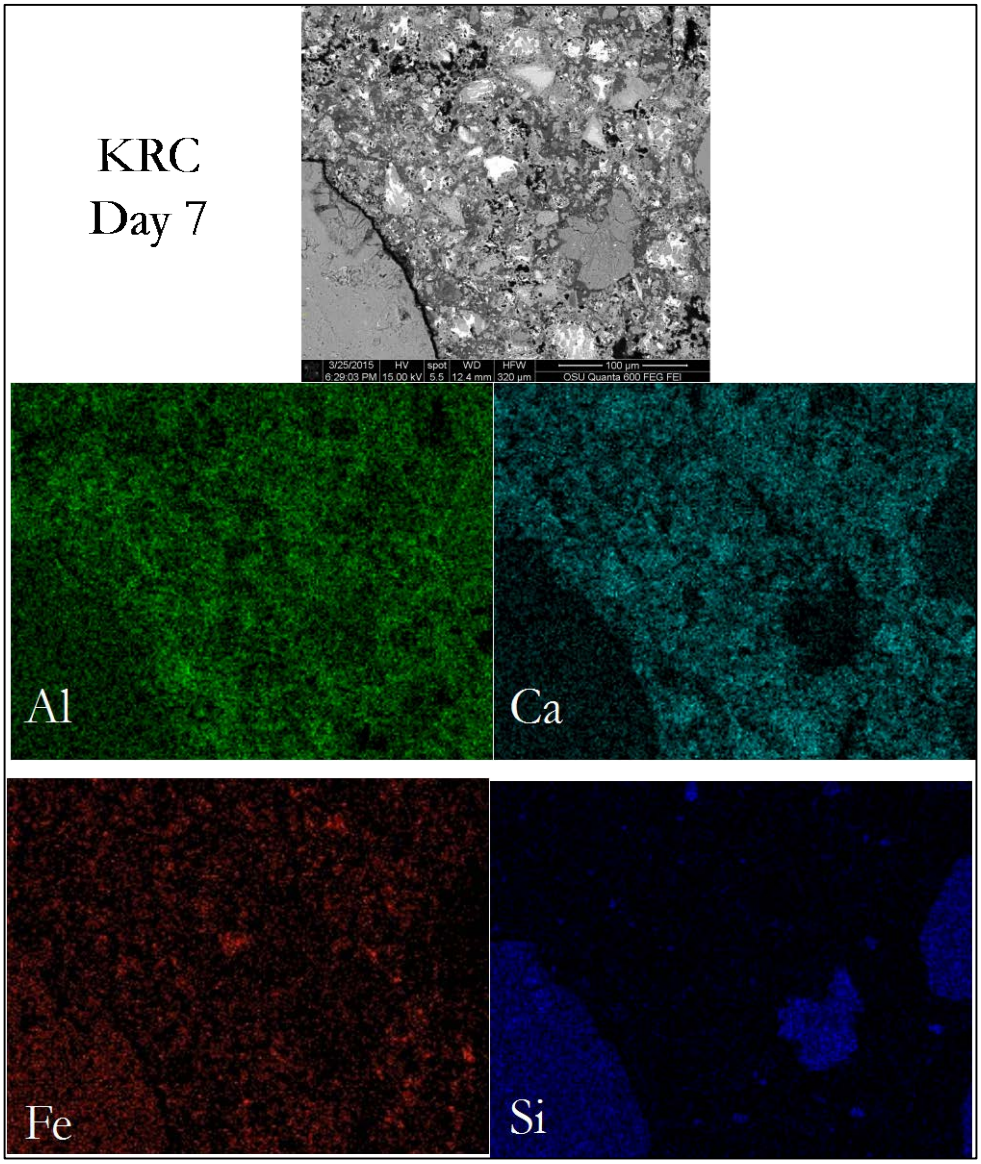

Figure B-25 A and B: Day 7 KRC EDX Map

B.1.4.4 Day 14

Figure B-26 A and B presents selected BSE-SEM images with corresponding EDX maps used for examining microstructure of the KRC system at Day 14.

A)

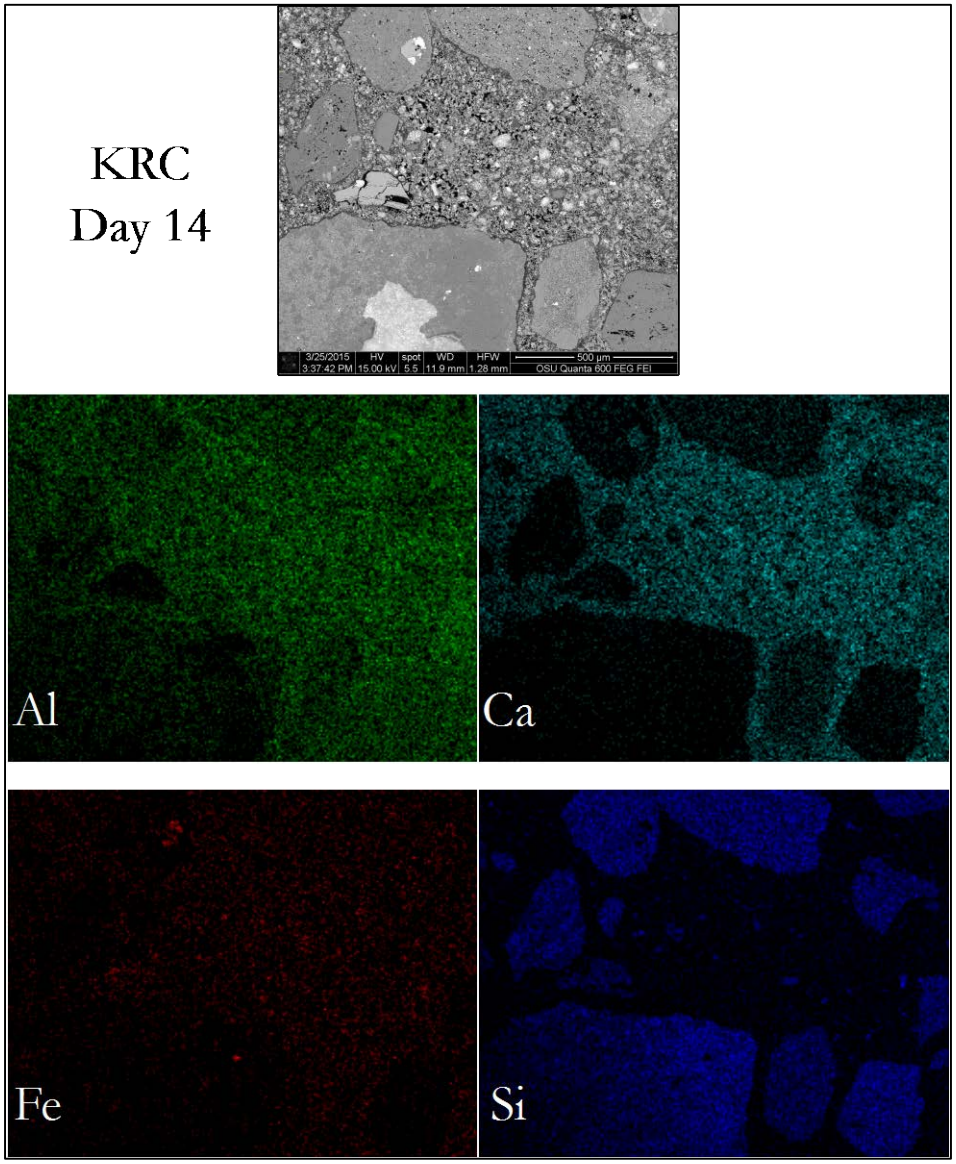

B)

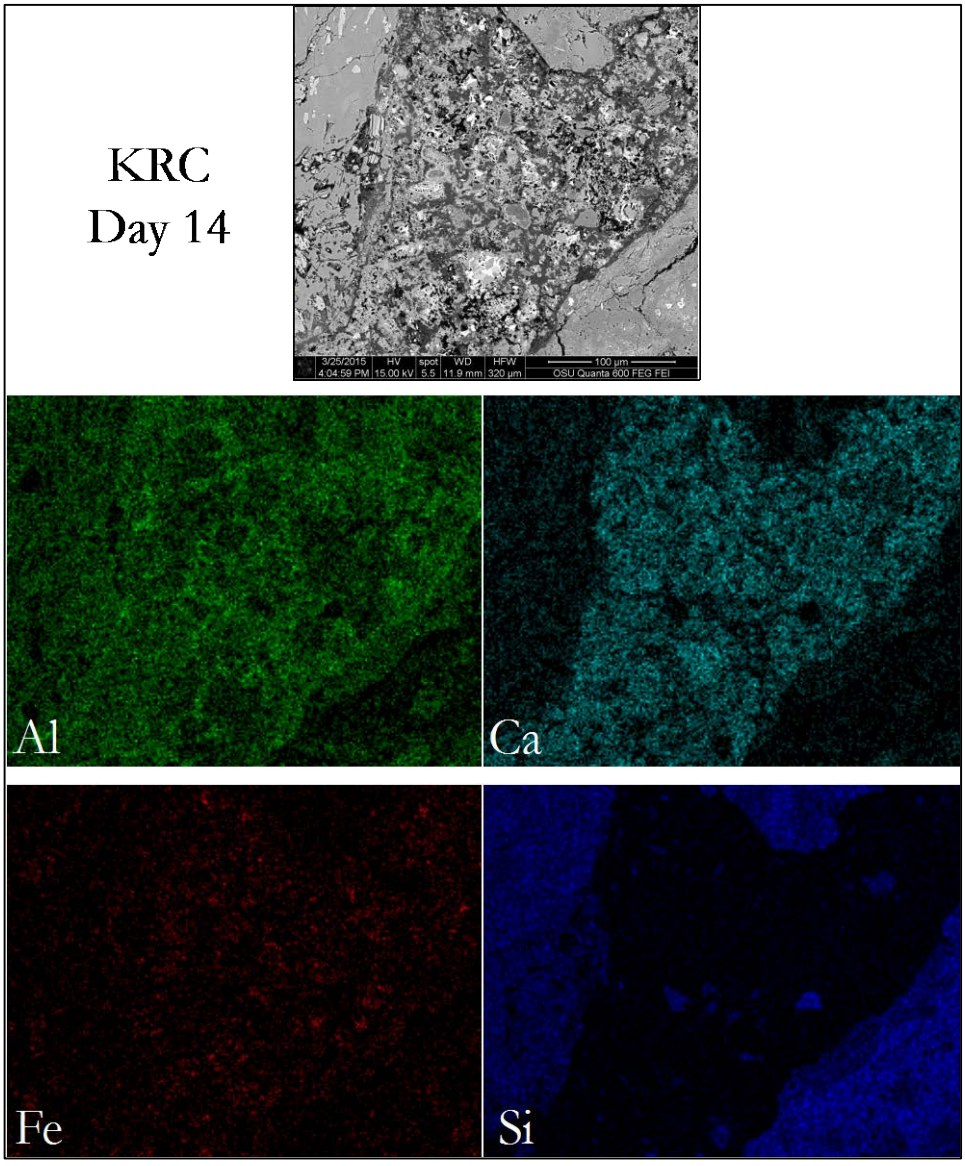

Figure B-26 A and B: Day 14 KRC EDX Map

B.1.5 Additional CRC System EDX Map

B.1.5.1 Day 1

Figure B-27 A and B presents selected BSE-SEM images with corresponding EDX maps used for examining microstructure of the CRC system at Day 1.

A)

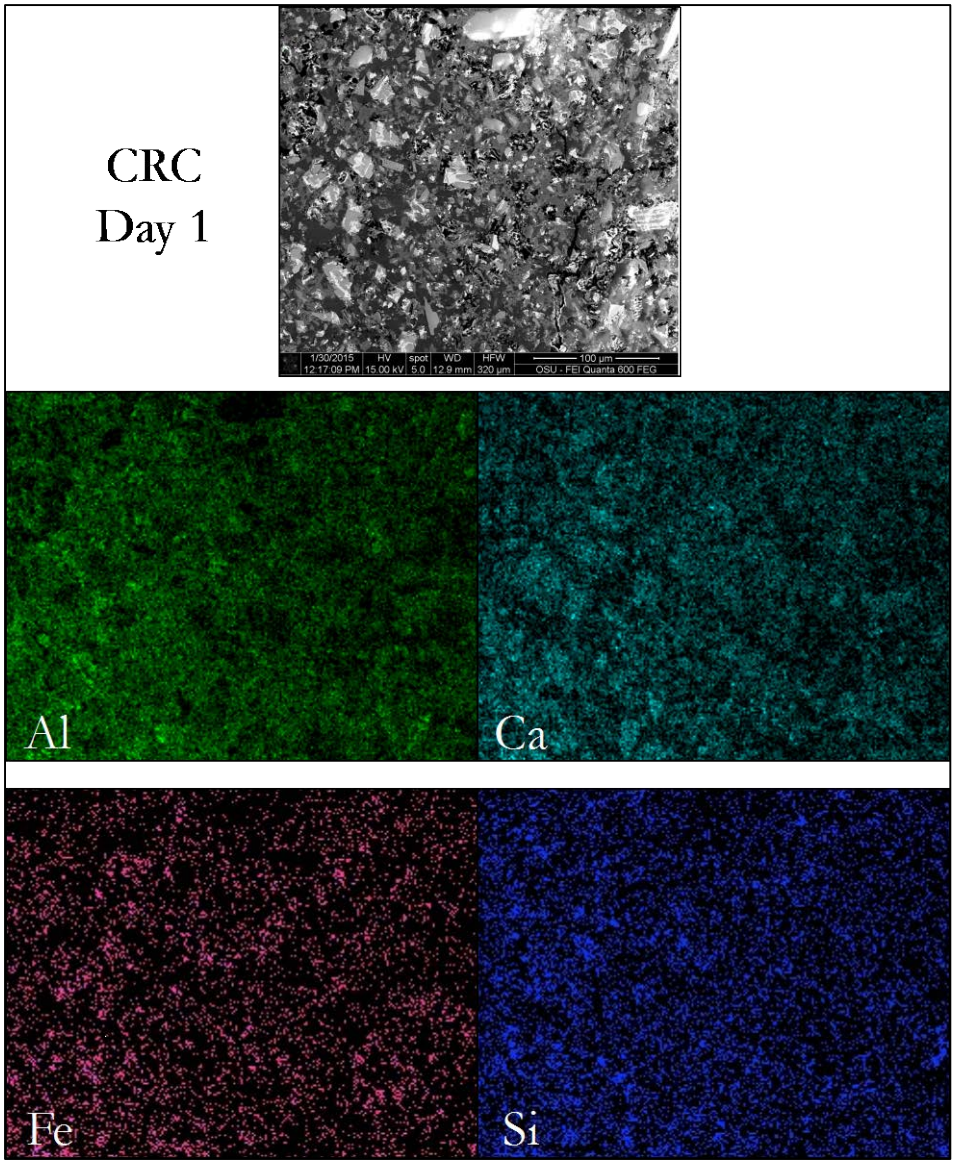

B)

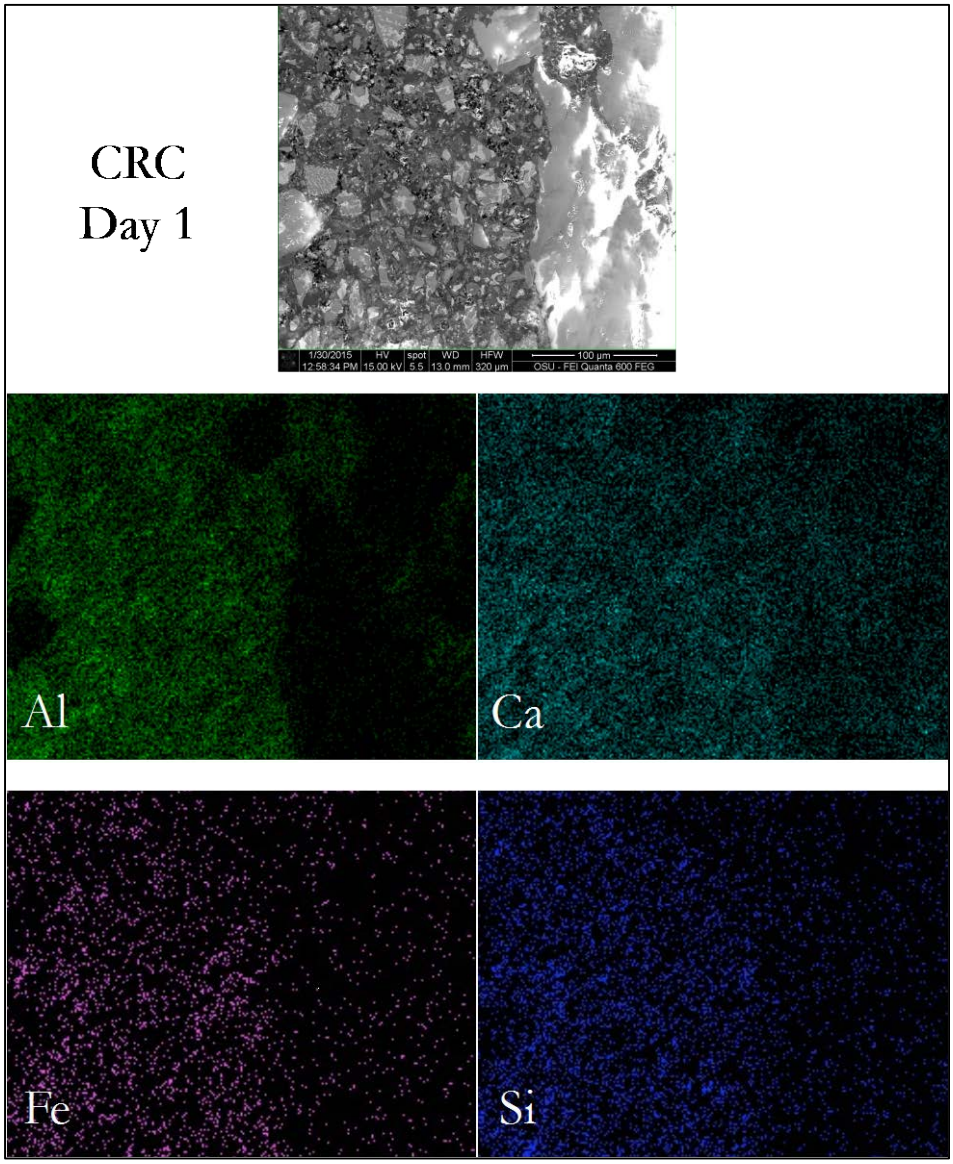

Figure B-27 A and B: Day 1 CRC EDX Maps

B.1.5.2 Day 3

Figure B-28 A and B presents selected BSE-SEM images with corresponding EDX maps used for examining microstructure of the CRC system at Day 3.

A)

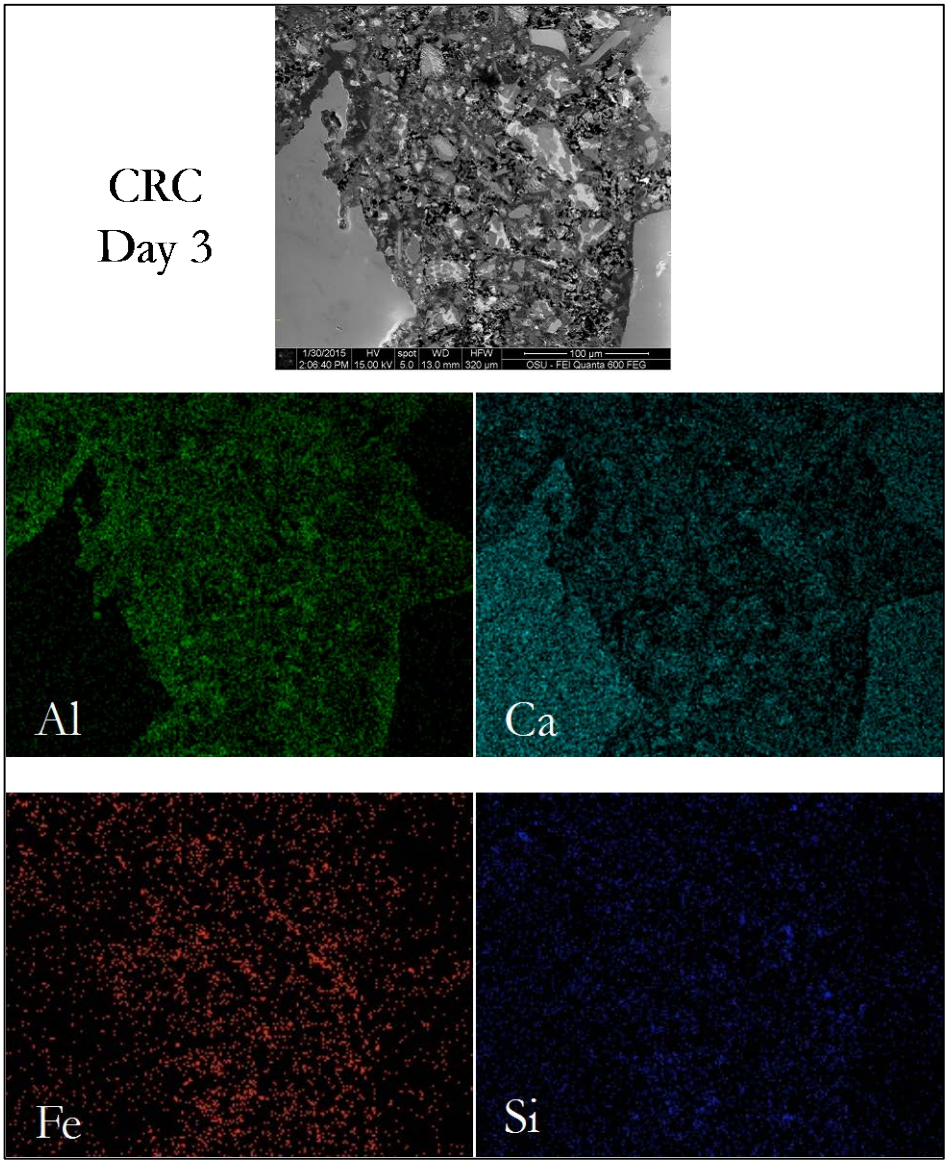

B)

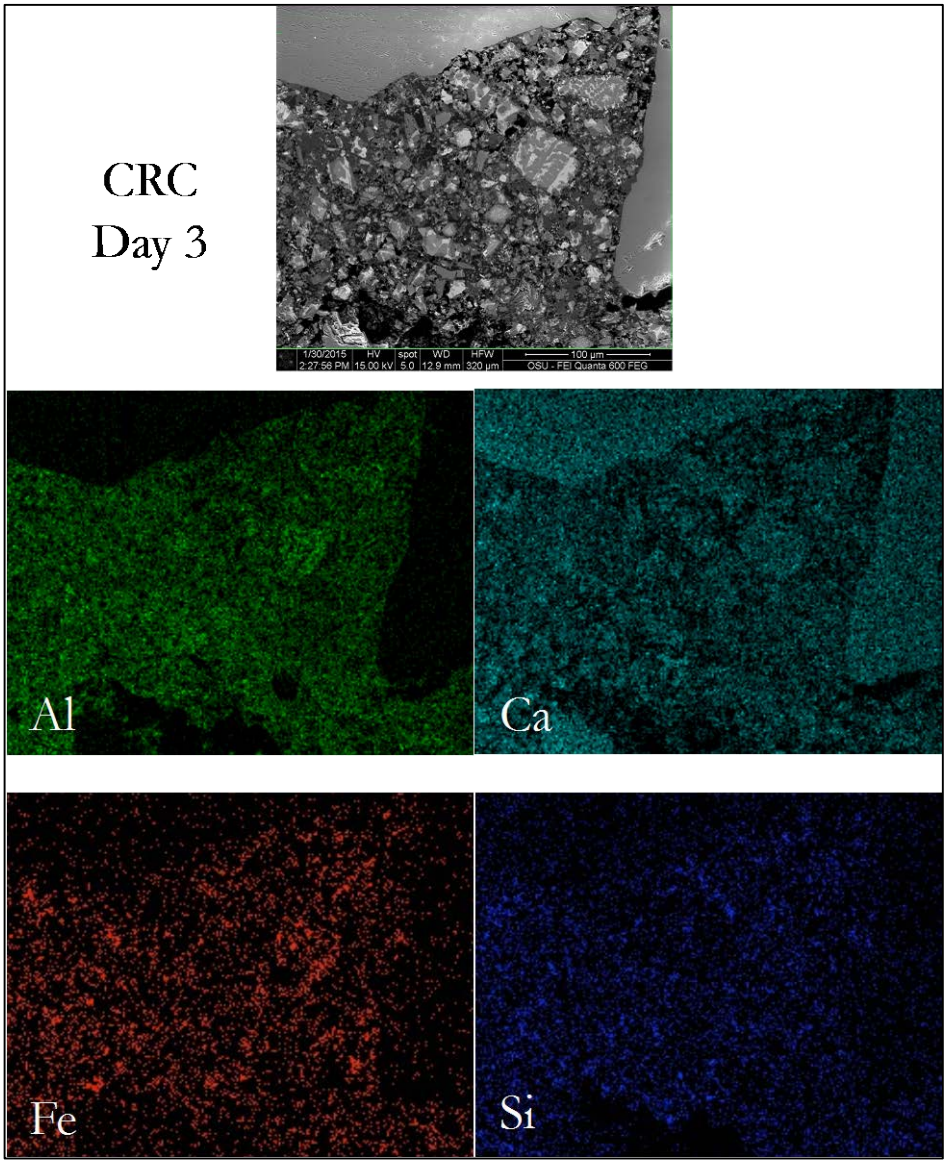

Figure B-28 A and B: Day 3 CRC EDX Maps

B.1.5.3 Day 7

Figure B-29 A and B presents selected BSE-SEM images with corresponding EDX maps used for examining microstructure of the CRC system at Day 7.

A)

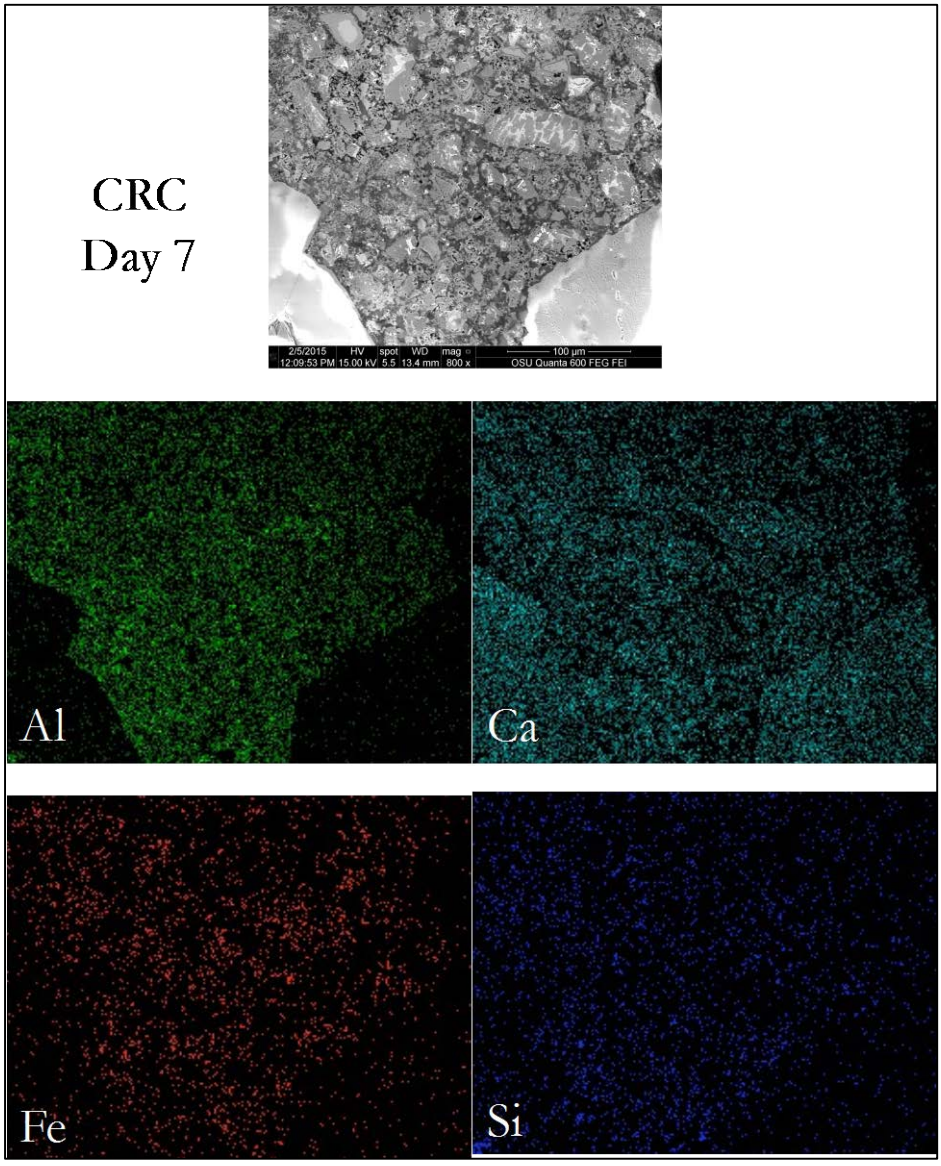

B)

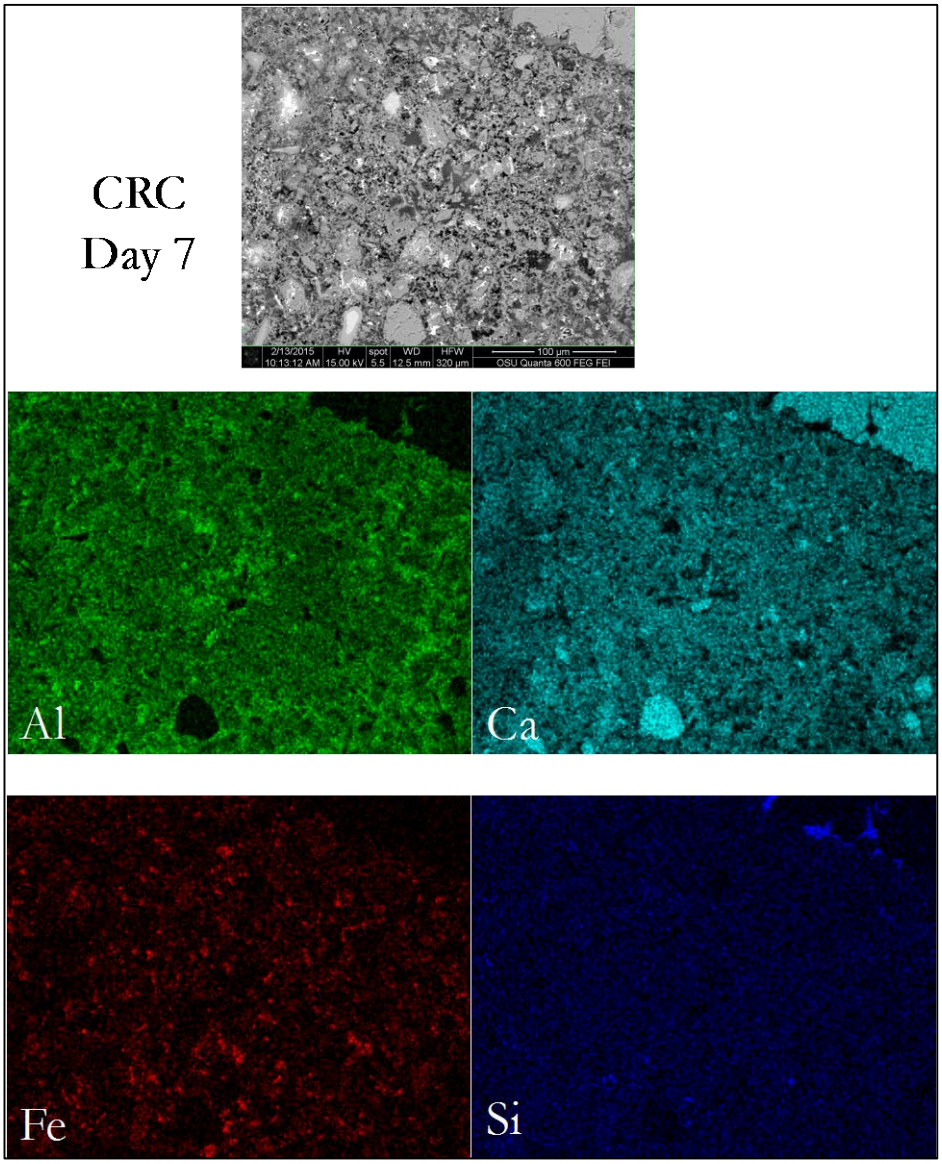

Figure B-29 A and B: Day 7 CRC EDX Maps

B.1.5.4 Day 14

Figure B-30 A and B presents selected BSE-SEM images with corresponding EDX maps used for examining microstructure of the CRC system at Day 14.

A)

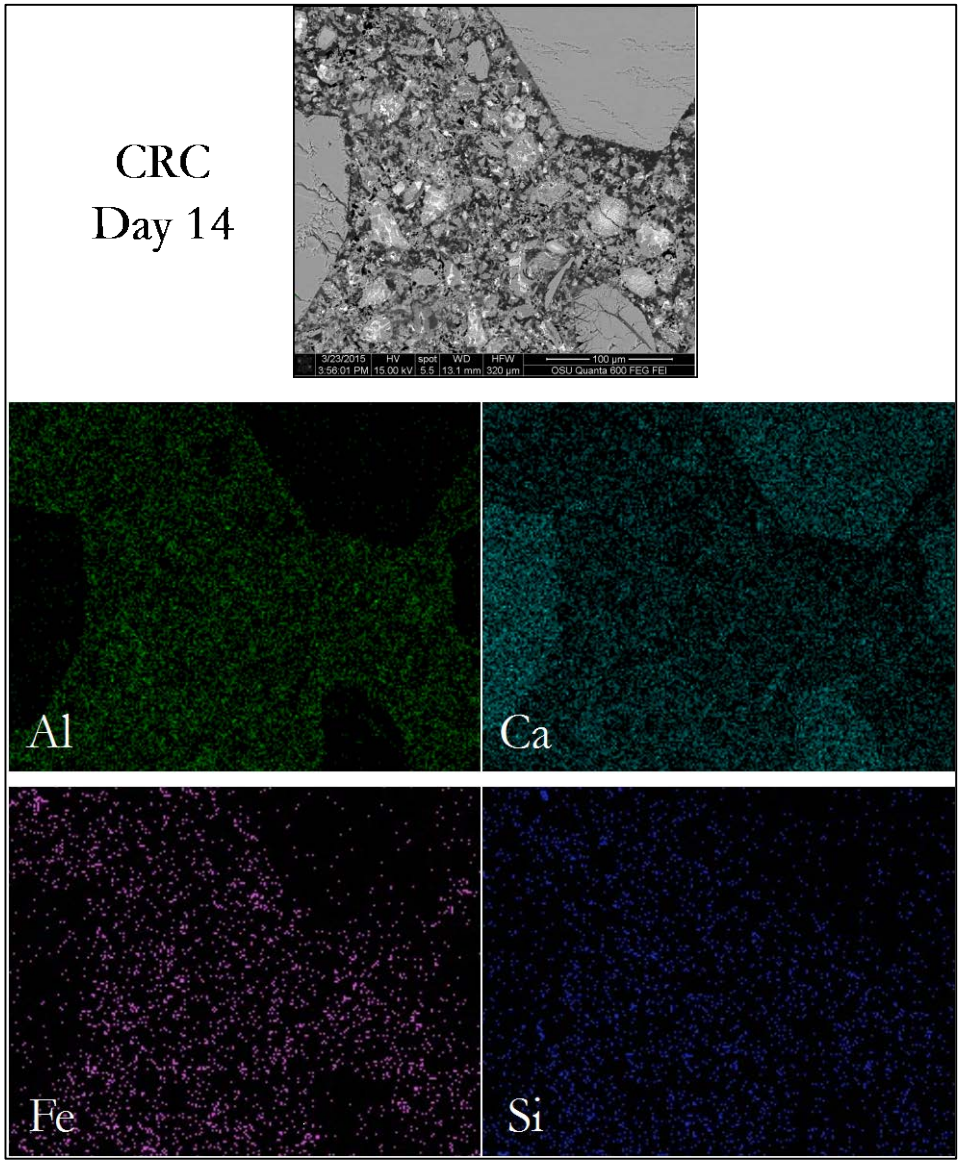

B)

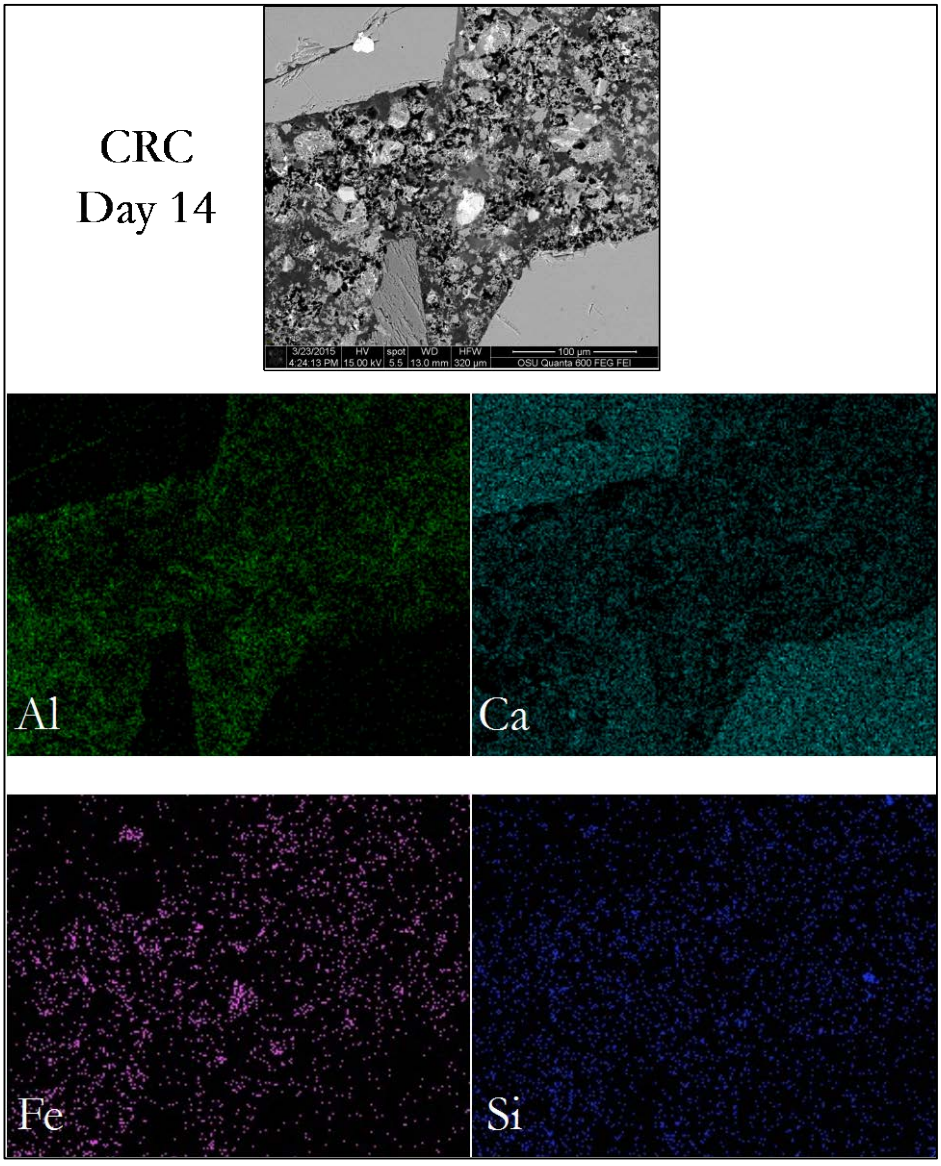

Figure B-30 A and B: Day 14 CRC EDX Maps